Advancing Conjugated Polymer Synthesis Through Catalyst Design

by

Kendra Delaine Souther

A dissertation submitted in partial fulfillment
of the requirements for the degree of
Doctor of Philosophy
(Chemistry)
in the University of Michigan
2018

Doctoral Committee:

Professor Anne J. McNeil, Chair
Professor Jinsang Kim
Professor John P. Wolfe
Associate Professor Paul M. Zimmerman

Kendra D. Souther

kendrads@umich.edu

ORCID iD: 0000-0002-2373-1434

DEDICATION

To my mother and father, Idalene and Garrison, for instilling the power of hardwork in me from a very young age and being a constant fountain of encouragement; lifting me up when I forget how.

To my sister, Deidre, for making my world a brighter place; always making me laugh and for always having a prayer ready to fill me up with love.

I love you all. MBT.

ACKNOWLEDGEMENTS

I must first begin by thanking my advisor and mentor, Professor Anne J. McNeil. Her commitment to pursuing challenging problems with integrity and fervor gave me a role model throughout my grad school experience and was a constant motivator. She encouraged me to be the best version of myself, for myself, and helped shape me into an independent scientist and problem solver. Next, I must thank my labmates past and present who made coming to work every day easy: Dr. Se Ryeon Lee, Dr. Kelsey Carter, Dr. Edmund Palermo, Dr. Fei Cheng, Dr. Zachary Bryan, Dr. Danielle Zurcher, Dr. Gesine Veits, Dr. Mitchell Smith, Dr. Peter Goldberg, Dr. Ariana Hall, Dr. Chen Kong, Amanda Leone, Matthew Hannigan, Justin Harris, Emily Mueller, Han Kim, Takunda Chazovachii, Dr. Patrick Lutz and Bri Barbu. A special thanks to my two mentors in lab, Se Ryeon and Zack. Both of them were patient, kind, and taught me the ropes of being a polymer chemist. Thank you to my personal thesis editing team, Amanda, Patrick, and Ariana, for taking the time and giving encouraging feedback.

Next, I must thank the fantastic collaborators I've had the pleasure of working with over the years. Thank you to Professor Paul Zimmerman and Andrew Vitek for being a computational force for our copolymerization system. Thank you to the ONR dream team, Professor Geoff Coates (Cornell), Dr. Anne LaPointe (Cornell), and our fearless leader Professor Robert Waymouth (Stanford) for providing synthetic insight and project feedback. Thank you to Geoff and Anne for allowing me to use their recycling GPC at Cornell, as well as perform high throughput experimentation and for being great hosts while I was there. Finally thank you to Professor Kevin Noonan (Carnegie Mellon) for giving invaluable advice at the Gordon Research Conference as well as many conversations via email and for assistance in characterizing my block copolymer.

During my time at Michigan, I have had the pleasure of having a fantastic support network. Before grad school began, I was given friends through the Rackham Merit Fellowship Summer Institute Program, and our bond has remained strong over grad school. Thank you to Dr. Kyle McDonald, Dr. Melissa Lee, Bryant James, Andrew Vitek, Autumn Bullard, Aeriel Murphy, Brad Keller, and Juan Lopez for all the laughter and good times. But before I even began the summer institute, I came into contact with an incoming chemistry PhD student, that has become one of the greatest friends I could ever have, Kyle McDonald. Kyle has been my biggest cheerleader, consistently showering me with love and encouragement, believing in me from day one, and I would not be on the other side of a PhD if were not for this amazing human. Kyle, I love you and thank you for being my rock. Through knowing Kyle, I also came to know another fabulous human, Rosalyn Kent. She is the epitome of a strong, independent woman who has a full heart and a willingness to share. Thank you Rosalyn for never a dull moment and for being a person I could always talk to when it all felt too much; I love you. While at Michigan, I also had the pleasure of becoming friends with women who are black girl magic: Aeriel, Autumn, Nkema, Aixa, Ciara, Lauren, Oleta, Crystal, and Yasmin. These women showed me how to knock down stereotypes while remaining true to myself, and have enabled me to grow beyond my career. I next must thank all permutations of my a capella group, the Graduate Troupe of Needlessly Educated Singers (GradTONES), that I have had the pleasure of singing with for five years. The TONES have been an amazing outlet during grad school, allowing me to express myself and put time into myself. I'd also like to take time and thank my spiritual counselor and phenomenal friend, Dr. Kayla Pyper. What an amazing woman who has filled me up with love through scripture and fellowship, so selfless. Thank you, Kayla. Finally, I need to thank my family, Ida, Garry, Deidre and my extended family for the unending support and love. Thank you. Lastly, I want to acknowledge funding support through a National Science Foundation Graduate Research Fellowship and a Rackham Merit Fellowship.

TABLE OF CONTENTS

LIST OF FIGURES

LIST OF SCHEMES

LIST OF EQUATIONS

LIST OF CHARTS

LIST OF APPENDICES

Abstract

Catalyst-transfer polymerization (CTP) is a living, chain-growth method for synthesizing conjugated polymers, which are attractive materials for organic electronics. What separates CTP from traditional cross-coupling polymerizations is a metal–polymer π-complex that enables the catalyst to stay associated to the growing polymer chain. This association yields polymers with targeted molecular weights, narrow dispersities, and tunable sequences. However, the utility of CTP is limited by a narrow monomer scope, wherein the most desirable polymers remain inaccessible via controlled methods. This thesis aims to advance CTP by designing catalysts capable of widening monomer pairings for block copolymers, exploring ligand electronics in designing an optimal CTP catalyst for previously inaccessible monomers, and optimizing a new user-friendly CTP method.

Chapter 1 briefly summarizes CTP with a focus on how understanding polymerization mechanisms can facilitate catalyst design. Specifically, how exploiting the metal-π complex has led to expanded, albeit limited monomer scope, and new copolymer sequences. The major conclusions of chapters 2–5 and our efforts to expand CTP catalyst scope are briefly outlined followed by the implications of this work on future CTP systems.

Chapter 2 reports the trials and tribulations of designing a single catalyst to perform two sequential, living polymerizations to access thiophene/olefin block copolymers in a one-pot synthesis. Lessons learned include the influence of catalyst reactive ligand and cocatalyst identity on successful thiophene polymerization as well as the inhibitory nature of olefins on thiophene polymerization, requiring olefin monomer removal to induce a switch-in-mechanisms. While a small amount of copolymer was synthesized, the major products were undesired homopolymer.

We attributed these homopolymers to a high-barrier reductive elimination when the catalyst switches mechanisms and subsequent chain-transfer during thiophene polymerization. This work highlights the need to identify conditions that facilitate living behavior for both polymerizations as well as promotes efficient cross-propagation.

Chapter 3 describes efforts to design catalysts for CTP that expand monomer scope by tuning ligand electronics to stabilize the metal-π complex. A pyrrolidinyl-based bisphosphine precatalyst was explored in poly(thiophene) and poly(hexylesterthiophene) synthesis and yields polymers with targeted molecular weights as well as high end-group fidelity, suggesting this newly designed catalyst forms a stabilized metal-π complex. While poly(phenylene) synthesis was attempted, gel permeation chromatography revealed a multimodal polymer trace, suggesting multiple catalytic species in the polymerization and an uncontrolled reaction. This catalyst should be further explored in polymerizing previously inaccessible monomers, whose polymerizations are often marred by chain-transfer events.

Chapter 4 describes efforts towards developing a more user-friendly CTP. An NHC-ligated palladium precatalyst with a 3–fluoropyridine ligand polymerized electron-rich and electron-poor monomers of the form, Ar–ZnCl•$Mg(OPiv)_2$, in-air via a controlled, chain-growth method. Ongoing work is focused on showing the utility of this method to a broader community in synthesizing relevant materials for organic electronics.

Chapter 5 summarizes each chapter and provides an outlook for how these results can be informative for the CTP community. The results in accessing conjugated/olefin block copolymers will inform the design of alternative precatalysts that promote Csp^2–Csp^3 reductive elimination in copolymerizations. The pyrrolidinyl-based bisphospine precatalyst for CTP will add to the toolbox of catalysts, particularly for electron-deficient polymerizations. Finally, our work in identifying a user-friendly CTP route will aid researchers from a variety of backgrounds in synthesizing conjugated polymers with control over molecular weight open-to-air.

Chapter 1
Introduction

Catalyst-transfer polymerization (CTP) is a transition-metal catalyzed, chain-growth polymerization method used for synthesizing conjugated (hetero)arene polymers, attractive materials for the active layer of organic electronics (e. g. solar cells, transistors, light-emitting diodes).[1] Because CTP is a living, chain-growth method, researchers can access polymers with targeted number average molecular weights (M_n), narrow dispersities (Đ), end groups, and specific sequences. The first reported living, chain-growth synthesis for conjugated polymers (poly(3-hexylthiophene) (P3HT)) were in 2004 by Yokozawa and McCullough independently, both using Ni bisphosphine catalysts.[2,3] This work has enabled the field of CTP to expand to other monomers; including thiazole,[4,5] pyrrole,[6] phenylene,[7] fluorene,[8,9] benzotriazole,[10] and most of the chalcogen analogues of thiophene (O, Se, Te)[11,12,13] (Chart 1.1). Organometallic functionality of (hetero)arene monomers has also expanded with monomer scope. While an aryl-magnesium species is a common motif used in CTP, researchers have also incorporated other functionalities such as zinc,[14] boronic acids[15]/esters,[16] stannanes,[17] and less commonly gold[18] and lithium[19]. While Ni bisphosphine catalysts are the common choice for CTP, expanding to other metals (Pd) as well as other ancillary ligands (N–heterocyclic carbenes (NHCs),[19,20] Buchwald ligands,[21] and diimines[22]) has provided routes for accessing alternative conjugated polymers.

Chart 1.1 Selected monomers polymerized via CTP.

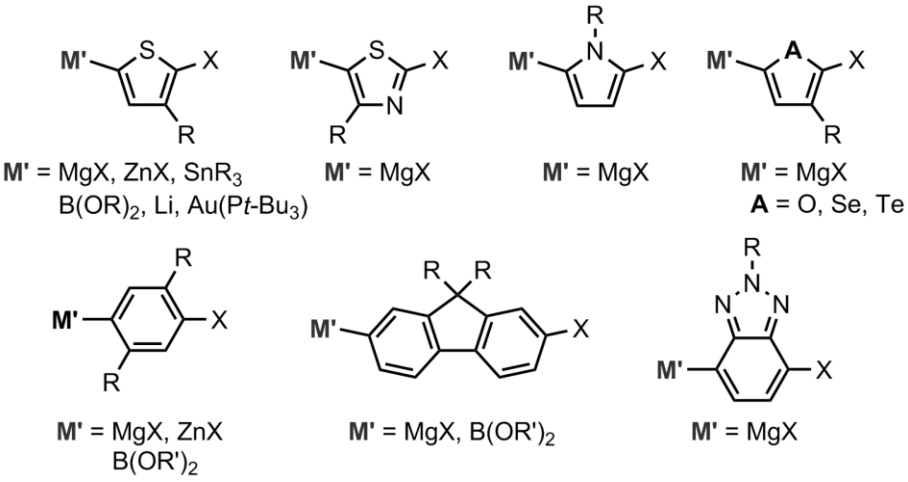

CTP advancements have only been possible through mechanistic understanding of the catalytic cycle (Scheme 1.1).[23] CTP is initiated via a transmetalation event between the organometallic (hetero)arene and a metal precatalyst, wherein the number of transmetalation events depends on the precatalyst identity. A dihalide precatalyst (L_nMX_2) requires a double transmetalation, while a precatalyst of the form L_nMArX require a single transmetalation. The resulting biaryl metal complex then undergoes reductive elimination to yield a metal–polymer π-complex (**I**). The catalyst stays associated with the polymer chain, ring-walking to the C–Br bond of the terminal arene (**II**), and enters propagation by intramolecular oxidative addition into the C–Br bond to yield complex **III**. Propagation additionally includes transmetalation with monomer (**IV**) and reductive elimination to yield a metal–polymer π-complex that has been extended by one monomer unit. Propagation continues until all monomers are consumed.

Scheme 1.1 Catalytic cycle in CTP (M = Ni or Pd, X = halide, RL = reactive ligand (Ar), M' = organometallic group).

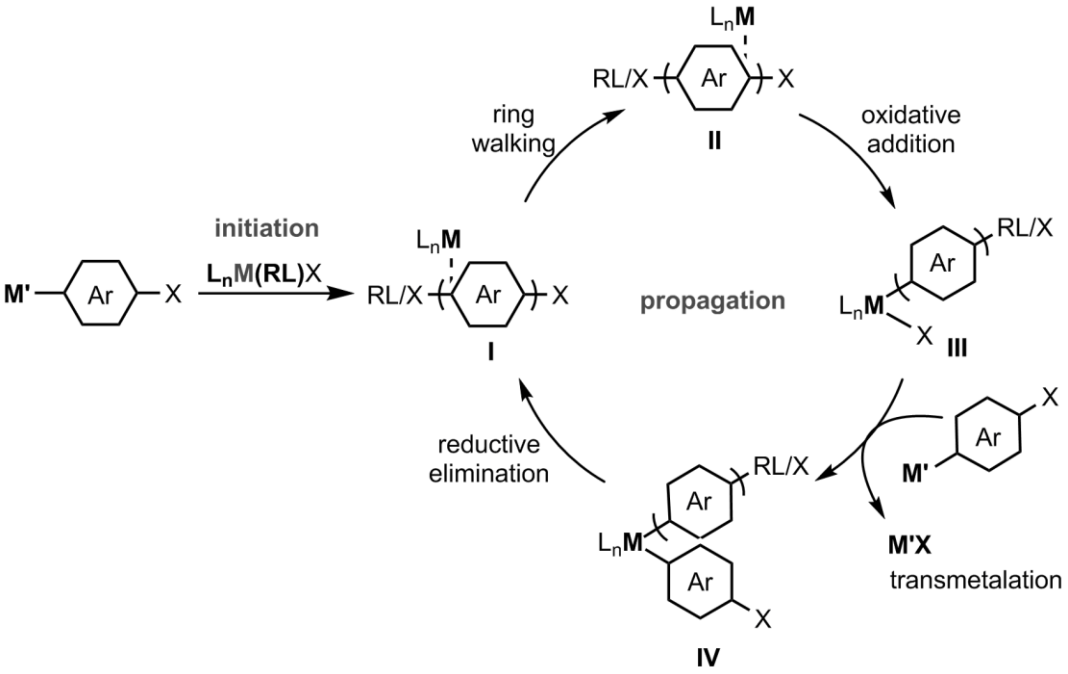

McNeil and coworkers have been at the forefront of elucidating the CTP mechanism of P3HT and poly(phenylene) syntheses using ^{31}P NMR spectroscopic analysis to support the various aforementioned intermediates throughout initiation and propagation.[24,25,26] While most intermediates can be observed using this technique, the metal–polymer π–complex **(I**) is often elusive during polymerization due to relatively fast intramolecular oxidative addition. Koeckelburghs observed a metal–π complex using ^{31}P NMR spectroscopy in an attempted thienothiophene polymerization. [27] The stability of this species enabled NMR spectroscopic detection, providing indirect evidence of the complex but stalled the catalytic cycle (no polymer formation). McNeil and Bryan have also used small-molecule competition experiments to probe the π-complex intermediate.[28]

Because the catalyst stays associated with the growing polymer chain and the chain ends remain active at the end of the polymerization, other CTP-compatible monomers can be enchained into the growing polymer and give rise to copolymers (e.g. block,[29] random,[29a,30] and gradient[29a,31]). These copolymers are used as donor materials in organic electronics (i. e., solar cells) and as compatibilizers[32,33] in thin films to promote film stability and inhibit phase separation, a process that decreases the efficiency of a

solar cell over time. Accessing copolymers can be streamlined when the monomers have similar polymerization mechanisms. However when the mechanisms are dissimilar, numerous synthetic steps and multiple purifications are required to make the pure copolymers.[34] We were interested in synthesizing block copolymers that contained insulating and conducting segments, as these block copolymers exhibit improved thin film morphology.[35,36]

In Chapter 2 we report our work in identifying a single catalyst ("multitasking catalyst") capable of enchaining monomers with dissimilar mechanisms in one pot (Scheme 1.2).[37] We evaluated a Ni diimine-ligated catalyst and optimized conditions for polymerizing 1-pentene and 3-hexylthiophene (**3HT**). While we were able to isolate the desired copolymer, albeit in low yields, the major products were both homopolymers, suggesting that catalysts dissociate during and/or after the switch-in-mechanism. Experimental and theoretical studies revealed a high-energy barrier for the catalyst to switch mechanisms, coupled with infrequent catalyst dissociation as the reason for low copolymer yield. Combined, these studies highlight the difficulties associated with identifying multitasking catalysts and further catalyst optimization (ancillary ligand, metal) is necessary for this specific copolymerization.

Scheme 1.2 Copolymerization between 1-pentene and 3HT via a Ni diimine precatalyst.

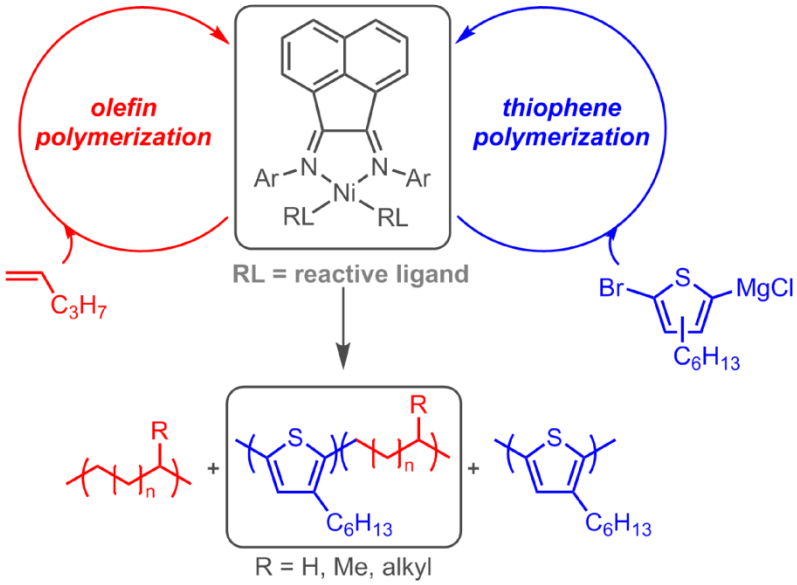

While we chose diimine precatalysts for our copolymerization system because they had literature precedent for polymerizing both olefins[38] and thiophenes,[22a] commercially available Ni(diphenylphosphinoethane)Cl_2 and Ni(diphenylphosphinopropane)Cl_2 are typically used in CTP. Moving beyond these catalysts, researchers have also expanded ligand scope to include bisalkylphosphinoethane and substituted bisarylphosphinoethane ligands and NHCs for CTP.[25,39] Increasing electron density of the catalyst via ligand modifications has provided a measurable increase in end-group control and narrow dispersities for conjugated polymers. We were interested in exploring a new ligand scaffold, nitrogen-based bisphosphinoethane, and comparing this catalyst to the previous work in the field through dispersity and end-group analysis.

Chapter 3 describes our efforts in synthesizing conjugated polymers via CTP with a new ligand scaffold (Figure 1.1). We synthesized a bis(dipyrrolidinylphopshino)ethane (dpyrpe) Ni dihalide precatalyst (L_2MX_2) that yielded poly(bishexyloxyphenylene) (**PBHP**) and **P3HT** with multimodal gel permeation chromatograms, suggesting numerous catalytic cycles. ^{31}P NMR spectroscopic studies of **BHP** polymerization revealed slow initiation. To ensure that all chains were initiating in unison, we modified our precatalyst to have a biphenyl reactive ligand, as work by McNeil and coworkers[40] showed that this biphenyl reactive ligand increased the rate of initiation in **PBHP** synthesis. While a multimodal peak persisted for **PBHP** using our new precatalyst (L_2MArX), a unimodal polymer peak was observed for **P3HT** with a narrow dispersity (Đ = 1.13) and almost complete end-group incorporation (99.5%). In addition, an electron deficient polymer, poly(3-hexylesterthiophene) (**P3HET**) was synthesized with L_2MArX with a moderate dispersity (Đ = 1.31) and 99% incorporation of end-groups. A low molecular weight tail was seen, suggesting slow initiation. Comparing our system to past work, dpyrpe–ligated Ni catalysts should be further explored for polymerizing electron-deficient monomers.

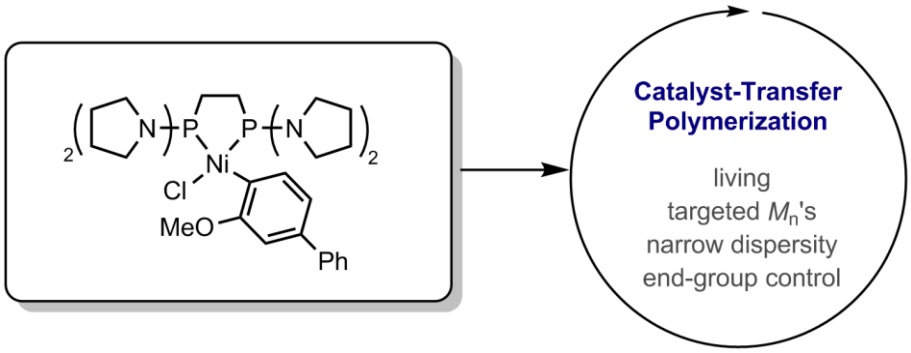

Figure 1.1 Dpyrpe-ligated Ni catalyst for CTP

Another limitation of CTP is that most catalysts and organometallic monomers suffer from air and/or moisture sensitivity, rendering researchers limited to working in gloveboxes and/or using Schlenk techniques. We were inspired by work from Knochel and coworkers,[41] wherein ArMgCl with $Zn(OPiv)_2$ salt produced an air- and moisture-tolerant ArZnCl and $Mg(OPiv)_2$. This combination was still >90% active material after 4 h exposed to air. Mechanistic work by Knochel in 2014 revealed stability is due $Mg(OPiv)_2$ salt absorbing H_2O, preventing hydrolysis of the Zn–C bond.[42] We hypothesized that a monomer with the above organometallic functionality would enable us to perform CTP in air and Chapter 4 describes our efforts in outlining a user-friendly, open-to-air synthesis. We reported a precatalyst that (**IPentF**) (Scheme 1.3) shows promise as a suitable precatalyst for an in-air conjugated polymer synthesis via CTP yielding polymers with targeted molecular weights and narrow dispersities. This motivating result suggests that CTP can be made available to a broader scientific community, as a glovebox is not necessary for polymerization.

Scheme 1.3 Open-to-air CTP polymerization conditions.

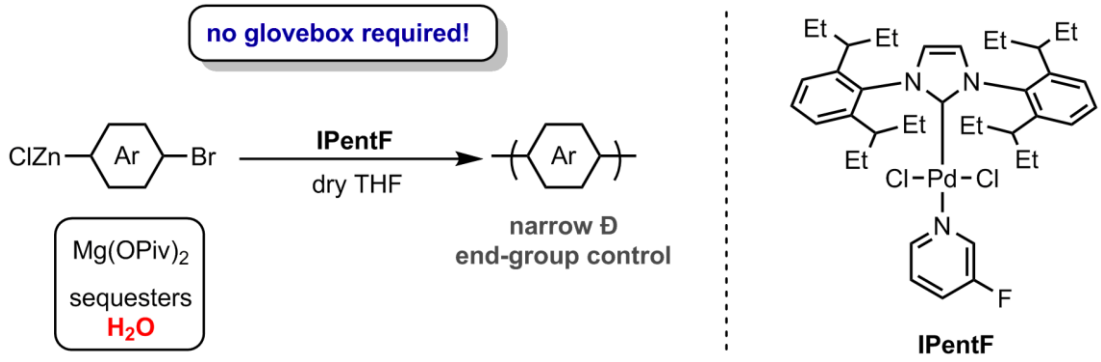

Overall, this thesis aims to advance copolymer sequence of CTP, design new CTP precatalysts, and provide an air-tolerant CTP route to the broader scientific community. Specifically, we look at accessing block copolymers with insulating and conducting segments in one-pot using a single catalyst. While some copolymer is generated, the major products of the reaction mixture are homopolymers due to a high energy barrier switching between mechanisms coupled with chain-transfer reactions. Lessons learned are also discussed that should aid in future "multitasking" catalyst design. We next seek to expand ligand scope of bisphopsphine–ligated Ni precatalysts to include dpyrpe ligands. These catalysts polymerize thiophene-based electron-rich and electron-poor monomers with exclusive end-group incorporation. Mechanistic studies are suggested for future work to understand this new catalyst's behavior in CTP. Finally, we provide an outline of a potential open-to-air route for accessing conjugated polymers via CTP that enables researchers to generate important materials for organic electronics without the need for a glovebox.

References

(1) Recent reviews (a) Bryan, Z. J.; McNeil, A. J. Conjugated Polymer Synthesis via Catalyst-Transfer Polycondensation (CTP): Mechanism, Scope and Applications. *Macromolecules* **2013**, *46*, 8395–8405. (b) Leone, A. K.; McNeil, A. J. Matchmaking in Catalyst-Transfer Polycondensation: Optimizing Catalysts based on Mechanistic Insight. *Acc. Chem. Res.* **2016**, *49*, 2822–2831. (c) Baker, M. A.; Tsai, C.-H.; Noonan, K. J. T. Diversifying Cross-Coupling Strategies, Catalysts and Monomers for the Controlled Synthesis of Conjugated Polymers. *Chem. Eur. J.* **2018**, *ASAP*, DOI: 10.1002/chem.201706102.

(2) Yokoyama, A.; Miyakoshi, R.; Yokozawa, T. Chain Growth Polymerization for Poly(3-hexylthiophene) with a Defined Molecular Weight and a Low Polydispersity. *Macromolecules* **2004**, *37*, 1169–1171.

(3) Sheina, E. E.; Liu, J.; Iovu, M. C.; Laird, D. W.; McCullough, R. D. Chain Growth Mechanism for Regioregular Nickel-Initiated Cross-Coupling Polymerizations. *Macromolecules* **2004**, *37*, 3526–3528.

(4) Pammer, F.; Jager, J.; Rudolf, B.; Sun, Y. Soluble Head-to-Tail Regioregular Polythiazoles: Preparation, Properties, and Evidence for Chain-Growth Behavior in the Synthesis via Kumada-Coupling Polycondensation. *Macromolecules* **2014**, *47*, 5904–5912.

(5) Smith, M. L.; Leone, A. K.; Zimmerman, P. M.; McNeil, A. J. Impact of Preferential π-Binding in Catalyst-Transfer Polycondensation of Thiazole Derivatives. *ACS Macro Lett.* **2016**, *5*, 1411–1415.

(6) Yokoyama, A.; Kato, A.; Miyakoshi, R.; Yokozawa, T. Precision Synthesis of Poly(N-hexylpyrrole) and its Diblock Copolymer with Poly(p-phenylene) via Catalyst-Transfer Polycondensation. *Macromolecules* **2008**, *41*, 7271–7273.

(7) Miyakoshi, R.; Shimono, K.; Yokoyama, A.; Yokozawa, T. Catalyst-Transfer Polycondensation for the Synthesis of Poly(*p*-phenylene) with Controlled Molecular Weight and Low Polydispersity. *J. Am. Chem. Soc.* **2006**, *128*, 16012–16013.

(8) Yokoyama, A.; Suzuki, H.; Kubota, Y.; Ohuchi, K.; Higashimura, H.; Yokozawa, T. Chain-Growth Polymerization for the Synthesis of Polyfluorene via Suzuki-Miyaura Coupling Reaction from an Externally Added Initiator Unit. *J. Am. Chem. Soc.* **2007**, *129*, 7236–7237.

(9) Sui, A.; Shi, X.; Wang, Y.; Geng, Y.; Wang, F. Kumada Catalyst Transfer Polycondensation for Controlled Synthesis of Polyfluorenes Using 1,3-bis(diarylphosphino)propanes as Ligands. *Polym. Chem*. **2015**, *6*, 4819–4827.

(10) Bridges, C. G.; McCormick, T. M.; Gibson, G. L.; Hollinger, J.; Seferos, D. S. Designing and Refining Ni(II)diimine Catalysts Toward the Controlled Synthesis of Electron-Deficient Conjugated Polymers. *J. Am. Chem. Soc.* **2013**, *135*, 13212–13219.

(11) Qiu, Y.; Fortney, A.; Tsai, C.-H.; Baker, M. A.; Gil, R. R.; Kowalewski, T.; Noonan, K. J. T. Synthesis of Polyfuran and Thiophene-Furan Alternating Copolymers Using Catalyst-Transfer Polycondensation. *ACS Macro Lett*. **2016**, *5*, 332–336.

(12) Hollinger, J.; Jahnke, A. A.; Coombs, N.; Seferos, D. S. Controlling Phase Separation and Optical Properties in Conjugated Polymers through Selenophene−Thiophene Copolymerization. *J. Am. Chem. Soc.* **2010**, *132*, 8546–8547.

(13) Ye, S.; Steube, M.; Carrera, E. I.; Seferos, D. S. What Limits the Molecular Weight and Controlled Synthesis of Poly(3- alkyltellurophene)s? *Macromolecules* **2016**, *49*, 1704–1711.

(14) Goto, E.; Nakamura, S.; Kawauchi, S.; Mori, H.; Ueda, M.; Higashihara, T. Precision Synthesis of Regioregular Poly(3-hexylthiophene) with Low Dispersity Using a Zincate Complex Catalyzed by Nickel with the Ligand of 1,2-Bis(dicyclohexylphosphino)ethane. *J. Polym. Sci., Part A: Polym. Chem.* **2014**, *52*, 2287–2296.

(15) Yokoyama, A.; Suzuki, H.; Kubota, Y.; Ohuchi, K.; Higashimura, H.; Yokozawa, T. Chain-Growth Polymerization for the Synthesis of Polyfluorene via Suzuki−Miyaura Coupling Reaction from an Externally Added Initiator Unit. *J. Am. Chem. Soc*. **2007**, *129*, 7236–7237.

(16) (a) Sui, A.; Shi, X.; Tian, H.; Geng, Y.; Wang, F. Suzuki–Miyaura Catalyst-Transfer Polycondensation with Pd(IPr)(OAc)2 as the Catalyst for the Controlled Synthesis of Polyfluorenes and Polythiophenes. *Polym. Chem*. **2014**, *5*, 7072–7080. (b) Yokozawa, T.; Kohno, H.; Yoshihiro, O.; Yokoyama, A. Catalyst-Transfer Suzuki−Miyaura Coupling Polymerization for Precision Synthesis of Poly(p-phenylene). *Macromolecules* **2010**, *43*, 7095–7100. (c) Elmalem, E.; Kiriy, A.; Huck, W.T.S. Chain-Growth Suzuki Polymerization of n-Type Fluorene Copolymers. *Macromolecules* **2011**, *44*, 9057–9061.

(17) Qiu, Y.; Mohin, J.; Tsai, C.-H.; Tristram-Nagle, S.; Gil, R.R.; Kowalewski, T.; Noonan, K. J. T. Stille Catalyst-Transfer Polycondensation Using Pd-PEPPSI-IPr for High Molecular-Weight Regioregular Poly(3-hexylthiophene). *Macromol. Rapid Commun.* **2015**, *36*, 840–844.

(18) Suraru, S. L.; Lee, J. A.; Luscombe, C. K. Preparation of an Aurylated Alkylthiophene Monomer via C–H Activation for Use in Pd-PEPPSI-iPr Catalyzed-Controlled Chain Growth Polymerization. *ACS Macro Lett.* **2016**, *5*, 533–536.

(19) Fuji, K.; Tamba, S.; Shono, K.; Sugie, A.; Mori, A. Murahashi Coupling Polymerization: Nickel(II)–N-Heterocyclic Carbene Complex-Catalyzed

Polycondensation of Organolithium Species of (Hetero)arenes. *J. Am. Chem. Soc*. **2013**, *135*, 12208–12211.

(20) (a) Bryan, Z. J.; Smith, M. L.; McNeil, A. J. Chain-growth Polymerization of Aryl Grignards Initiated by Stabilized NHC-Pd Precatalysts. *Macromol. Rapid Commun.* **2012**, *33*, 842–847. (b) Tamba, S.; Shono, K.; Sugie, A.; Mori, A. C–H Functionalization Polycondensation of Chlorothiophenes in the Presence of Nickel Catalyst with Stoichiometric or Catalytically Generated Magnesium Amide. *J. Am. Chem. Soc.* **2011**, *133*, 9700–9703.

(21) (a) Zhang, H.H.; Xing, C.H.; Hu, Q.S. Controlled Pd(0)/t-Bu3P-Catalyzed Suzuki CrossCoupling Polymerization of AB-Type Monomers with PhPd(t-Bu3P)I or Pd2(dba)3/tBu3P/ArI as the Initiator. *J. Am. Chem. Soc*. **2012**, *134*, 13156–13159. (b) Kosaka, K.; Uchida, T.; MIkami, K.; Ohta, Y.; Yokozawa, T. AmPhos Pd-Catalyzed Suzuki-Miyaura Catalyst-Transfer Condensation Polymerization: Narrow Dispersity by Mixing the Catalyst and Base Prior to Polymerization. *Macromolecules* **2018**, *51*, 364–369.

(22) (a) Magurudeniya, H. D.; Sista, P.; Westbrook, J. K.; Ourso, T. E.; Nguyen, K.; Maher, M. C.; Alemseghed, M. G.; Biewer, M. C.; Stefan, M. C. Nickel(II) α-Diimine Catalyst for Grignard Metathesis (GRIM) Polymerization. *Macromol. Rapid Commun.* **2011**, *32*, 1748–1752. (b) Leone, A. K.; Souther, K. D.; Vitek, A. K.; LaPointe, A. M.; Coates, G. W.; Zimmerman, P. M.; McNeil, A. J. Mechanistic Insight into Thiophene Catalyst-Transfer Polymerization Mediated by Nickel Diimine Catalysts. *Macromolecules* **2017**, *50*, 9121–9127.

(23) Yokozawa, T.; Ohta, Y. Transformation of Step-Growth Polymerization into Living Chain-Growth Polymerization. *Chem. Rev*. **2016**, *116*, 1950–1968.

(24) Lanni, E. L.; McNeil, A. J. Mechanistic Studies on Ni(dppe)Cl_2-Catalyzed Chain-Growth Polymerizations: Evidence for Rate-Determining Reductive Elimination. *J. Am. Chem. Soc.* **2009**, *131*, 16573–16579.

(25) Lanni, E. L.; McNeil, A. J. Evidence for Ligand-Dependent Mechanistic Changes in Nickel-Catalyzed Chain-Growth Polymerizations. *Macromolecules* **2010**, *43*, 8039–8044.

(26) Lanni, E. L.; Locke, J. R.; Gleave, C. M.; McNeil, A. J. Ligand Based Steric Effects in Ni-Catalyzed Chain-Growth Polymerizations Using Bis(dialkylphosphino)ethanes. *Macromolecules* **2011**, *44*, 5136–5145.

(27) Willot, P.; Koeckelberghs, G. Evidence for Catalyst Association in the Catalyst Transfer Polymerization of Thieno[3,2-b]thiophene. *Macromolecules* **2014**, *47*, 8548–8555.

(28) Bryan, Z. J.; McNeil, A. J. Evidence for a Preferential Intramolecular Oxidative Addition in Ni-catalyzed Cross-Coupling Reactions and Their Impact on Chain-Growth Polymerizations. *Chem. Sci.* **2013**, *4*, 1620–1624.

(29) (a) Willot, P.; Govaerts, S.; Koeckelberghs, G. The Controlled Polymerization of Poly(cyclopentadithiophene)s and Their All Conjugated Block Copolymers. *Macromolecules* **2013**, *46*, 8888–8895. (b) Palermo, E. F.; McNeil, A. J. Impact of Copolymer Sequence on Solid-State Properties for Random, Gradient and Block Copolymers containing Thiophene and Selenophene. *Macromolecules* **2012**, *45*, 5948–5955. (c) Song, I. Y.; Kim, J.; Im, M. J.; Moon, B. J.; Park, T. Synthesis and Self-Assembly of Thiophene-Based All-Conjugated Amphiphilic Diblock Copolymers with a Narrow Molecular Weight Distribution. *Macromolecules* **2012**, *45*, 5058–5068. (d) Umezawa, K.; Oshima, T.; Yoshizawa-Fujita, M.; Takeoka, Y.; Rikukawa, M. Synthesis of Hydrophilic−Hydrophobic Block Copolymer Ionomers Based on Polyphenylenes. *ACS Macro Lett.* **2012**, *1*, 969–972. (e) Verswyvel, M.; Monnaie, F.; Koeckelberghs, G. AB Block Copoly(3-alkylthiophenes): Synthesis and Chiroptical Behavior. *Macromolecules* **2011**, *44*, 9489–9498. (f) Zhang, Y.; Tajima, K.; Hashimoto, K. Nanostructure Formation in Poly(3-hexylthiophene-block-3-(2-ethylhexyl)thiophene)s. *Macromolecules* **2009**, *42*, 7008–7015. (g) Ohshimizu, K.; Ueda, M. Well-Controlled Synthesis of Block Copolythiophenes. *Macromolecules* **2008**, *41*, 5289–5294.

(30) Willot, P.; Steverlynck, J.; Moerman, D.; Leclere, P.; Lazzaroni, R.; Koeckelberghs, G. Poly(3-alkylthiophene) with Tuneable Regioregularity: Synthesis and Self-Assembling Properties. *Polym. Chem.* **2013**, *4*, 2662–2671.

(31) Locke, J. R.; McNeil, A. J. Syntheses of Gradient π-Conjugated Copolymers of Thiophene. *Macromolecules* **2010**, *43*, 8709–8710.

(32) Palermo, E. F.; van der Laan, H. L.; McNeil, A. J. Impact of π- conjugated Gradient Sequence Copolymers on Polymer Blend Morphology. *Polym. Chem*. **2013**, *4*, 4606–4611.

(33) Palermo, E. F.; McNeil, A. J. Conjugated Gradient Copolymers Suppress Phase Separation and Improve Stability in Bulk Heterojunction Solar Cells. *J. Mater. Chem. C.* **2014**, *2*, 3401–3406.

(34) (a) Moon, H. C.; Anthonysamy, A.; Lee, Y.; Kim, J. K. Facile Synthesis of Well-Defined Coil−Rod−Coil Block Copolymer Composed of Regioregular Poly(3-hexylthiophene) via Anionic Coupling Reaction. *Macromolecules* **2010**, *43*, 1747–1752. (b) Radano, C. P.; Scherman, O. A.; Stingelin-Stutzmann, N.; Muller, C.; Breiby, D. W.; Smith, P.; Janssem, R. A. J.; Meijer, E. W. Crystalline-Crystalline Block Copolymers of Regioregular Poly(3-hexylthiophene) and Polyethylene by Ring-Opening Metathesis Polymerization. *J. Am. Chem. Soc.* **2005**, *127*, 12502–12503.

(35) Müller, C.; Goffri, S.; Breiby, D. W.; Andreasen, J. W.; Chanzy, H. D.; Janssen, R. A. J.; Nielsen, M. M.; Radano, C. P.; Sirringhaus, H.; Smith, P.; Stingelin-Stutzmann, N.

Tough, Semiconducting Polyethylene-poly(3-hexylthiophene) Diblock Copolymers. *Adv. Funct. Mater.* **2007**, *17*, 2674–2679.

(36) Lo, C.-T.; Lin, C.-J.; Lee, J.-Y.; Tung, S.-H.; Tsai, J.-C.; Chen, W.-C. Molecular Stacking Structure and Field-Effect Transistor Characteristics of Crystalline Poly(3-hexylthiophene)-block-Syndiotactic Polypropylene Through Solvent Selectivity. *RSC Adv.* **2014**, *4*, 23002–23009.

(37) Souther, K. D.; Leone, A. K.; Vitek, A. K.; Palermo, E. F.; LaPointe, A. M.; Coates, G. W.; Zimmerman, P. M.; McNeil, A. J. Trials and Tribulations of Designing Multitasking Catalysts for Olefin/Thiophene Block Copolymerizations. *J. Polym. Sci. Part A: Polym. Chem.* **2018**, *56*, 132–137.

(38) (a) Cherian, A. E.; Rose, J. M.; Lobkovsky, E. B.; Coates, G. W. A C_2-Symmetric, Living α-Diimine Ni(II) Catalyst: Regioblock Copolymers from Propylene. *J. Am. Chem. Soc.* **2005**, *127*, 13770–13771. (b) Rose, J. M.; Cherian, A. E.; Coates, G. W. Living Polymerization of α-Olefins with an α-Diimine Ni(II) Catalyst: Formation of Well-Defined Ethylene-Propylene Copolymers through Controlled Chain-Walking. *J. Am. Chem. Soc.* **2006**, *128*, 4186–4187. (c) Rose, J. M.; Deplace, F.; Lynd, N. A.; Wang, Z.; Hotta, A.; Lobkovsky, E. B.; Kramer, E. J.; Coates, G. W. C_2-Symmetric Ni(II) α-Diimines Featuring Cumyl-Derived Ligands: Synthesis of Improved Elastomeric Regioblock Polypropylenes. *Macromolecules* **2008**, *41*, 9548–9555.

(39) Lee, S. R.; Bryan, Z. J.; Wagner, A. M.; McNeil, A. J. Effect of Ligand Electronic Properties on Precatalyst Initiation and Propagation in Ni-Catalyzed Cross-Coupling Polymerizations. *Chem. Sci.* **2012**, *3*, 1562–1566.

(40) Hall, A. O.; Lee, S. R.; Bootsma, A. N.; Bloom, J. W. G.; Wheeler, S. E.; and McNeil, A. J. Reactive Ligand Influence on Initiation in Phenylene Catalyst Transfer Polymerization. *J. Polym. Sci. Part A: Polym. Chem*. **2017**, 1530–1535.

(41) (a) Stathakis, C. I.;Bernhardt, S.; Quint, V.; Knochel, P. Improved Air-Stable Solid Aromatic and Heterocyclic Zinc Reagents by Highly Selective Metalations for Negishi Cross-Couplings. *Angew. Chem. Int. Ed.* **2012**, *51*, 9428–9432. (b) Manolikakes, S. M.; Ellwart, M.; Stathakis, C. I.; Knochel, P. Air-Stable Solid Aryl and Heteroaryl Organozinc Pivalates: Syntheses and Applications in Organic Synthesis. *Chem. Eur. J.* **2014**, *20*, 12289–12297.

(42) Hernán-Gómez, A.; Herd, E.; Hevia, E.; Kennedy, A. R.; Knochel, P.; Koszinowski, K.; Manolikakes, S. M.; Mulvey, R. E.; Schnegelsberg, C. Organozinc Pivalate Reagents: Segregation, Solubility, Stabilization, and Structural Insights. *Angew. Chem. Int. Ed.* **2014**, *53*, 2706–2710.

Chapter 2

Trials and Tribulations of Designing Multitasking Catalysts for Olefin/Thiophene Block Copolymerizations*

INTRODUCTION

Block copolymers have had an outsized impact on materials science, with applications including templating nanostructures[1,2] and thermally stabilizing polymer blends.[3–6] Synthesizing block copolymers is facile when the co-monomers are similar because they can be enchained sequentially in the same flask via the same mechanism (Scheme 2.1A). In contrast, synthesizing block copolymers from dissimilar monomers is significantly more challenging. Most approaches require multiple synthetic and purification steps to isolate the desired copolymer from unreacted polymer precursors.

Scheme 2.1. One-pot approaches for synthesizing block copolymers.

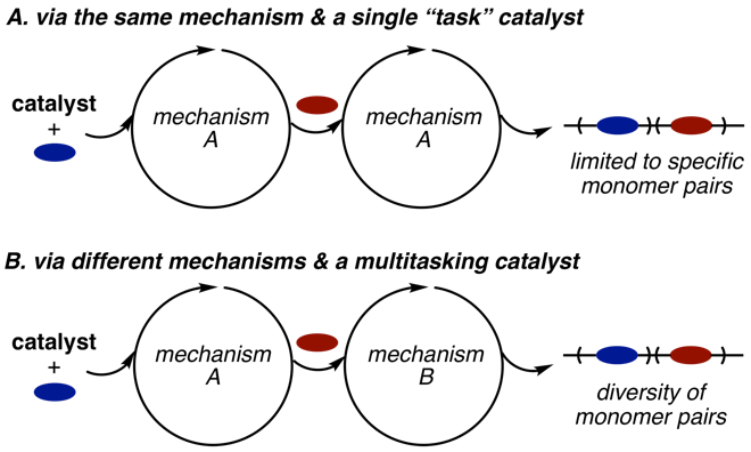

* Reproduced with permission from Souther, K. D.; Leone, A. K.; Vitek, A. K.; Palermo, E. F.; LaPointe, A. M.; Coates, G. W.; Zimmerman, P. M.; McNeil, A. J. Trials and Tribulations of Designing Multitasking Catalysts for Olefin/Thiophene Block Copolymerizations. *J. Polym. Sci. Part A: Polym. Chem.* **2018**, *56*, 132–137.

** A.K.L. identified living, chain-growth conditions for Ni-diimine mediated 3HT polymerization. A.K.V. performed all computations. E.F.P. ran an initial diimine catalyst screen with precatalysts provided by G.W.C. and ran control experiments for Et_2AlCl and THF influence on the copolymerization.

An alternative strategy involves using “switchable catalysts” that rely on an external stimulus to alter their reactivity.[7] This approach requires installing stimuli-responsive functional groups on the catalyst, which usually adds synthetic steps and can generate compatibility issues. Moreover, this method has so far only been demonstrated with monomers enchained via the same mechanism.

Another strategy would be to identify a single “multitasking” catalyst that can mediate sequential, mechanistically distinct polymerizations (Scheme 2.1B). Deming and Novak reported an early example of a multitasking polymerization catalyst in 1991.[8] A single, cationic Ni(II) species was used to sequentially polymerize butadiene via a coordination/insertion mechanism, followed by isocyanide via a coordination/nucleophilic addition mechanism. This work was later extended to other co-monomer pairs using similar Ni precatalysts.[9–19] In each example, the same active catalyst mediates mechanistically distinct polymerizations to generate a block copolymer.

Motivated by these studies, we sought to identify a single multitasking catalyst for copolymerizing olefins with thiophene to generate insulating/conductive block copolymers. Similar materials have been made with multi-step processes.[20] For example, Stingelin-Stutzmann showed that even with only 10 wt% thiophene in the copolymer, the resulting materials exhibited higher charge mobility, strength and flexibility than poly(3-hexylthiophene) (P3HT).[21] Similarly, Chen and co-workers showed that a thiophene/syndiotactic polypropylene block copolymer exhibited higher charge mobilities and air-stability than P3HT alone.[22]

While both Ni and Pd catalysts have been used for poly(olefin) and poly(thiophene) syntheses, we focused on Ni because it out-performs Pd in the latter case.[23] Diimines were selected as the ancillary ligands for our multitasking catalyst based on their wide use in poly(olefin) synthesis,[24–26] with recent applications in conjugated polymer synthesis.[27–31] Both olefin and thiophene enchainment mechanisms involve a Ni(II) intermediate, suggesting that switching from one mechanism to the other may be possible.

We report herein our efforts to synthesize olefin/thiophene block copolymers using Ni-diimine precatalysts. Extensive optimization was needed to identify the appropriate reactive ligands, activator, olefin monomer, and reaction conditions for the copolymerization. Although some block copolymer was isolated, the reaction mixture contained mostly homopolymers, suggesting widespread chain termination and/or chain transfer. This result was traced to a high activation barrier for the "switch" from one mechanism of enchainment to the other, with concomitant chain transfer and/or catalyst dissociation.

EXPERIMENTAL

Activation of 2,5-Dibromo-3-Hexylthiophene (eq 1)

In the glovebox, 2,5-dibromo-3-hexylthiophene (250 mg, 0.768 mmol, 1 equiv.), *n*-docosane (approx. 4 mg), and tetrahydrofuran (THF, 7.40 mL) were added sequentially to a 20 mL vial equipped with a stir bar. To this solution iPrMgCl (268 µL, 0.537 mmol, 2.00 M in THF, 0.7 equiv.) was added. The resulting thiophene Grignard solution was stirred for 30 min at rt and then titrated using salicylaldehyde phenylhydrazone.[32] An aliquot of the Grignard solution (0.3 mL, 0.070 M) was quenched with aq. HCl (0.5 mL, 12 M) outside the glovebox, extracted with $CHCl_3$ (2 mL), dried over $MgSO_4$, and analyzed by gas chromatography (GC) to show a mixture of regioisomers (79:21).

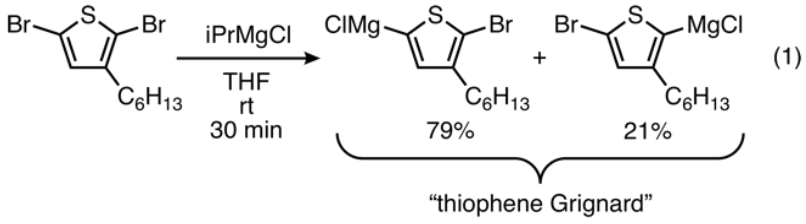

(1)

Copolymerization of 1-Pentene and Thiophene

In the glovebox, precatalyst **C2** (15.7 mg, 0.0177 mmol, 1.0 equiv.) and cold 1-pentene (2.00 mL, kept at −30 °C) were added to a 4 mL vial while stirring. After 2 min, the mixture was filtered through a PTFE syringe filter (0.2 µm) into a 50 mL round-bottom flask equipped with a stir bar. A solution of $B(C_6F_5)_3$ (18.0 mg, 0.0354 mmol, 2.0

equiv.) in cold 1-pentene (1 mL) was added and the reaction stirred for 20 s. Then, THF (5.0 mL) and toluene (3.0 mL) were added. The flask was then held under reduced pressure for 30 min (until ~2 mL solvent remained). An aliquot (0.50 mL) of the remaining solution was added to a J-Young tube and analyzed by ^{1}H NMR spectroscopy before quenching with MeOH (2 mL) and concentrating *in vacuo*. The residue was redissolved in THF (1.5 mL), passed through a PTFE syringe filter (0.2 μm), and analyzed by gel permeation chromatography (GPC) to estimate the macroinitiator molecular weight. THF (8.0 mL) and thiophene Grignard (4.0 mL) were added to the remaining macroinitiator solution. After 2 h, the reaction was quenched with aq. HCl (10 mL, 12 M). The resulting polymer was extracted with $CHCl_3$ (2 × 15 mL), dried over $MgSO_4$, and filtered using a Buchner funnel. An aliquot (0.5 mL) of this solution was split into two equal portions. The first portion was diluted with $CHCl_3$ (2.0 mL) and analyzed by GC to determine the thiophene conversion. The second portion was concentrated *in vacuo* and then redissolved in THF/toluene (99:1; 1.5 mL) with mild heating, passed through a PTFE filter, and analyzed by GPC. After analysis, both portions were recombined with the mother liquor and the solvent was removed *in vacuo*, yielding a maroon solid (25 mg).

Block Copolymer Purification

The maroon solid was dissolved in $CHCl_3$ (0.5 mL) and precipitated with MeOH (15.0 mL). The mixture was spun in a centrifuge for 10 min. The supernatant was decanted and saved. The precipitate was dried under reduced pressure, yielding 15 mg of polymer. ^{1}H NMR spectroscopic analysis revealed that this solid resembled P3HT homopolymer. The supernatant was concentrated under reduced pressure to generate a purple solid (10 mg). MeOH (10 mL) was added followed by sonication for 1 min. The resulting mixture was spun in the centrifuge for 10 min, and then the supernatant was removed and saved. This process was repeated three times. Hexanes (10 mL) was added to the remaining solid, followed by centrifugation (10 min). The resulting yellow supernatant was collected, passed through a PTFE syringe filter (0.2 μm), and concentrated in vacuo to yield a solid (4 mg). ^{1}H NMR spectroscopic analysis revealed

that the solid contained a mixture of the desired copolymer and poly(1-pentene) homopolymer.

Computational Details

Quantum chemical simulations were performed on key reaction steps, with pathways and transition states optimized using the growing string method.[33–35] Reported energies come from the ωB97X-D density functional[36] using the triple-zeta, polarized cc-pVTZ basis set,[37] and the SMD solvation model[38] with THF as the solvent.

RESULTS AND DISCUSSION

Identifying Reactive Ligands

We initially selected Ni precatalyst **C1** (Chart 2.1), which was chosen based on its reported living, chain-growth olefin polymerization behavior[39–43] as well as its ability to synthesize P3HT with a targeted number-average molecular weight (M_n) and moderate dispersity (Đ).[44,45] Due to the high sensitivity of the olefin polymerization to coordinating substrates, including thiophene and THF, we synthesized the polyolefin block first, followed by polythiophene.

Chart 2.1 Precatalyst Structures

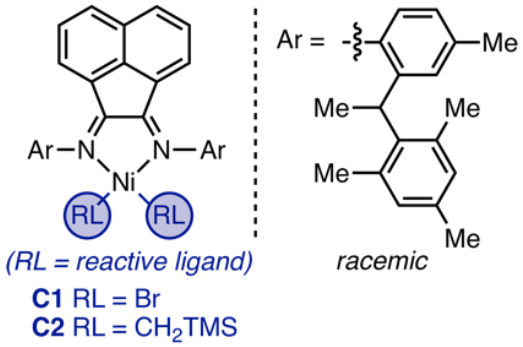

To initiate thiophene polymerization, the two reactive ligands in **C1** (i.e., Br) are displaced via two sequential transmetalations with thiophene Grignard, followed by reductive elimination to generate bithiophene. In contrast, to initiate olefin polymerization, an alkyl aluminum reagent (e.g., Et_2AlCl) is needed to perform the sequential transmetalations followed by alkyl group abstraction to generate a cationic

catalyst. We hypothesized that the residual Et_2AlCl and generated alkyl aluminum species may interfere with the thiophene polymerization. Indeed, no P3HT was formed when Et_2AlCl was added to the standard thiophene polymerization conditions (Figure S1.6). Most likely, the Grignard and aluminum reagents formed a less reactive mixed aggregate.[46,47] To avoid using an aluminum activator, the Br reactive ligands in precatalyst **C1** were replaced with trimethylsilylmethylene ("$TMSCH_2$") to yield precatalyst **C2** (Chart 2.1).[44]

Selecting a Cocatalyst

We next sought to identify a co-catalyst that could generate a cationic Ni(II) species by abstracting one $TMSCH_2$ from precatalyst **C2**. Triarylboranes were evaluated based on their known ability to act as a co-catalyst for poly(olefin) synthesis[48] and their anticipated lack of reactivity with Grignard reagents. Indeed, PH3T synthesis was unaffected by the presence of tris(pentafluorophenyl)borane ($B(C_6F_5)_3$) (eq 2, Figure S1.10). Note that, in this case, initiation involves thiophene transmetalation with a cationic Ni(II) intermediate; computational studies revealed a low activation barrier (10.2 kcal/mol) for this step (Figure S1.26b).

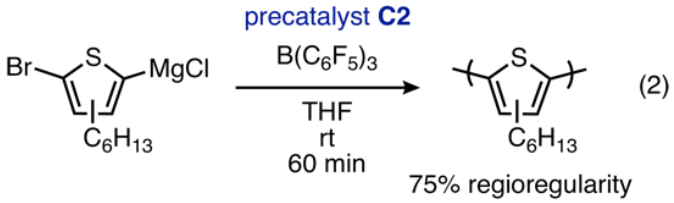

(2)

In addition, this precatalyst/co-catalyst combination led to poly(1-hexene) with narrow dispersities and molecular weights that tracked linearly with time, suggesting a living, chain-growth polymerization (Figure S1.9). The olefin polymerization mechanism involves predominantly 1,2-insertion, followed by chain-walking to generate mostly linear polyolefin (eq 3, Figure S1.8). Under these conditions, however, neat olefin was necessary because borane-activated catalysts have lower reactivity than aluminum-activated catalysts.

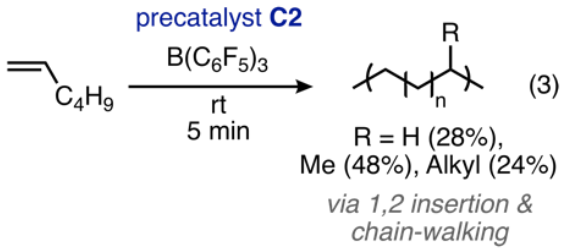

First Copolymerization

Olefin enchainment begins when the borane co-catalyst is added to a solution containing precatalyst **C2** and 1-hexene (eq 4). After a few minutes, an aliquot of THF is added to stall the polymerization and to target a lower molecular weight macroinitiator. THF should bind to the open coordination site on Ni(II), inhibiting further olefin binding and insertion. Indeed, a control experiment confirmed that adding THF prevents further olefin incorporation (Figure S1.12). The thiophene monomer was subsequently added to the reaction mixture and the polymerization continued for 60 min.

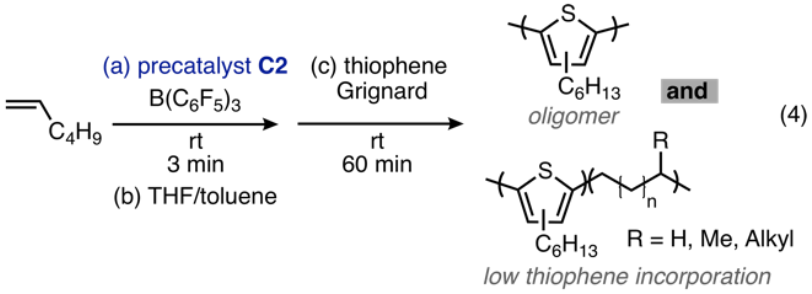

Gel permeation chromatography (GPC) was used to monitor block copolymer formation (Fig. 2.1(A)). Almost no change in number-average molecular weight of the macroinitiator was observed, suggesting minimal thiophene addition into the chains. Nevertheless, the UV and RI traces exhibit similar peak shapes, suggesting that some thiophene units were incorporated. In addition, a new polymer peak with a lower molecular weight was observed, which is consistent with shorter thiophene homopolymers. Thiophene conversion in the block copolymerization was significantly lower than observed in thiophene homopolymerization (cf., 11% vs. 70%), suggesting that not all catalysts were actively enchaining monomer. Combined, these results suggest low thiophene incorporation in the block copolymer with a subsequent chain-

transfer or chain-termination event releasing catalysts capable of synthesizing P3HT, albeit slowly.

To understand these results, we considered the differences between the copolymerization and thiophene homopolymerization. The most significant change is the presence of unreacted olefin during the copolymerization. Based on this observation, we suspected that olefin competitively displaces the polymer from Ni(0).[49] This hypothesis is based on studies by McCullough and coworkers[50,51] and Pickel and coworkers,[52] where added olefin attenuated catalyst reactivity during P3HT synthesis. To probe this hypothesis, the relative binding energies for 1-hexene and thiophene to diimine-ligated Ni(0) were calculated and found to be similar ($\Delta G = 0.6$ kcal/mol; eq 5), suggesting that olefin can displace the copolymer from Ni(0) under the reaction conditions. This hypothesis is further supported by our data showing that even 1 equiv. of 1-hexene (relative to thiophene Grignard) inhibits thiophene homopolymerization with precatalyst **C2** [Figure 2.1(B)]

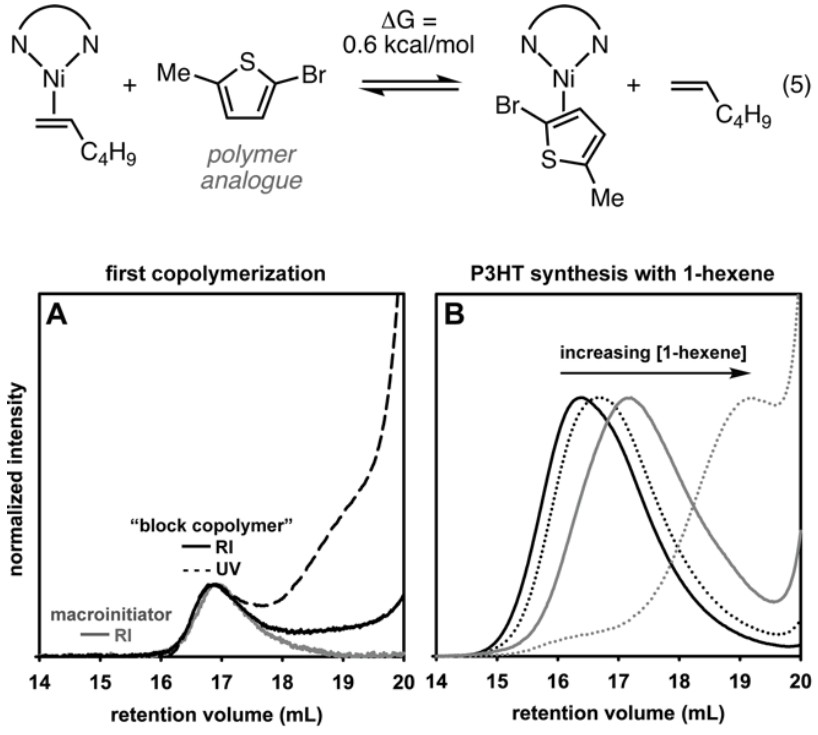

Figure 2.1 Gel permeation chromatograms for (A) 1-hexene and thiophene Grignard copolymerization, and (B) thiophene homopolymerization in the presence of 1-hexene.

To overcome olefin inhibition, we replaced 1-hexene (bp = 63 °C) with the more volatile 1-pentene (bp = 30 °C). As a consequence, the olefin can be removed prior to adding thiophene Grignard (Figure S1.15), preventing competitive displacement on Ni(0).

Second Copolymerization

An apparent, significant chain extension was observed when the copolymerization was performed with 1-pentene [eq 6 and Figure 2.2(A)]. This result suggests that the desired block copolymer was formed. However, the ^{1}H NMR spectrum of the crude reaction mixture (by precipitation in $CHCl_3$/MeOH) suggested the major product was P3HT homopolymer (Figure S1.18). After removing the P3HT and unreacted monomer, a mixture of poly(olefin) and apparent block copolymer was isolated (Figure S1.20).

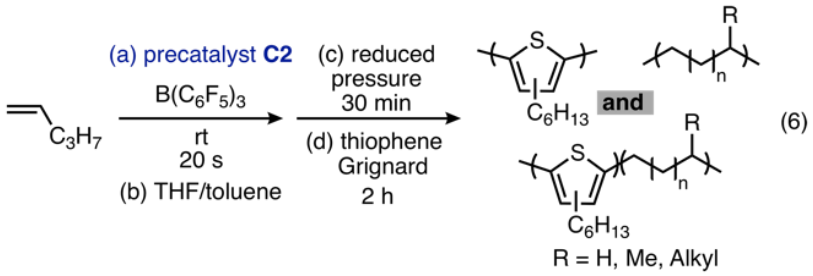

(6)

Identifying whether or not block copolymer was synthesized was difficult due to overlapping NMR signals from the CH_2 moieties on the hexyl side chain on thiophene and poly(olefin). Nevertheless, comparing the ^{1}H NMR spectra of independently synthesized homopolymers (P3HT and poly(olefin)) versus the copolymer mixture revealed two new resonances at 2.92 and 3.04 ppm [Figure 2.2(B)]. These resonances were tentatively assigned to hydrogens on the poly(olefin) carbon directly attached to the first thiophene unit. Further evidence was provided by their NOE correlations with the aromatic–^{1}H resonances from poly(thiophene) (7.0–7.1 ppm) via ^{1}H/^{1}H NOESY (Figure S1.21). Combined, these data suggest successful copolymer formation.

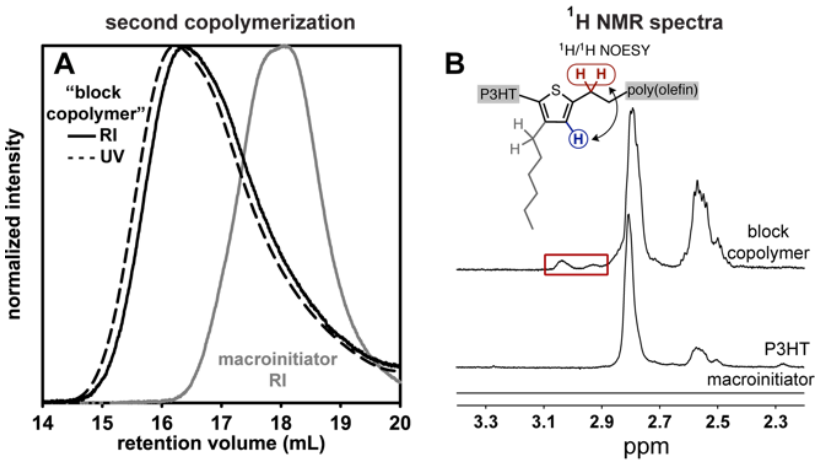

Figure 2.2 (A) Gel permeation chromatograms for 1-pentene and thiophene Grignard copolymerization. (B) ^{1}H NMR spectral comparison of the macroinitiator, P3HT, and the isolated block copolymer.

Obtaining some block copolymer (albeit in low quantities) demonstrates that this multitasking catalyst does sequentially polymerize two dissimilar monomers via distinct mechanisms. To increase the yield, an understanding of the unproductive pathways is needed.

Identifying the Problematic Step(s)

To understand the origin(s) of the unproductive pathways, we considered the key intermediate between the two mechanistically distinct polymerizations. For the catalyst to switch enchainment mechanisms, a reductive elimination must occur between poly(olefin) (Csp^3) and a thiophene monomer (Csp^2) (Scheme 2.2).

Scheme 2.2 Comparison of reductive elimination barriers.

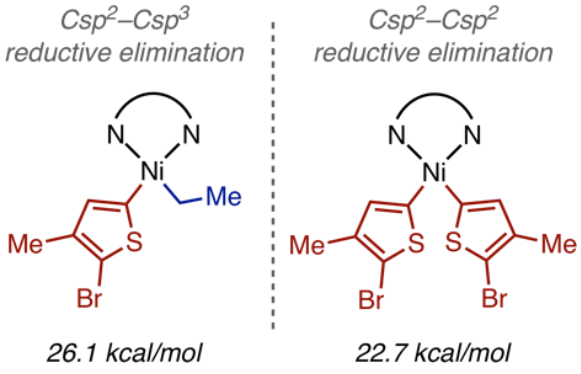

To provide insight into this step, DFT computations were used to assess the relative rates of Csp^2–Csp^3 and Csp^2–Csp^2 reductive eliminations. These computations found that the barrier for the Csp^3–Csp^2 elimination was 3.4 kcal/mol higher, and the reaction would therefore be approximately 300 times slower than bis-thiophene reductive elimination [Figure S1.26(c)]. To probe the Csp^3–Csp^2 elimination experimentally, we synthesized a neutral precatalyst (**C3**) containing both a $TMSCH_2$ and Br reactive ligand. After transmetalation with thiophene Grignard, a Csp^2–Csp^3 reductive elimination should occur. Indeed, P3HT was observed with precatalyst **C3** (eq 7). Nevertheless, the isolated polymer exhibited a higher number-average molecular weight than expected based on the initial monomer/precatalyst ratio (Figure S1.25),[53] suggesting that not all catalysts are active. To determine whether the precatalyst initiation proceeded through the proposed Csp^2–Csp^3 reductive elimination, polymer end-groups were analyzed via MALDI-TOF-MS. The data showed negligible $TMSCH_2$ incorporation (Figure S1.24), suggesting that initiation proceeds either by the proposed reductive elimination followed by dissociation from the chain, or by disproportionation to generate Ni(0) and Ni(II), both of which are active for P3HT synthesis.

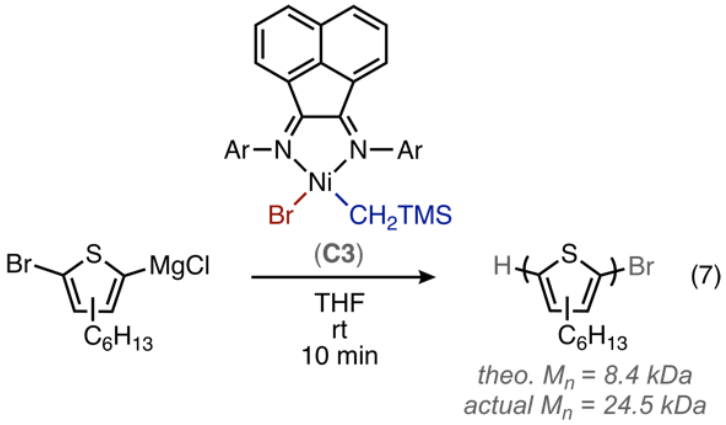

(7)

We suspect dissociation might be occurring based on our concurrent work with precatalyst **C1**,[45] where we observe some catalyst dissociation. In this case, however, the catalyst preferentially re-inserts into polymer chains rather than the monomer. This result was attributed to a statistical effect, where the polymer chain outcompetes the monomer for Ni(0) based on the greater number of π-binding sites. In contrast, in the

block copolymerization described herein, catalyst re-association into a polymer is less likely to occur because the polymer chains are predominantly poly(olefin), which have no π-binding sites. Therefore, we suspect that the macroinitiator undergoes initiation followed by some propagation and ultimately dissociation. Subsequent insertion into a thiophene monomer leads to P3HT homopolymers. In addition, we believe that only a small percentage of catalysts are active at any time due to the slow Csp^2–Csp^3 reductive elimination.

CONCLUSIONS

Combined, these studies highlight the challenges associated with identifying multitasking catalysts that can enchain different monomers via distinct mechanisms in the same pot. Even though both homopolymerizations were optimized under identical conditions, their combination in the same pot led to unanticipated challenges. Specifically, the diimine-ligated Ni precatalyst studied herein suffered from slow "switching" between the mechanisms, and from catalyst dissociation, resulting in a mixture of poly(olefin), P3HT, and block copolymer. However, our systematic investigation into the elementary steps of this polymerization provides fundamental insight that should be leveraged when designing new multitasking catalyst systems.

References

(1) Schacher, F. H.; Rupar, P. A.; Manners, I. Functional Block Copolymers: Nanostructured Materials with Emerging Applications. *Angew. Chem. Int. Ed.* **2012**, 51, 7898–7921.

(2) Mai, Y.; Eisenberg, A. Self-assembly of Block Copolymers. *Chem. Soc. Rev.* **2012**, 41, 5969–5985.

(3) Kipp, D.; Verduzco, R.; Ganesan, V. Block Copolymer Compatibilizers for Ternary Blend Polymer Bulk Heterojunction Solar Cells – An Opportunity for Computation Aided Molecular Design. *Mol. Syst. Des. Eng.* **2016**, *1*, 353–369.

(4) Zhu, M.; Kim, H.; Jang, Y. J.; Park, S.; Ryu, D. Y.; Kim, K.; Tang, P.; Qiu, F.; Kim, D. H.; Peng, J. Toward High Efficiency Organic Photovoltaic Devices with Enhanced Thermal Stability Utilizing P3HT-b-P3PHT Block Copolymer Additives. *J. Mater. Chem. A.* **2016**, *4*, 18432–18443.

(5) Lee, J. U.; Jung, J. W.; Emrick, T.; Russell, T. P.; Jo, W. H. Morphology Control of a Polythiophene-Fullerene Bulk Heterojunction for Enhancement of the High-Temperature Stability of Solar Cell Performance by a New Donor-Acceptor Diblock Copolymer. *Nanotechnology* **2010**, *21*, 105201–105209.

(6) Sivula, K.; Ball, Z. T.; Watanabe, N.; Fréchet, J. M. J. Amphiphilic Diblock Copolymer Compatibilizers and Their Effect on the Morphology and Performance of Polythiophene:Fullerene Solar Cells. *Adv. Mater.* **2006**, *18*, 206–210.

(7) Teator, A. J.; Lastovickova, D. N.; Bielawski, C. W. Switchable Polymerization Catalysts. *Chem. Rev.* **2016**, *116*, 1969–1992.

(8) Deming, T. J.; Noavk, B. M. "Change of Mechanism" Block Copolymerizations: Formation of Block Copolymers Containing Helical Polyisocyanide and Elastomeric Polybutadiene Segments. *Macromolecules* **1991**, *24*, 5478–5480.

(9) Deming, T. J.; Novak, B. M.; Ziller, J. W. Living Polymerization of Butadiene at Both Chain Ends via a Bimetallic Nickel Initiator. Preparation of Hydroxytelechelic Poly(butadiene) and Symmetric Poly(isocyanide-b-butadiene-b-isocyanide) Elastomeric Triblock Copolymers. *J. Am. Chem. Soc.* **1994**, *116*, 2366–2374.

(10) Tomita, I.; Taguchi, K.; Takagi, K.; Endo, T. Block Copolymerization of Allene Derivatives with Isocyanides by the Coordination Polymerization with π-allyl Nickel Catalyst. *J. Polym. Sci. Part A; Polym. Chem.* **1997**, *35*, 431–437.

(11) Taguchi, M.; Tomita, I.; Yoshida, Y.; Endo, T. Block Copolymerization of Allene Derivatives with 1,3-butadiene by Living Coordination Polymerization with π-allyl Nickel Catalyst *J. Polym. Sci. Part A: Polym. Chem.* **1999**, *37*, 3916–3921.

(12) Zhu, Y.-Y.; Yin, T.-T.; Yin, J.; Liu, N.; Yu, Z.-P.; Zhu, Y.-W.; Ding, Y.-S.; Yin, J.; Wu, Z.-Q. Poly(3-hexylthiophene)-*block*-poly(5,8-di-*p*-tolylquinoxaline-2,3-diyl) Conjugated

Rod-Rod Copolymers: One Pot Synthesis, Self-assembly and Highly Selective Sensing of Cobalt. *RSC Adv.* **2014**, *4*, 40241–40250.

(13) Ono, R. J.; Todd, A. D.; Hu, Z.; Vanden Bout, D. H.; Bielawski, C. W. Synthesis of a Donor-Acceptor Diblock Copolymer via Two Mechanistically Distinct, Sequential Polymerizations Using a Single Catalyst. *Macromol. Rapid Commun.* **2014**, *35*, 204–209.

(14) Wu, Z.-Q.; Qi, C.-G.; Liu, N.; Wang, Y.; Jin, Y.; Zhu, Y.-Y.; Qiu, L.-Z.; Lu, H.-B. One-pot Synthesis of Conjugated Poly(3-hexylthiophene)-*b*-poly(phenyl isocyanide) Hybrid Rod-Rod Block Copolymers and its Self-assembling Properties. *J. Polym. Sci. Part A: Polym. Chem.* **2013**, *51*, 2939–2947.

(15) Wu, Z.-Q.; Liu, D.-F,; Wang, Y.; Liu, N.; Yin, J.; Zhu, Y.-Y.; Qiu, L.-Z.; Ding, Y.-S. One Pot Synthesis of a Poly(3-hexylthiophene)-**b**-oly(quinoxaline-2,3-diyl) Rod-Rod Diblock Copolymer and its Tunable Light Emission Properties. *Polym. Chem.* **2013**, *4*, 4588–4595.

(16) Liu, N.; Qi, C.-G.; Wang, Y.; Liu, D.-F.; Yin, J.; Zhu, Y.-Y.; Wu, Z.-Q. Solvent-Induced White-Light Emission of Amphiphilic Rod-Rod Poly(3-triethylene glycol thiophene)-*block*-poly(phenyl isocyanide) Copolymer. *Macromolecules* **2013**, *46*, 7753–7758.

(17) Wu, Z.-Q.; Radcliffe, J. D.; Ono, R. J.; Chen, Z.; Li, Z.; Bielawski, C. W. Synthesis of Conjugated Diblock Copolymers: Two Mechanistically Distinct, Sequential Living Polymerizations using a Single Catalyst. *Polym. Chem.* **2012**, *3*, 874–881.

(18) Wu, Z.-Q.; Ono, R. J.; Chen, Z.; Bielawski, C. W. Synthesis of Poly(3-alkylthiophene)-block-poly(arylisocyanide): Two Sequential, Mechanistically Distinct Polymerizations Using a Single Catalyst. *J. Am. Chem. Soc.* **2010**, *132*, 14000–14001.

(19) Wu, Z.-Q; Chen. Y.; Wang, Y.; He, X.-Y.; Ding, Y.-S.; Liu, N. One Pot Synthesis of Poly(3-hexylthiophene)-block-poly(hexadecyloxylallene) by Sequential Monomer Addition. *Chem. Commun.* **2013**, *49*, 8069–8071.

(20) For examples see: (a) Moon, H. C.; Anthonysamy, A.; Lee, Y.; Kim, J. K. Facile Synthesis of Well-Defined Coil−Rod−Coil Block Copolymer Composed of Regioregular Poly(3-hexylthiophene) via Anionic Coupling Reaction. *Macromolecules* **2010**, *43*, 1747–1752. (b) Radano, C. P.; Scherman, O. A.; Stingelin-Stutzmann, N.; Muller, C.; Breiby, D. W.; Smith, P.; Janssem, R. A. J.; Meijer, E. W. Crystalline-Crystalline Block Copolymers of Regioregular Poly(3-hexylthiophene) and Polyethylene by Ring-Opening Metathesis Polymerization. *J. Am. Chem. Soc.* **2005**, *127*, 12502–12503.

(21) Müller, C.; Goffri, S.; Breiby, D. W.; Andreasen, J. W.; Chanzy, H. D.; Janssen, R. A. J.; Nielsen, M. M.; Radano, C. P.; Sirringhaus, H.; Smith, P.; Stingelin-Stutzmann, N. Tough, Semiconducting Polyethylene-poly(3-hexylthiophene) Diblock Copolymers. *Adv. Funct. Mater.* **2007**, *17*, 2674–2679.

(22) Lo, C.-T.; Lin, C.-J.; Lee, J.-Y.; Tung, S.-H.; Tsai, J.-C.; Chen, W.-C. Molecular Stacking Structure and Field-effect Transistor Characteristics of Crystalline Poly(3-hexylthiophene)-block-syndiotactic polypropylene Through Solvent Selectivity. *Rsc. Adv.* **2014**, *4*, 23002–23009.

(23) Leone, A. K.; McNeil, A. J. Matchmaking in Catalyst-Transfer Polycondensation: Optimizing Catalysts based on Mechanistic Insight. *Acc. Chem. Res.* **2016**, *49*, 2822–2831.

(24) Guan, Z.; Popeney, C. S. Recent Progress in Late Transition Metal α-Diimine Catalysts for Olefin Polymerization. *Top. Organomet. Chem.* **2009**, *26*, 179–220.

(25) Baier, M. C.; Zuideveld, M. A.; Mecking, S. Post-Metallocenes in the Industrial Production of Polyolefins. *Angew. Chem. Int. Ed.* **2014**, *53*, 9722–9744.

(26) Guo, L.; Dai, S.; Sui, X.; Chen, C. Palladium and Nickel Catalyzed Chain Walking Olefin Polymerization and Copolymerization. *ACS Catal.* **2016**, *6*, 428–441.

(27) Magurudeniya, H. D.; Sista, P.; Westbrook, J. K.; Ourso, T. E.; Nguyen, K.; Maher, M. C.; Alemseghed, M. G.; Biewer, M. C.; Stefan, M. C. Nickel(II) α-Diimine Catalyst for Grignard Metathesis (GRIM) Polymerization. *Macromol. Rapid Commun*. **2011**, *32*, 1748–1752.

(28) Pollit, A. A.; Obhi, N. K.; Lough, A. J.; Seferos, D. S. Evaluation of an External Initiating Ni(II) Diimine Catalyst for Electron-deficient π-conjugated Polymers. *Polym. Chem.* **2017**, *8*, 4108–4113.

(29) Bridges, C. R.; Yan, H.; Pollit, A. A.; Seferos, D. S. Controlled Synthesis of Fully π-Conjugated Donor-Acceptor Block Copolymers Using a Ni(II) Diimine Catalyst. *ACS. Macro Lett.* **2014**, *3*, 671–674.

(30) Bridges, C. R.; McCormick, T. M.; Gibson, G. L.; Hollinger, J.; Seferos, D. S. Designing and Refining Ni(II)diimine Catalysts Toward the Controlled Synthesis of Electron-Deficient Conjugated Polymers. *J. Am. Chem. Soc.* **2013**, *135*, 13212–13219

(31) Pollit, A. A.; Bridges, C. R.; Seferos, D. S. Evidence for the Chain-Growth Synthesis of Statistical π-Conjugated Donor-Acceptor Copolymers. *Macromol. Rapid. Commun.* **2015**, *36*, 65–70.

(32) Love, B. E.; Jones, E. G. The Use of Salicylaldehyde Phenylhydrazone as an indicator for the Titration of Organometallic Reagents. *J. Org. Chem.* **1999**, *64*, 3755–3756.

(33) Zimmerman, P. M. Growing String method with Interpolation and Optimization in Internal Coordinates: Method and Examples. *J. Chem. Phys.* **2013**, *138*, 184102-1–184102-10.

(34) Zimmerman, P. M. Reliable Transition State Searches Integrated with the Growing String Method. *J. Chem. Theory Comput.* **2013**, *9*, 3043–3050.

(35) Zimmerman, P. M. Single-ended Transition State Finding with the Growing String Method. *J. Comput. Chem.*, **2015**, *36*, 601–611.

(36) Chai, J. D.; Head-Gordon, M. Long-range Corrected Hybrid Density Cunctionals with Damped Atom-Atom Dispersion Corrections. *Phys. Chem. Chem. Phys.* **2008**, *10*, 6615–6620.

(37) Dunning Jr., T. H. Gaussian Basis Sets for use in Correlated Molecular Calculations. 1. The Atoms Boron through Neon and Hydrogen. *J. Chem. Phys.* **1989**, *90*, 1007–1023.

(38) Marenich, A. V.; Cramer, C. J.; Truhlar, D. G. Universal Solvation Model Based on Solute Electron Density and on a Continuum Model of the Solvent Defined by the Bulk Dielectric Constant and Atomic Surface Tensions. *J. Phys. Chem. B* **2009**, *113*, 6378–6396.

(39) Cherian, A. E.; Rose, J. M.; Lobkovsky, E. B.; Coates, G. W. A C_2-Symmetric, Living α-Diimine Ni(II) Catalyst: Regioblock Copolymers from Propylene. *J. Am. Chem. Soc.* **2005**, *127*, 13770–13771.

(40) Rose, J. M.; Cherian, A. E.; Coates, G. W. Living Polymerization of α-Olefins with an α-Diimine Ni(II) Catalyst: Formation of Well-Defined Ethylene-Propylene Copolymers through Controlled Chain-Walking. *J. Am. Chem. Soc.* **2006**, *128*, 4186–4187.

(41) Rose, J. M.; Deplace, F.; Lynd, N. A.; Wang, Z.; Hotta, A.; Lobkovsky, E. B.; Kramer, E. J.; Coates, G. W. C_2-Symmetric Ni(II) α-Diimines Featuring Cumyl-Derived Ligands: Synthesis of Improved Elastomeric Regioblock Polypropylenes. *Macromolecules* **2008**, *41*, 9548–9555.

(42) Ruiz-Orta, C.; Fernandez-Blazquez, J. P.; Anderson-Wile, A. M.; Coates, G. W.; Alamo, R. G. Isotactic Polypropylene with (3,1) Chain-Walking Defects: Characterization, Crystallization, and Melting Behaviors. *Macromolecules* **2011**, *44*, 3436–3451.

(43) The racemic (RS, SR) ligand generates a C_2-symmetric Ni catalyst that predominantly gives ω,2-enchainment with 1-hexene, resulting in amorphous ethylene-propylene copolymers.

(44) Precatalyst geometries not specified in Chart 1. Precatalyst C1 is tetrahedral (as evidence by a single-crystal X-ray structure, see ref. 39). Precatalyst C2 is expected to be square planar based on a related diimine$Ni(CH_2TMS)_2$ crystal structure (for ref, see Schleis, T.; Spaniol, T.P.; Okuda, J.; Heinemann, J.; Mülhaupt, R. Ethylene Polymerization Catalysts based on Nickel(II) 1,4-Diazadiene Complexes: The Influence of the 1,4-Diazadiene Backbone Substituents on Structure and Reactivity. *J. Organomet. Chem.* **1998**, *569*, 159–167). Moreover, the ^{1}H NMR spectrum of precatalyst **C1** displays peak shape/positions consistent with a paramagnetic complex (Figure S1.3), while precatalyst **C2** displays peak shape/positions consistent with a diamagnetic complex (Figure S1.4).

(45) Leone, A. K.; Souther, K. D.; Vitek, A. K.; LaPointe, A. M.; Coates, G. W.; Zimmerman, P. M.; McNeil, A. J. Mechanistic Insight into Thiophene Catalyst-Transfer Polymerization Mediated by Nickel Diimine Catalysts. *Macromolecules* **2017**, *50*, 9121–9127.

(46) Michel, O.; Meermann, C.; Törnoos, K. W.; Anwander, R. Alkaline-Earth Metal Alkylaluminate Chemistry Revisited. *Organometallics* **2009**, *28*, 4783–4790.

(47) An alternative explanation is that a mixed aggregate undergoes 1,2-addition into the diimine, altering catalyst reactivity. For ref, see: Michel, O.; Yamamoto, K.; Tsurugi, H.; Maichle-Mössmer, C.; Törnroos, K. W.; Mashima, K.; Anwander, R. Reactivity of Permethylated Magnesium Complexes toward β-Diimines. *Organometallics* **2011**, *30*, 3818–3825.

(48) Chen, E. Y.-X.; Marks, T. J. Cocatalysts for Metal-Catalyzed Olefin Polymerization: Activators, Activation Processes, and Structure-Activity Relationships. *Chem. Rev.* **2000**, *100*, 1391–1434.

Chapter 3

Bis(pyrrolidinylphosphino)ethane Ni Mediated Catalyst-Transfer Polymerization

Introduction

The 2004 discovery of a living, chain-growth method for conjugated polymer synthesis, catalyst-transfer polymerization[1] (CTP), has enabled access to many materials for use in the active layer of organic electronics (e. g., solar cells, transistors, and light-emitting diodes).[2,3,4,5,6] Since this advent, McNeil and coworkers elucidated the mechanism of bis(aryl/alkylphosphino)-,[7,8,9] and diimine-ligated[10] nickel catalysts in CTP. In CTP, a precatalyst must first undergo initiation, yielding a metal-π complex that persists as an intermediate throughout propagation (Scheme 3.1). It has been hypothesized that the stability and reactivity of this complex dictates CTP behavior, ensuring that intramolecular oxidative addition occurs after the catalyst ring walks to the terminal Ar–Br bond. The stability of this complex can be directly correlated to the σ-donating (bonding) and π-accepting properties of the ancillary ligand which influence metal backbonding interactions into the antibonding π-orbitals of the arene monomer.

McNeil and coworkers have specifically looked at σ-donating properties of bisphosphine ligands and hypothesized that electron-rich phosphines would yield a stable π-complex as well as induce faster intramolecular oxidative addition. This hypothesis was explored via small molecule competition experiments in which product ratios of *intra*molecular versus *inter*molecular oxidative addition into a biaryl complex generated in situ were measured.[11] All four electron-rich ligands screened (diphenylphosphinoethane (dppe), triphenylphosphine, diethylphosphinoethane (depe), and diparamethoxyphenylphosphinoethane) yielded the major intramolecular oxidative addition product, suggesting that the metal-π complex was forming. An additional experiment showed that the most electron-rich ligand (depe), had

the fastest relative rates of intramolecular oxidative addition. These results supported their hypothesis that more σ-donating ligands stabilize the metal π-complex as well as increase rates of intramolecular oxidative addition. The CTP literature has thus focused on varying steric and electronic properties of metal-ligand pairs to achieve the aforementioned polymer properties and access new conjugated polymers.[12,13,14]

Scheme 3.1 Catalytic cycle for CTP.

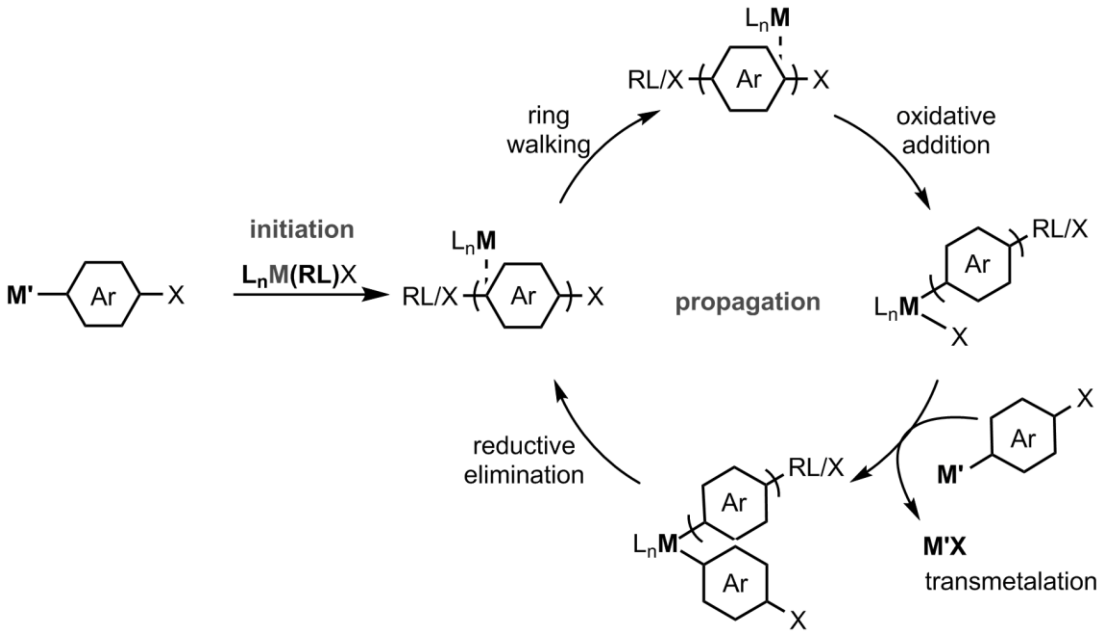

McNeil and coworkers have also hypothesized that varying σ-donating properties of bisphosphine ligands in polymerizations would enhance the metal's binding affinity to the polymer as well as increase intramolecular oxidative addition rate, yielding better CTP behavior. Evidence for improved CTP behavior in a polymerization can be supported through accessing polymers with narrow dispersities (Đ) as well as exclusive end-group incorporation (analyzed using Matrix-Assisted Laser Desorption/Ionization-Time of Flight/Mass Spectrometry (MALDI-TOF/MS)). In 2011, McNeil and coworkers screened three electron-donating ligands complexed with Ni for CTP (Chart 3.1), and found that ($Ni(depe)Cl_2$) yielded polymers with narrower dispersities and complete end-group control for poly(phenylene), poly(thiophene), and poly(pyrrole) compared to the more common bisphosphine CTP catalysts $Ni(dppe)Cl_2$ and $Ni(dppp)Cl_2$, with complete end-group fidelity.

Chart 3.1 Selected bisphosphine ligands explored in CTP

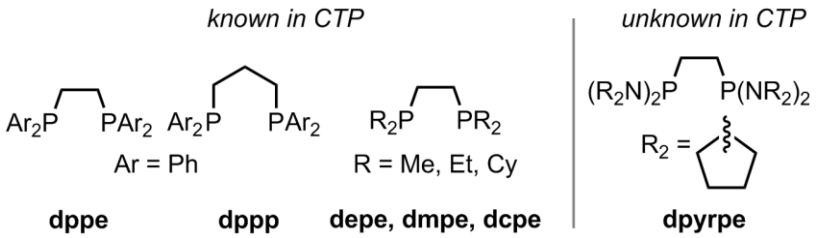

However, metal-π complex formation in CTP is dependent on σ-donating and π-accepting properties of the ligand, as well as monomer identity. Motivated by McNeil's work, we sought to explore the scope of electron-donating ligands in Ni-catalyzed CTP. Infrared spectroscopy can be used to measure electron-donating abilities of ligands by measuring CO stretching frequencies in ligand–metal–CO complexes; an electron-donating ligand lengthens and weakens the CO bond, leading to a smaller CO frequency. A bis(pyrrolidinylphosphino)ethane (dpyrpe) ligand was recently reported to yield similar (Chart 3.1) wavenumbers to dppe when ligated to a metal-CO complex (1960 cm^{-1} vs 1961 cm^{-1} respectively).[16] This result suggests that dpyrpe-ligated Ni catalysts would most likely yield polymers with similar CTP properties to dppe-ligated Ni catalysts, leading us to consider the π-acceptor character of dpyrpe.

Work by Michalak and coworkers measured differences in orbital energies of a variety of substituted phosphines and found that while alkyl and alkoxy substituted phosphines had similar sigma donating strength; alkoxy substituted phosphines were better π-acceptors, represented by a smaller energy difference between orbitals.[17] Overall, phosphines substituted with more electronegative atoms were better π-acceptors. While amino-substituted phosphines were not measured directly in the above work, the small increase in electronegativity from carbon to nitrogen suggests that nitrogen-based phosphino ligands should be better π-acceptors. We hypothesized that dpypre's π-acidity coupled with its σ-donating abilities may show improved CTP polymerization behavior compared to carbon-based bisphosphines. Herein, we report a dpyrpe–ligated Ni precatalyst for CTP that yields poly(3-hexylthiophene) (**P3HT**) with better dispersity and comparable end-groups compared to a dppe-ligated Ni precatalyst. We also expanded monomer scope for this catalyst to include an electron-deficient

hexylesterthiophene (**3HET**). While we sought to expand monomer scope of this precatalyst to 2,5-bishexyloxyphenylene (**BHP**), the polymerization was marred by slow initiation and the presence of multiple catalytic species.

Precatalyst synthesis

Ligand exchange between dpyrpe (synthesized in 1 step with 76% yield) and dimethoxyethylene glycol (DME) from $Ni(DME)Br_2$ in DCM at rt overnight yielded **C1** (44% yield) (Scheme 3.2). Ligand exchange between the *trans*-triphenylphosphine ligands on nickel precursor (1) (synthesized in 1 step with 65% crude yield) and dpyrpre at rt for 90 min in THF yielded **C2** (54% yield).

Scheme 3.2 C1 and **C2** synthesis.

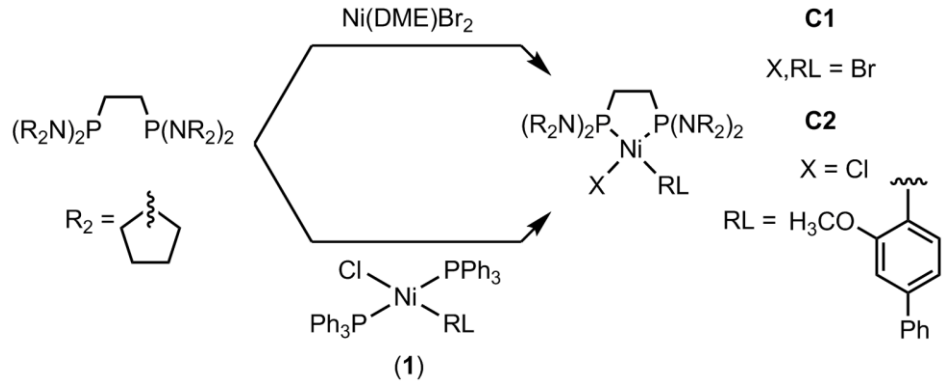

Results and Discussion

Precatalyst **C1** was screened in **BHP** polymerization, yielding **PBHP** with a multimodal gel permeation chromatography (GPC) trace (M_n = 16.9 kDa, Đ = 4.81, 89% conversion) (Figure 3.1). This result suggests multiple catalytic species are present throughout the polymerization. ^{31}P nuclear magnetic resonance (NMR) spectroscopy was performed to monitor the catalytic species present. Reacting **C1** with 15 equiv of **BHP** yielded two species: a pair of doublets (117.65, 111.90 ppm, J = 40.5 Hz) and a singlet (121.70 ppm) (Figure 3.2). The doublet was assigned to complex **II** (Figure 3.1) based on similar coupling constants seen for **C2**. Complex II forms after an initial **BHP** transmetalation event with **C1**, giving rise to a non-symmetric phosphine precatalyst. Complex **II** is then converted to complex **III** via a second transmetalation event with

BHP, yielding a symmetric bisphosphine precatalyst. As the reaction proceeds, the singlet at 121.70 ppm begins to disappear as reductive elimination occurs and a new set of doublets appear (117.36, 111.60 ppm, J = 37.7 Hz). Given the similar chemical shifts to complex **II** and coupling constants to **C2**, we assigned this complex **IV**, representing the catalyst resting state for propagation. While complex **III** completely disappears after 50 min, complex **II** persists; suggesting the second transmetalation is slow, possibly due to steric crowding around the metal center from the **BHP** monomer.

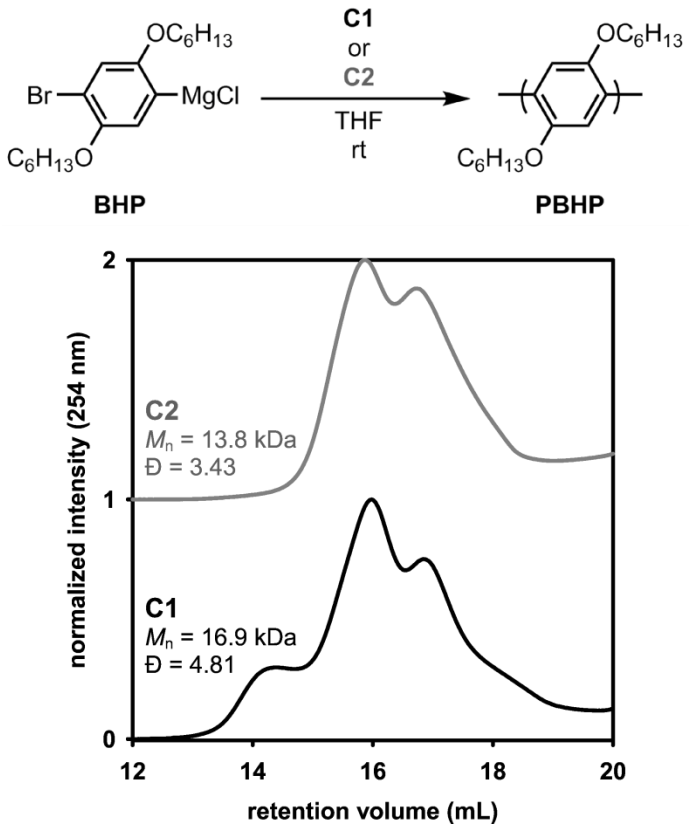

Figure 3.1 GPC trace of **PBHP** synthesized with **C1** or **C2** (1.3 mol%) ([mon] = 0.1 M, [cat] = 1.36 mM) at rt for 8 h. (theor. M_n = 20.7 kDa)

We synthesized a potentially faster initiating precatalyst with a biphenyl reactive ligand (RL) (Scheme 3.2, **C2**) containing an *ortho*-methoxy group, requiring only a single transmetalation with the **BHP** monomer. McNeil and coworkers have also used this precatalyst in **PBHP** synthesis.[18] When **BHP** was polymerized using **C2**, a bimodal GPC trace was observed with a narrower dispersity (M_n = 13.8 kDa, Đ = 3.43, 86 %

conversion) compared to **PBHP** synthesized via **C1**. This data suggests that multiple catalytic species still remain leading us to explore other monomers for polymerization.

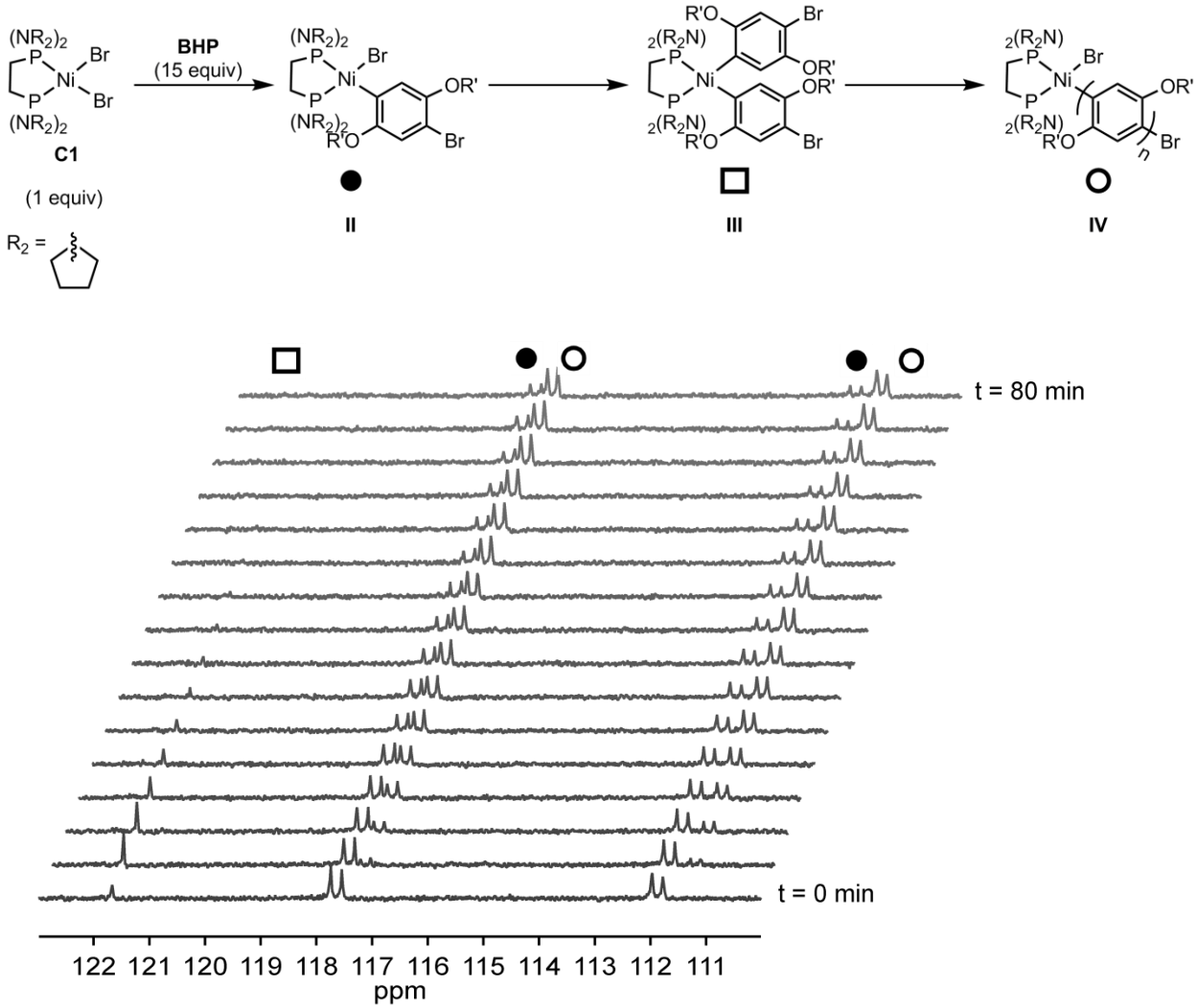

Figure 3.2 ^{31}P NMR spectra for polymerizing **BHP** (15 equiv) with **C1** (1 equiv) and the various catalytic species throughout the polymerization ([mon] = 0.17 M, [cat] = 9.0 mM).

Polymerizing **3HT** with **C1** yields **P3HT** at approximately the theoretical molecular weight (M_n = 11.8 kDa, theor. M_n = 12.5 kDa) and Đ = 1.34, with only the major regioisomer consumed and a bimodal peak observed via GPC (Figure 3.3). When polymerizing **3HT** with **C2**, **P3HT** (M_n = 14.9 kDa, theor. M_n = 14.0 kDa) with a narrower dispersity (Đ = 1.11) and unimodal GPC trace was observed (Figure 3.3). Similar to **C1**,

only the major **3HT** regioisomer is consumed with precatalyst **C2**. Luscombe polymerized **3HT** with a dppe-ligated Ni precatalyst with a tolyl-reactive ligand to give **P3HT** (Mn = 9.8 kDa, Đ = 1.2) with complete end-group incorporation.[19] Compared to our system, the narrower dispersity obtained using **C2** (compared to Luscombe's precatalyst) supports our hypothesis that the dpyrpe ligand may stabilizing the metal-π complex and enhancing oxidative addition rates. Given the above polymer properties, the living and chain-growth nature of **C2**-mediated **3HT** polymerization was explored.

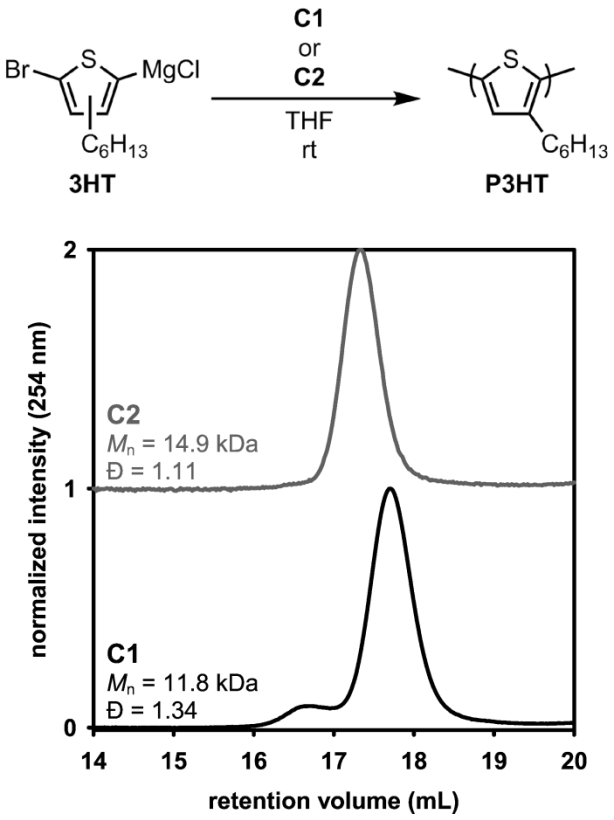

Figure 3.3 GPC trace of **P3HT** synthesized with **C1** or **C2** (1 mol%) ([mon] = 0.02 M, [cat] = 0.3 mM) for 90 min at rt.

As expected for a chain-growth polymerization, a linear relationship between monomer conversion and polymer molecular weight was observed (Figure 3.4A). Living chains ends were supported by a chain-extension experiment in which a second monomer aliquot is added to the polymerization after the initial monomer is mostly consumed (99%). Comparing GPC traces before and after monomer addition, show a shift to a higher molecular weight polymer without broadening the dispersity. (Figure

S2.16, $P3HT_{initial}$ = 7.3 kDa, Đ = 1.13, $P3HT_{extended}$ = 14.9 kDa, Đ = 1.13). Approximately theoretical molecular weights were also achieved at each catalyst loading (mon:cat = 25:1, 50:1, 75:1) with consistently narrow Đ < 1.13, (Figure 3.4B), indicating that most catalysts initiate and polymerize a single chain. Finally, end-group analysis after quenching with acid using MALDI-TOF/MS revealed exclusive RL/H end-groups (Figure 3.4C). This result suggests that the catalyst stays associated to the growing polymer chain throughout propagation. Combined, successful chain-extension, targeted molecular weight, and high end-group fidelity all indicate that **C2** polymerizes **3HT** via a living, chain-growth mechanism with minimal side reactions or catalyst dissociation.

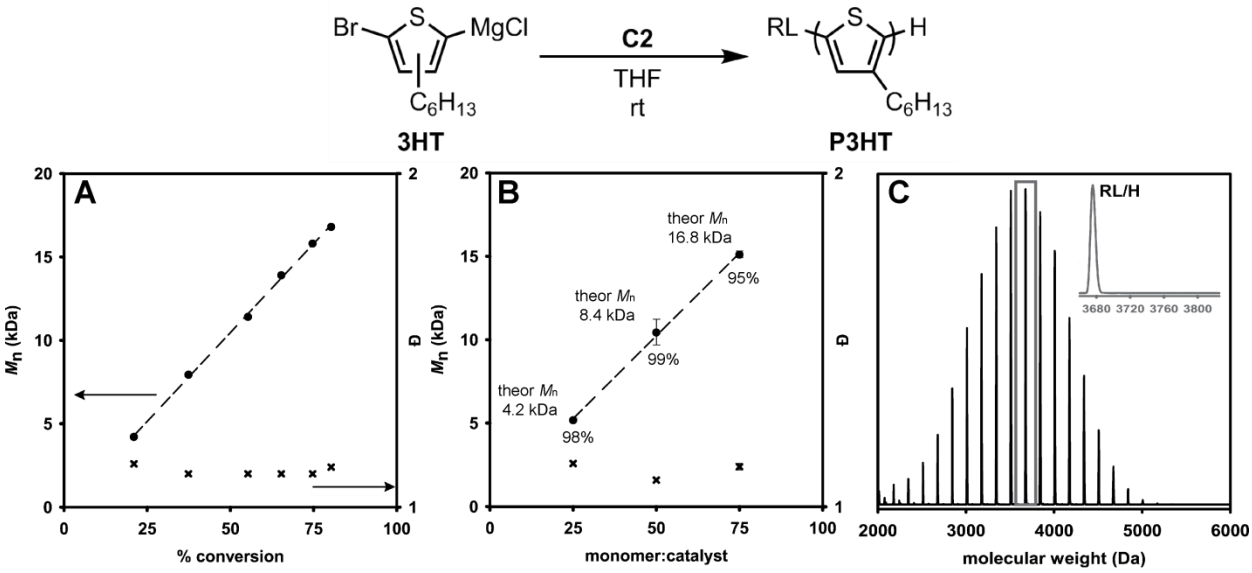

Figure 3.4 3HT polymerizations with **C2** to support chain-growth behavior showing **A)** number-average molecular weight (M_n) versus percent conversion of **3HT**, **B)** varying monomer:catalyst ratio (25:1, 50:1, 75:1) with percent monomer conversion and **C)** MALDI-TOF MS of P3HT (M_n = 5.25 kDa, Đ = 1.13).

While the living chain-growth synthesis for electron-deficient polymers are of continued interest in the CTP field, reports of these syntheses are few.[20,21,22,23] Polymerizing electron-deficient monomers via CTP can be difficult, as low catalyst-turnover in these reactions can potentially lead to unproductive pathways. However, Noonan and coworkers polymerized 3-hexylesterthiophene, **3HET**, an emerging monomer of interest for donor-acceptor copolymers, under Suzuki CTP conditions with various nickel precatalysts, including $Ni(dppe)Cl_2$.[23] While living conditions were

identified, MALDI-TOF/MS showed end groups consistent with chain-transfer. We were thus interested in applying **C2** to a **3HET** polymerization. Monomer **3HET** was synthesized herein via zinc metalation with hexyl 2-bromo-3-thiophenecarboxylate and 2,2,6,6-tetramethylpiperidinylzinc chloride at 65 °C to give the monomer as a single regioisomer. This mild activation route was necessary as esters are sensitive to Grignards, and could not be synthesized via Grignard metathesis. Precatalyst **C2** yielded poly(3-hexylesterthiophene) (**P3HET**) with a targeted M_n = 3.6 kDa (theor. M_n = 3.2 kDa) (for MALDI-TOF/MS analysis) and moderate Đ (1.31). Because a single regioisomer reacts with the precatalyst, the resulting **P3HET** is regioregular (head-to-tail). MADLI-TOF/MS analysis of **P3HET** revealed high end-group incorporation (99% RL/H–polymers), indicating that chain-transfer to monomer was not occurring. Nevertheless, low molecular weight tailing in the GPC trace suggests **3HET** polymerization suffers from slow initiation. Future work probing the mechanism should glean insight into the rate-limiting step, which could assist our design of an optimal catalyst to increase the initiation rate and narrow the resulting polymer's dispersity.

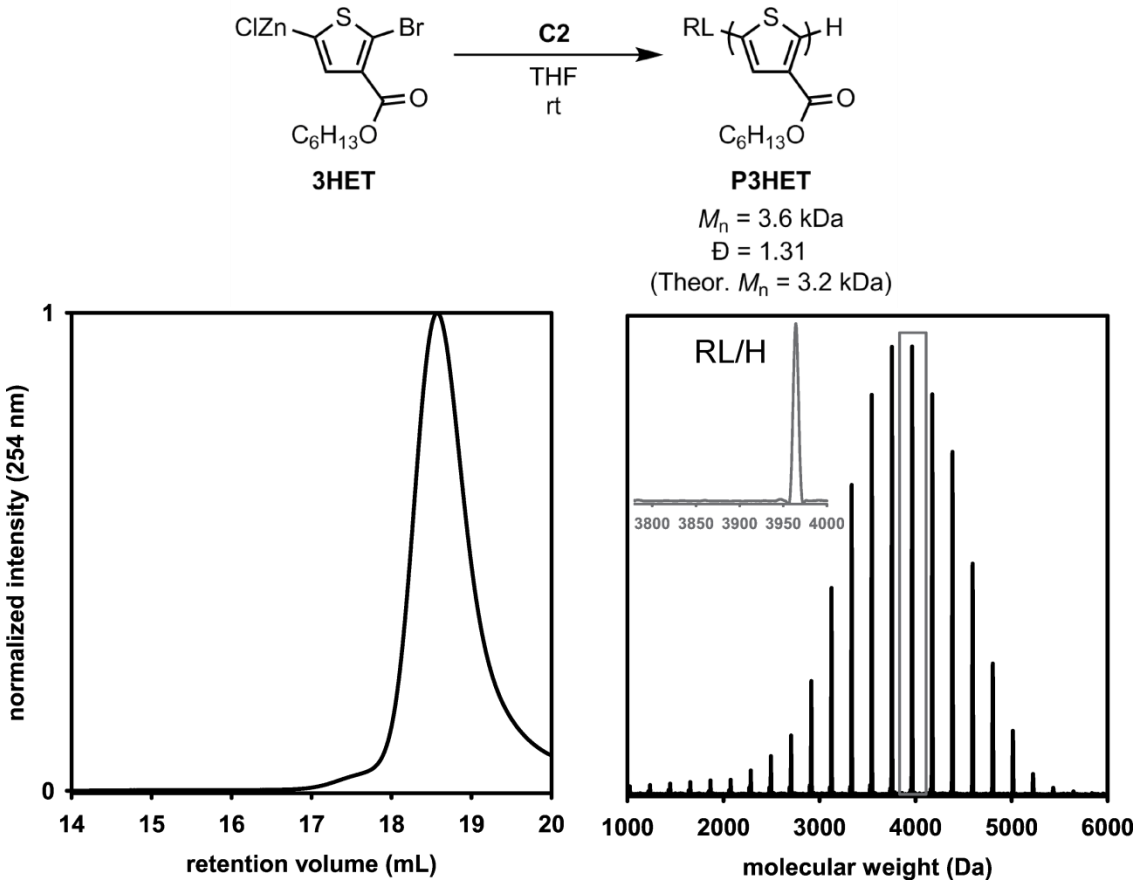

Figure 3.5 GPC and MALDI-TOF/MS trace for **P3HET** synthesized with **C2** (5.8 mol%) ([mon] = 0.02 M, [cat] = 0.3 mM) for 3 h at rt.

Conclusions and Future Directions

We hypothesized that dpyrpe, a strong σ-donating ligand with increased π-acceptor character compared to dppe, would promote CTP behavior. Using **C2**, **P3HT** was synthesized with a narrow dispersity (Đ = 1.11) and complete incorporation of reactive ligand/H end groups. This precatalyst also polymerized an electron-deficient monomer, **3HET**; yielding polymer with high end-group fidelity. Future work should focus on expanding monomer scope to other electron-poor monomers. Finally, while a **BHP** polymerization was attempted, multimodal GPC peaks were observed using **C1** and **C2**, suggesting multiple catalytic species and an uncontrolled polymerization. Overall, future work should include kinetic and spectroscopic studies to probe the CTP mechanism of this new catalyst. Mechanistic insight will inform future catalyst design for

tuning the σ-donating and π-accepting character of ancillary ligands to influence productive CTP pathways.

References

(1) (a) Yokoyama, A.; Miyakoshi, R.; Yokozawa, T. Chain Growth Polymerization for Poly(3-hexylthiophene) with a Defined Molecular Weight and a Low Polydispersity. *Macromolecules* **2004**, *37*, 1169–1171. (b) Sheina, E. E.; Liu, J.; Iovu, M. C.; Laird, D. W.; McCullough, R. D. Chain Growth Mechanism for Regioregular Nickel-Initiated Cross-Coupling Polymerizations *Macromolecules* **2004**, *37*, 3526–3528.

(2) Yeh, N.; Yeh, P. Organic solar cells: Their Developments and Potentials. *Renew. Sust. Energ. Rev.* **2013**, *21*, 421–431.

(3) Cataldo, S.; Pignataro, B. Polymeric Thin Films for Organic Electronics: Properties and Adaptive Structures. *Materials* **2013**, *6*, 1159–1190.

(4) Li, G.; Zhu, R.; Yang, Y. Polymer Solar Cells. *Nature Photonics* **2012**, *6*, 153–161.

(5) Boudreault, P.-L. T.; Najari, A.; Leclerc, M. Processable Low-Bandgap Polymers for Photovoltaic Applications. *Chem. Mater*. **2011**, *23*, 456–469. 36

(6) Facchetti, A. π-Conjugated Polymers for Organic Electronics and Photovoltaic Cell Applications *Chem. Mater*. **2011**, *23*, 733–758.

(7) Lanni, E. L.; Locke, J. R.; Gleave, C. M.; McNeil, A. J. LigandBased Steric Effects in Ni-Catalyzed Chain-Growth Polymerizations Using Bis(dialkylphosphino)ethanes *Macromolecules,* **2011**, *44*, 5136–5145.

(8) Lanni, E. L.; McNeil, A. J. Evidence for Ligand-Dependent Mechanistic Changes in Nickel-Catalyzed Chain-Growth Polymerizations *Macromolecules,* **2010**, *43*, 8039–8044.

(9) Lanni, E. L.; McNeil, A. J. Mechanistic Studies on Ni(dppe)Cl_2- Catalyzed Chain-Growth Polymerizations: Evidence for Rate-Determining Reductive Elimination *J. Am. Chem. Soc.,* **2009**, *131*, 16573–16579.

(10) Leone, A. K.; Souther, K. D.; Vitek, A. K.; LaPointe, A. M.; Coates, G. W.; Zimmerman, P. M.; McNeil, A. J. Mechanistic Insight into Thiophene Catalyst-Transfer Polymerization Mediated by Nickel Diimine Catalysts *Macromolecules*, **2017**, *50*, 9121–9127.

(11) Bryan, Z. J.; McNeil, A. J. Evidence for a Preferential Intramolecular Oxidative Addition in Ni-Catalyzed Cross-Coupling Reactions and their Impact on Chain-Growth Polymerizations. Chem. Sci. **2013**, *3*, 1620–1624.

(12) Baker, M. A.; Tsai, C.-H.; Noonan, K. J. T. Diversifying Cross-Coupling Strategies, Catalysts and Monomers for the Controlled Synthesis of Conjugated Polymers. *Chem. Eur. J.* **2018**, *ASAP*, DOI: 10.1002/chem.201706102.

(13) Leone, A. K.; McNeil, A. J. Matchmaking in Catalyst-Transfer Polycondensation: Optimizing Catalysts based on Mechanistic Insight. *Acc. Chem. Res.* **2016**, *49*, 2822–2831.

(14) Bryan, Z. J.; McNeil, A. J. Conjugated Polymer Synthesis via Catalyst-Transfer Polycondensation (CTP): Mechanism, Scope and Applications. *Macromolecules* **2013**, *46*, 8395–8405.

(15) Lee, S. R.; Bryan, Z. J.; Wagner, A. M.; McNeil, A. J. Effect of Ligand Electronic Properties on Precatalyst Initiation and Propagation in Ni-Catalyzed Cross-Coupling Polymerizations. *Chem. Sci.* **2012**, *3*, 1562–1566.

(16) Beach, M. T.; Walker, J. M.; Wang, R.; Spivak, G. J. Ruthenium Piano-Stool Complexes Containing Mono- or Bidentate Pyrrolidinylalkylphosphines and Their Reactions with Small Molecules. *J. Organomet. Chem.* **2011**, *20*, 3198–3205.

(17) Mitoraj; M. P.; Michalak, A. σ-Donor and π-Acceptor Properties of Phosphorus Ligands: An Insight from the Natural Orbitals for Chemical Valence. *Inorg. Chem.* **2010**, *49*, 578–582.

(18) Hall, A. O.; Lee, S. R.; Bootsma, A. N.; Bloom, J. W. G.; Wheeler, S. E.; McNeil, A. J. Reactive Ligand Influence on Initiation in Phenylene Catalyst-Transfer Polymerization. *J. Polym. Sci. Part A: Polym. Chem.* **2017**, *55*, 1530–1535.

(19) Bronstein, H. A.; Luscombe, C. K. Externally Initiated Regioregular P3HT with Controlled Molecular Weight and Narrow Polydispersity. *J. Am. Chem. Soc.* **2009**, *131*, 12894–12895.

(20) Pammer, F.; Jager, J.; Rudolf, B.; Sun, Y. Soluble Head-to-Tail Regioregular Polythiazoles: Preparation, Properties, and Evidence for Chain-Growth Behavior in the Synthesis via Kumada-Coupling Polycondensation. *Macromolecules* **2014**, *47*, 5904–5912.

(21) Smith, M. L.; Leone, A. K.; Zimmerman, P. M.; McNeil, A. J. Impact of Preferential π-Binding in Catalyst-Transfer Polycondensation of Thiazole Derivatives. *ACS Macro Lett,* **2016**, *5*, 1411–1415.

(22) Bridges, C. G.; McCormick, T. M.; Gibson, G. L.; Hollinger, J.; Seferos, D. S. Designing and Refining Ni(II)diimine Catalysts Toward the Controlled Synthesis of Electron-Deficient Conjugated Polymers. *J. Am. Chem. Soc.* **2013**, *135*, 13212–13219.

(23) Qiu, Y.;Worch, J. C.; Fortney, A.; Gayathri, C.; Gil, R. R.; Noonan, K. J. T. Nickel-Catalyzed Suzuki Polycondensation for Controlled Synthesis of Ester-Functionalized Conjugated Polymers. *Macromolecules* **2016**, *49*, 4757–4762.

Chapter 4

User-Friendly Synthesis for Conjugated Polymers

Introduction

Transition metal-catalyzed cross-coupling is an often utilized method for forming carbon–carbon bonds in the pharmaceutical, agrochemical and material fields.[1,2,3,4] A particularly useful application of cross-coupling chemistry is in conjugated polymer synthesis via catalyst-transfer polymerization (CTP), a living, chain-growth method.[5,6,7] This polymerization proceeds through a Ni(0)/Ni(II) catalytic cycle (Scheme 4.1) in which the catalyst stays associated to the growing polymer chain via a metal-π polymer complex.[8,9,10] This association ensures addition into the same chain, enabling access to targeted molecular weight polymers, a narrow molecular weight distribution (dispersity, Đ), and sequence control.[11]

Scheme 4.1 General mechanism for catalyst-transfer polymerization.

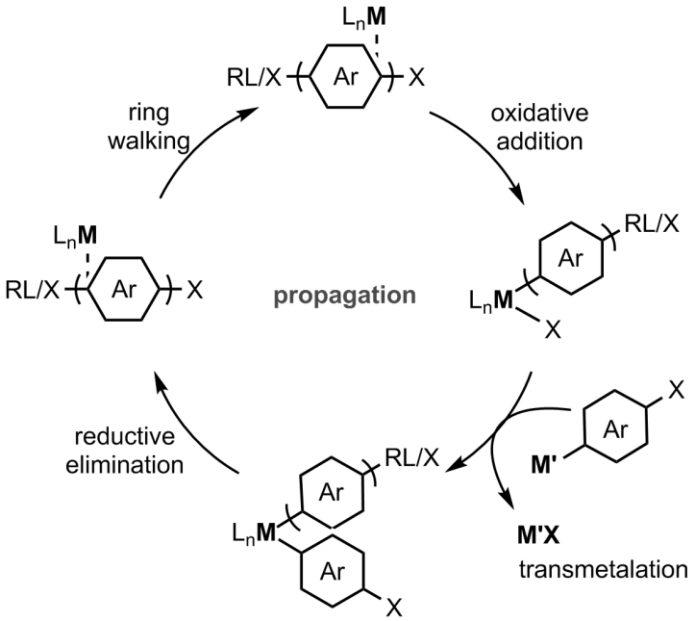

A major limitation with cross-coupling chemistry is that the organometallic transmetalating agent and transition metal catalyst are often air- and moisture-sensitive. When exposed to water, organometallic reagents hydrolyze making them inactive for synthesis. Additionally, transition metal catalysts are often poisoned by oxygen and/or water. Combined, these oxygen/water sensitivities require many cross-coupling reactions to be conducted in inert atmospheres (i.e., N_2 or Ar). To circumvent these limitations, Knochel and coworkers first reported an air-stable cross-coupling reagent by reacting ArMgX (X = Cl, Br, I) with $Zn(OPiv)_2$ to generate ArZnCl with a noncoordinated $Mg(OPiv)_2$ salt (Figure 4.1, ***past work***).[12,13] The organozinc arenes were then used in high-yielding Negishi cross-coupling reactions via air-tolerant N-heterocyclic carbene(NHC)-ligated palladium (Pd) precatalysts, known as PEPPSI (pyridine-enhanced precatalyst preparation, stabilization, and initiation).[14] Mechanistic studies by Knochel hypothesized that the $Mg(OPiv)_2$ sequesters H_2O, reducing the probability of hydrolyzing the Zn–C bond.[15] We were motivated to expand this work to CTP (Figure 4.1, ***this work***). Herein we report our initial work in identifying an open-to-air synthesis for poly(3-hexylthiophene) (**P3HT**) and poly(3-hexylesterthiophene) (**P3HET**).

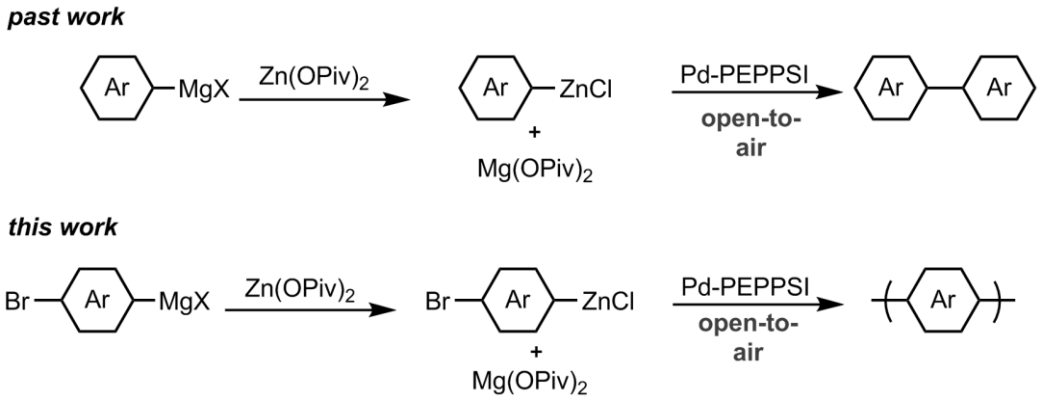

Figure 4.1 Air-tolerant Negishi cross-couplings with Pd-PEPPSI precatalysts (**past work**). Air-tolerant catalyst-transfer polymerization with Pd-PEPPSI precatalyst (**this work**).

As a control, **P3HT** synthesis was first performed in the glovebox. Monomer **Zn-3HT** was generated via Grignard metathesis between iPrMgCl-LiCl with 2,5-dibromo-3-hexylthiophene, followed by transmetalation with $Zn(OPiv)_2$ (95% conversion). After transmetalation, a new shift in the ^1H nuclear magnetic resonance (^1H NMR) spectrum of the thiophene aromatic proton downfield (Δ = 0.03 ppm) was observed (Figure S3.4). Commercially available NHC-ligated Pd precatalysts were first screened for **Zn-3HT** polymerization (Chart 4.1).

Chart 4.1 Selected commercially available NHC-ligated Pd precatalysts

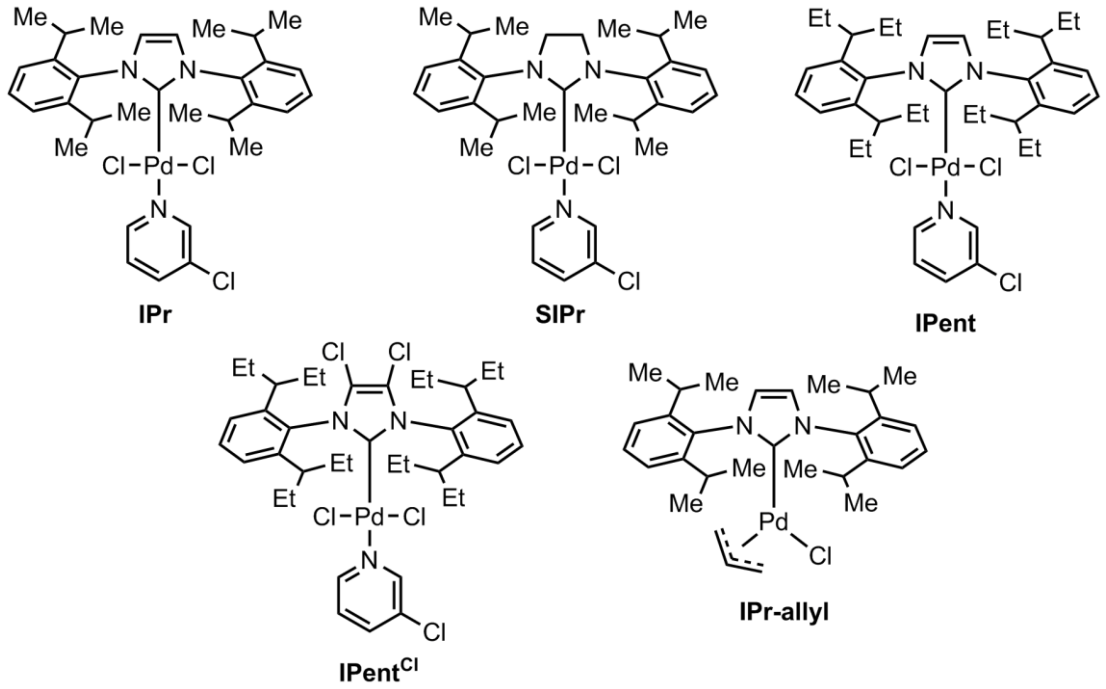

When **Zn-3HT** was polymerized with **IPr** and its saturated analogue **SIPr** in the glovebox, targeted molecular weight polymers (theor. M_n = 15.5 kDa) were achieved for **IPr** (M_n = 17.7 kDa) and **SIPr** (M_n = 12.3 kDa) albeit with broad dispersities (IPr: Đ = 2.25, SIPr: Đ = 2.10) (Figure 4.2). This result is in contrast to Kumada-CTP reported by McNeil and coworkers in which **IPr** yielded **P3HT** (M_n = 28.2 kDa) with narrow dispersity (Đ = 1.19) with Mg-3HT.[16] End-group analysis of our polymers via matrix-assisted laser desorption ionization-time of flight mass spectrometry (MALDI-TOF/MS), showed Br/H (83%), Br/Br (17%) for **IPr** and Br/H (78%), Br/Br (8%), iPr/H (3%) for **SIPr** with 11% of end-groups unaccounted for (Figure 4.2). These results suggest that catalyst

dissociation from the growing polymer chain is happening, indicated by Br/Br end-groups coupled with broad dispersity. Precatalyst **IPent** polymerized **Zn-3HT** to yield **P3HT** with a narrower dispersity (Đ = 1.55) than **IPr/SIPr** and a higher percentage of Br/H end-groups (Br/H (91%) and Br/Br (9%)), indicating fewer catalysts were dissociating. Fewer catalysts dissociating could be due to an increase in electron density at the metal center compared to **IPr** and a stronger metal-π complex. We also explored an **IPent** derivative with chlorines replacing the H's on the NHC (**IPent**$^{\mathbf{Cl}}$). This precatalyst gave **P3HT** (M_n = 12.3 kDa) with a narrower dispersity (Đ = 1.33) compared to **IPent**. Unfortunately end-group analysis revealed poor end-group fidelity (Br/H (73%), Br/Br (11%), iPr/Br (9%), iPr/H (6%)). Loss of end-group control could stem from a weaker metal-polymer complex with the electron-withdrawing chlorines compared to **IPent**. Finally, an NHC-ligated Pd precatalyst with an allyl stabilizing ligand, **IPr-allyl**, was evaluated. A polymer with M_n greater than 3 times the theoretical molecular weight (M_n = 87 kDa, theor. M_n = 15.5 kDa) with a broad dispersity (Đ = 2.57) was synthesized. These results suggest that fewer catalysts were initiated than anticipated, generating higher-than targeted molecular weight polymers. Summarizing these results, **IPent** polymerized **Zn-3HT** with a narrow dispersity and highest end-group fidelity among screened precatalysts and was selected for further catalyst optimization.

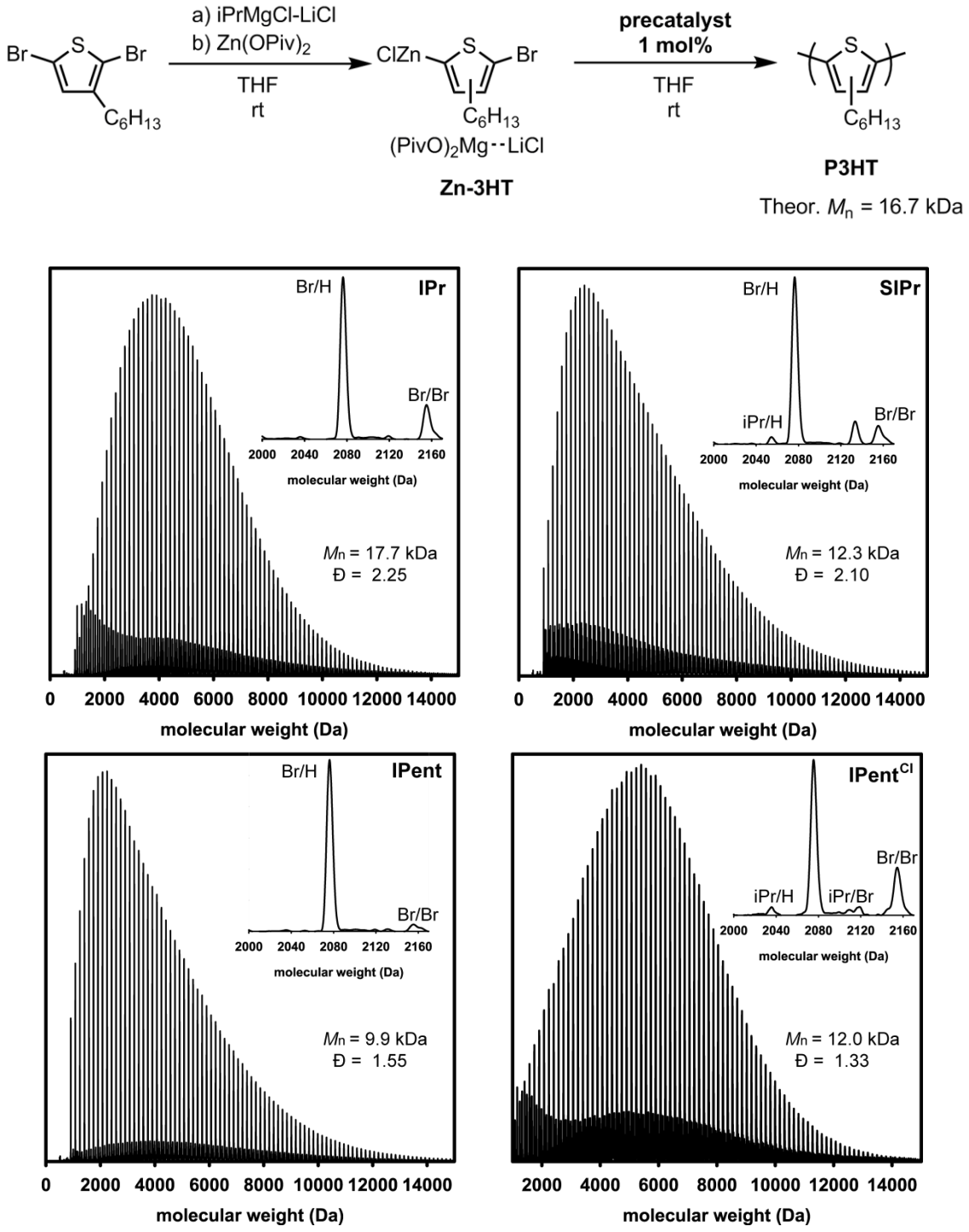

Figure 4.2 Zn-3HT monomer synthesis and polymerization with commercially available NHC-ligated Pd precatalysts and corresponding MALDI-TOF/MS plots ([mon] = 0.02 M, [cat] = 0.3 mM).

Computational work by Zimmerman and coworkers has recently elucidated the role of 3-chloropyridine during Kumada CTP of thiophene via **IPr**.[17] While initially thought of as only a "throw-away" ligand,[18] 3-chloropyridine participates in both initiation and propagation. During initiation, the pyridine must dissociate from the metal center. However, 3-chloropyridine was also found to bind the metal catalyst center during propagation, creating an off-cycle species and limiting catalyst-turnover. We hypothesized that using a more electron-withdrawing group on the pyridine would enable faster pyridine dissociation, as well as decrease the binding affinity of pyridine to the metal center during propagation resulting in polymers with narrower dispersities. Thus we generated 3–fluoro and 3–trifluoromethylpyridine **IPent** derivatives and applied them to **Zn-3HT** polymerization (Figure 4.3). Both precatalysts yield **P3HT** with narrower dispersities than **IPent** (Đ = 1.49), 3-trifluoromethyl **IPent** (Đ = 1.41) and 3-fluoro **IPent** (Đ = 1.39). While a dramatic change in dispersity was not observed, we were encouraged to see a small decrease (Δ = 0.10), suggesting that a more electron-withdrawing group on pyridine may influence binding affinity to the metal center. Having designed an optimal precatalyst, **IPentF**, we next evaluated the air-tolerance of this system.

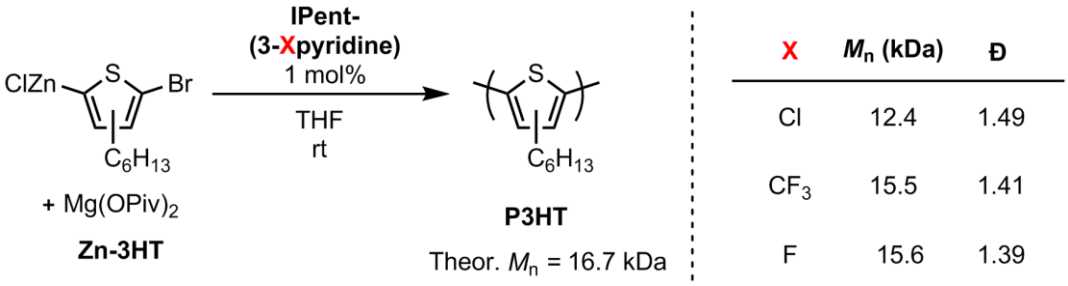

Figure 4.3 Zn-3HT polymerization using **IPent** with various pyridine ligands ([mon] = 0.02 M, [cat] = 0.3 mM) for 30 min.

To evaluate the air-tolerance of **Zn-3HT** with **IPentF**, both monomer and catalyst solutions were prepared and then capped and removed from the glovebox. Outside of the glovebox, the caps were removed from each vial, monomer solution was injected into the catalyst solution, and the polymerization vial was re-capped and stirred for 30 min (Figure 4). Using this initial setup, a higher than targeted molecular weight (M_n =

19.7 kDa, theor. M_n = 14.0 kDa) polymer was synthesized with a dispersity similar to glovebox polymerizations (Đ = 1.40). A lower molecular weight polymer (M_n = 4.11 kDa, Đ = 1.70, Figure S3.9) was also synthesized for end-group analysis by MALDI-TOF/MS, showing 93% Br/H and 7% Br/Br. The percentage of active chain-ends was assessed via a chain-extension experiment, in which a second aliquot of monomer is injected after initial monomer is mostly consumed (conversion of 1st aliquot = 93%). The chain-extension experiment generated a higher molecular weight polymer (**P3HT$_{initial}$:** M_n = 8.96 kDa, Đ = 1.51, **P3HT$_{extended}$:** M_n = 18.3 kDa, Đ = 1.38), wherein the entire polymer peak shifts, suggesting most chain-ends are active. These results were promising and encouraged us to expand monomer scope using the polymerization setup describe above.

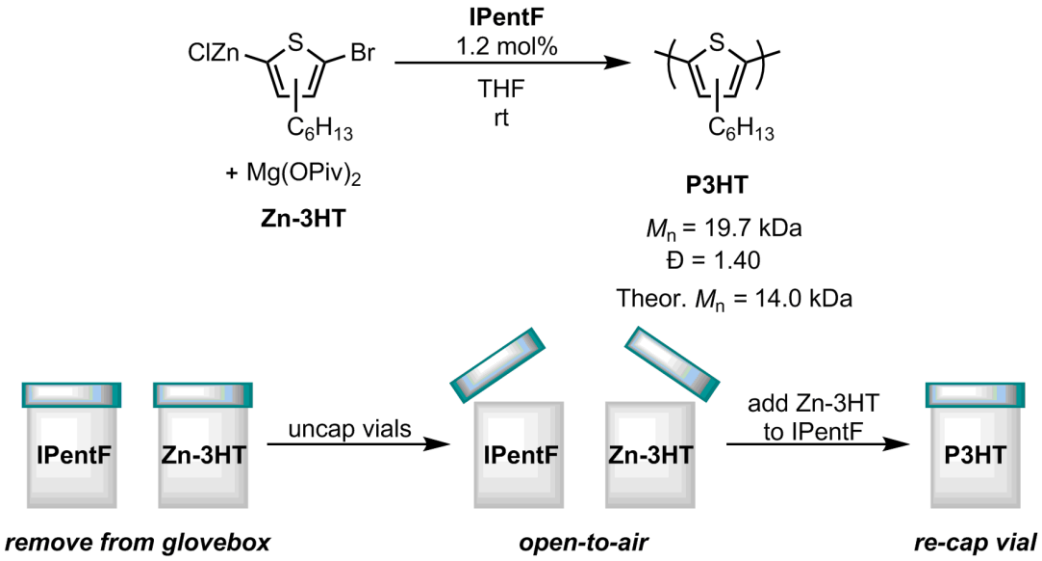

Figure 4.4 Zn-3HT polymerization exposed to air using **IPentF** and experimental setup ([mon] = 0.02 M, [cat] = 0.35 mM) for 30 min.

Poly(3-hexylesterthiophene) (**P3HET**) has emerged as an attractive polymer for potential use in donor-acceptor copolymers,[19] and inspired us to explore this polymer's synthesis open-to-air. However, the ester functionality is sensitive to Grignard reagents, requiring us to modify our monomer synthesis. Knochel and coworkers accessed air-tolerant organometallic arenes with sensitive functional groups by reacting a 2,2,6,6-tetramethylpiperidinylmagnesium chloride lithium chloride solution with $Zn(OPiv)_2$

(Scheme 4.2).[20] This complex metalates the most acidic proton in arenes. Applying this route to **Zn-3HET** synthesis yielded the monomer in 51% yield.

Scheme 4.2 Synthetic route for accessing ZnCl–Ar with sensitive functional groups.

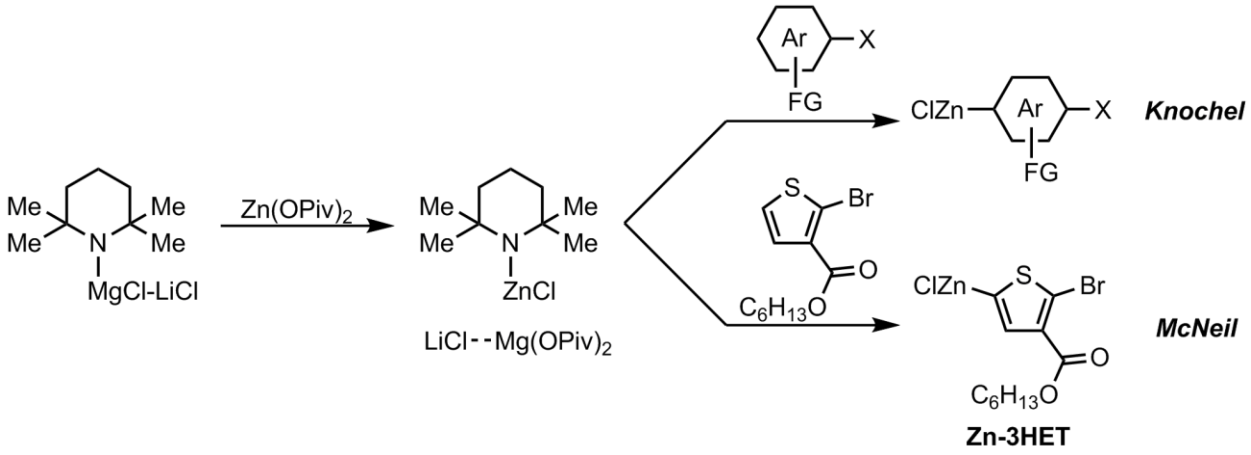

We next polymerized **Zn-3HET** with **IPentF** open-to-air as well as in the glovebox for a control. Similar molecular weight polymers (glovebox: M_n = 12.1 kDa, Đ = 1.54, open-to-air: M_n = 12.2 kDa, Đ = 1.35) were observed in each environment with similar peak shapes (Figure 4.5). Because a single regioisomer of **Zn-3HET** is reacted with the precatalyst, a regioregular polymer (head-to-tail coupling) is generated. A lower molecular weight **P3HET** (M_n = 2.56 kDa, Đ = 1.40) was also synthesized open-to-air using **IPentF** for MALDI-TOF/MS analysis, revealing 92% Br/H and 8% Br/Br end-groups. These results suggest that open-to-air conjugated polymer synthesis can be achieved for an electron-deficient monomer using **IPentF**.

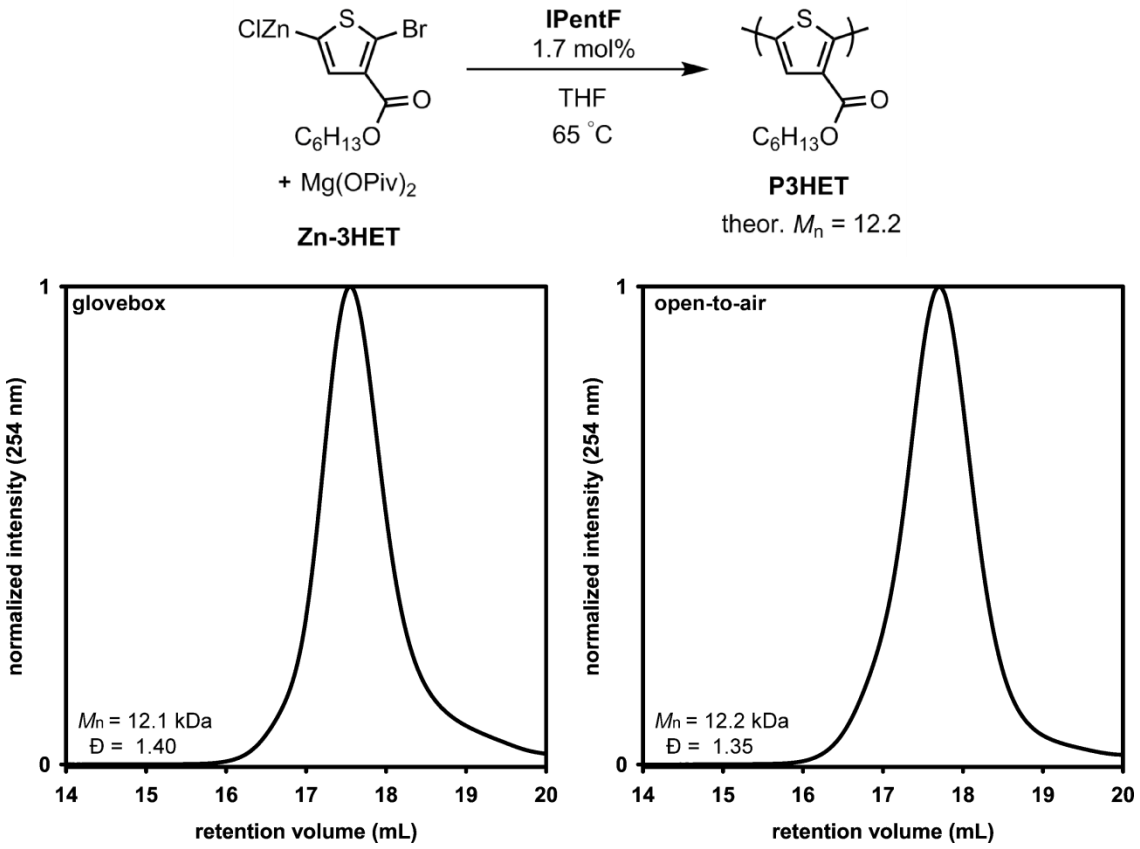

Figure 4.5 P3HET generated in the glovebox versus open-to-air ([mon] = 0.02 M, [cat] = 0.25 mM) for 15 min.

In conclusion, we described a new route for accessing **P3HT** and **P3HET** open-to-air using **IPentF**. This route yields polymers with targeted molecular weights and end-group fidelity. Future work will include identifying a synthetic route that includes monomer activation outside of the glovebox coupled with our conditions for open-to-air polymer synthesis. This work is applicable to chemists and engineers interested in having a quick and efficient route to accessing conjugated polymers, and thus the utility of this reaction must be further explored. One's ability to access polymers with different M_n is important to those interested in materials for organic electronics, as some reports show the dependence of device performance on polymer molecular weight.[21] Future work will show the range of accessible molecular weights for both **P3HT** and **P3HET**.

References

(1) Hazari, N.; Melvin, P. R.; Beromi, M. M. Well-defined Nickel and Palladium Precatalysts for Cross–Coupling. *Nature Reviews Chemistry* **2017**, *1*, 0025, 1–16.

(2) Liu, C.; Zhang, H.; Shi, W.; Lei, A. Bond Formations Between Two Nucleophiles: Transition Metal Catalyzed Oxidative Cross–Coupling Reactions. *Chem. Rev.* **2011**, *111*, 1780–1824.

(3) Fortman, G. C.; Nolan, S. P. *N*-Heterocyclic Carbene (NHC) Ligands and Palladium in Homogeneous Cross–Coupling Catalysis: A Perfect Union. *Chem. Soc. Rev.* **2011**, *40*, 5151–5169.

(4) Corbet, J.-P.; Mignani, G. Selected Patented Cross–Coupling Reaction Technologies. *Chem. Rev.* **2006**, *106*, 2651–2710.

(5) Bryan, Z. J.; McNeil, A. J. Evidence for a Preferential Intramolecular Oxidative Addition in Ni-Catalyzed Cross-Coupling Reactions and their Impact on Chain-Growth Polymerizations. Chem. Sci. **2013**, *3*, 1620–1624.

(6) Leone, A. K.; McNeil, A. J. Matchmaking in Catalyst-Transfer Polycondensation: Optimizing Catalysts based on Mechanistic Insight. *Acc. Chem. Res.* **2016**, *49*, 2822–2831.

(7) Baker, M. A.; Tsai, C.-H.; Noonan, K. J. T. Diversifying Cross-Coupling Strategies, Catalysts and Monomers for the Controlled Synthesis of Conjugated Polymers. *Chem. Eur. J.* **2018**, *ASAP*, DOI: 10.1002/chem.201706102.

(8) Lanni, E. L.; McNeil, A. J. Mechanistic Studies on Ni(dppe)Cl_2- Catalyzed Chain-Growth Polymerizations: Evidence for Rate-Determining Reductive Elimination *J. Am. Chem. Soc.,* **2009**, *131*, 16573–16579.

(9) Lanni, E. L.; McNeil, A. J. Evidence for Ligand-Dependent Mechanistic Changes in Nickel-Catalyzed Chain-Growth Polymerizations *Macromolecules,* **2010**, *43*, 8039–8044.

(10) Lanni, E. L.; Locke, J. R.; Gleave, C. M.; McNeil, A. J. LigandBased Steric Effects in Ni-Catalyzed Chain-Growth Polymerizations Using Bis(dialkylphosphino)ethanes *Macromolecules,* **2011**, *44*, 5136–5145.

(11) (a) Yokoyama, A.; Miyakoshi, R.; Yokozawa, T. Chain Growth Polymerization for Poly(3-hexylthiophene) with a Defined Molecular Weight and a Low Polydispersity. *Macromolecules* **2004**, *37*, 1169–1171. (b) Sheina, E. E.; Liu, J.; Iovu, M. C.; Laird, D. W.; McCullough, R. D. Chain Growth Mechanism for Regioregular Nickel-Initiated Cross-Coupling Polymerizations *Macromolecules* **2004**, *37*, 3526–3528.

(12) Bernhardt, S.; Manolikakes, G.; Kunz, T.; Knochel, P. Preparation of Solid Salt-Stabilized Functionalized Organozinc Compounds and their Applications in Cross–Coupling and Carbonyl Addition Reactions. *Angew. Chem. Int. Ed.* **2011**, *50*, 9205–9209.

(13) Stathakis, C. I.; Bernhardt, S.; Quint, V.; Knochel, P. Improved Air-Stable Solid Aromatic and Heterocyclic Zinc Reagents by Highly Selective Metalations for Negishi Cross–Couplings. *Angew. Chem. Int. Ed.* **2012**, 51, 9428–9432.

(14) Organ, M. G.; Avola, S.; Dubovyk, I.; Hadei, N.; Kantchev, E. A. B.; O'Brein, C. J.; Valente, C. A User-Friendly, All-Purpose Pd–NHC (NHC = N-Heterocyclic Carbene) Precatalyst for the Negishi Reaction: A Step Towards a Universal Cross–Coupling Catalyst. *Chem. Eur. J.* **2006**, *12*, 4749–4755.

(15) Hernán-Gómez, A.; Herd, E.; Hevia, E.; Kennedy, A. R.; Knochel, P.; Koszinowski, K.; Manolikakes, S. M.; Mulvey, R. E.; Schnegelsberg, C. Organozinc Pivalate Reagents: Segregation, Solubility, Stabilization, and Structural Insights. *Angew. Chem. Int. Ed.* **2014**, *53*, 2706–2710.

(16) Bryan, Z. J.; Smith, M. L., McNeil, A. J. Chain-growth Polymerization of Aryl Grignards Initiated by a Stabilized NHC–Pd Precatalyst. *Macromol. Rapid Commun.* **2012**, *33*, 842–847.

(17) Nasielski, J.; Hadei, N.; Achonduh, G.; Kantchev, E. A. B.; O'Brein, C. J.; Lough, A.; Organ, M. G. Structure-Activity Analysis of Pd-PEPPSI Complexes in Cross–Couplings: A Close Inspection of the Catalytic Cycle and the Precatalyst Activation Model. *Chem. Eur. J.* **2010**, *16*, 10844–10853.

(18) Zhao, Y.; Nett, A. J.; McNeil, A. J.; Zimmerman, P. M. Computational Mechanism for Initiation and Growth of Poly(3-hexylthiophene) Using Palladium N-Heterocyclic Carbene Precatalysts. *Macromolecules* **2016**, *49*, 7632–7641.

(19) Qiu, Y.;Worch, J. C.; Fortney, A.; Gayathri, C.; Gil, R. R.; Noonan, K. J. T. Nickel-Catalyzed Suzuki Polycondensation for Controlled Synthesis of Ester-Functionalized Conjugated Polymers. *Macromolecules* **2016**, *49*, 4757–4762.

(20) Stathakis, C. I.; Manolikakes, S. M.; Knochel, P. TMPZnOPiv•LiCl: A New Base for the Preparation of Air-Stable Solid Zinc Pivalates of Sensitive Aromatics and Heteroaromatics. *Org. Lett.* **2013**, *15*, 1302–1305.

(21) Bruner, C.; Dauskardt, R. Role of Molecular Weight on the Mechanical Device Properties of Organic Polymer Solar Cells. *Macromolecules* **2014**, *47*, 1117–1121.

Chapter 5

Conclusions and Future Directions

Over the past decade, catalyst-transfer polymerization has enabled access to a wide variety of conjugated polymers,[1,2,3] although monomer scope has been limited to electron-rich hetero(arene) with similar structures and few reports of electron deficient arenes. This thesis first describes our efforts in expanding monomer pairings in synthesizing copolymers containing conducting/insulating segments in a one-pot synthesis.[4] While we designed a catalyst capable of polymerizing each monomer independently, copolymer yield was low due to a high-energy barrier for the catalyst to switch mechanisms. We also expanded monomer scope to an electron-deficient monomer with high end-group fidelity by using a pyrrolidinyl-based bisphosphine nickel catalyst. Finally, a user-friendly CTP method was optimized and shown to polymerize an electron-rich and electron poor monomer.

In Chapter 2 we were interested in synthesizing copolymers whose monomers had two mechanistically distinct living polymerizations in one-pot using a single catalyst. We hypothesized this route would give a streamlined approach to accessing a wide variety of monomer pairings for conjugated/insulating copolymers. Our approach was to identify a precatalyst that could polymerize each monomer independently via a living, chain-growth mechanism and then optimize reaction conditions to induce successful copolymerization.[5,6] Since poly(olefin) metal complexes are sensitive to coordinating substrates, it was necessary for poly(olefin) to be used as the macroinitiator. An initial control experiment revealed aluminum reagents (a cocatalyst for diimine-Ni(II) mediated olefin polymerization) inhibited thiophene polymerization, leading us to redesign our precatalyst and replace the halide reactive ligands with alkyl groups. This modification enabled us to use a boron cocatalyst which did not inhibit thiophene polymerization. A consequence of this change in cocatalyst required poly(olefin) synthesis to be performed under neat monomer conditions, with olefin remaining after

macroinitiator synthesis. Combined computational and experimental work revealed olefin inhibited thiophene polymerization, presumably due to competitive binding to the nickel center. Thus, our optimized copolymerization system required us to remove olefin before extending the macroinitiator with thiophene. However, the major products of the copolymerization were thiophene and olefin homopolymers. Computations revealed a high-energy reductive elimination barrier for the catalyst to switch mechanisms coupled with chain-transfer events, as likely sources for homopolymer formation.

Work in our lab by Amanda Leone has focused on circumventing this dilemma by inducing a “ligand-switch” from a diimine ancillary ligand on the olefin macroinitiator complex to a bisphosphine ancillary ligand (Scheme 5.1). Preliminary thiophene polymerization studies that use this ligand-switch approach show unproductive chain-transfer reactions have been mitigated. Studies are ongoing in our lab to apply this approach to copolymerizing olefin and thiophene as a model system. If successful, we envision this method being applied to synthesizing relevant block copolymers for organic electronics. A recent multistep synthesis for block copolymers containing poly(fluorene) and isoindigo-functionalized polyacrylates,[7] a promising material for resistive memory applications, gave 70% copolymer yield (from the 2nd step) suggesting the synthesis could be improved. Our “ligand-switch” approach would be attractive for this particular block copolymer synthesis as Ni diimines have polymerized methacrylates[8] and dppp-ligated Ni precatalyst has synthesized poly(fluorene)[9], leading us to hypothesize a successful ligand-switch induced copolymerization possible.

Scheme 5.1 Ligand-switch approach for accessing conjugated/olefin block copolymers

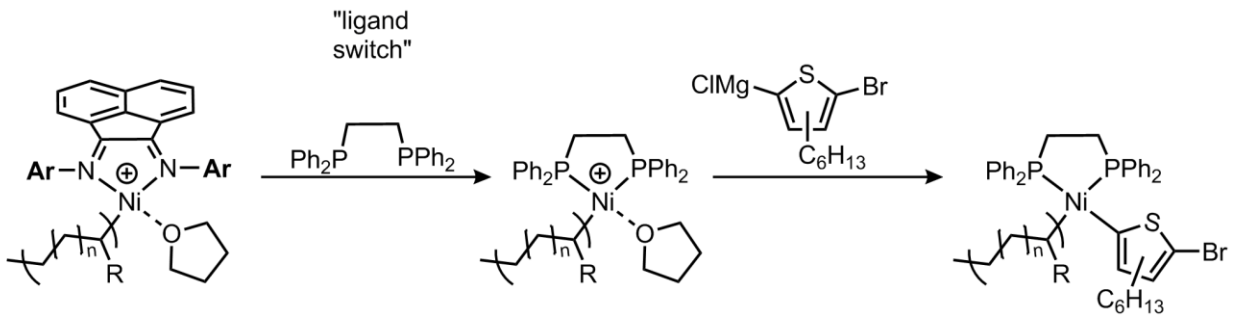

In Chapter 3 we were interested in exploiting ancillary ligand electronics to gain access to new catalysts for CTP that stabilized the metal-π complex and enhanced intramolecular oxidative addition. While most ligand modification in catalyst design of bis(phosphine)ethane complexes has focused on σ-donating properties of the phosphine,[10] exploring the influence of π-acceptor character on CTP behavior is rare.[11] We selected a pyrrolidinyl bisphosphine ancillary ligand for our study as the σ-donating properties are the same as a commonly used ligand for CTP: dppe. It has been reported that phosphines with more electronegative atoms are better π-acceptors.[12] Since nitrogen is slightly more electronegative than carbon, we thought this ligand would be favor formation of the metal-π complex in CTP, enabling narrower dispersities and end-group control.

A pyrrolidinyl bisphosphine-ligated Ni precatalyst (**C1**) with dihalide reactive ligands gave both poly(phenylene) and P3HT with multimodal GPC traces, suggesting multiple catalytic species present in the polymerization. A ^{31}P NMR spectroscopic study of phenylene polymerization revealed second transmetalation rate-limiting for initiation. enhance the rate of transmetalation, we synthesized an analogue to **C1** to include a biphenyl reactive ligand where only one transmetalation event would be required, referred to as **C2**. This new precatalyst gave poly(phenylene) with a multimodal GPC trace, suggesting an uncontrolled polymerization. However, when **P3HT** was synthesized using **C2**, a unimodal GPC trace was observed, as well as polymer with consistently narrow dispersity (Đ = 1.11–1.13) and high-end group fidelity. Comparing these results to **P3HT** synthesis via a similar dppe-ligated Ni catalyst, our system yieleded polymers with narrower dispersity and improved end-groups. Future work exploring the mechanism of **C2** in conjugated polymer synthesis can glean insight into the effect of pyrrolidinyl-based bisphosphine ligands on CTP.

We also expanded monomer scope of **C2** polymerization to include an electron-deficient polymer, poly(3-hexylesterthiophene). High end-group fidelity was observed for this polymerization, suggesting that chain-transfer reactions, which can inhibit access to high molecular weight polymers, were not occurring. Our catalyst should be further explored in polymerizing electron-deficient monomers not currently accessible via CTP.

A monomer of specific interest is thienopyrrole-dione (TPD) (Scheme 5.2), which has been used as an acceptor unit in donor-acceptor copolymers for the active layer in a photovoltaic solar cell with high power conversion efficiency (7.3%), a measure of the device efficiency in converting sunlight to electricity.[13] The controlled synthesis of this monomer could enable access to new donor-acceptor copolymers, specifically coupled with donor polymers already accessed via CTP.

Scheme 5.2 TPD polymerization with **C2**

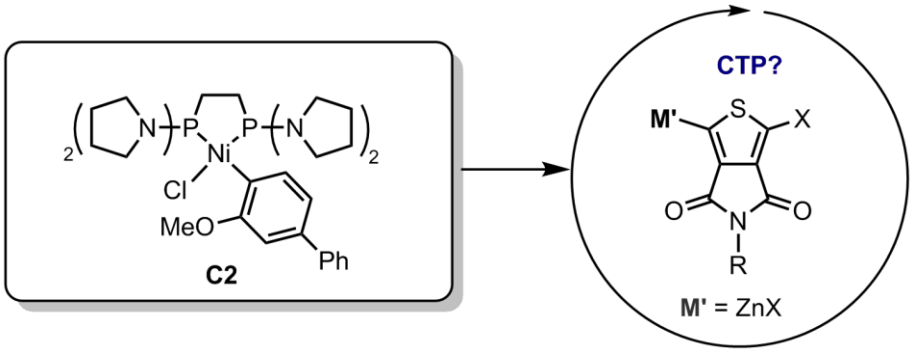

Finally, Chapter 4 described our efforts in identifying user-friendly CTP conditions. Organometallic arenes, Ar-ZnCl $Mg(OPiv)_2$, have shown remarkable air stability.[13] This functionality was incorporated into monomers of interest for CTP polymerization. These monomers were then polymerized in air using a new NHC–ligated Pd catalyst with 3-fluoropyridine as a stabilizing ligand to yield P3HT and poly(hexylesterthiophene). Using this route, targeted molecular weights were accessed as well as end-group fidelity observed (> 90% Br/H) for both polymers. Future work will focus on optimizing a synthesis to be done without the use of a glovebox (including monomer activation). We envision this work being easily accessible to undergraduate laboratories, where a lab focused on CTP and the importance of controlling polymer properties (molecular weight, dispersity, sequence) can be fully explored by studying the resulting polymer's optoelectronic behavior and morphology.

This work aims to advance conjugated polymer synthesis by expanding monomer scope of CTP through catalyst design. The implications of this thesis should enable researchers to expand monomer pairings in accessing block copolymers with

conducing/insulating segments in one-pot, to synthesize thiophene-based electron deficient monomers, while also providing a user-friendly CTP route.

References

(1) Bryan, Z. J.; McNeil, A. J. Conjugated Polymer Synthesis via Catalyst-Transfer Polycondensation (CTP): Mechanism, Scope and Applications. *Macromolecules* **2013**, *46*, 8395–8405.

(2) Leone, A. K.; McNeil, A. J. Matchmaking in Catalyst-Transfer Polycondensation: Optimizing Catalysts based on Mechanistic Insight. *Acc. Chem. Res.* **2016**, *49*, 2822–2831.

(3) Baker, M. A.; Tsai, C.-H.; Noonan, K. J. T. Diversifying Cross-Coupling Strategies, Catalysts and Monomers for the Controlled Synthesis of Conjugated Polymers. *Chem. Eur. J.* **2018**, *ASAP*, DOI: 10.1002/chem.201706102.

(4) Souther, K. D.; Leone, A. K.; Vitek, A. K.; Palermo, E. F.; LaPointe, A. M.; Coates, G. W.; Zimmerman, P. M.; McNeil, A. J. Trials and Tribulations of Designing Multitasking Catalysts for Olefin/Thiophene Block Copolymerizations. *J. Polym. Sci. Part A: Polym. Chem.* **2018**, *56*, 132–137.

(5) (a) Cherian, A. E.; Rose, J. M.; Lobkovsky, E. B.; Coates, G. W. A C_2-Symmetric, Living α-Diimine Ni(II) Catalyst: Regioblock Copolymers from Propylene. *J. Am. Chem. Soc.* **2005**, *127*, 13770–13771. (b) Rose, J. M.; Cherian, A. E.; Coates, G. W. Living Polymerization of α-Olefins with an α-Diimine Ni(II) Catalyst: Formation of Well-Defined Ethylene-Propylene Copolymers through Controlled Chain-Walking. *J. Am. Chem. Soc.* **2006**, *128*, 4186–4187. (c) Rose, J. M.; Deplace, F.; Lynd, N. A.; Wang, Z.; Hotta, A.; Lobkovsky, E. B.; Kramer, E. J.; Coates, G. W. C_2-Symmetric Ni(II) α-Diimines Featuring Cumyl-Derived Ligands: Synthesis of Improved Elastomeric Regioblock Polypropylenes. *Macromolecules* **2008**, *41*, 9548–9555.

(6) Leone, A. K.; Souther, K. D.; Vitek, A. K.; LaPointe, A. M.; Coates, G. W.; Zimmerman, P. M.; McNeil, A. J. Mechanistic Insight into Thiophene Catalyst-Transfer Polymerization Mediated by Nickel Diimine Catalysts. *Macromolecules* **2017**, *50*, 9121–9127.

(7) Wang, J.-T.; Saito, K.; Wu, H.-C.; Sun, H.-S.; Hung, C.-C.; Chen, Y.; Isono, T.; Kakuchi, T.; Satoh, T.; Chen, W.-C. High-performance Stretchable Resistive Memories using Donor-Acceptor Block Copolymers with Fluorene Rods and Pendent Isoindigo Coils. *NPG Asia Materials* **2016**, *8*, 1–11.

(8) He, X.; Deng, Y.; Jiang, X.; Wang, Z.; Yang, Y.; Han, Z.; Chen, D. Copolymerization of Norbornene and Butyl Methacrylate at Elevated Temperatures by a Single Centre

Nickel Catalyst Bearing Bulky Bis(α-Diimine) Ligand with Strong Electron-Withdrawing Groups. *Polym. Chem.* **2017**, *8*, 2390–2396.

(9) Sui, A.; Shi, X.; Wang, Y.; Geng, Y.; Wang, F. Kumada Catalyst Transfer Polycondensation for Controlled Synthesis of Polyfluorenes Using 1,3-bis(diarylphosphino)propanes as Ligands. *Polym. Chem.* **2015**, *6*, 4819−4827.

(10) Lanni, E. L.; Locke, J. R.; Gleave, C. M.; McNeil, A. J. Ligand Based Steric Effects in Ni-Catalyzed Chain-Growth Polymerizations Using Bis(dialkylphosphino)ethanes. *Macromolecules* **2011**, *44*, 5136–5145.

(11) Lee, S. R.; Bryan, Z. J.; Wagner, A. M.; McNeil, A. J. Effect of Ligand Electronic Properties on Precatalyst Initiation and Propagation in Ni-Catalyzed Cross-Coupling Polymerizations. *Chem. Sci.* **2012**, *3*, 1562–1566.

(12) Mitoraj; M. P.; Michalak, A. σ-Donor and π-Acceptor Properties of Phosphorus Ligands: An Insight from the Natural Orbitals for Chemical Valence. *Inorg. Chem.* **2010**, *49*, 578–582.

(13) Piliego, C.; Holcombe, T. W.; Douglas, J. D.; Woo, C. W.; Beaujuge, P. M.; Fréchet, J. M. J. Synthetic Control of Structural Order in *N*-Alkylthieno[3,4-*c*]pyrrole-4,6-dione-Based Polymers for Efficient Solar Cells. *J. Am. Chem. Soc.* **2010**, *132*, 7595–7597.

(14) (a) Stathakis, C. I.;Bernhardt, S.; Quint, V.; Knochel, P. Improved Air-Stable Solid Aromatic and Heterocyclic Zinc Reagents by Highly Selective Metalations for Negishi Cross-Couplings. *Angew. Chem. Int. Ed.* **2012**, *51*, 9428–9432. (b) Manolikakes, S. M.; Ellwart, M.; Stathakis, C. I.; Knochel, P. Air-Stable Solid Aryl and Heteroaryl Organozinc Pivalates: Syntheses and Applications in Organic Synthesis. *Chem. Eur. J.* **2014**, *20*, 12289–12297.

Appendix 1

Supporting Information for Chapter 2

Trials and Tribulations of Designing Multitasking Catalysts for Olefin/Thiophene Block Copolymerizations

I. Materials

Flash chromatography was performed on SiliCycle silica gel (40–63 μm). Thin layer chromatography was performed on Merck TLC plates (pre-coated with silica gel 60 F254). iPrMgCl (2M in THF) was purchased in 25 mL quantities from Aldrich. All other reagent grade materials and solvents were purchased from Aldrich, Acros, ArkPharm, or Fisher and used without further purification unless otherwise noted. 3HT was purified via flash chromatography with hexanes as the eluent. THF was dried and deoxygenated using an Innovative Technology solvent purification system composed of activated alumina, a copper catalyst, and molecular sieves. The glovebox in which specified procedures were carried out was an MBraun LABmaster 130 with a N_2 atmosphere and H_2O levels below 4 ppm. Compounds **S1**,[1] **S2**,[1] **C1**,[1] **C2**,[2] **C3**[2] were prepared using modified literature procedures.

II. General Experimental

NMR Spectroscopy: Unless otherwise noted, ^{1}H and ^{13}C spectra for all compounds were acquired at rt in CD_2Cl_2, $CDCl_3$, C_6D_6 on a Varian vnmrs 700 operating at 700 and 176 MHz or a Varian vnmrs 500 operating at 500 and 126 MHz, respectively. For ^{1}H and ^{13}C spectra in deuterated solvents, the chemical shift data are reported in units of δ (ppm) relative to tetramethylsilane (TMS) and referenced with residual solvent. Multiplicities are reported as follows: singlet (s), doublet (d), apparent doublet, (ad), doublet of doublets (dd), apparent doublet of doublets (add), triplet (t), apparent triplet (at), quartet (q), multiplet (m), and broad resonance (br). * denotes Si grease.

Mass Spectrometry: HRMS data were obtained on a Micromass AutoSpec Ultima Magnetic Sector mass spectrometer.

MALDI-TOF-MS: MALDI-TOF mass spectra were recorded using a Bruker AutoFlex Speed in linear or reflectron mode. The matrix trans-2-[3-(4-tert-butylphenyl)-2-methyl-2-propenylidene]malononitrile (DCTB), was prepared at a concentration of 0.1M in $CHCl_3$. The instrument was calibrated with a sample of polythiophene with H/Br endgroups. The polymer sample was dissolved in THF or CH_2Cl_2 to obtain an approx.1 mg/mL solution. A 2.5 μL aliquot of polymer solution was mixed with 2.5 μL of the DCTB. This mixture (1 μL) was placed on the target plate and then air-dried. The data was analyzed using flexAnalysis.

Gel-Permeation Chromatography: Polymer molecular weights were determined by comparison with polystyrene standards (Varian, EasiCal PS-2 MW 580–377,400) on a Malvern Viscotek GPCMax VE2001 equipped with two Viscotek LT-5000L 8 mm (ID) × 300 mm (L) columns and analyzed with Viscotek TDA 305 (with R.I., UV-PDA detector model 2600 (190–500 nm), RALS/LALS, and viscometer). Samples were dissolved in THF (with mild heating) and passed through a 0.2 μm PTFE filter prior to analysis. The RI detector was used for determining poly(olefin) MWs while the UV-PDA detector was used for determining poly(thiophene) and poly(olefin)-*b*-poly(thiophene) MWs.

Titrations of the Grignard Reagents: An accurately weighed sample of salicylaldehyde phenylhydrazone[3] (typically between 90–100 mg) was dissolved in 5.00 mL of THF. An aliquot (0.25 mL) of this solution was stirred at rt while the Grignard of interest was added dropwise using a 500 μL syringe. The initial solution is yellow and turns bright orange at the end-point.

Gas Chromatography: Gas chromatography was carried out using a Shimadzu GC 2010 containing a Shimadzu SHRX5 (crossbound 5% diphenyl – 95% dimethyl polysiloxane; 15 m, 0.25 mm ID, 0.25 μm df) column.

III. Synthetic Procedures of S1, S2, C1, C2, C3

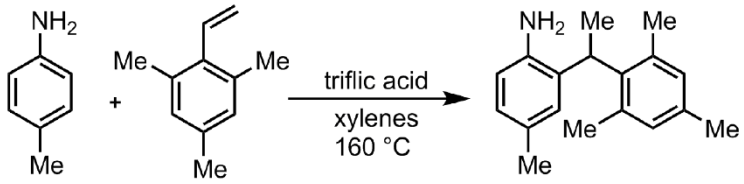

S1

2-(1-mesitylethyl)-4-methylaniline (S1): To a 50 mL bomb flask equipped with a stir bar were added 2,4,6-trimethylstyrene (1.07 mL, 6.62 mmol, 1.0 equiv), ρ-toluidine (1.06 g, 9.93 mmol, 1.5 equiv) and xylenes (1.73 mL). To the stirring solution was added triflic acid (0.12 mL, 1.3 mmol, 0.2 equiv). The flask was sealed and stirred at 160 °C for 18 h. After 18 h the reaction solution was cooled to rt, diluted with EtOAc (10 mL), transferred to a round-bottom flask, concentrated *in vacuo*, and subjected to flash chromatography with hexanes/EtOAc (90:10) as the eluent to produce 709 mg of **S1** as a white solid (42% yield). HRMS (EI): Calcd. for $C_{18}H_{23}N$ [M] 253.1830, found 253.1835.

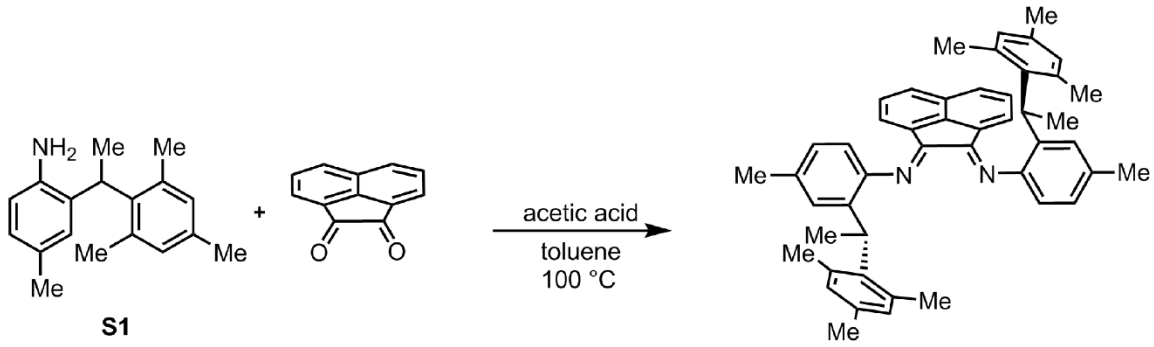

S1 **S2**

(1E,2E)-N1-N2-bis(2-(1-mesitylethyl)-4-methylphenyl)acenaphthylene-1,2-diimine (S2): To a 20 mL vial equipped with a stir bar were added **S1** (171 mg, 0.675 mmol, 2.05 equiv), acenaphthylenequinone (60.1 mg, 0.329 mmol, 1.0 equiv), glacial acetic acid (0.75 mL, 13 mmol, 40 equiv), and toluene (0.39 mL). The reaction was stirred at 100 °C for 3 h and then cooled to rt. The yellow precipitate that formed after cooling was then collected by vacuum filtration, washed with MeOH (10 mL) and hexanes (10 mL), and dried under vacuum to produce 144 mg of **S2** as a yellow solid (77% yield). HRMS (EI): Calcd. for $C_{48}H_{48}N_2$ [M] 652.3817, found, 652.3829.

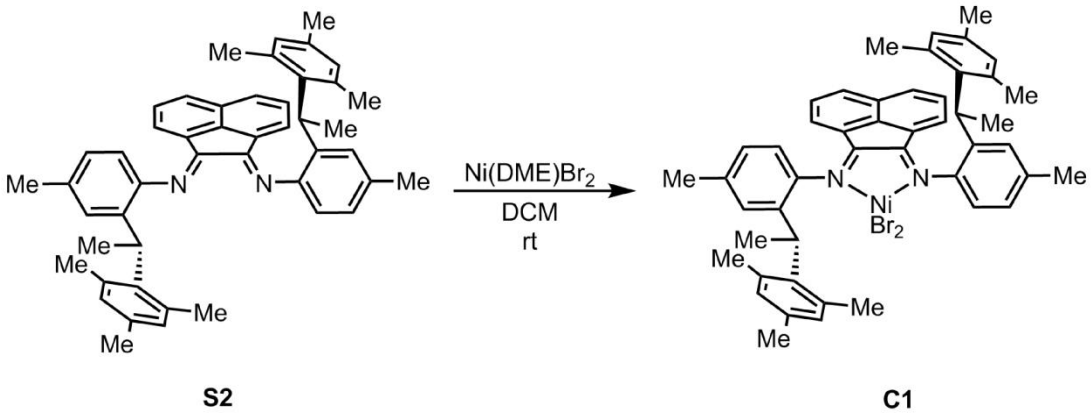

S2 C1

(1E,2E)-N1-N2-bis(2-(1-mesitylethyl)-4-methylphenyl)acenapythylene-1,2-diimine nickel dibromide (C1): To a 50 mL Schlenk flask equipped with a stir bar was added **S2** (152 mg, 0.233 mmol, 1.00 equiv), Ni(DME)Br_2 (75.0 mg, 0.244 mmol, 1.05 equiv) and DCM (4.7 mL). The flask was sealed with a rubber septum and the reaction stirred for 16 h at rt under an N_2 atmosphere. The dark red solution was then filtered through celite and concentrated *in vacuo*. The crude product was redissolved in a minimal amount of DCM (3 mL), layered with pentanes (20 mL), and recrystallized in a -20 °C freezer to afford 126 mg of **C1** as dark red crystals (62% yield).

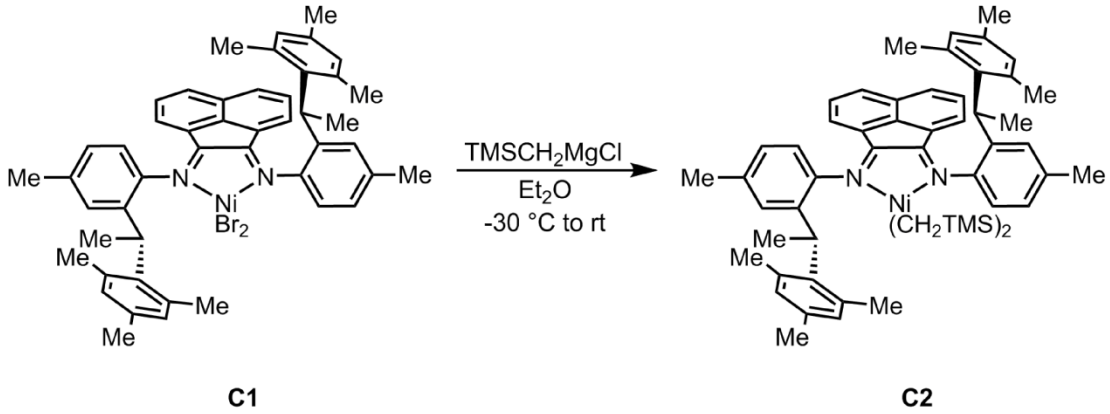

C1 C2

(1E,2E)-N1-N2-bis(2-(1-mesitylethyl)-4-methylphenyl)acenaphthylene-1,2-diimine nickel bismethylenetrimethylsilyl (C2): In the glovebox were added **C1** (119 mg, 0.137 mmol, 1.0 equiv) and Et_2O (3.7 mL) to a 20 mL vial equipped with a stir bar. The vial was sealed with a teflon cap and placed in the freezer (-30 °C) for 15 min. After 15 min, the vial was removed and to the stirring mixture was added $TMSCH_2MgCl$ (340 µL, 0.850 M in Et_2O, 3.00 equiv). The reaction was warmed to rt and stirred for 30 min after which the initial dark green solution turned dark purple. The Et_2O was removed under high vac until 0.5 mL remained, then cold MeOH (5 mL) was added and the solution was passed through a syringe equipped with a 0.2 µm PTFE filter into a 20 mL vial. The solvent was removed under vacuum giving 55 mg of **C2** as a purple solid (45% yield).

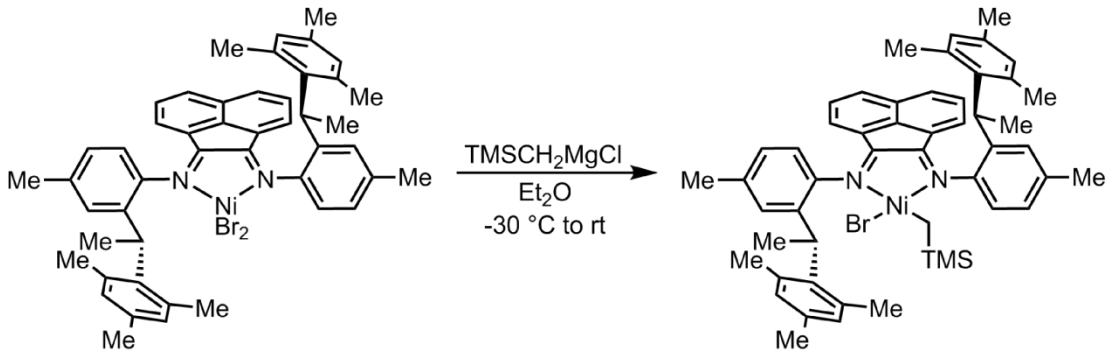

C1 **C3**

(1E,2E)-N1-N2-bis(2-(1-mesitylethyl)-4-methylphenyl)acenaphthylene-1,2-diimine nickel monomethylenetrimethylsilyl monobromide (C3): In the glovebox were added **C1** (14.0 mg, 0.0169 mmol, 1.00 equiv) and Et_2O (0.45 mL) to a 20 mL vial equipped with a stir bar. The vial was sealed with a teflon cap and placed in the freezer (-30 °C) for 15 min. After 15 min, the vial was removed and to the stirring mixture was added $TMSCH_2MgCl$ (17.0 µL, 0.0145 mmol, 0.850 M in Et_2O, 0.900 equiv). The reaction was warmed to rt and stirred for 30 min, turning a dark green over time. After 30 min, the Et_2O solution was filtered through a glass wool plug to remove unreacted **C1**. The glass wool plug was rinsed with additional Et_2O (2.0 mL). The solvent was removed under high vac to produce a dark green solid. The solid was then dissolved in cold MeOH (1.0 mL) and filtered through a glass wool plug to produce a dark green filtrate. The solvent was removed under vacuum giving a green solid. The solid was dissolved in a minimal amount of Et_2O (0.5 mL) and pentane (5 mL) was added to the vial, producing a green precipitate. The mixture was filtered through a glass wool plug, leaving behind the solid at the top of the plug. This solid was rinsed with additional pentanes (1 mL). The solid was then redissolved in THF (1 mL) by passing the solvent through the glass wool plug into a new 20 mL vial. The solvent was then removed under vacuum to yield 7 mg of **C3**. (50% yield).

IV. NMR spectra of S1, S2, C1, C2, C3

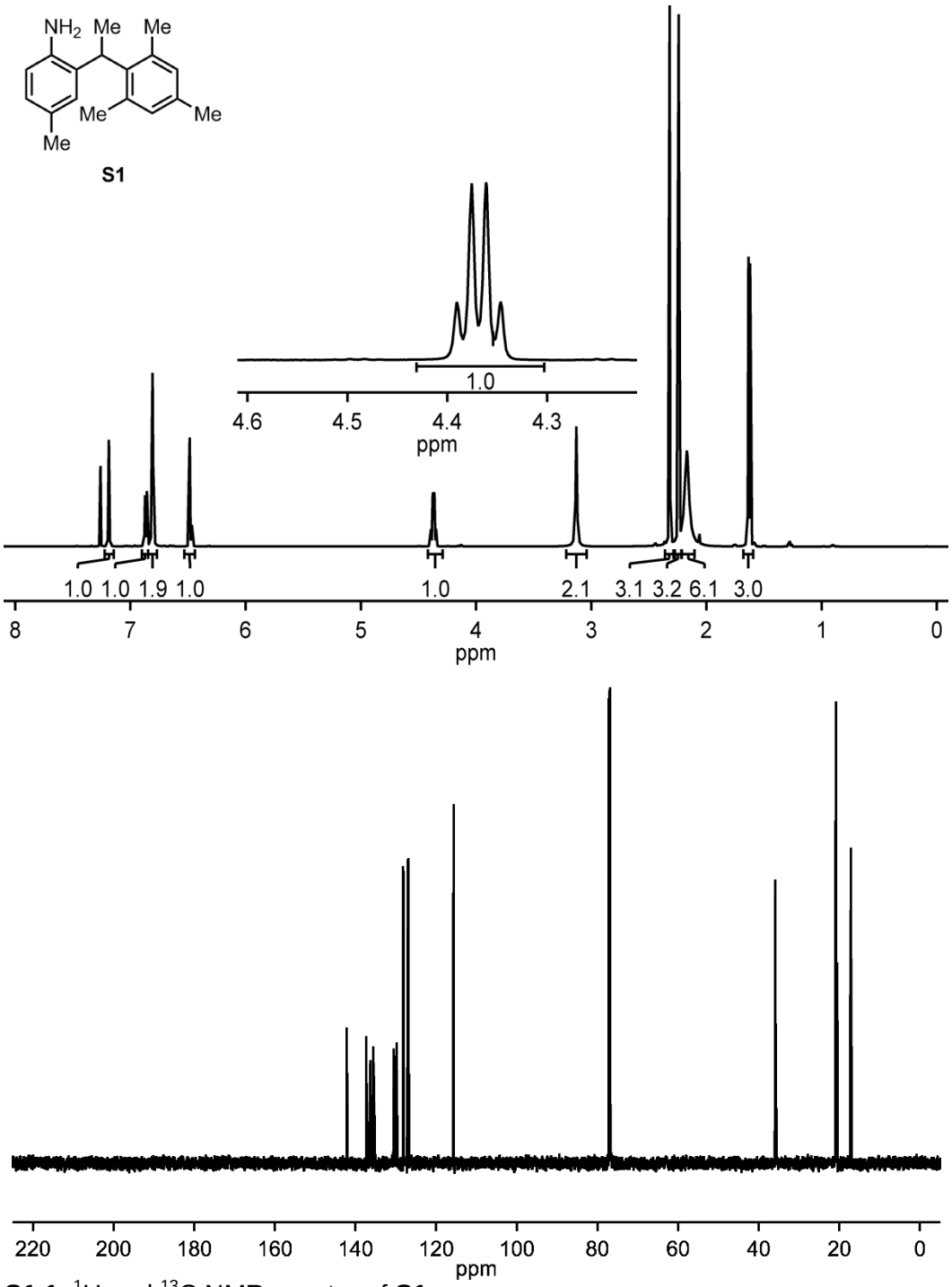

Figure S1.1. ^{1}H and ^{13}C NMR spectra of **S1**

^{1}H NMR (500 MHz, $CDCl_3$) δ 7.19 (s, 1H), 6.86 (dd, *J* = 7.9, 1.9 Hz, 1H), 6.81 (s, 2H), 6.48 (d, *J* = 7.9 Hz, 1H), 4.37 (q, *J* = 7.3 Hz, 1H), 3.13 (s, 2H), 2.32 (s, 3H), 2.24 (s, 3H), 2.17 (br s, 6H), 1.63 (d, *J* = 7.3 Hz, 3H)

^{13}C NMR (126 MHz, $CDCl_3$) δ 142.21, 137.36, 136.32, 135.64, 130.49, 129.80, 128.17, 127.23, 126.98, 115.72, 35.91, 20.89, 20.77, 20.57, 17.17

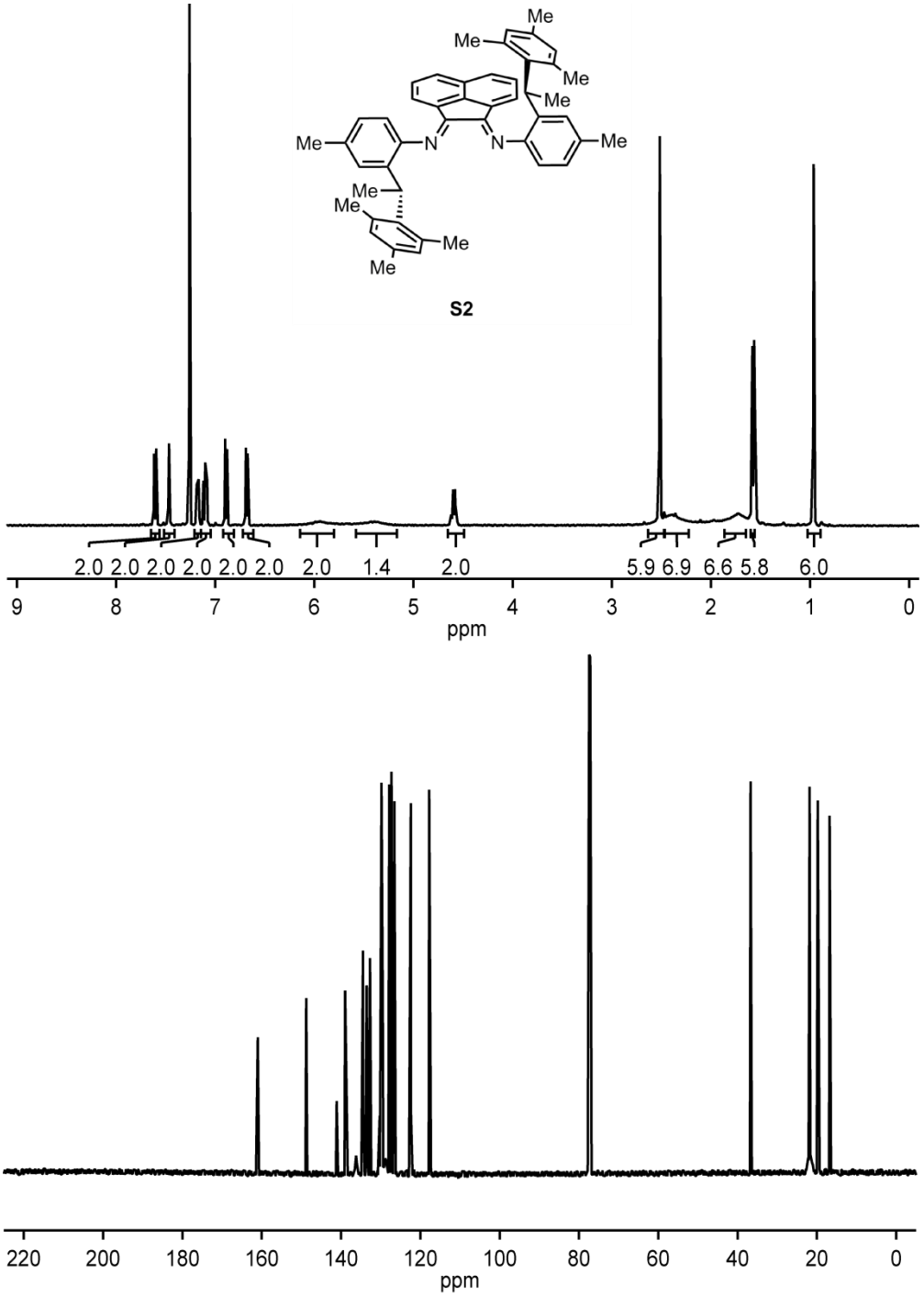

Figure S1.2. ^{1}H and ^{13}C NMR spectra of **S2**
^{1}H NMR (500 MHz $CDCl_3$) δ 7.61 (d, *J* = 8.2 Hz, 2H), 7.46 (d, *J* = 1.8 Hz, 2H), 7.18 (dd, *J* = 8.2, 1.8 Hz, 2H), 7.10 (dd, *J* = 8.2, 7.2 Hz, 2H), 6.89 (d, *J* = 7.8 Hz, 2H), 6.68 (d, *J* = 7.2 Hz, 2H), 5.95 (br s, 2H), 5.40 (br s, 2H), 4.59 (q, *J* = 7.4 Hz, 2H), 2.52 (s, 6H), 2.38 (br s, 6H), 1.73 (br s, 6H), 1.57 (d, *J* = 7.4 Hz, 6H), 0.96 (s, 6H)
^{13}C NMR (126 MHz, $CDCl_3$) δ 160.75, 148.55, 140.87, 138.74, 136.7 (br), 134.21, 133.32, 132.45, 130.02, 129.56, 129.25, 127.60, 127.03, 126.33, 122.16, 117.53, 36.50, 25.77, 21.60, 19.55, 16.56

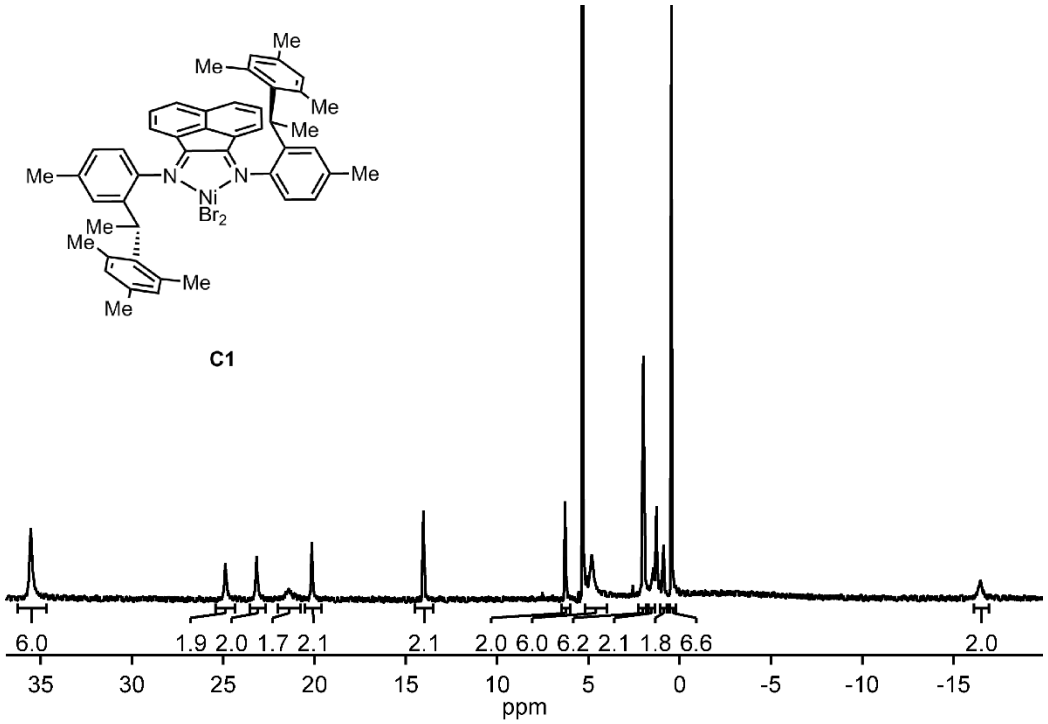

Figure S1.3. ^{1}H NMR spectrum of **C1**

^{1}H NMR (500 MHz CD_2Cl_2) δ 35.53 (s, 6H), 24.88 (s, 2H), 23.17 (s, 2H), 21.45 (br s, 2H), 20.14 (s, 2H), 14.03 (s, 2H), 6.27 (s, 2H), 4.82 (br s, 6H), 1.99 (s, 6H), 1.44 (s, 2H) 0.87 (s, 2H), 0.45 (s, 6H), -16.43 (br s, 2H) (One Ar-CH_3 (6H) is unaccounted for. Spectrum matches literature[1])

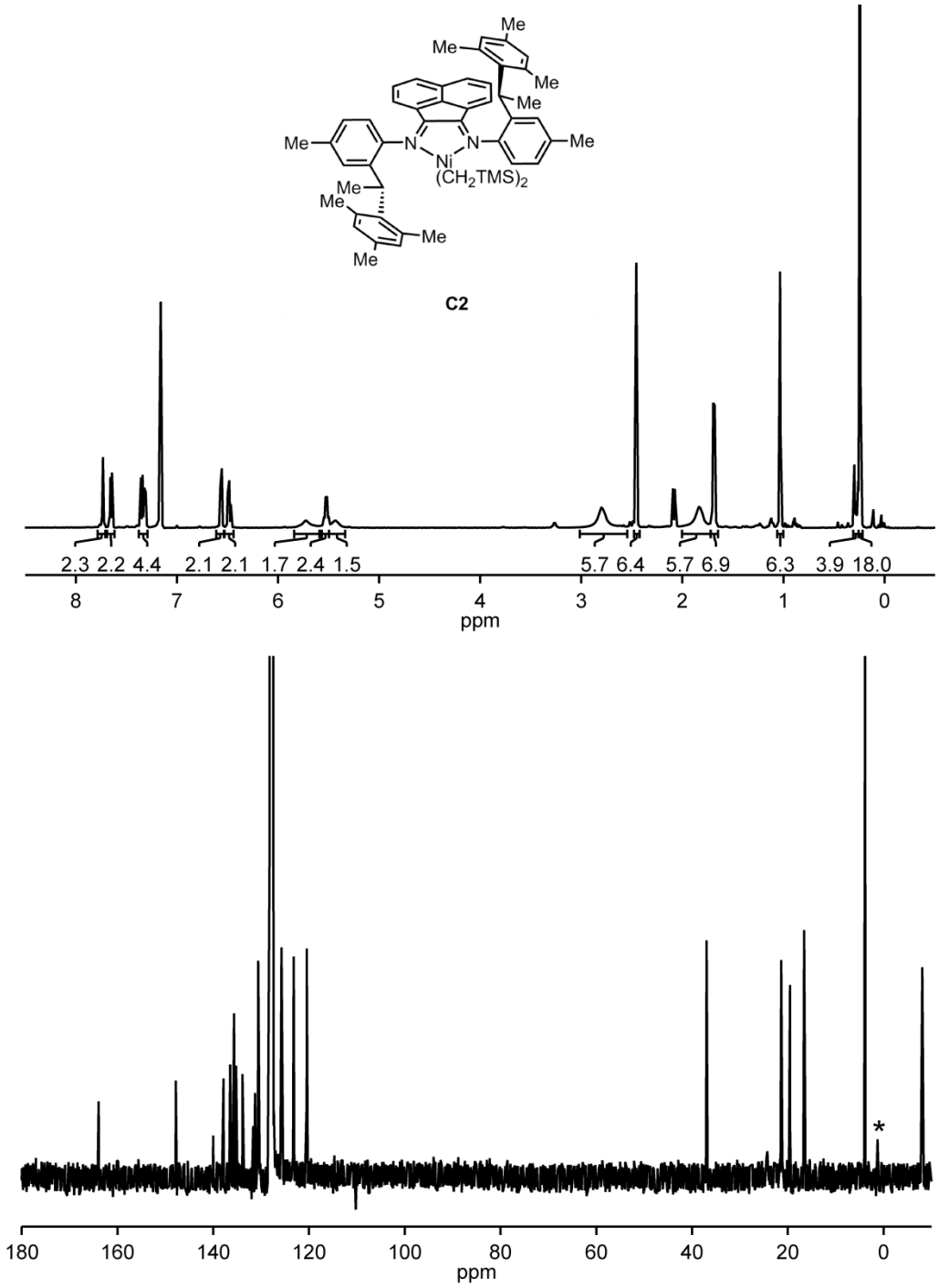

Figure S1.4. ^{1}H and ^{13}C NMR spectra of **C2**
^{1}H NMR (700 MHz, C_6D_6) δ 7.73 (s, 2H), 7.65 (d, *J* = 7.7 Hz, 2H), 7.35 (d, *J* = 8.2 Hz, 2H), 7.32 (d, *J* = 7.8 Hz, 2H), 6.56 (ad, J = 7.2 Hz, 2H), 6.48 (dd, *J* = 7.8, 7.7 Hz, 2H), 5.72 (br s, 2H), 5.52 (q, *J* = 7.4 Hz, 2H), 5.43 (br s, 2H), 2.80 (s, 6H), 2.46 (s, 6H), 1.83 (s, 6H), 1.69 (d, *J* = 7.4 Hz, 6H), 1.03 (s, 6H), 0.33 (m, 4H), 0.24 (s, 18H)
^{13}C NMR (176 MHz, C_6D_6) δ 163.93, 147.81, 140.02, 137.85, 136.46, 135.65, 135.22, 133.89, 131.66, 131.26, 130.60, 127.33, 123.19, 120.47, 36.96, 24.07, 21.37, 19.54, 16.59, 3.85, –8.09 (* denotes Si grease)

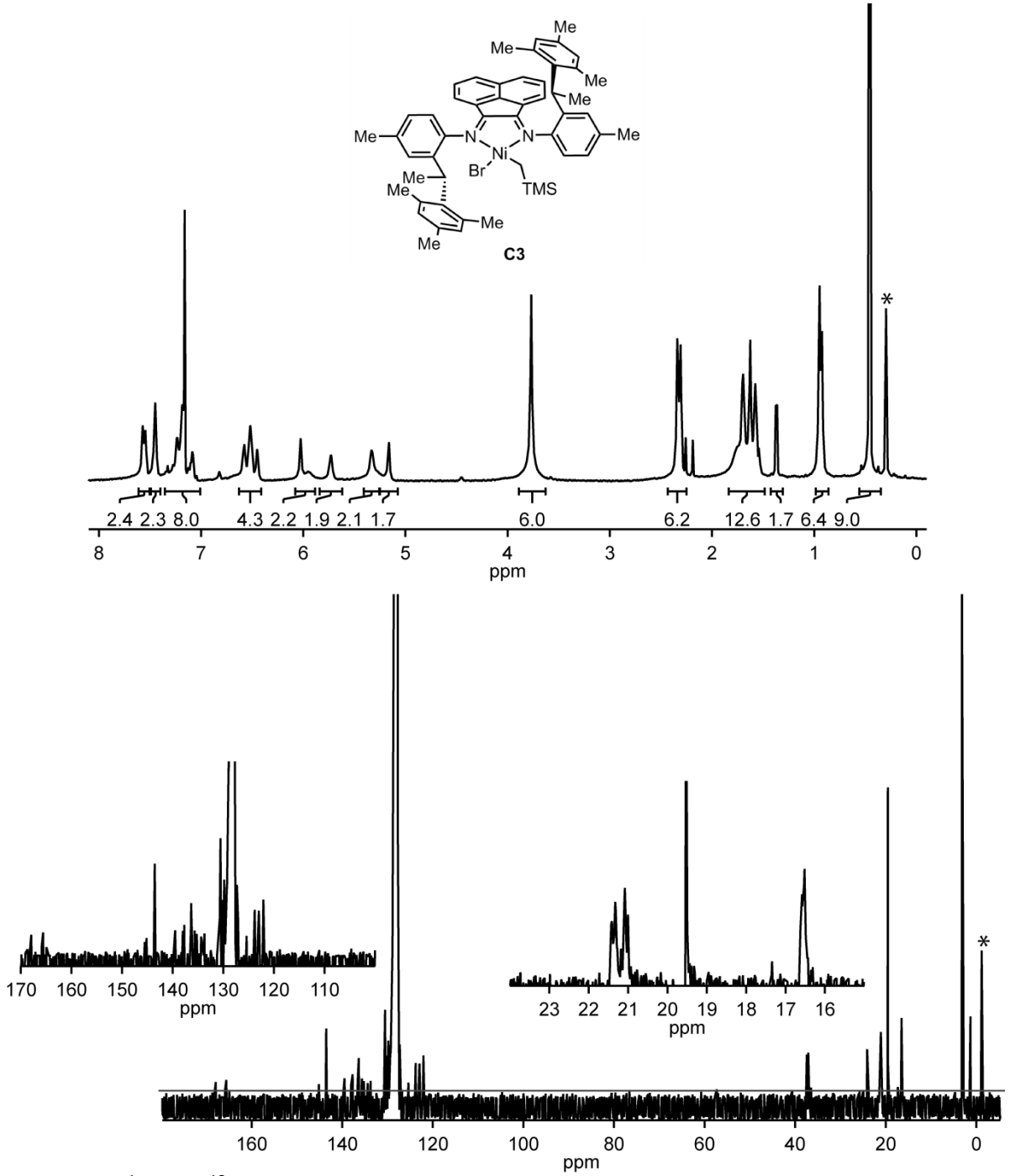

Figure S1.5. ^{1}H and ^{13}C NMR spectra of **C3**

^{1}H NMR (700 MHz, C_6D_6) δ 7.56 (ad, 2H), 7.45 (s, 2H), 7.36 – 7.00 (m, 2H(C3), 6H (C_6D_6)), 6.52 (at, 4H), 6.14 – 5.87 (m, 2H), 5.73 (br s, 2H), 5.33 (br s, 2H), 5.16 (br s, 2H), 3.77 (s, 6H), 2.32 (ad, 6H), 1.87– 1.47 (m, 12H), 1.37 (d, *J* = 9.4 Hz, 2H), 0.94 (add, 6H), 0.46 (s, 9H)

^{13}C NMR(176 MHz, C_6D_6) δ 167.95, 165.59, 143.54, 139.54, 138.06, 138.00, 137.70, 136.55, 136.52, 136.12, 136.09, 136.08,135.65, 135.62, 135.23, 135.21, 135.19, 134.36, 134.34, 133.76, 133.72, 130.66, 130.55, 130.21, 127.25, 127.07, 125.38, 123.79, 122.95, 122.09, 121.93, 37.43, 37.10, 24.11, 21.43, 21.41, 21.33, 21.09, 21.00, 19.53, 16.51, 3.19, 1.30

(⎯ = baseline used, * denotes Si grease)

V. Polymerization of 3HT monomer with precatalyst C1 and Et_2AlCl

General Procedure: Activation of 2,5-dibromo-3-hexylthiophene with iPrMgCl

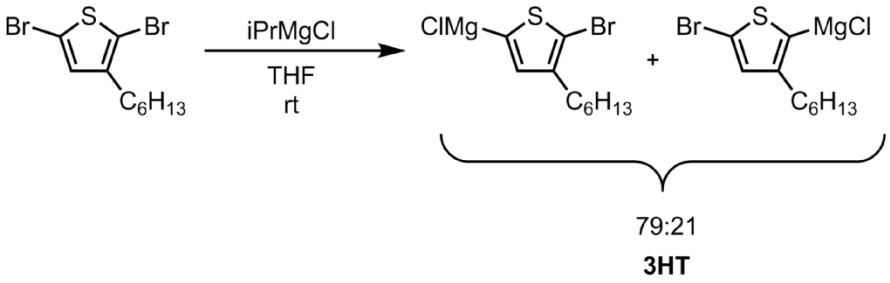

In the glovebox 2,5-dibromo-3-hexylthiophene (169 mg, 0.518 mmol, 1 equiv) was added to a 20 mL vial equipped with a stir bar, n-docosane (approx. 4.0 mg) and THF (4.99 mL). To the stirring solution was added iPrMgCl (196 µL, 0.363 mmol, 2.00 M in THF, 0.900 equiv) and stirred for 30 min. **3HT** was titrated to be 0.071 M using salicylaldehyde phenylhydrazone. An aliquot (0.3 mL) of **3HT** was quenched with aq. HCl (0.50 mL, 12 M) outside of the box. The quenched monomer was extracted with $CHCl_3$ (2.0 mL), dried over $MgSO_4$, and analyzed by GC to show a mixture of regioisomers (79:21).

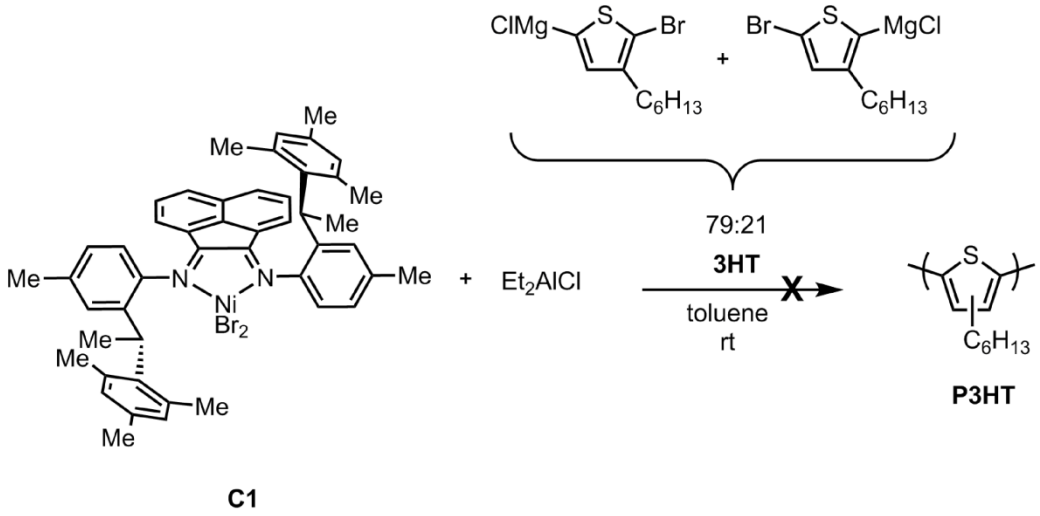

In the glovebox to a 20 mL vial equipped with a stir bar were added Et_2AlCl (0.14 mL, 1.6 M in toluene, 200 equiv), toluene (2.5 mL), and **C1** (2.8 mg, 0.0060 mmol, 1 equiv) in 0.5 mL DCM to yield a purple opaque solution. To the stirring solution was added **3HT** (1.00 mL, 0.0720 mmol, 100 equiv). After 30 min the reaction was taken out of the box and quenched with aq. HCl (2 mL, 12 M). The reaction mixture was extracted with $CHCl_3$ (5 mL), dried over $MgSO_4$, filtered through a glass wool plug and split into two portions. The first portion was analyzed by GC showing 24% conversion of **3HT**. All solvent was removed from the other portion under reduced pressure. The oil was then dissolved in THF:PhMe (99:1) with mild heating, passed through a PTFE filter (0.2 µm), and analyzed by GPC.

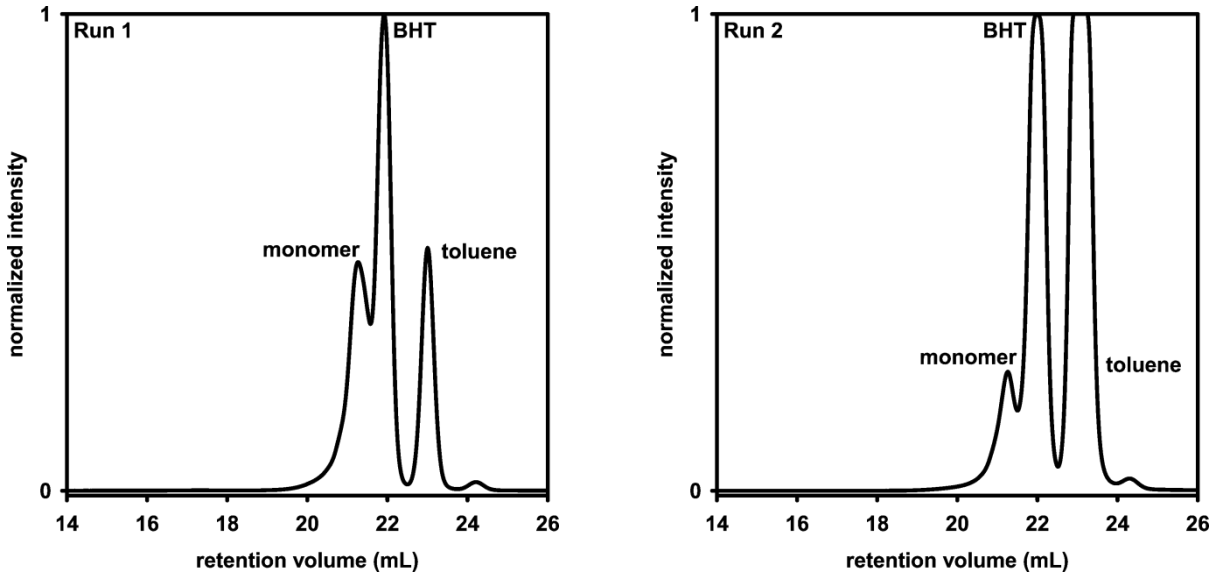

Figure S1.6. GPC trace for polymerization of **3HT** monomer with catalyst **C1** and **Et_2AlCl**. (BHT (Butylated hydroxytoluene) = THF stabilizer)

VI. Polymerization of 1-hexene monomer with precatalyst C2 and $B(C_6F_5)_3$

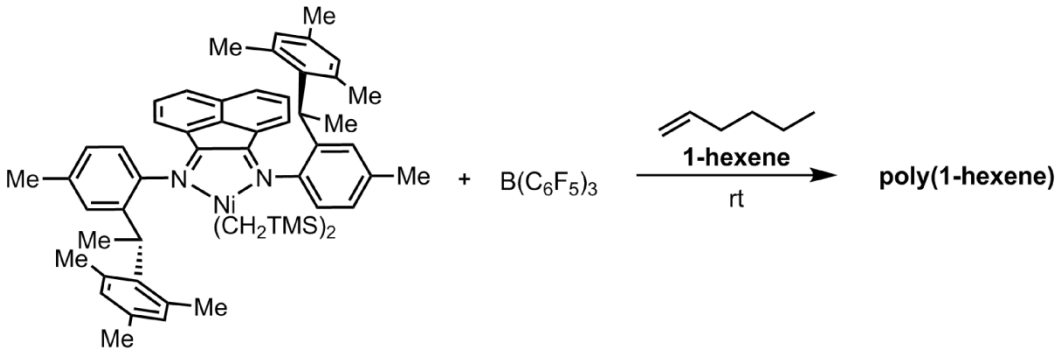

C2

To a 4 mL vial in the glovebox were added **C2** (2.7 mg, 0.0030 mmol, 1.0 equiv) and 1-hexene (1.00 mL). This solution was then passed through a syringe fitted with a PTFE filter (0.2 µm) into a 20 mL vial equipped with a stir bar. In another 4 mL vial were added **$B(C_6F_5)_3$** (3.1 mg, 0.0061 mmol, 2.0 equiv) and 1-hexene (0.50 mL). The **$B(C_6F_5)_3$** solution was then injected into the **C2** solution. The solution immediately turned dark green and then transitioned to a light pink. The polymerization was stirred for 5 min, turning slightly viscous, before being quenched outside of the box with MeOH (3 mL), precipitating **poly(1-hexene)** as a white solid (13.0 mg). The solvent was removed by decanting and the polymer was dissolved in THF:PhMe (99:1) (1.5 mL), and after mild heating passed through a PTFE filter (0.2 µm) to be analyzed by GPC. Integrated area on GPC trace is from retention volume of 14 mL to 20 mL.

Run 1: M_n **=** 78.2 kDa, **Đ =** 1.60 (13.0 mg)
Run 2: M_n **=** 64.1 kDa**, Đ =** 1.59 (8.0 mg)

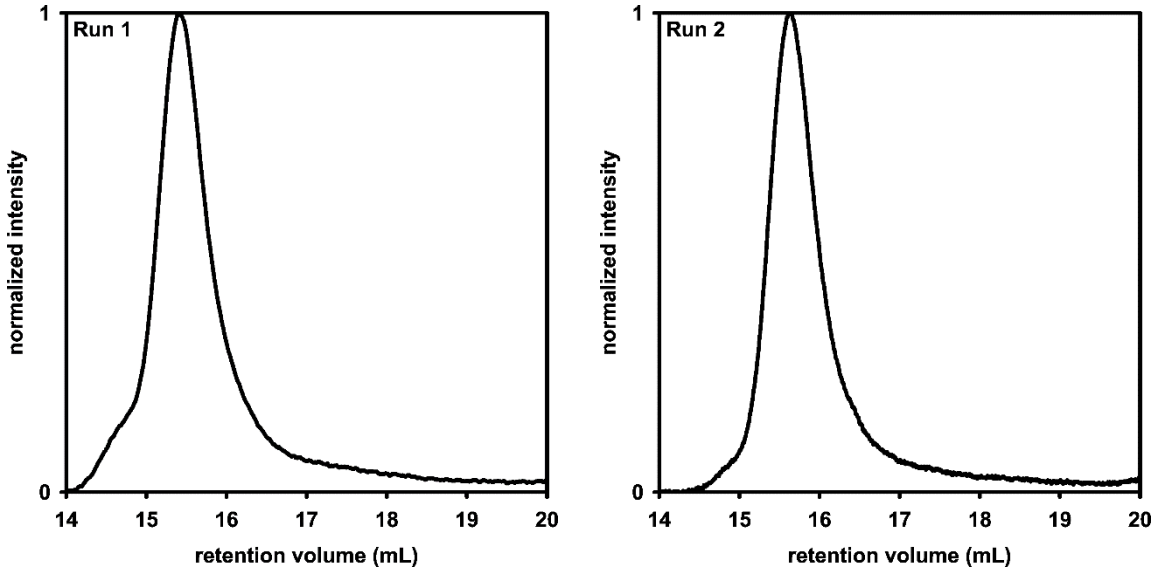

Figure S1.7. GPC trace for polymerization of **1-hexene** monomer with catalyst **C2** and **$B(C_6F_5)_3$.**

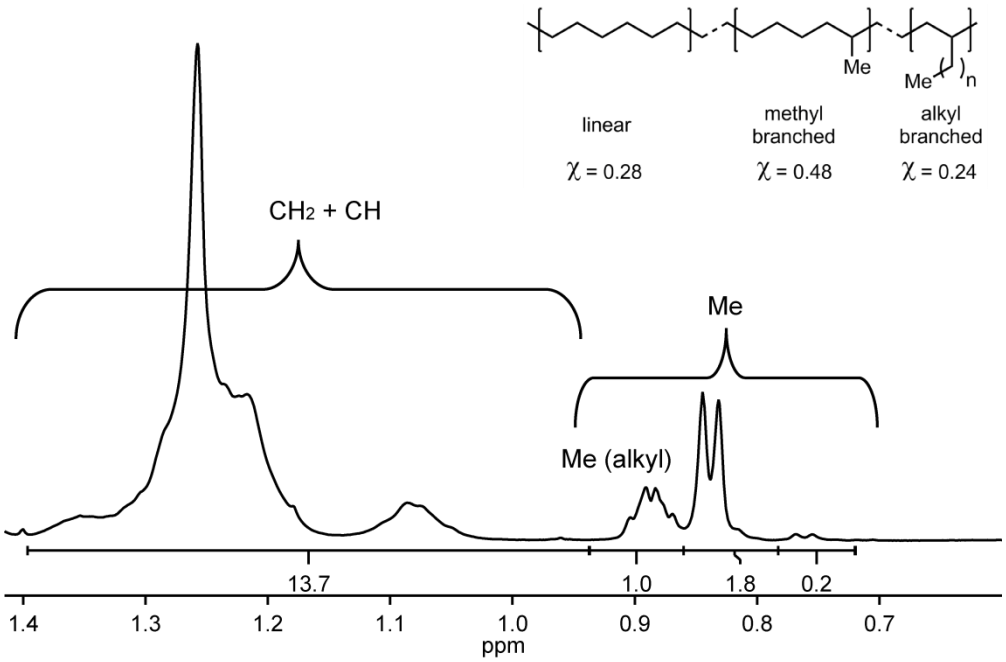

Figure S1.8. ^{1}H NMR spectrum of **poly(1-hexene)** generated with catalyst **C2** and **$B(C_6F_5)_3$**

$$R = \frac{[CH_3]}{[CH_2]} = \frac{(3/3)}{(13.7-1)/2} = 0.157$$

$$\chi_{linear} = \frac{[1-(\omega-2)R]}{[1+2R]} = 0.280$$

carbons in 1-hexene = $\omega = 6$

$$\chi_{alkyl} + \chi_{methyl} = 1 - \chi_{linear} = 0.717$$

$$\frac{\chi_{alkyl}}{\chi_{methyl}} = \frac{CH_3\,(Me\,(alkyl))}{CH_3\,(Me)} = \frac{1.0}{2.0} = 0.500$$

$$\chi_{alkyl} = (0.50)\,\chi_{methyl}$$

$$(0.50)\,\chi_{methyl} + \chi_{methyl} = 0.717$$

$$\chi_{methyl} = 0.480$$

$$\chi_{alkyl} = 0.240$$

Equation S1.1. Calculating br/1000C of **poly(1-hexene)** using ^{1}H NMR spectroscopy[3]

Procedure: M_n versus time of 1-hexene polymerization with precatalyst C2 and $B(C_6F_5)_3$

C2 and $B(C_6F_5)_3$ stock solutions

In the glovebox were added **C2** (12.0 mg, 0.014 mmol, 0.50 mM) and 1-hexene (2.71 mL) to a 20 mL vial. In another 20 mL vial were added **$B(C_6F_5)_3$** (19 mg, 0.0074 mmol, 0.50 mM) and 1-hexene (7.42 mL).

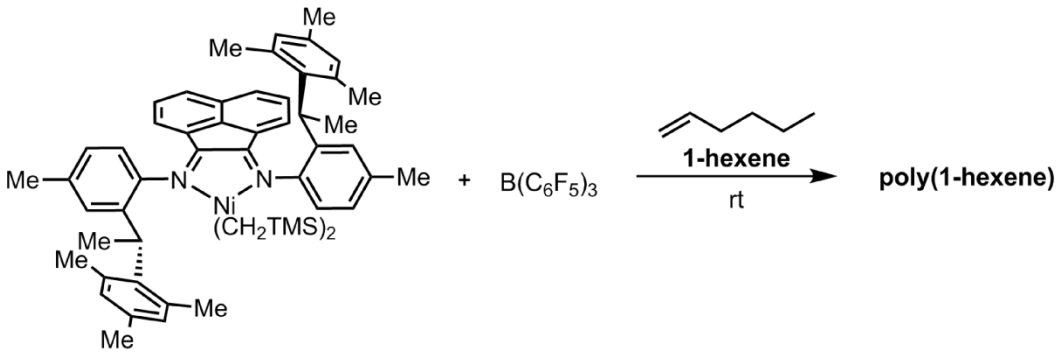

C2

In the glovebox to a 20 mL vial equipped with a stir bar were added **C2** (0.50 mL, 0.0025 mmol, 0.50 mM solution in 1-hexene, 1.0 equiv) and **$B(C_6F_5)_3$** (1.0 mL, 0.0050 mmol, 0.50 mM solution in 1-hexene, 2.0 equiv). Aliquots were taken at 125, 210, 290, 385, and 530 s. Each aliquot was taken out of the glovebox and quenched with MeOH. If polymer did not precipitate, the solvent was removed under reduced pressure. If polymer did precipitate after quenching, the solvent was removed by decanting. The aliquots were then dissolved in THF:PhMe (99:1) (1.5 mL) and after mild heating were passed through a PTFE filter (0.2 µm) to be analyzed by GPC.

Run 1

aliquot (sec)	M_n (kDa)	Đ
125	27.2	1.27
210	39.2	1.34
290	49.6	1.38
385	60.0	1.41
530	69.0	1.45

Run 2

aliquot (sec)	M_n (kDa)	Đ
180	30.8	1.57
255	37.3	1.59
360	46.9	1.53
480	57.8	1.51

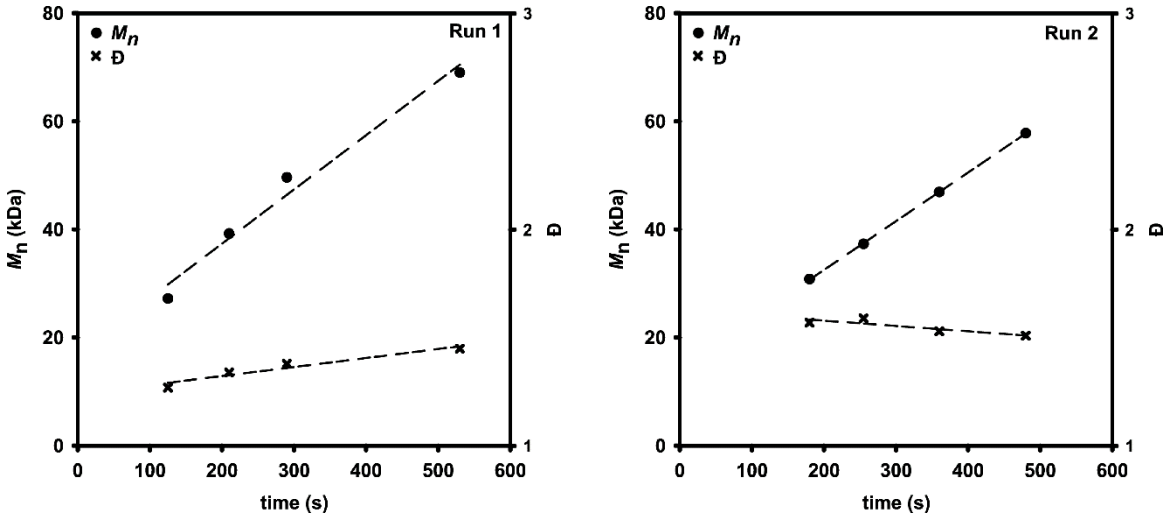

Figure S1.9. M_n versus time for polymerizing **1-hexene** monomer with precatalyst **C2** and **$B(C_6F_5)_3$.**

VII. Polymerization of 3HT monomer with precatalyst C2 and $B(C_6F_5)_3$

Activation of 2,5-dibromo-3-hexylthiophene with iPrMgCl

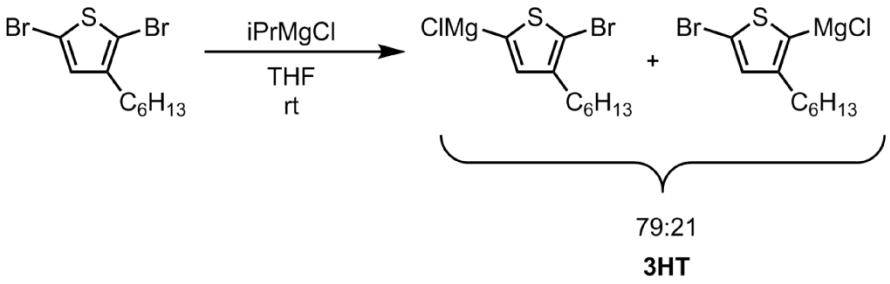

In the glovebox 2,5-dibromo-3-hexylthiophene (90.0 mg, 0.276 mmol, 1.00 equiv) was added to a 20 mL vial equipped with a stir bar, n-docosane std. (approx. 4 mg) and THF (2.66 mL). To the stirring solution was added iPrMgCl (100 µL, 0.193 mmol, 1.89 M in THF, 0.700 equiv) and stirred for 30 min. **3HT** was titrated to be 0.071 M using salicylaldehyde phenylhydrazone. An aliquot (0.3 mL) of the Grignard solution was quenched with aq. HCl (0.5 mL, 12M) outside of the glovebox. The quenched monomer was extracted with $CHCl_3$ (2 mL), dried over $MgSO_4$, and analyzed by GC to show a mixture of regioisomers (79:21).

C2 and $B(C_6F_5)_3$ stock solutions

In the glovebox were added **C2** (5.2 mg, 0.0059 mmol, 0.50 mM) and toluene (1.18 mL) to a 4 mL vial. In another 4 mL vial were added **$B(C_6F_5)_3$** (3.8 mg, 0.0074 mmol, 0.50 mM) and toluene (1.48 mL). **C2** solutions were made fresh for each **3HT** polymerization

Activation of precatalyst C2 with $B(C_6F_5)_3$

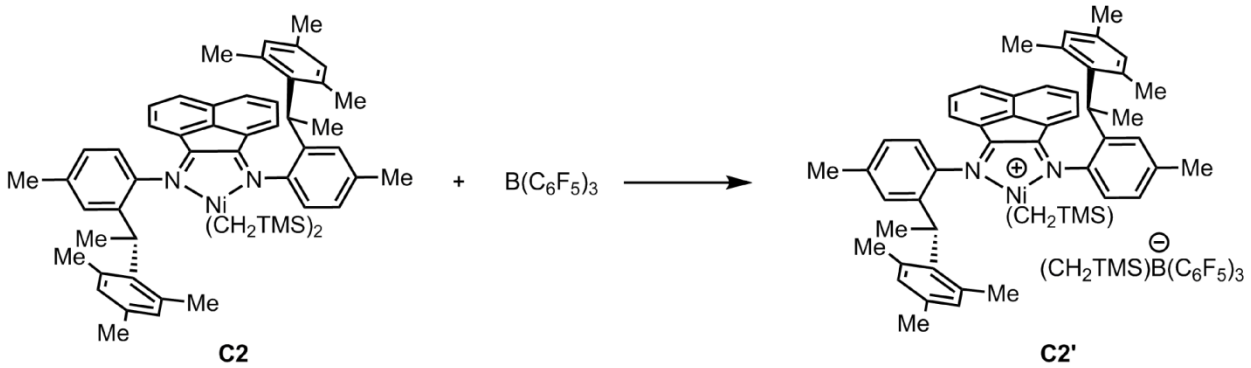

C2 (0.11 mL, 0.50 mM in toluene, 1.0 equiv) and **$B(C_6F_5)_3$** (0.11 mL, 0.50 mM in toluene, 1.0 equiv) were added to a 4 mL vial equipped with a stir bar and stirred for 5 min. **C2'** solution must be made fresh for each **3HT** polymerization.

Procedure: Polymerization of 3HT monomer with catalyst C2'

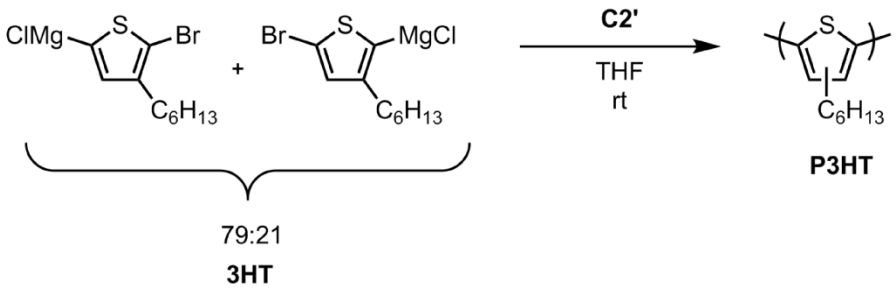

In the glovebox to a 20 mL vial equipped with a stir bar was added **3HT** (1.00 mL, 0.0700 mmol, 125 equiv relative to **C2'**) and THF (1.63 mL) to give an overall [**3HT**] of 0.02 M. To the stirring solution was added **C2'** (0.22 mL, 0.57 µmol, 1.0 equiv). The polymerization was stirred for 1 h before being quenched outside of the box with aq. HCl (2.0 mL, 12 M). The reaction mixture was extracted with $CHCl_3$ (5.0 mL), dried over $MgSO_4$, and filtered through glass wool. The organic layer was then split into two equal portions. The first portion was diluted with additional $CHCl_3$ (2.0 mL) and analyzed by GC to show 70% conversion. The other portion was concentrated in vacuo and then redissolved in THF:PhMe (99:1) (1.5 mL) with mild heating, passed through a PTFE filter (0.2 µm), and analyzed by GPC. After GC and GPC analysis, both portions were recombined and the solvent removed *in vacuo* to yield a purple solid. The solid was dissolved in a minimum amount of $CHCl_3$ (0.5 mL), and precipitated with MeOH (15.0 mL). The mixture was then centrifuged, the solvent decanted, and the solid dried under vacuum to afford **P3HT** as a purple solid. Regioregularity of P3HT was calculated to be 75%.

Run 1: M_n **=** 23.5 kDa, **Đ =** 1.98 (6.7 mg, 58% yield)
Run 2: M_n **=** 19.5 kDa, **Đ =** 2.05 (5.5 mg, 47% yield)

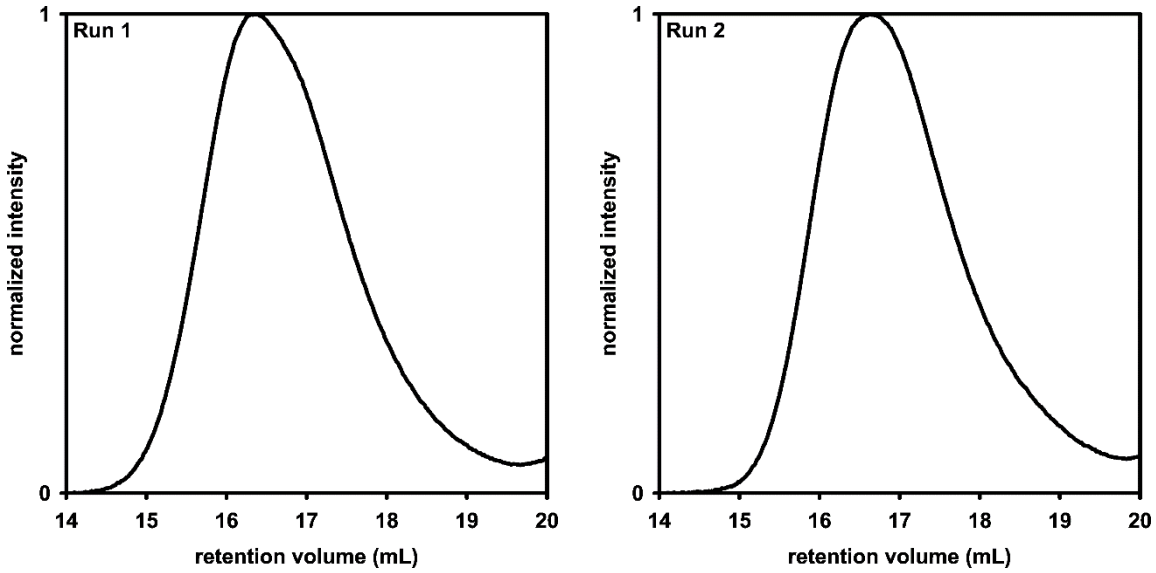

Figure S1.10. GPC trace of **P3HT** generated with catalyst **C2'**

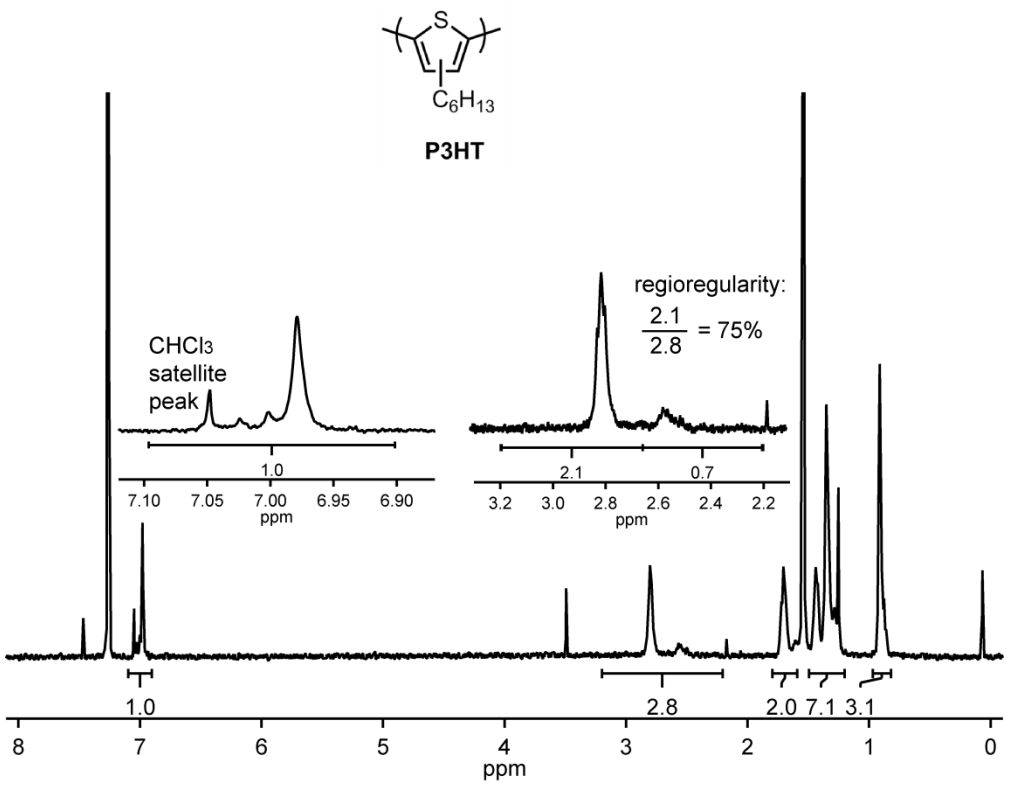

Figure S1.11. ^{1}H NMR spectrum of **P3HT** generated with **C2'**.

VIII. THF impact on 1-hexene polymerization

$B(C_6F_5)_3$ solution preparation

In a 4 mL vial were added **$B(C_6F_5)_3$** (2.5 mg, 0.0050 mmol, 2.0 equiv) and **1-hexene** (0.5 mL).

Procedure

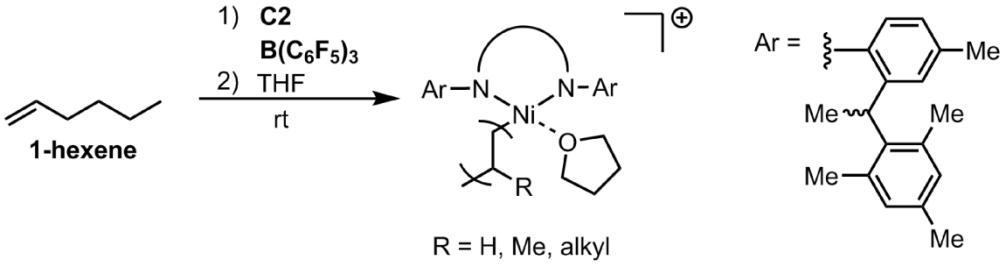

In the glovebox was added **C2** (2.2 mg, 0.0025 mmol, 1 equiv) and **1-hexene** (1.0 mL) to a 4 mL vial. This solution was then passed through a syringe fitted with a PTFE filter (0.2 µm) into a 20 mL vial equipped with a stir bar. The **$B(C_6F_5)_3$** solution was then injected into the 20 mL vial. Upon adding the activator, the solution immediately turned dark green and then transitioned to a light pink. The reaction stirred for 3 min and THF (3.0 mL) was added to the vial. An aliquot (0.3 mL) was taken and quenched outside of the box with MeOH (2.0 mL). After 1 h the reaction was quenched outside of the box with MeOH (5.0 mL). The solvent was removed under reduced for both the first aliquot and final polymer. The resulting residues were dissolved in THF:PhMe (99:1) (1.5 mL), and after mild heating, passed through a PTFE filter (0.2 µm) to be analyzed by GPC.

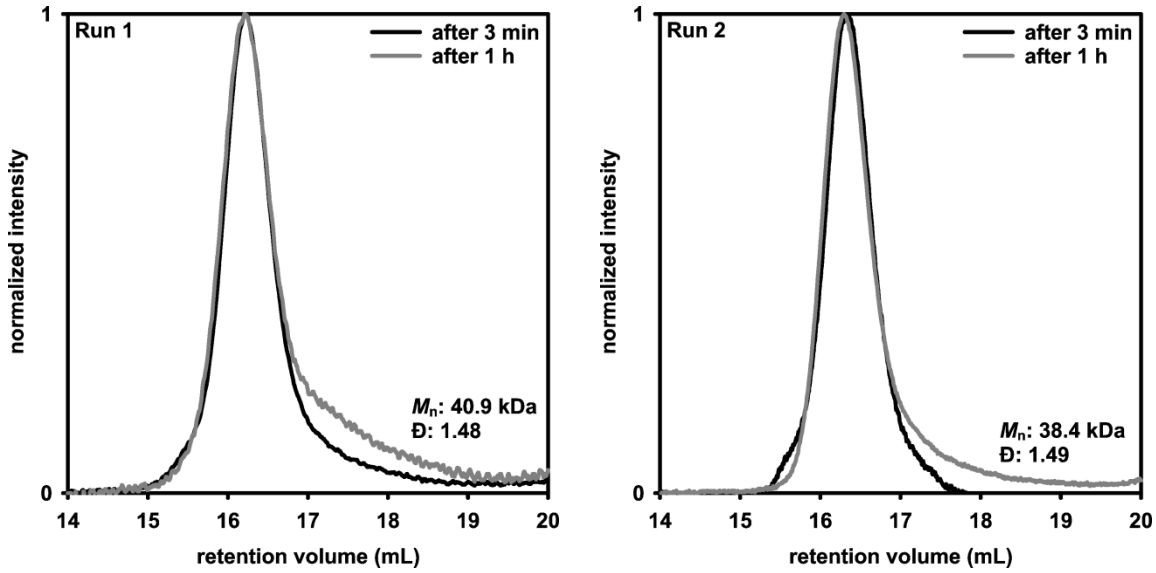

Figure S1.12. GPC trace of **1-hexene** polymerization at 3 min and 1 h after THF addition.

IX. Copolymerization of 3HT and 1-hexene monomers with precatalyst C2 and $B(C_6F_5)_3$

$B(C_6F_5)_3$ stock solution prep

In a 4 mL vial was added **$B(C_6F_5)_3$** (3.1 mg, 0.0062 mmol, 2.0 equiv) and **1-hexene** (0.5 mL).

Procedure

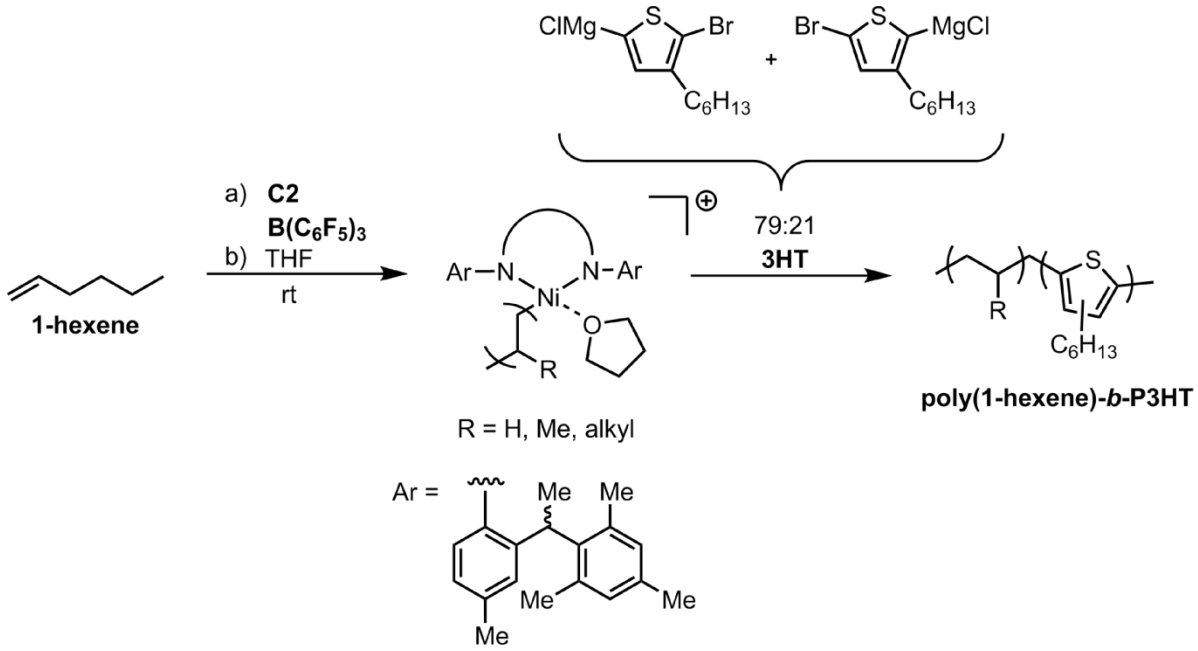

In the glovebox was added **C2** (2.8 mg, 0.0031 mmol, 1.0 equiv) and **1-hexene** (1.0 mL) to a 4 mL vial. This solution was then passed through a syringe fitted with a PTFE filter into a 20 mL vial equipped with a stir bar. The **$B(C_6F_5)_3$** solution was then injected into the **C2** solution. Upon adding the activator, the solution immediately turned dark green and then transitioned to a light pink. The reaction stirred for 3 min at rt and THF (3.00 mL) was added to the vial. Then an aliquot (0.5 mL) was taken and quenched outside of the glovebox with neutral MeOH (2 mL). To the remaining reaction was added **3HT** (1.0 mL, 0.070 mmol, 23 equiv). After 1 h the polymerization was quenched with aq HCl (2.00 mL, 12 M) outside of the glovebox. The mixture was extracted with $CHCl_3$ (5.00 mL), dried over $MgSO_4$, and filtered through glass wool. The organic layer was then split into two portions. The first portion was analyzed by GC to show 11% conversion. The solvent was removed under reduced pressure from the second portion. The resulting solid was dissolved in THF:PhMe (99:1) (1.5 mL) with mild heating, passed through a PTFE filter (0.2 µm), and analyzed by GPC.

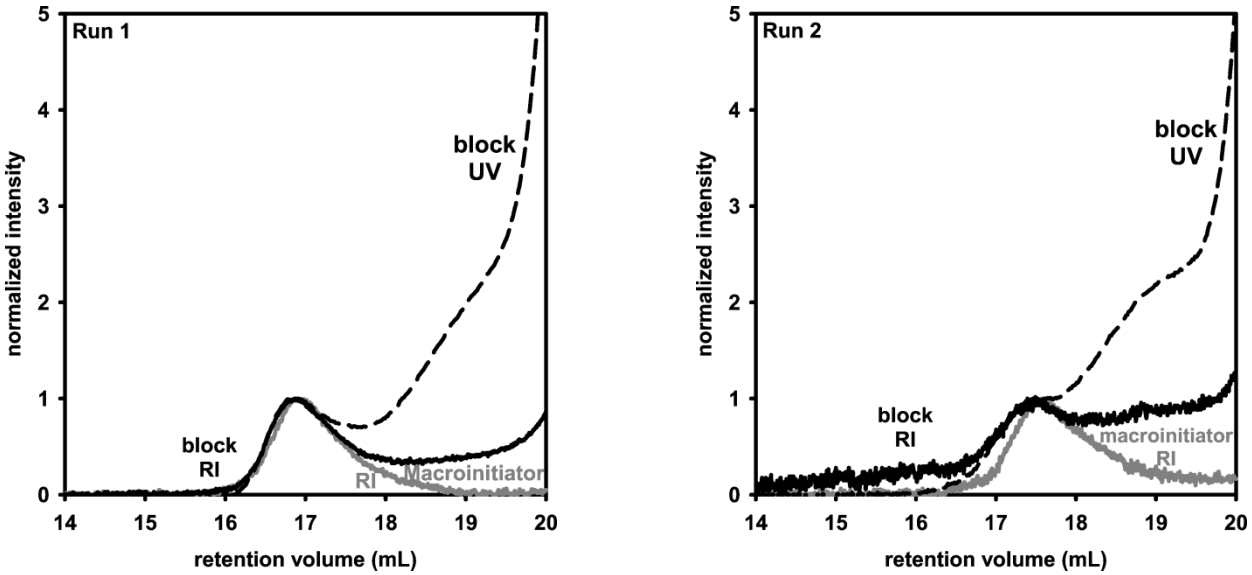

Figure S1.13. GPC trace of copolymerization of **1-hexene** and **3HT** product mixture.

X. Polymerization of 3HT monomer with varying amounts of 1-hexene

Activation of 2,5-dibromo-3-hexylthiophene with iPrMgCl

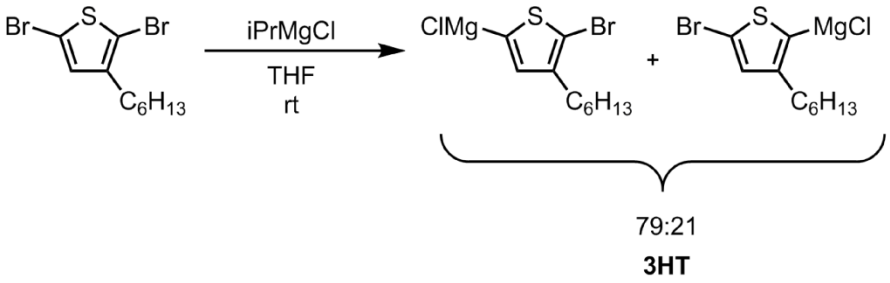

In the glovebox 2,5-dibromo-3-hexylthiophene (45.0 mg, 0.138 mmol, 1.00 equiv) was added to a 20 mL vial equipped with a stir bar, n-docosane (approx. 4.0 mg) and THF (1.33 mL). To the stirring solution was added iPrMgCl (48.0 µL, 0.0966 mmol, 2.00 M in THF, 0.700 equiv) and stirred for 30 min. **3HT** was titrated to be 0.070 M using salicylaldehyde phenylhydrazone. An aliquot (0.3 mL) of **3HT** was quenched with aq HCl (0.50 mL, 12 M) outside of the box. The quenched monomer was extracted with $CHCl_3$ (2.0 mL), dried over $MgSO_4$, and analyzed by GC to show a mixture of regioisomers (79:21).

C2 and $B(C_6F_5)_3$ stock solutions

In the glovebox were added **C2** (6.0 mg, 0.0068 mmol, 0.50 mM) and toluene (1.35 mL) to a 4 mL vial. In another 4 mL vial were added **$B(C_6F_5)_3$** (7.0 mg, 0.014 mmol, 0.50 mM) and toluene (2.73 mL). **C2** solutions were made fresh for each **3HT** polymerization

Activation of precatalyst C2 with $B(C_6F_5)_3$

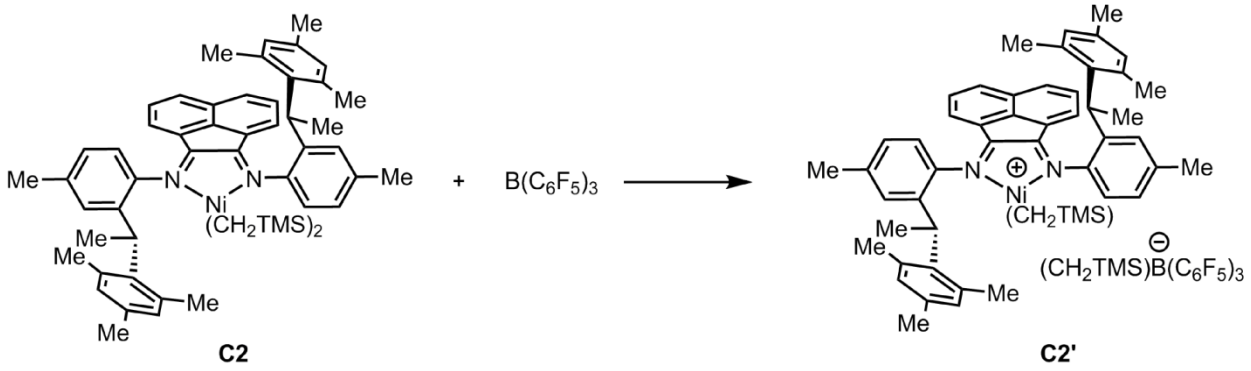

C2 (0.10 mL, 0.50 mM in toluene, 1.0 equiv) and **$B(C_6F_5)_3$** (0.10 mL, 0.50 mM in toluene, 1.0 equiv) were added to a 4 mL vial equipped with a stir bar and stirred for 5 min. **C2'** solution must be made fresh prior to use in **3HT** polymerization.

3HT stock solution preparation

In the glovebox to four separate 20 mL vials equipped with a stir bar was added **3HT** (100 equiv rel. to cat.), THF (X mL, 0.02 M), **1-hexene**

Vial 1: 3HT (1 mL, 0.07 M), THF (2.4 mL), **1-hexene** (0 mL, 0 equiv)
Vial 2: 3HT (1 mL, 0.07 M), THF (1.65 mL), **1-hexene** (0.75 mL, 12000 equiv)
Vial 3: 3HT (1 mL, 0.07 M), THF (2.34 mL), **1-hexene** (60 µL, 1000 equiv)
Vial 4: 3HT (1 mL, 0.07 M), THF (2.39 mL), **1-hexene** (10 µL, 50 equiv)

Procedure

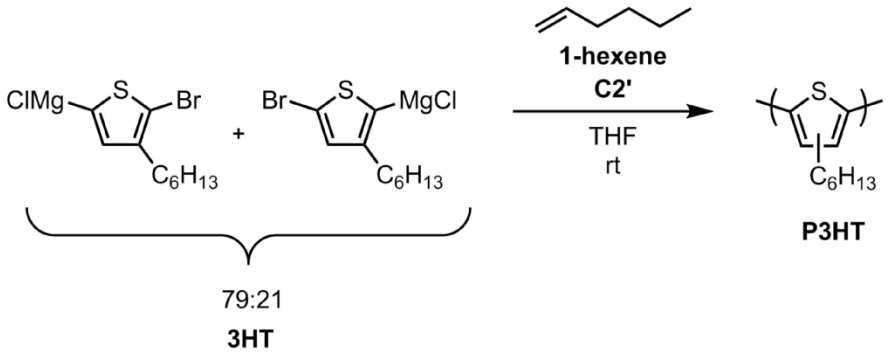

To each vial was added the **C2'** solution (0.20 mL, 0.50 µmol, 1 equiv). The reactions were stirred at rt for 1 h before being quenched outside of the box with aq HCl (2.0 mL, 12 M). Each vial was extracted $CHCl_3$ (2.0 mL), dried over $MgSO_4$, and filtered through glass wool. The organic layer was then split into two portions The first portion was analyzed by GC. The solvent was removed under reduced pressure from the second portion. The resulting solid was then dissolved in THF (1.5 mL) with mild heating, passed through a PTFE filter (0.2 µm), and analyzed by GPC.

Table S1.1: P3HT synthesis with varying equiv of **1-hexene**

Run 1:

X equiv 1-hexene	% conversion 3HT	M_n P3HT kDa	Đ
12000	12.6	5.87	1.85
1000	22.1	14.6	1.96
50	35.9	20.3	2.05
0	71.1	26.5	1.89

Run 2:

X equiv 1-hexene	% conversion 3HT	M_n P3HT kDa	Đ
12000	7.5	6.67	1.80
1000	13.7	15.8	2.02
50	35.0	24.2	2.02
0	93.6	24.8	2.03

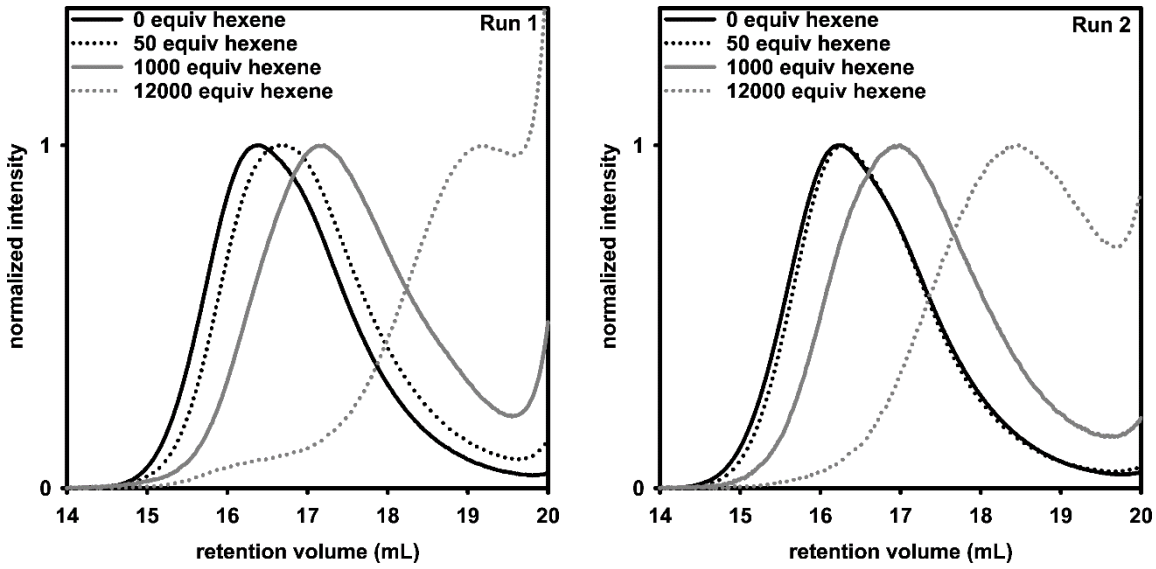

Figure S1.14. GPC trace of **P3HT** synthesis with varying equiv of **1-hexene**.

XI. Copolymerization of 1-pentene and 3HT monomers with precatalyst C2 and $B(C_6F_5)_3$

Activation of 2,5-dibromo-3-hexylthiophene with iPrMgCl

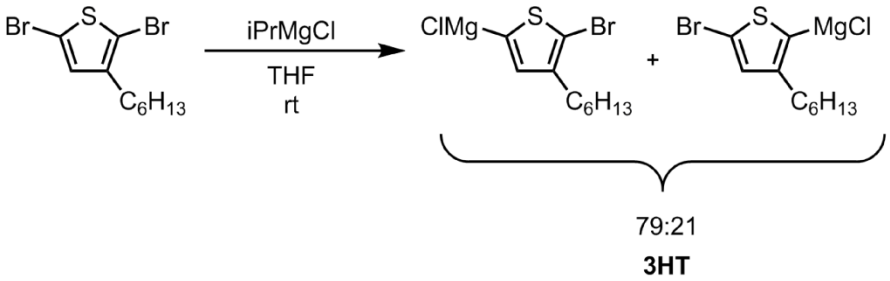

In the glovebox, 2,5-dibromo-3-hexylthiophene (250 mg, 0.768 mmol, 1 equiv), n-dodecane (approx. 4 mg), and tetrahydrofuran (THF, 7.40 mL) were added sequentially to a 20 mL vial equipped with a stir bar. To this solution iPrMgCl (268 µL, 0.537 mmol, 2.00 M in THF, 0.7 equiv) was added. The resulting thiophene Grignard solution was stirred for 30 min at rt and then titrated using salicylaldehyde phenylhydrazone.[i] An aliquot of the Grignard solution (0.3 mL, 0.070 M) was quenched with aq. HCl (0.5 mL, 12 M) outside the glovebox, extracted with $CHCl_3$ (2 mL), dried over $MgSO_4$, and analyzed by gas chromatography (GC) to show a mixture of regioisomers (79:21).

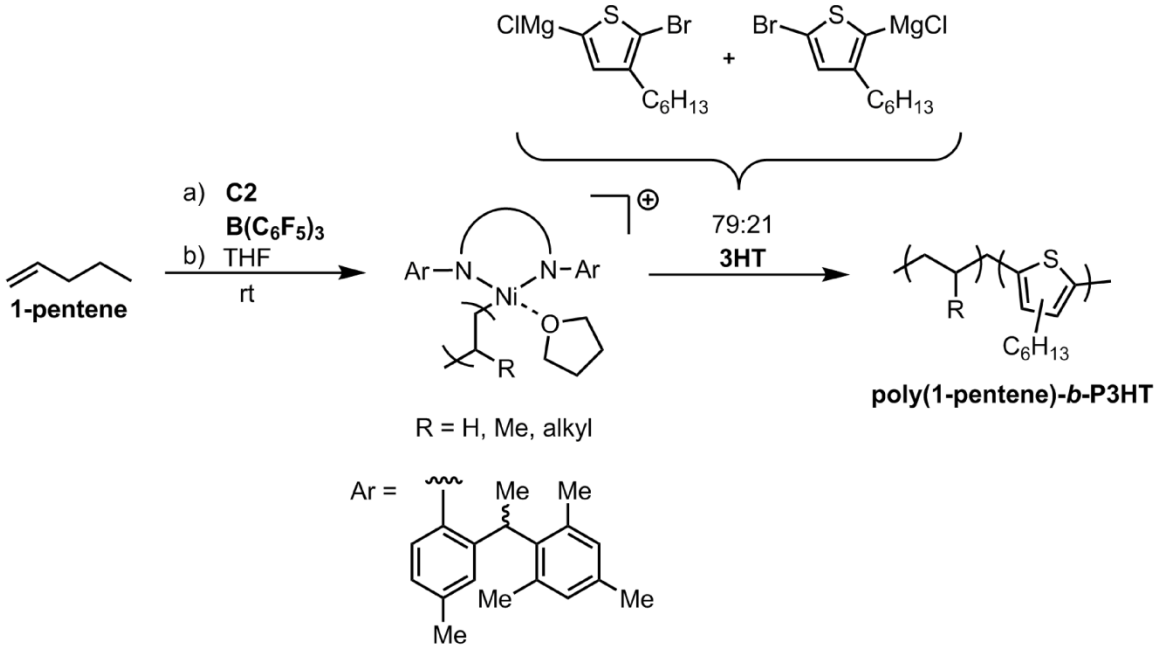

Copolymerization procedure

In the glovebox, precatalyst **C2** (15.7 mg, 0.0177 mmol, 1.0 equiv) and cold 1-pentene (2.00 mL, kept at -30 °C) were added to a 4 mL vial while stirring. After 2 min, the mixture was filtered through a PTFE filter (0.2 µm) into a 50 mL round-bottom flask equipped with a stir bar. A solution of $B(C_6F_5)_3$ (18.0 mg, 0.0354 mmol, 2.0 equiv) in cold 1-pentene (1 mL) was added and the reaction stirred for 20 s. Then, THF (5.0 mL) and toluene (3.0 mL) were added. The flask was then held under reduced pressure for 30 min (until ~2 mL solvent remained).

An aliquot (0.50 mL) of the remaining solution was added to a J-Young tube and analyzed by ^{1}H NMR spectroscopy (**Figure S15**) before quenching with MeOH (2 mL) and concentrating in vacuo. The residue was redissolved in THF (1.5 mL), passed through a PTFE syringe filter (0.2 µm), and analyzed by gel permeation chromatography (GPC) to estimate the macroinitiator molecular weight. THF (8.0 mL) and thiophene Grignard (4.0 mL) were added to the remaining macroinitiator solution. After 2 h, the reaction was quenched with aq. HCl (10 mL, 12 M). The resulting polymer was extracted with $CHCl_3$ (2 x 15 mL), dried over $MgSO_4$, and filtered using a Buchner funnel. An aliquot (0.5 mL) of this solution was split into two equal portions. The first portion was diluted with $CHCl_3$ (2.0 mL) and analyzed by GC to determine the thiophene conversion. The second portion was concentrated in vacuo and then redissolved in THF/toluene (99:1; 1.5 mL) with mild heating, passed through a PTFE filter, and analyzed by GPC. After analysis, both portions were recombined with the mother liquor and the solvent was removed in vacuo, yielding a maroon solid (25 mg).

Block Copolymer Purification

The maroon solid was dissolved in $CHCl_3$ (0.5 mL) and precipitated with MeOH (15.0 mL). The mixture was spun in a centrifuge for 10 min. The supernatant was decanted and saved. The precipitate was dried under reduced pressure, yielding 15 mg of polymer. ^{1}H NMR spectroscopic analysis revealed that this solid resembled P3HT homopolymer (**Figure S18**). The supernatant was concentrated under reduced pressure to generate a purple solid (10 mg). MeOH (10 mL) was added followed by sonication for 1 min. The resulting mixture was spun in the centrifuge for 10 min, and then supernatant was removed and saved. This process was repeated 3 times. Hexanes (10 mL) was added to the remaining solid, followed by centrifugation (10 min). The resulting yellow supernatant was collected, passed through a PTFE syringe filter (0.2 µm), and concentrated in vacuo to yield a solid (4 mg). ^{1}H NMR spectroscopic analysis revealed that the solid contains a mixture of the desired copolymer and poly(1-pentene) homopolymer (Figure S20).

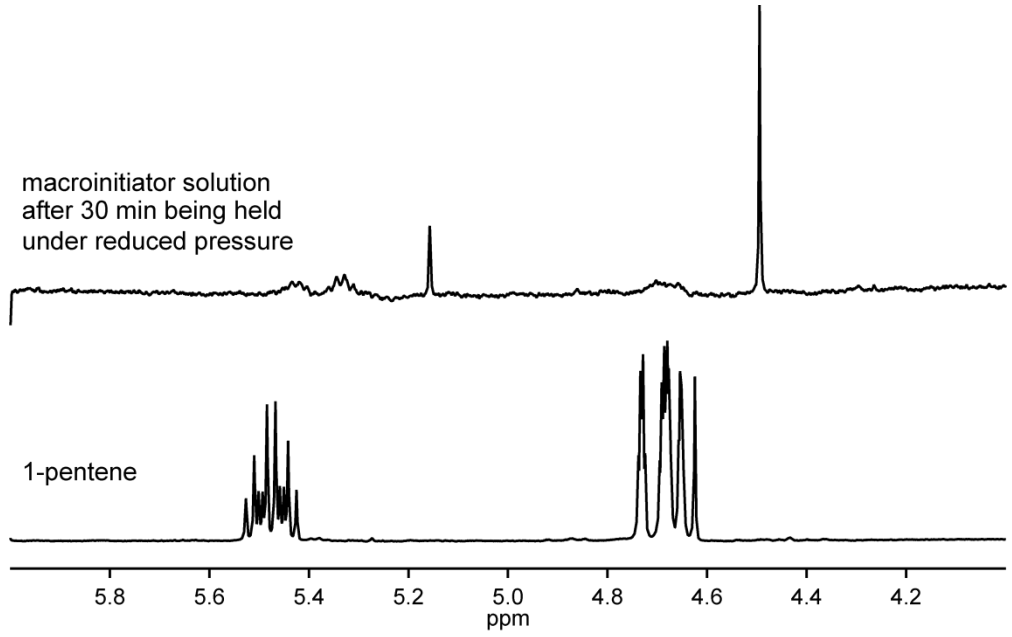

Figure S1.15. ^{1}H NMR spectrum of the poly(1-pentene) macroinitiator from glovebox after being held reduced pressure for 30 min.

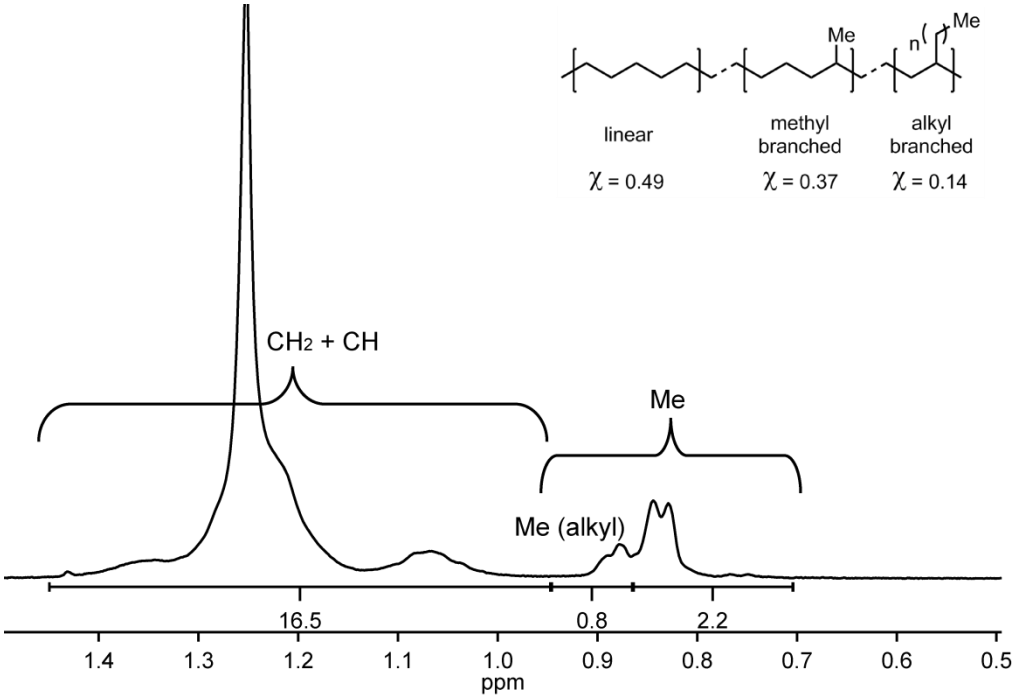

Figure S1.16. ^{1}H NMR spectrum of **poly(1-pentene)** macroinitiator

$$R = \frac{[CH_3]}{[CH_2]} = \frac{(3/3)}{(16.5\text{-}1)/2} = 0.129$$

$$\chi_{linear} = \frac{[1-(\omega-2)R]}{[1+2R]} = 0.487$$

carbons in 1-pentene = $\omega = 5$

$$\chi_{alkyl} + \chi_{methyl} = 1 - \chi_{linear} = 0.513$$

$$\frac{\chi_{alkyl}}{\chi_{methyl}} = \frac{CH_3\,(Me\ (alkyl))}{CH_3\,(Me)} = \frac{0.8}{2.2} = 0.364$$

$$\chi_{alkyl} = (0.364)\chi_{methyl}$$

$$(0.364)\chi_{methyl} + \chi_{methyl} = 0.513$$

$$\chi_{methyl} = 0.376$$

$$\chi_{alkyl} = 0.137$$

Equation S1.2. Calculating br/1000C of **poly(1-pentene)** using ^{1}H NMR spectroscopy.[3]

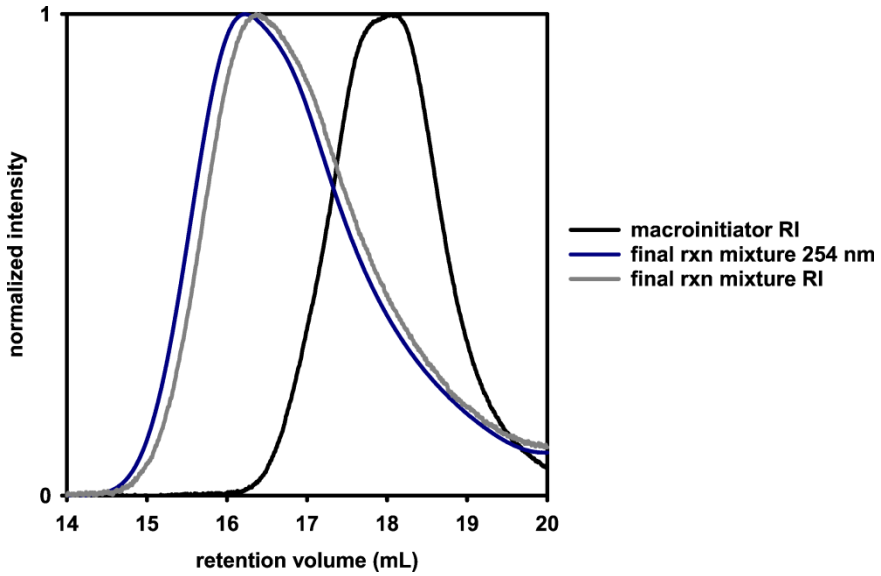

Figure S1.17. GPC trace of product mixture from copolymerization between **1-pentene** and **3HT** monomers using catalyst **C2** and **$B(C_6F_5)_3$**.

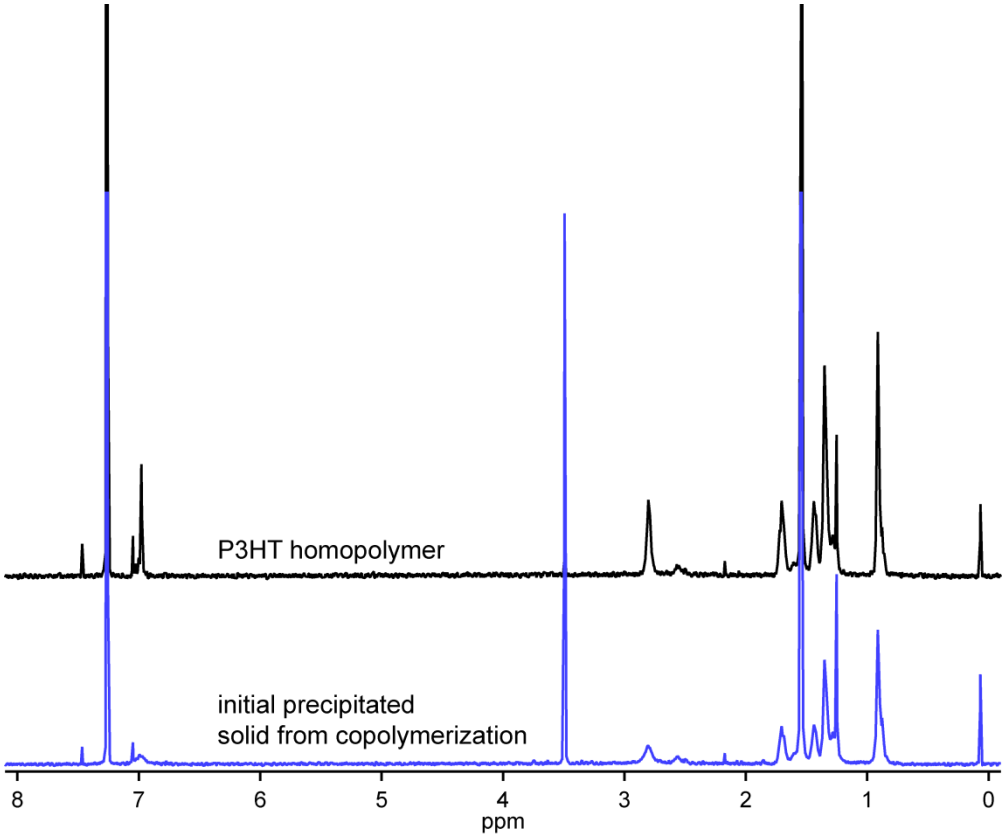

Figure S1.18. ^{1}H NMR spectrum after initial precipitation from copolymerization

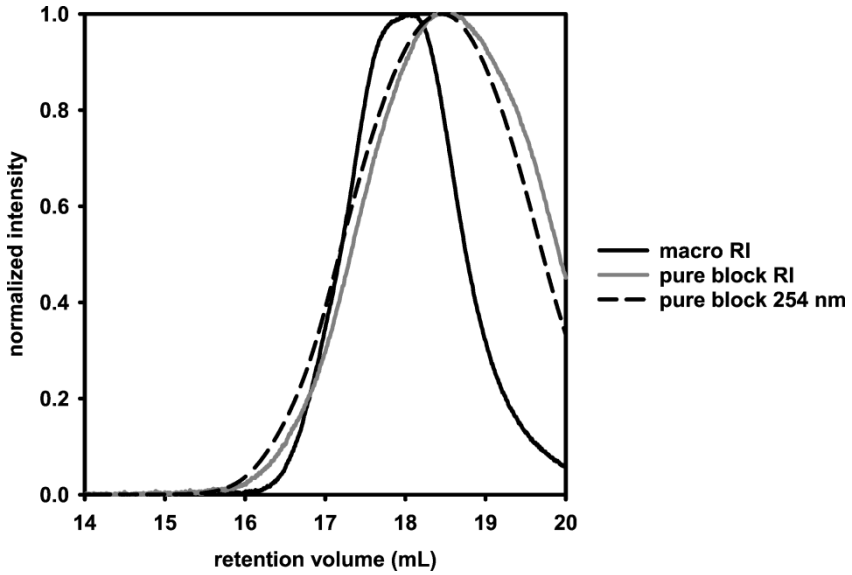

Figure S1.19. GPC trace of block copolymer (**poly(1-pentene)-*b*-P3HT**) after purification from copolymerization between **1-pentene** and **3HT** monomers using catalyst **C2** and **$B(C_6F_5)_3$**

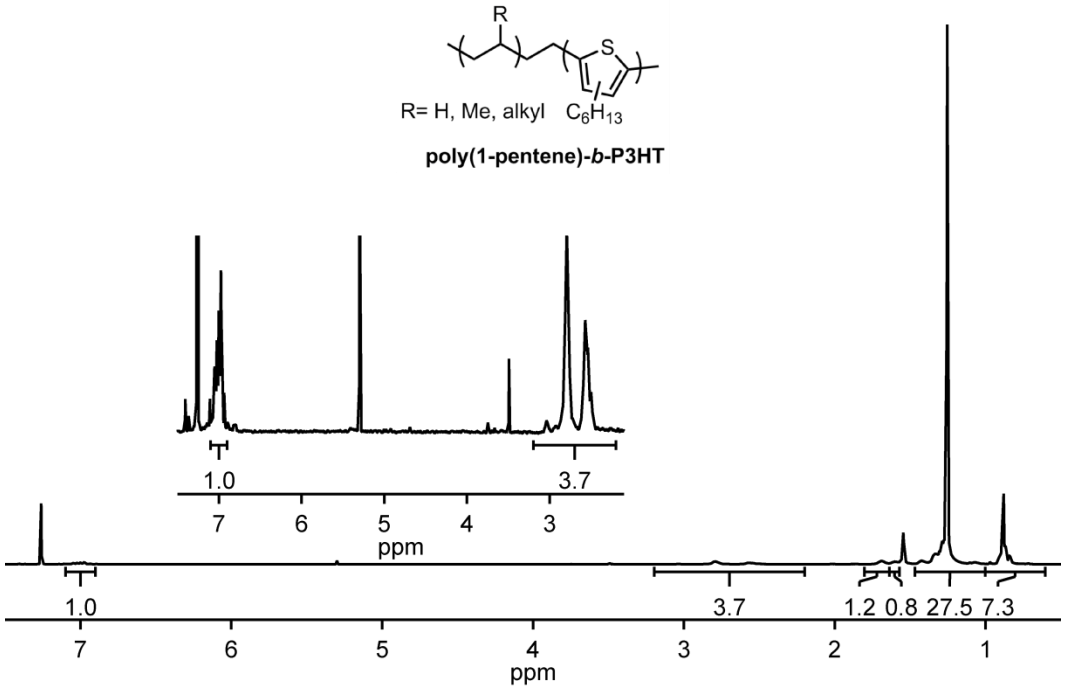

Figure S1.20. ^{1}H NMR spectrum of purified **poly(1-pentene)-*b*-P3HT**.

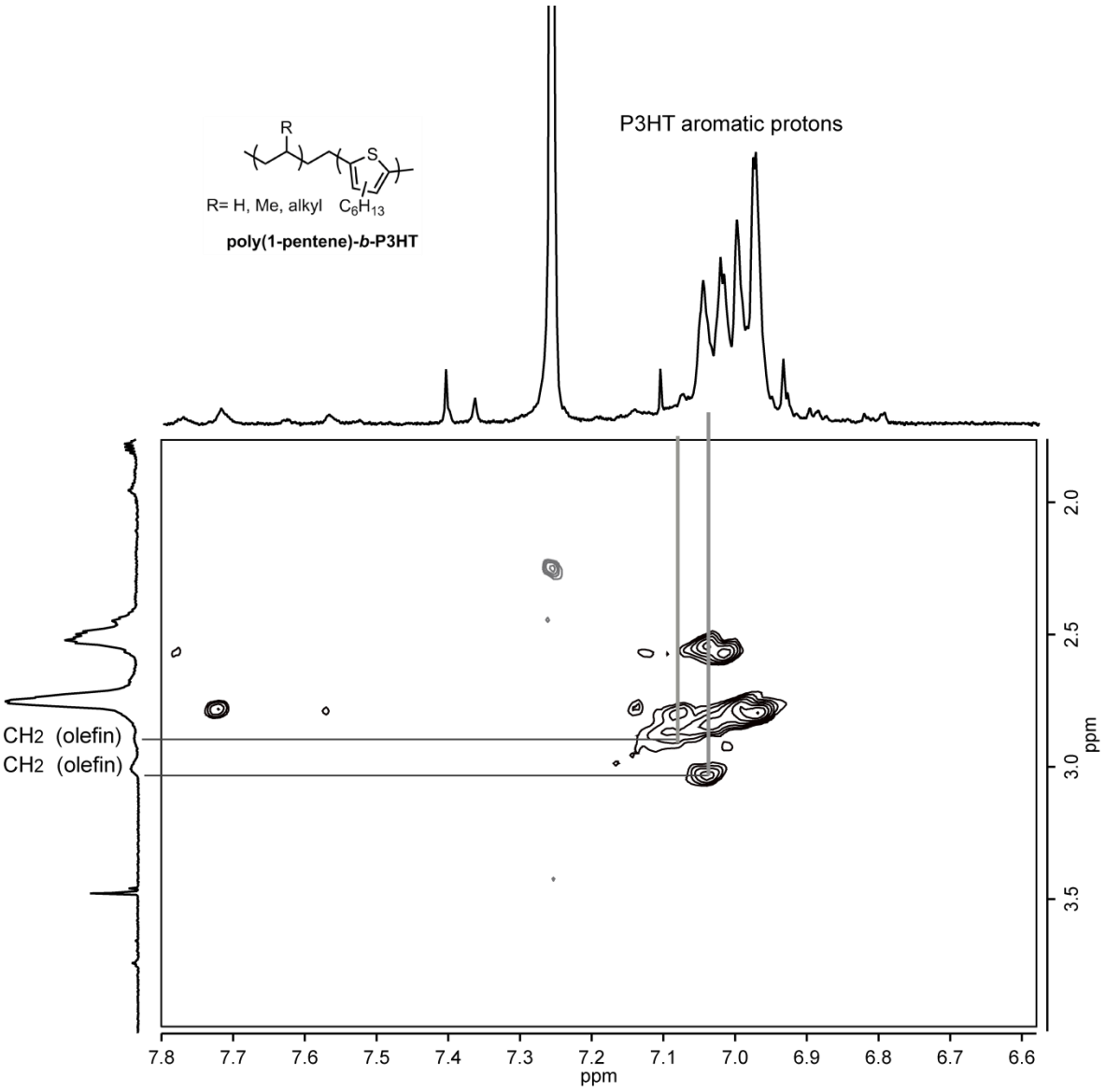

Figure S1.21. $^{1}H/^{1}H$ NOESY spectrum of purified **poly(1-pentene)-*b*-P3HT**.

XII. M_n versus percent conversion in polymerization of 3HT monomer with precatalyst C2 and $B(C_6F_5)_3$

Activation of 2,5-dibromo-3-hexylthiophene with iPrMgCl

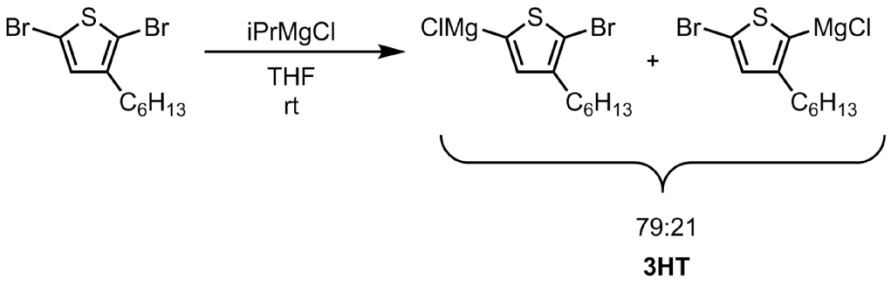

In the glovebox 2,5-dibromo-3-hexylthiophene (70.0 mg, 0.215 mmol, 1.00 equiv) was added to a 20 mL vial equipped with a stir bar, n-docosane (approx. 4.0 mg) and THF (2.07 mL). To the stirring solution was added iPrMgCl (80.0 µL, 0.150 mmol, 2.00 M in THF, 0.700 equiv) and stirred for 30 min. **3HT** was titrated to be 0.070 M using salicylaldehyde phenylhydrazone. An aliquot (0.3 mL) of **3HT** was quenched with aq HCl (0.50 mL, 12 M) outside of the box. The quenched monomer was extracted with $CHCl_3$ (2.0 mL), dried over $MgSO_4$, and analyzed by GC to show a mixture of regioisomers (79:21).

C2 and $B(C_6F_5)_3$ stock solutions

In the glovebox were added **C2** (6.0 mg, 0.0068 mmol, 0.50 mM) and toluene (1.35 mL) to a 4 mL vial. In another 4 mL vial were added **$B(C_6F_5)_3$** (7.0 mg, 0.014 mmol, 0.50 mM) and toluene (2.73 mL). **C2** solutions were made fresh for each **3HT** polymerization

Activation of precatalyst C2 with $B(C_6F_5)_3$

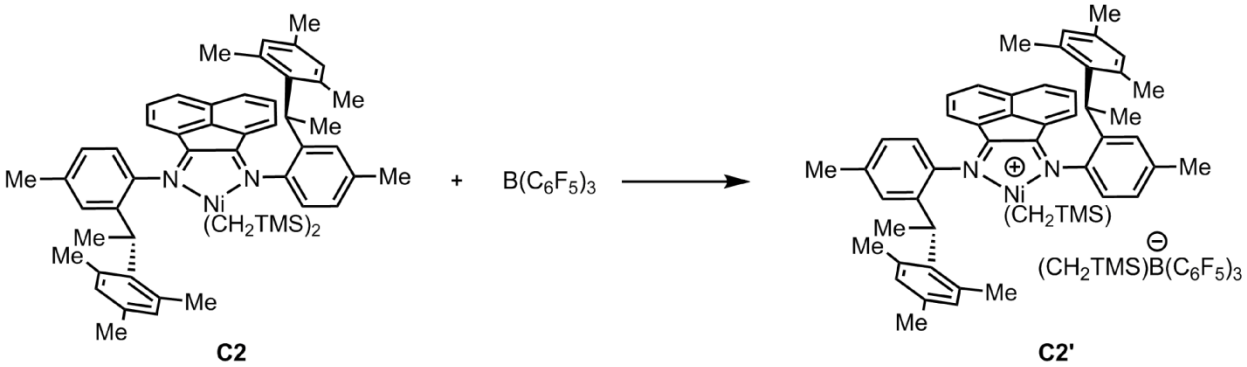

C2 (0.11 mL, 0.50 mM in toluene, 1.0 equiv) and **$B(C_6F_5)_3$** (0.11 mL, 0.50 mM in toluene, 1.0 equiv) were added to a 4 mL vial equipped with a stir bar and stirred for 5 min. **C2'** solution must be prepared fresh for each **3HT** polymerization.

Procedure

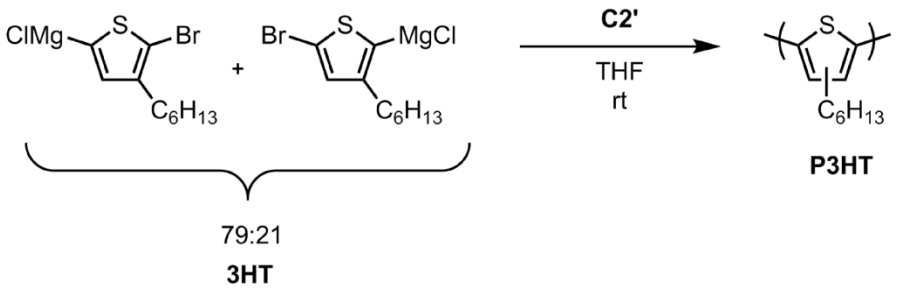

In the glovebox to a 20 mL vial equipped with a stir bar were added **3HT** (1.00 mL, 0.07 mmol, 125 equiv relative to **C2'**) and THF (1.63 mL) to give an overall [**3HT**] of 0.02 M. To the stirring solution was added **C2'** (0.22 mL, 0.57 µmol, 1 equiv). Aliquots were taken at 2 min, 4 min, 6 min, 8 min, and 10 min and quenched with aq. HCl (2.0 mL, 12 M) outside of the box. Each aliquot was extracted with $CHCl_3$ (2.0 mL), dried over $MgSO_4$, and filtered through glass wool. The organic layer was then split into two equal portions. The first portion was diluted with additional $CHCl_3$ (2.0 mL) and analyzed by GC. The second portion was concentrated in vacuo and then redissolved in THF (1.5 mL) with mild heating, passed through a PTFE filter (0.2 µm), and analyzed by GPC.

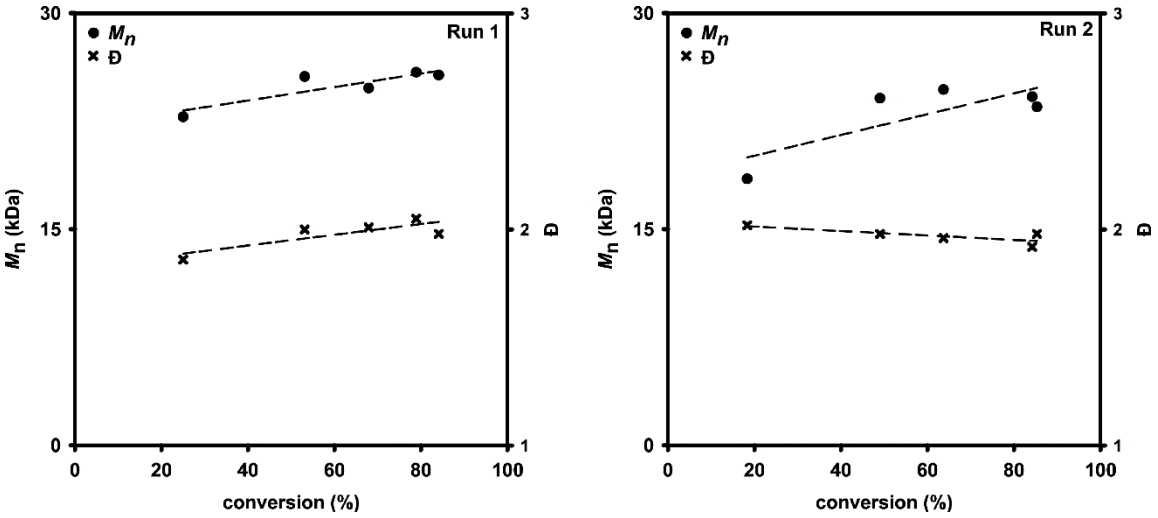

Figure S1.22. M_n versus percent conversion for polymerization of **3HT** monomer with catalyst **C2'**.

XIII. Polymerizations of 3HT monomer with precatalyst C3

Procedure: M_n versus percent conversion for polymerization of 3HT monomer with catalyst C3

Activation of 2,5-dibromo-3-hexylthiophene with iPrMgCl

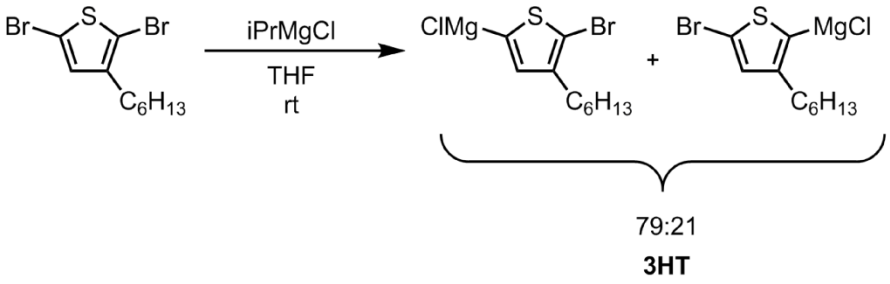

In the glovebox 2,5-dibromo-3-hexylthiophene (68.0 mg, 0.209 mmol, 1.00 equiv) was added to a 20 mL vial equipped with a stir bar, n-docosane (approx. 2.0 mg) and THF (2.01 mL). To the stirring solution was added iPrMgCl (73.0 µL, 0.146 mmol, 2.00 M in THF, 0.700 equiv) and stirred for 30 min. **3HT** was titrated to be 0.070 M using salicylaldehyde phenylhydrazone. An aliquot (0.3 mL) of **3HT** was quenched with aq HCl (0.50 mL, 12 M) outside of the box. The quenched monomer was extracted with $CHCl_3$ (2.0 mL), dried over $MgSO_4$, and analyzed by GC to show a mixture of regioisomers (79:21).

C3 stock solution: C3 (2.0 mg, 0.0023 mmol, 0.50 mM) was added to a 4 mL vial equipped with a stir bar, followed by THF (0.46 mL). The solution was stirred for 5 min before using.

Procedure

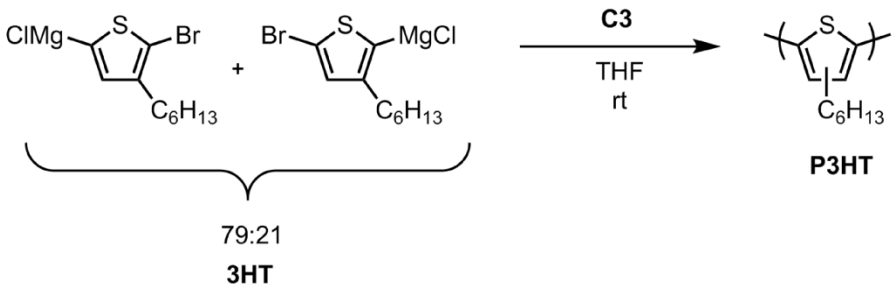

In the glovebox, to a 20 mL vial equipped with a stir bar was added **3HT** (0.50 mL, 0.035 mmol, 117 equiv relative to **C3**) and THF (5.00 mL) to give an overall [**3HT**] of 0.005 M. To the stirring solution was added the **C3** solution (60.0 µL, 0.300 µmol, 1.00 equiv). Aliquots were taken at 2, 4, 6, 8, and 10 min and quenched with aq. HCl (0.5 mL, 12 M) outside of the box. Each aliquot was extracted with $CHCl_3$ (2.0 mL), dried over $MgSO_4$, and filtered through glass wool. The organic layer was then split into two equal portions. The first portion was diluted with $CHCl_3$ (2.0 mL) and analyzed by GC. The second portion was concentrated in vacuo and redissolved in THF (1.5 mL) with mild heating, passed through a PTFE filter (0.2 µm), and analyzed by GPC.

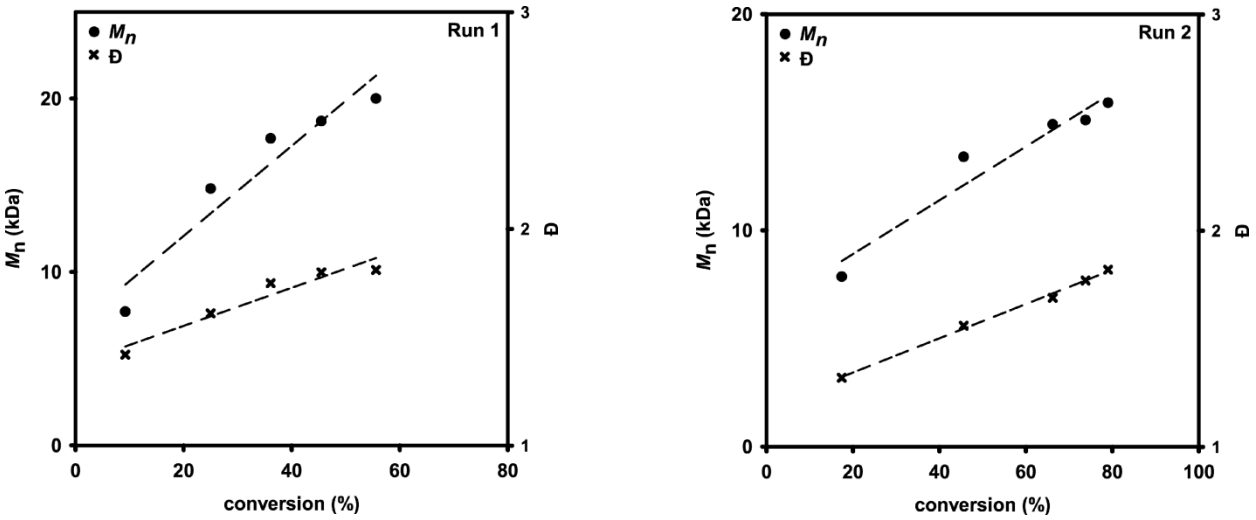

Figure S1.23. M_n versus percent conversion for polymerization of **3HT** monomer with precatalyst **C3**.

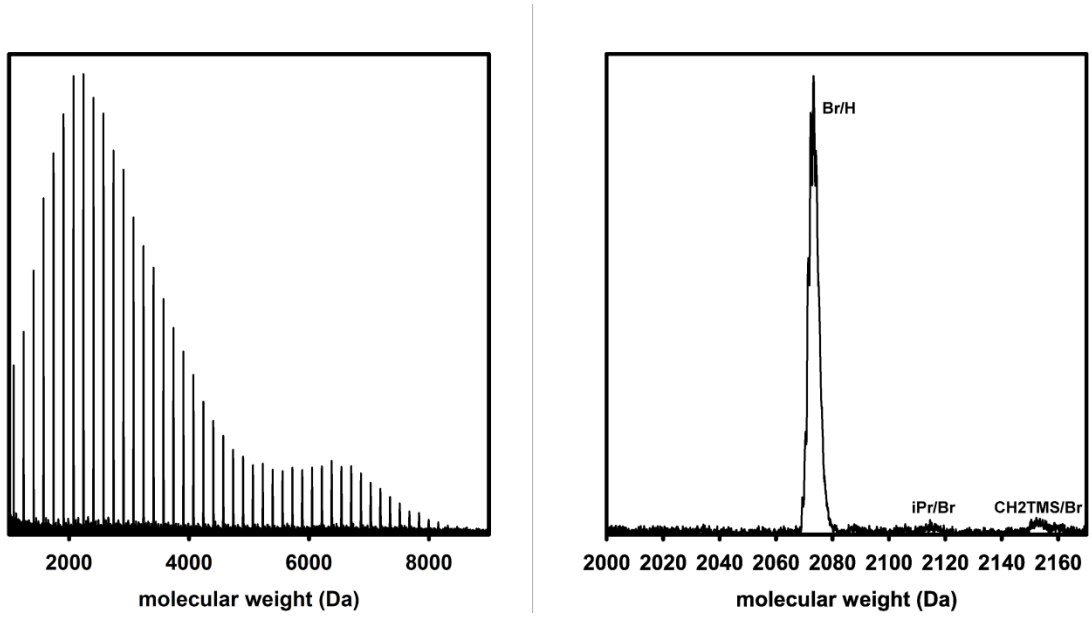

Figure S1.24. MALDI-TOF spectrum of the aliquot taken at 2 min in the polymerization of **3HT** monomer with precatalyst **C3**.

Procedure: M_n vs varying monomer:catalyst ratio in polymerization of 3HT monomer with catalyst C3

Activation of 2,5-dibromo-3-hexylthiophene with iPrMgCl

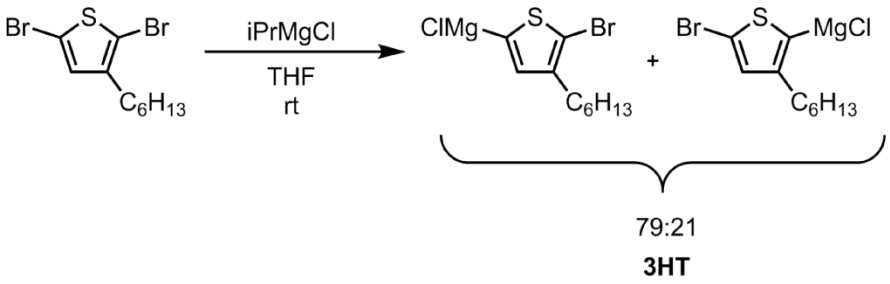

In the glovebox 2,5-dibromo-3-hexylthiophene (73.0 mg, 0.224 mmol, 1.00 equiv) was added to a 20 mL vial equipped with a stir bar, n-docosane (approx. 2.0 mg) and THF (2.16 mL). To the stirring solution was added iPrMgCl (78.0 µL, 0.157 mmol, 2.00 M in THF, 0.700 equiv) and stirred for 30 min. 3HT was titrated to be 0.070 M using salicylaldehyde phenylhydrazone. An aliquot (0.3 mL) of 3HT was quenched with aq HCl (0.50 mL, 12 M) outside of the box. The quenched monomer was extracted with $CHCl_3$ (2.0 mL), dried over $MgSO_4$, and analyzed by GC to show a mixture of regioisomers (79:21).

C3 stock solution: C3 (1.7 mg, 0.0019 mmol, 0.50 mM) was added to a 4 mL vial equipped with a stir bar, followed by THF (0.39 mL). The solution was stirred for 5 min before using.

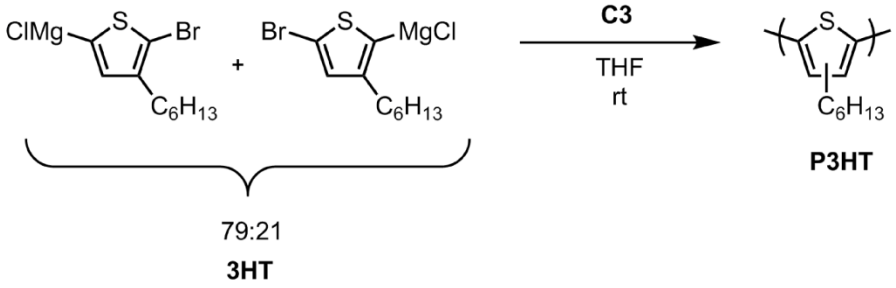

To three 4 mL vials equipped with stir bars were added the **C3** solution (50 µL, 0.25 µmol) and the respective amounts of THF and **3HT** listed below.

Vial 1: THF (0.2 mL), **3HT** (0.10 mL, 0.0070 mmol, 28 equiv)
Vial 2: THF (0.4 mL), **3HT** (0.20 mL, 0.014 mmol, 56 equiv)
Vial 3: THF (0.8 mL), **3HT** (0.40 mL, 0.028 mmol, 112 equiv)

The polymerizations were stirred for 1 h at rt, after which each vial was removed from the box and quenched with aq. 12 M HCl (0.5 mL). Each vial was extracted with $CHCl_3$ (1.0 mL), dried over $MgSO_4$, and filtered through glass wool. The organic layer was then split into two equal portions. The first portion was diluted with $CHCl_3$ (2.0 mL) and analyzed by GC. The second portion was concentrated in vacuo and redissolved in THF (1.5 mL) with mild heating, passed through a PTFE filter (0.2 µm), and analyzed by GPC.

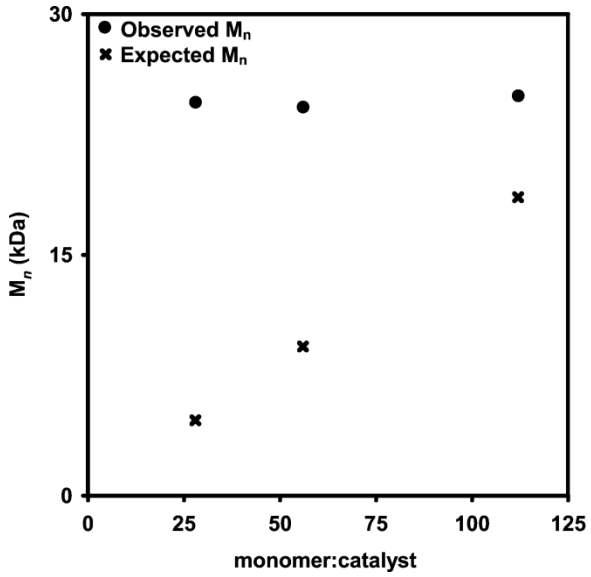

ratio 3HT:C3	% conversion 3HT	M_n (kDa)	Đ
28:1	98.3	24.5	1.91
56:1	98.2	24.2	1.86
112:1	93.3	24.9	2.07

Figure S1.25. Plot of M_n versus monomer:catalyst ratio in polymerization of **3HT** monomer with precatalyst **C3**.

XIV. Computational Details*

All quantum chemical calculations were performed using density functional theory (DFT) in the Q-Chem quantum chemistry package.[4] The restricted B3LYP density functional[5-6] with singlet spin was used with the LANL2DZ basis set and core potential[7-8] to acquire geometries for all intermediates and transition states. The growing string method was used to optimize reaction paths and transition states,[9-11] followed by eigenvector optimization to fully refine these structures. The ωB97X-D density functional[12] and the triple-zeta, polarized cc-pVTZ basis set[13] were used to calculate energies with the SMD solvation model[14] using THF as the implicit solvent. The long alkyl chain of the polyolefin macroinitiator and the hexyl group of the 3-hexylthiophene Grignard monomer were substituted with methyl groups to reduce computational cost. Thermodynamic corrections were applied to the solvated energies at a temperature of 298 K.

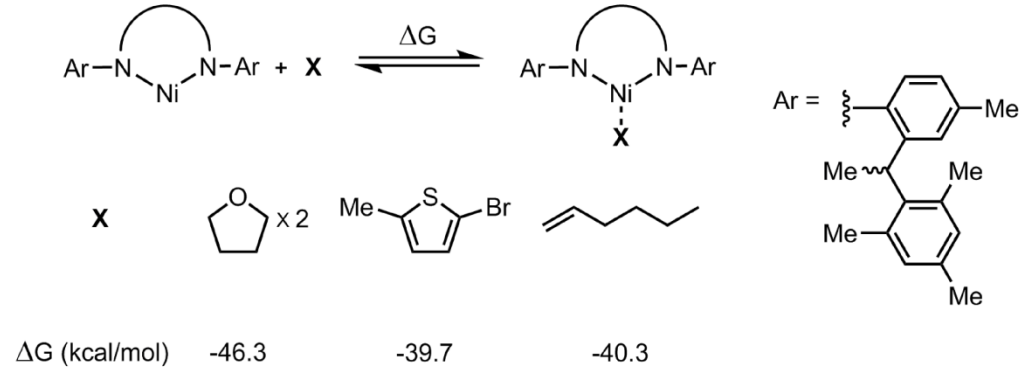

Figure S1.26a. Binding energy calculations of Ni(0) to species in copolymerization

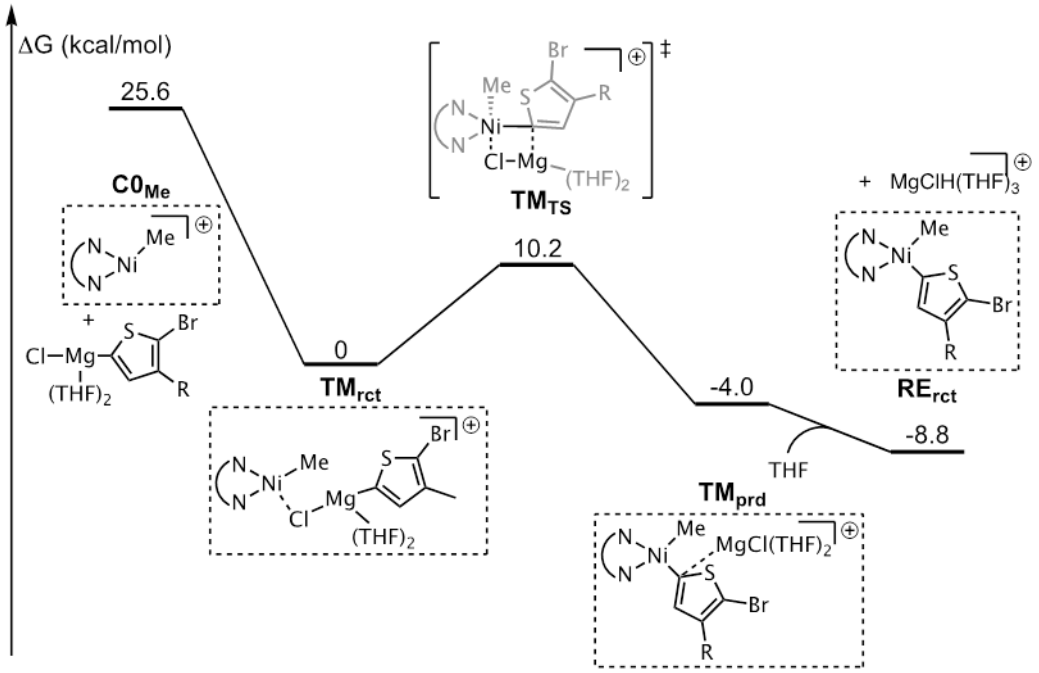

Figure S1.26b. The potential energy surface for transmetalation with thiophene at the cationic nickel center

*All XYZ coordinates for structures used to calculate binding energies (Figure S26a), tranmetalation (Figure S26b), and reductive elimination barriers (Figure S26c) are provided in original publication

After borane activation of **C2** and olefin enchainment, the resulting cationic macroinitiator must undergo transmetalation via thiophene monomer to begin thiophene polymerization. This reaction, which transforms the active nickel complex from cationic to neutral, is shown in Figure S26b. Transmetalation at the cationic macroinitiator, $\mathbf{C0_{Me}}$, begins after a thiophene monomer binds to the catalyst to form $\mathbf{TM_{rct}}$. In $\mathbf{TM_{rct}}$, the chloride of the thiophene monomer acts as a bridging ligand between the monomer and catalyst with a strong binding energy (over 25 kcal/mol). A facile transmetalation occurs via $\mathbf{TM_{TS}}$ with a barrier of 10.2 kcal/mol. The transmetalation product, $\mathbf{TM_{prd}}$, exhibits a lingering interaction between the nucleophilic carbon atom of thiophene and the electrophilic magnesium. Alkyl – aryl reductive elimination at $\mathbf{TM_{prd}}$ was performed but proved to be kinetically infeasible with a barrier over 30 kcal/mol. Upon addition of THF to $\mathbf{TM_{prd}}$, the MgCl complex dissociates from the nickel complex as cationic $MgCl(THF)_3$. This dissociation results in the neutral nickel species, $\mathbf{RE_{rct}}$, which can undergo reductive elimination.

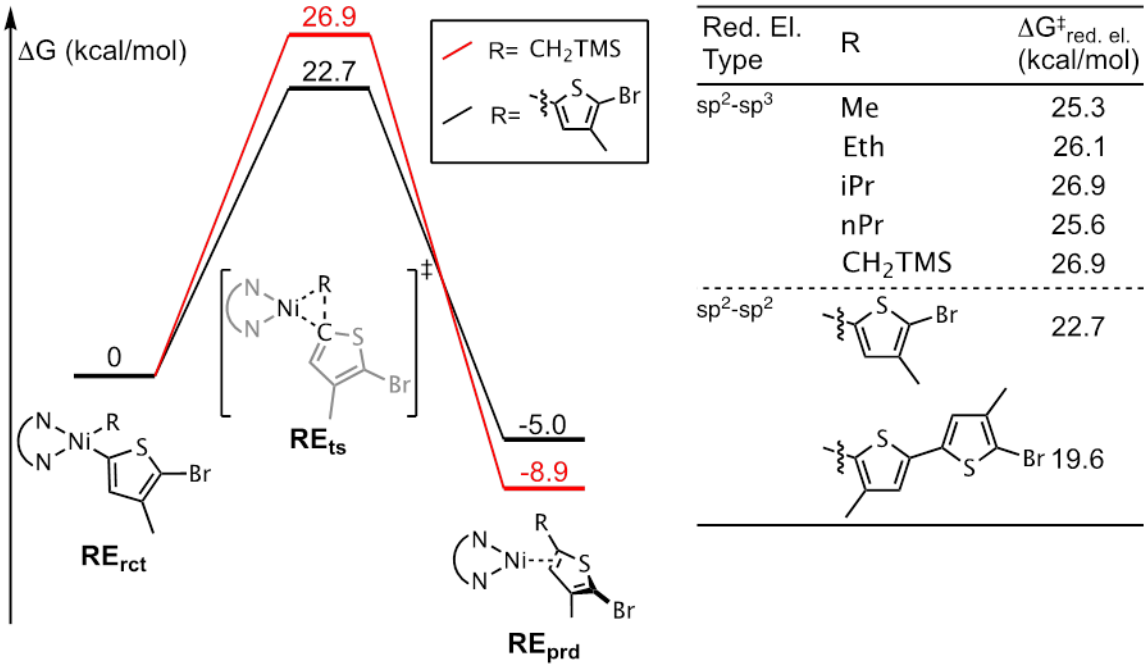

Red. El. Type	R	$\Delta G^{\ddagger}_{red.\ el.}$ (kcal/mol)
sp^2-sp^3	Me	25.3
	Eth	26.1
	iPr	26.9
	nPr	25.6
	CH_2TMS	26.9
sp^2-sp^2		22.7
		19.6

Figure S1.26c. The potential energy surfaces for sp^2-sp^3 and sp^2-sp^2 reductive elimination

The relative rates of sp^2-sp^3 reductive elimination, (Figure S26b, red pathway) compared to thiophene homopolymerization (sp^2-sp^2 reductive elimination, black pathway) were computed for catalyst **C2**. The reaction begins at RE_{rct} and proceeds through the three-membered transition state, RE_{ts} to form the π-complex intermediate RE_{prd}. The calculated difference between the two reductive elimination pathways predicts slow sp^2-sp^3 reductive elimination and fast thiophene homocoupling. At room temperature, the 4.2 kcal/mol preference for the black pathway would result in a switching step that is approximately 1,000 times slower than thiophene homocoupling. This is in good agreement with experiments that exhibited slow switching (main text, eq 3 and eq 4). The reductive elimination barriers for other alkyl and thiophene ligands were examined in the ligand survey in Figure S26b. These calculations showed that sp^2-sp^3 reductive elimination barriers slightly decrease with decreasing size of the alky reactive ligand. Reductive elimination involving two thiophene ligands remains fast in comparison, and the activation barrier decreases by about 3 kcal/mol for the dithiophene reactive ligand.

X. References

1. Cherian, A. E.; Rose, J. M.; Lobkovsky, E. B.; Coates, G. W. A C_2-Symmetric, Living α-Diimine Ni(II) Catalyst: Regioblock Copolymers from Propylene. *J. Am. Chem. Soc.* **2005**, *127*, 13770–13771.

2. Schleis, T.; Spaniol, T. P.; Okuda, J.; Heinemann, J.; Mülhaupt, R. Ethylene Polymerization Catalysts Based on Nickel(II) 1,4-Diazadiene Complexes: The Influence of the 1,4-Diazadiene Backbone Substituents on Structure and Reactivity *J. Organomet. Chem.* **1998**, *569*, 159–167.

3. Vaidya, T.; Klimovica, K.; LaPointe, A. M.; Keresztes, I.; Lobkovsky, E. B.; Daugulis, O.; Coates, G. W. Secondary Alkene Insertion and Precision Chain-Walking: A New Route to Semicrystalline "Polyethylene" from α-Olefins by Combining Two Rare Catalytic Events. *J. Am. Chem. Soc.* **2014**, *136*, 7213–7216.

4. Y. Shao et al., Advances in Molecular Quantum Chemistry Contained in the Q-Chem 4 Program Package. *Mol. Phys.* **2015**, *113*, 184–215.

5. Becke, A. D. Density-Functional Thermochemistry. III. The Role of Exact Change. *J. Chem. Phys.* **1993**, *98*, 5648–5652.

6. Lee, C.; Yang, W.; Parr, R. G. Development of the Colle-Salvetti Correlation-Energy Formula into a Functional of the Electron Density. *Phys. Rev. B.* **1988**, *37*, 785–789.

7. Hay, P. J.; Wadt, W. R. *Ab initio* Effective Core Potentials for Molecular Calculations. Potentials for K to Au Including the Outermost Core Orbitals. *J. Chem. Phys.* **1985**, *82*, 299–310.

8. Hay, P. J.; Wadt, W. R. *Ab initio* Effective Core Potentials for Molecular Calculations. Potentials for the Transition Metal Atoms Sc to Hg. *J. Chem. Phys.* **1985**, *82*, 270–283.

9. Zimmerman, P. M. Growing String Method with Interpolation and Optimization in Internal Coordinates: Methods and Examples. *J. Chem. Phys.* **2013**, *138*, 184102-1–184102-10.

10. Zimmerman, P. M. Reliable Transition State Searches Integrated with the Growing String Method. *J. Chem. Theory Comput.* **2013**, *9*, 3043–3050.

11. Zimmerman, P. M. Single-ended Transition State Finding with the Growing String Method. *J. Comput. Chem.* **2015**, *36*, 601–611.

12. Chai, J. D.; Head-Gordon, M. Long-range Corrected Hybrid Density Functionals with Damped Atom-Atom Dispersion Corrections. *Phys. Chem. Chem. Phys.* **2008**, *10*, 6615–6620.

13. Dunning, Jr., T. H.; Gaussian Basis Sets for Use in Correlated Molecular Calculations. I. The Atoms Boron through Neon and Hydrogen. *Chem. Phys.* **1989**, *90*, 1007–1023.

14. Marenich, A. V.; Cramer, C. J.; Truhlar, D. G. Universal Solvation Model Based on Solute Electron Density and on a Contiuum Model of the Solvent Defined by the Bulk Dielectric Constant and Atomic Surface Tensions. *J. Phys. Chem. B*, **2009**, *113*, 6378–6396.

Appendix 2

Supporting Information for Chapter 3

Bis(pyrrolidinylphosphino)ethane Nickel Mediated Catalyst Transfer Polymerization

I. Materials

Flash chromatography was performed on SiliCycle silica gel (40–63 μm). Thin layer chromatography was performed on Merck TLC plates (pre-coated with silica gel 60 F254). iPrMgCl (2M in THF) was purchased in 25 mL quantities from Aldrich and titrated as described below. 2,2,6,6-tetramethylpiperidinylmagnesium chloride lithium chloride complex solution was purchased from Aldrich and titrated as described below. Bis(cyclooctadiene)nickel ($Ni(cod)_2$) was purchased from Strem. All other reagent grade materials and solvents were purchased from Aldrich, Acros, ArkPharm, or Fisher and used without further purification unless otherwise noted. 2,5-dibromo-3-hexylthiophene was sourced from McNeil lab; synthesis previously reported.[1] purified via flash chromatography with hexanes as the eluent. 1,4-dibromo-2,5-bishexyloxyphenylene used THF was dried and deoxygenated using an Innovative Technology (IT) solvent purification system composed of activated alumina, a copper catalyst, and molecular sieves. The glovebox in which specified procedures were carried out was an MBraun LABmaster 130 with a N_2 atmosphere and H_2O levels below 0.1 ppm. Compounds **S1,**[2] **C1,**[3] **S2,**[1] **C2,**[1] **S4,**[4] were prepared using modified literature procedures.

II. General Experimental

NMR Spectroscopy: Unless otherwise noted, ^{1}H, ^{13}C, ^{31}P spectra for all compounds were acquired at rt in CD_2Cl_2 or $CDCl_3$ on a Varian vnmr 500 operating at 500, 126, 202 MHz, respectively. For ^{1}H, ^{13}C, ^{31}P spectra in deuterated solvents, the chemical shift data are reported in units of δ (ppm) relative to tetramethylsilane (TMS) and referenced with residual solvent. Multiplicities are reported as follows: singlet (s), doublet (d), apparent doublet (ad), triplet (t), apparent triplet (at), quartet (q), multiplet (m).

Mass Spectrometry: HRMS data were obtained on a Micromass AutoSpec Ultima Magnetic Sector mass spectrometer.

MALDI-TOF-MS: MALDI-TOF mass spectra were recorded using a Bruker AutoFlex Speed in linear or reflectron mode. The matrix trans-2-[3-(4-tert-butylphenyl)-2-methyl-2-propenylidene]malononitrile (DCTB), was prepared at a concentration of 0.1 M in THF. The instrument was calibrated with a sample of poly(3-decylthiophene) with H/Br end-groups. The polymer sample was dissolved in THF to obtain an approx.1 mg/mL solution. A 5.00 μL aliquot of polymer solution was mixed with 2.5 μL of the DCTB solution. This mixture (1 μL) was placed on the target plate and then air-dried. The data were analyzed using flexAnalysis.

GC and GPC Prep: An aliquot of the heterogenous reaction mixture was extracted with $CHCl_3$ (5.0 mL), dried over $MgSO_4$, and filtered through glass wool. The organic layer was then split into two equal portions. The first portion was diluted with additional $CHCl_3$ (2.0 mL) and analyzed by GC. The other portion was concentrated in vacuo and then redissolved in THF:PhMe (99:1) (1.5 mL) with mild heating, passed through a PTFE filter (0.2 μm), and analyzed by GPC.

Gas Chromatography: Gas chromatography was carried out using a Shimadzu GC 2010 containing a Shimadzu SHRX5 (crossbound 5% diphenyl – 95% dimethyl polysiloxane; 15 m, 0.25 mm ID, 0.25 μm df) column.

Gel-Permeation Chromatography: Polymer molecular weights were determined by comparison with polystyrene standards (Varian, EasiCal PS-2 MW 580-377,400) on a Malvern Viscotek GPCMax VE2001 equipped with two Viscotek LT-5000L 8 mm (ID) × 300 mm (L) columns and analyzed with Viscotek TDA 305 (with R.I., UV-PDA Detector Model 2600 (190–500 nm),

RALS/LALS, and viscometer). Samples were dissolved in THF (with mild heating) and passed through a 0.2 µm PTFE filter prior to analysis. UV-PDA was used for all polymer MWs.

Titrations of the Grignard Reagents: An accurately weighed sample of salicylaldehyde phenylhydrazone[4] recrystallized from $CHCl_3$ (typically between 90–100 mg) was dissolved in 5.00 mL of THF. An aliquot (0.25 mL) of this solution was stirred at rt while the Grignard of interest was added dropwise using a 500 µL syringe. The initial solution is yellow and turns bright orange at the end-point.

III. Synthetic Procedures for S1, C1, S2, C2, S3

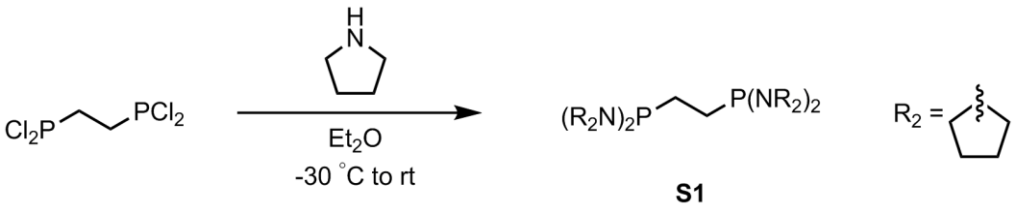

S1

1,2-bis(pyrrolidinylphosphino)ethane (S1): In the glovebox to a 20 mL vial equipped with a stir bar were added 1,2-bis(dichlorophosphino)ethane (0.15 mL, 1.0 mmol, 1.0 equiv) and Et_2O (4.6 mL). To an 8 mL vial were added pyrrolidine (0.83 mL, 10 mmol, 10 equiv) and Et_2O (2.3 mL). Both vials were placed in a -30 °C freezer and chilled for 10 min. After this time, the vials were removed from the freezer and the vial containing the dichlorophosphinoethane was put under vigorous stirring (1500 rpm). To the stirring vial was added the pyrrolidine solution dropwise over 1 min. Upon addition, a white solid immediately began to precipitate. The vial was sealed, warmed to rt, and stirred for 4 h. The heterogeneous mixture was filtered, and the solid was washed with Et_2O (15 mL) and the filtrate collected. The volatiles were removed under vacuum to yield 284 mg of **S1** in 77% yield as a white solid.

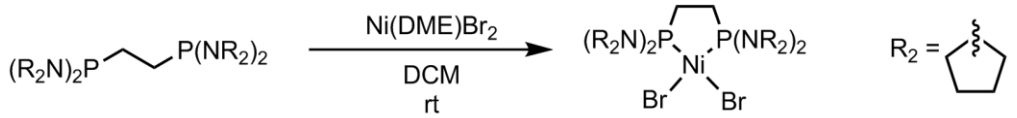

S1 **C1**

1,2-bis(pyrrolidinylphosphino)ethane nickel dibromide (cat 1): In the glovebox to a 20 mL vial equipped with a stir bar were added $Ni(DME)Br_2$ (36.0 mg, 0.117 mmol, 1.00 equiv) and DCM (3.8 mL). **S1** (47 mg, 0.127 mmol, 1.09 equiv) was dissolved in DCM (1.5 mL) and then added via pipette to the stirring nickel solution. The reaction was stirred overnight yielding an orange solution. The volatiles were removed under vacuum yielding an orange/yellow solid that was washed with pentanes (20 mL) and filtered through a PTFE filter. DCM (5 mL) was then passed through the filter to dissolve the solids into a 20 mL vial. The volatiles were removed under vacuum to yield 30 mg of **C1** as an orange powder (44% yield).

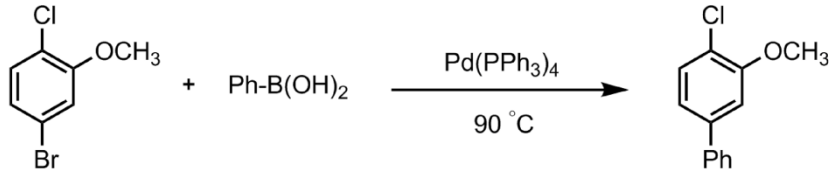

S2

2-chloro-5-phenylanisole (S2): A 25 mL Schlenk flask was equipped with a stir bar in the glovebox and charged with $Pd(PPh_3)_4$ (136 mg, 0.118 mmol, 0.0600 equiv). The flask was then removed from the glovebox and charged with phenylboronic acid (358 mg, 2.94 mmol, 1.50 equiv) and K_2CO_3 (813 mg, 5.89 mmol, 3.00 equiv). A solution of 1,4-dioxane and water (20 mL, 9:1) was sparged with N_2 for 30 min. Then, 9 mL were added to the flask. 4-bromo-1-chloro-2-methoxy-benzene (434 mg, 1.96 mmol, 1.00 equiv) dissolved in the dioxane/water solution (6 mL) was then added to the reaction mixture. The reaction mixture was heated to 90 °C for 6 h. The reaction was quenched with saturated NH_4Cl (50 mL), extracted with EtOAc (3 x 30 mL), washed with brine (30 mL), dried over $MgSO_4$, filtered, and concentrated in vacuo. The product was purified by silica gel chromatography using 10/90 (v/v) EtOAc/hexanes to give 322 mg of **S2** a colorless oil (75% yield). HRMS (EI): [M+] Calc'd for $C_{13}H_{11}ClO$, 218.0498; found, 218.0499.

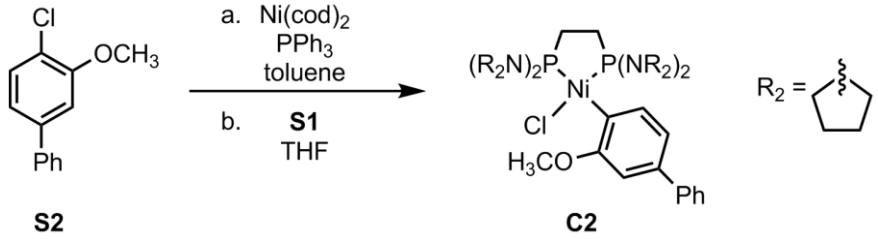

S2 **C2**

1,2-bis(pyrrolidinylphosphinoethane [3-methoxy(1,1'-biphenyl)-4-yl] nickel(II) chloride (C2): In the glovebox, a 20 mL vial equipped with a stirbar was charged with $Ni(cod)_2$ (296 mg, 1.07 mmol, 1.00 equiv) and PPh_3 (564 mg, 2.15 mmol, 2.00 equiv) and dissolved in THF (6 mL) with stirring. In a separate 20 mL vial, 2-chloro-5-phenylanisole (306 mg, 1.40 mmol, 1.3 equiv) was dissolved in THF (4 mL) and transferred to the stirring $Ni(cod)_2/PPh_3$ solution via pipette. The now red solution was stirred for 4 h. Then the volatiles were removed under vacuum until 0.5 mL of solvent remained. Adding hexanes (15 mL) lead to a yellow precipitate. This precipitate was filtered, washed with hexanes (10 mL), and the solids collected (561 mg, 65% crude yield) and used without further purification. A new 20 mL vial equipped with a stir bar was charged with the isolated solid (119 mg, 0.149 mmol, 1.00 equiv) and THF (1.0 mL). **S1** (66.0 mg, 0.178 mmol, 1.20 equiv) was dissolved in THF (1.0 mL) and added via pipette to the stirring nickel solution. The yellow solution turned orange upon ligand addition. The reaction was stirred for 60 min before the volatiles were removed under vacuum until 0.5 mL of solvent remained. Adding hexanes (15 mL) precipitated a yellow solid. The vial was placed in a freezer (-30 °C) for 16 h, after which the mixture was filtered, washed with hexanes (15 mL), and the solid collected and dried under vacuum to yield 52 mg of **C2** (54% yield) as a yellow solid. Elemental Analysis: Calcd for $C_{31}H_{47}ClN_4NiOP_2$, C, 57.47; H, 7.31; N, 8.35 Found C, 57.22; H, 7.33; N, 8.62.

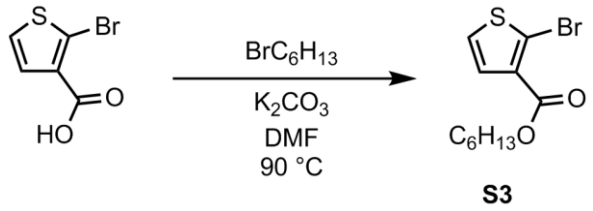

S3

Hexyl 2-bromothiophene-3-carboxylate (S4): To an oven dried 25 mL round-bottom flask equipped with a stir bar were added 2-bromothiophene-3-carboxylic acid (1.015 g, 4.902 mmol, 1.00 equiv), K_2CO_3 (2.03 g, 14.7 mmol, 3.00 equiv) and DMF (6.5 mL). Then 1-bromohexane (1.37 mL, 9.80 mmol, 2.00 equiv) was added. The flask was sealed with a rubber septum, placed under N_2, and stirred at 90 °C for 12 h. The reaction was then cooled to rt and then H_2O (20 mL) was added. The resulting mixture was added to a separatory funnel and the aqueous layer extracted with Et_2O (3 x 10 mL) and the combined organic extracts washed with brine (2 x 10 mL), dried over $MgSO_4$, and filtered. The filtrate solvent was concentrated in vacuo leaving behind a yellow oil. The yellow oil was purified by flash chromatography with a gradient of hexanes/EtOAc (99:1 to 94:6) as the eluent to afford 956 mg of **S3** as a clear oil (67% yield).

IV. NMR spectra of S1, C1, S2, C2, S3

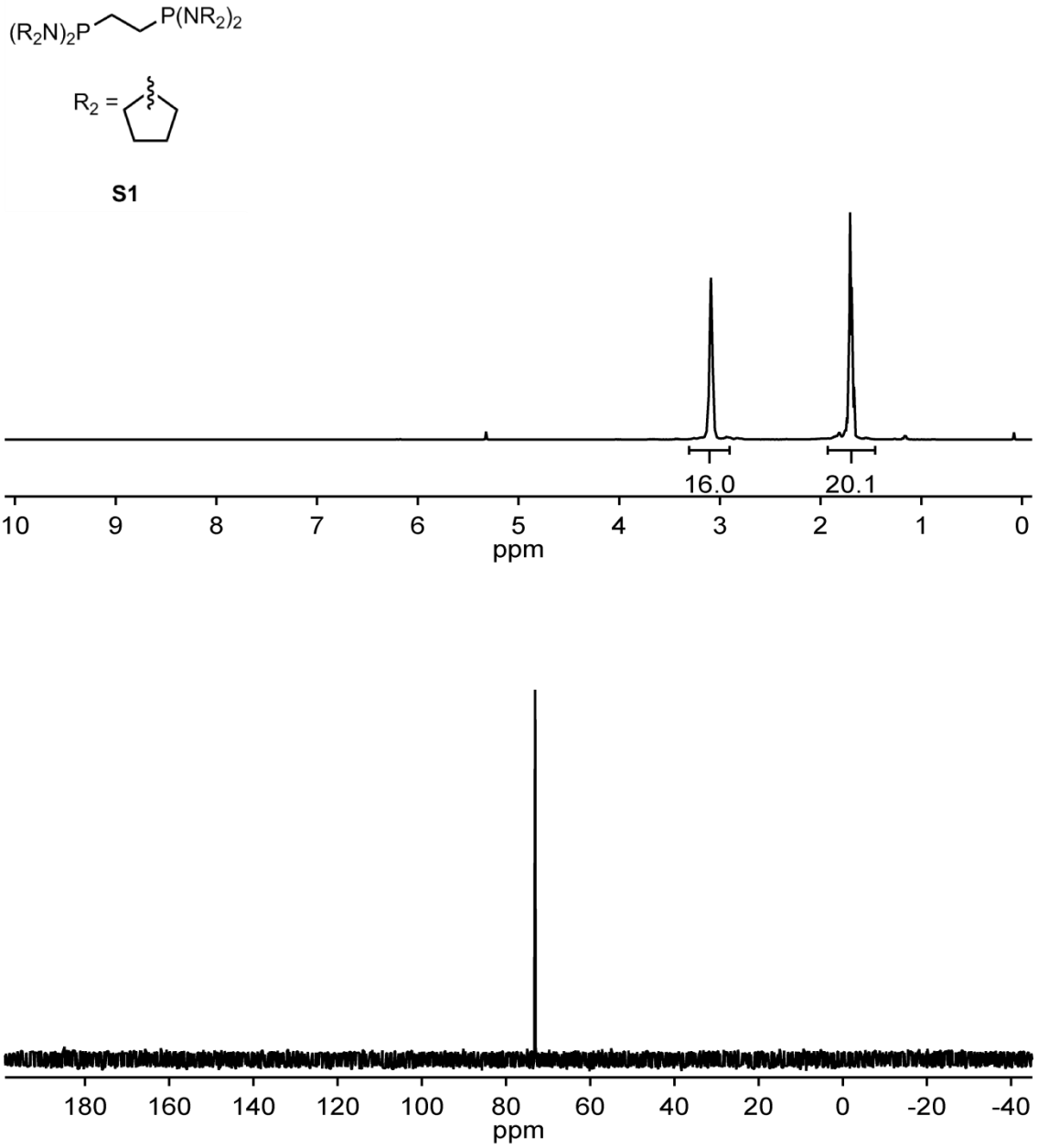

Figure S2.1. ^{1}H and ^{31}P NMR spectra of **S1**.
^{1}H NMR (500 MHz, CD_2Cl_2) δ 3.34–2.74 (m, 16H), 1.94–1.31 (m, 20H) ppm.
^{31}P NMR (202 MHz, CD_2Cl_2) δ 73.07 ppm.

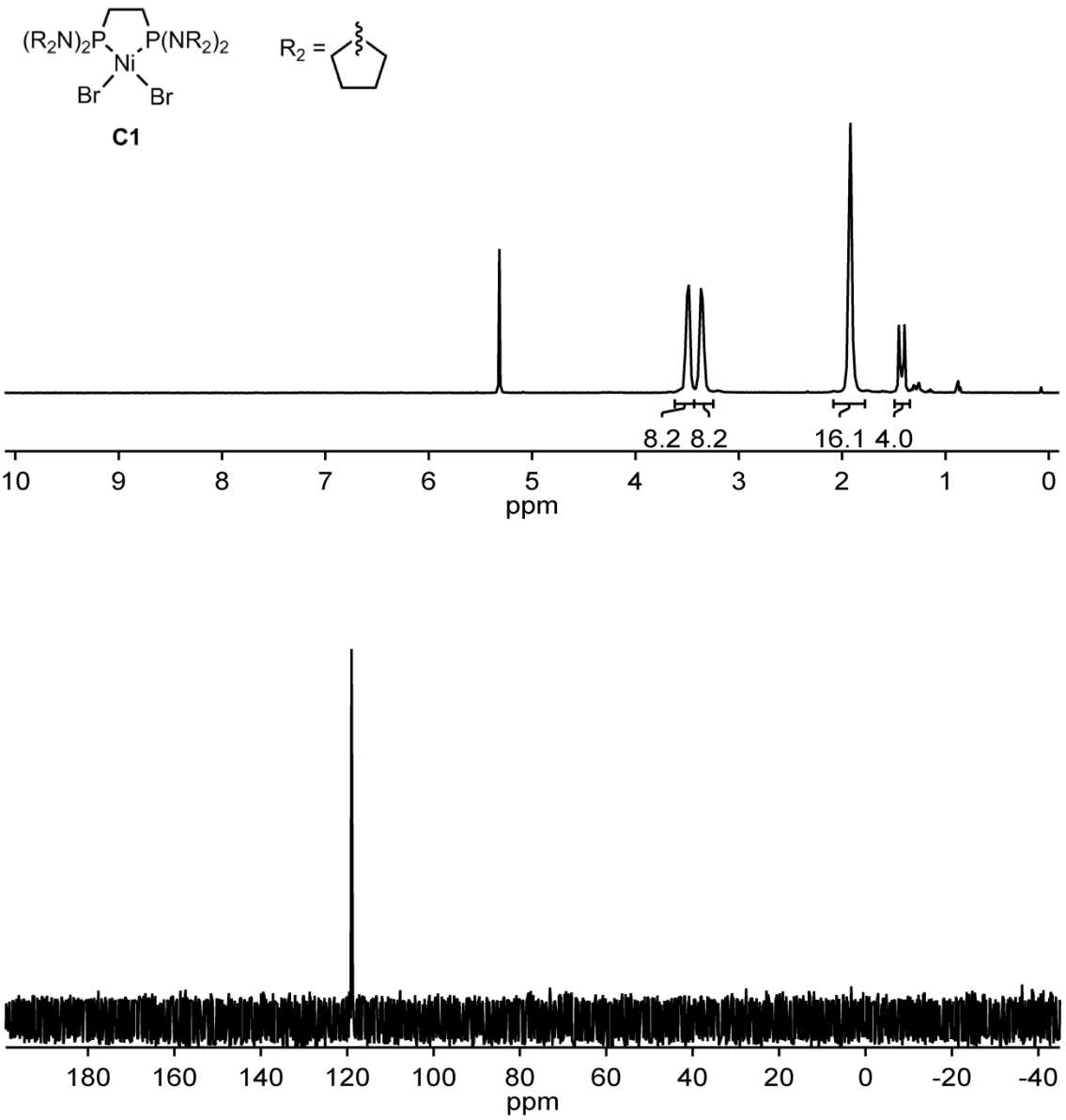

Figure S2.2. ^{1}H and ^{31}P NMR spectra of **C1**.
^{1}H NMR (500 MHz, CD_2Cl_2) δ 3.57–3.43 (m, 8H), 3.43–3.27 (m, 8H), 2.07–1.73 (m, 16H), 1.49–1.31 (m, 4H) ppm.
^{31}P NMR (202 MHz, CD_2Cl_2) δ 118.97 ppm.

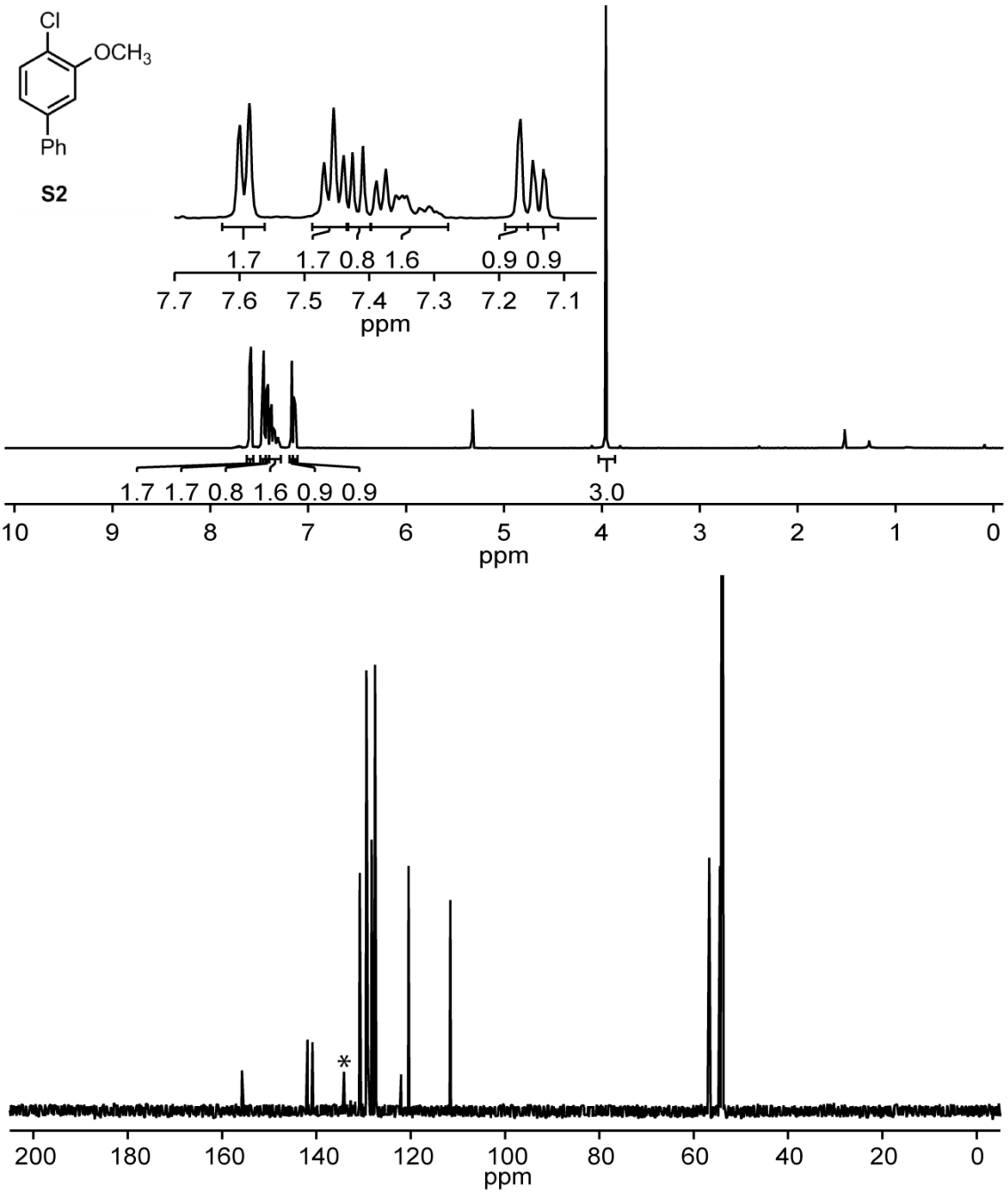

Figure S2.3. ^{1}H and ^{13}C NMR spectra of **S2**
^{1}H NMR (500 MHz, CD_2Cl_2) δ 7.62–7.56 (m, 2H), 7.45 (app t, 2H), 7.42–7.35 (m, 2H), 7.17 (m, 1H), 7.15 (m dd, 1H), 3.97 (s, 3H) ppm
^{13}C NMR (126 MHz, CD_2Cl_2) δ 155.18, 141.28, 140.23, 130.23, 128.79, 127.70, 126.97, 121.41, 119.86, 110.98, 56.11 ppm *denotes impurity

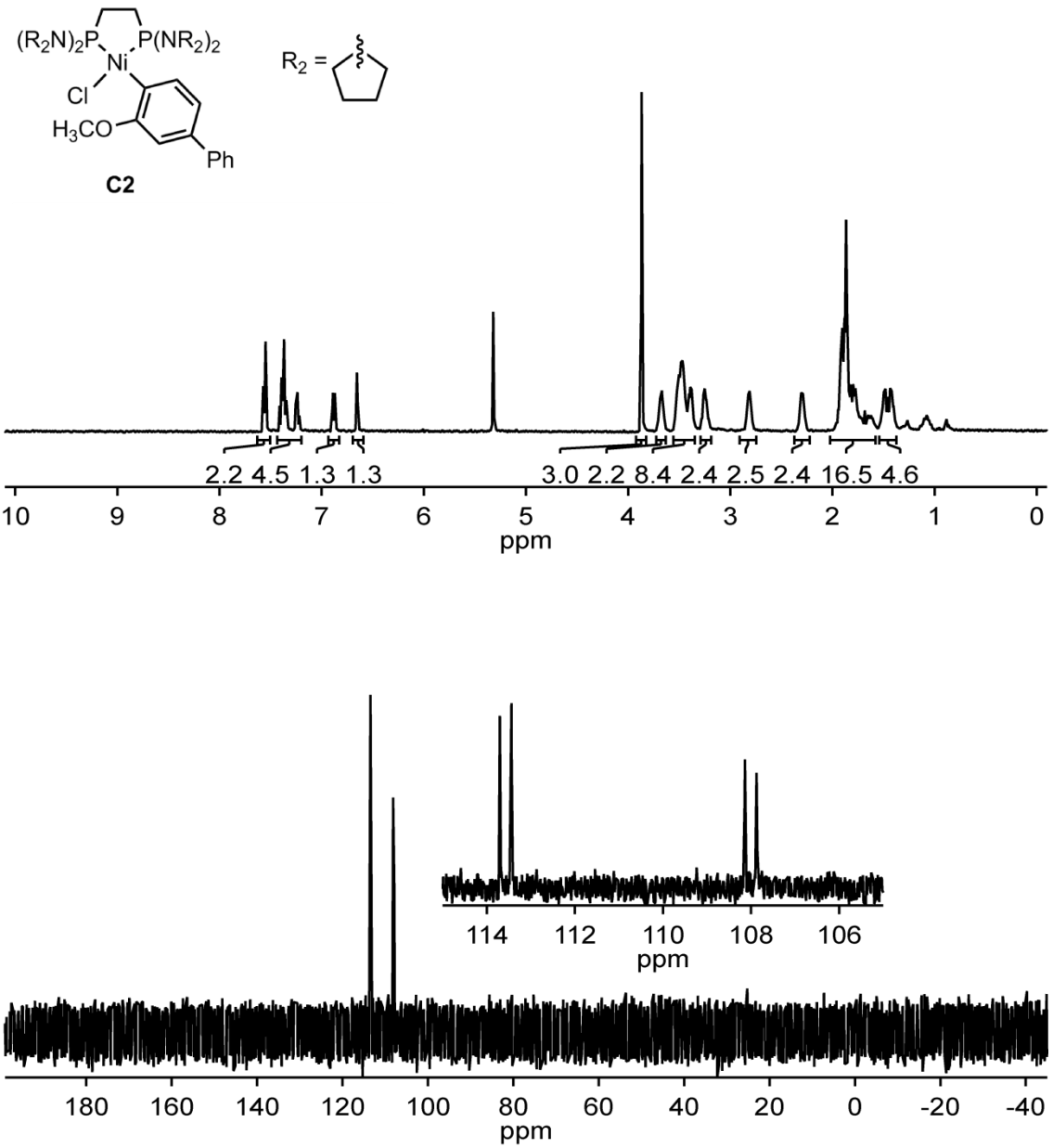

Figure S2.4. ^{1}H and ^{31}P NMR spectra of **C2**
^{1}H NMR (500 MHz, CD_2Cl_2) δ 7.59–7.52 (m, 2H), 7.44–7.18 (m, 5H), 6.88 (app d, 1H), 6.65 (app dd, 1H), 3.87 (s, 3H), 3.75–3.60 (m, 2H), 3.59–3.32 (m, 8H), 3.31–3.18 (m, 2H), 2.85–2.74 (m, 2H), 2.39–2.22 (m, 2H), 2.02–1.57 (m, 16H), 1.58–1.31 (m, 4H) ppm
^{31}P NMR (202 MHz, CD_2Cl_2) δ 113.57 (d, *J* = 42.7 Hz), 108.01 (d, *J* = 42.8 Hz) ppm.

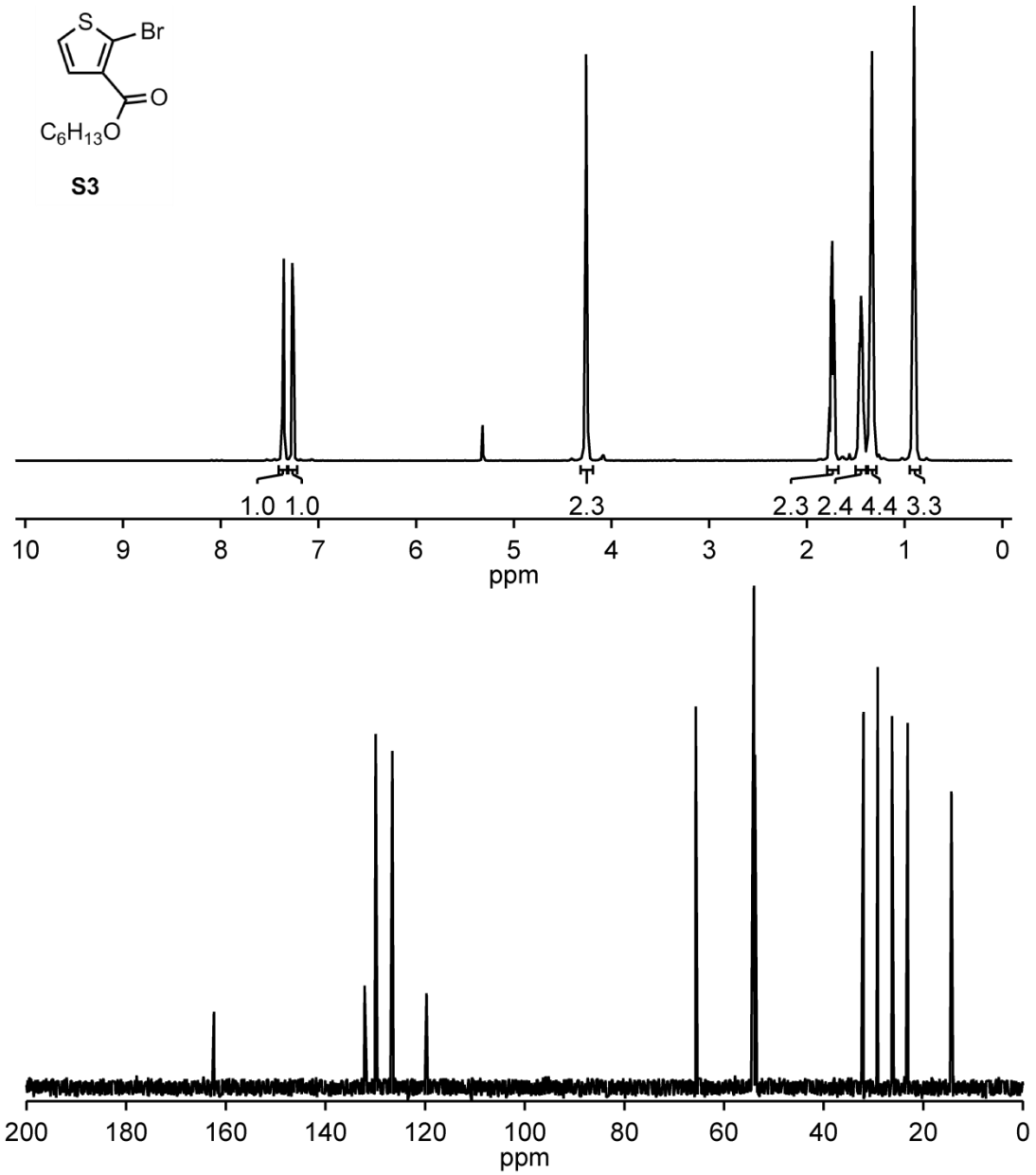

Figure S2.5. ^{1}H and ^{31}P NMR spectra of **S3**.
^{1}H NMR (500 MHz, CD_2Cl_2) δ 7.36 (d, *J* = 5.8 Hz, 1H), 7.26 (d, *J* = 5.7 Hz, 1H), 4.26 (t, *J* = 6.6 Hz, 2H), 1.81–1.67 (m, 2H), 1.51–1.39 (m, 2H), 1.39–1.27 (m, 4H), 0.99–0.81 (m, 3H) ppm.
^{13}C NMR (126 MHz, CD_2Cl_2) δ 162.37, 132.13, 129.92, 126.56, 119.70, 65.68, 32.02, 29.15, 26.29, 23.13, 14.36 ppm.

V. BHP polymerizations using C1 and C2

Representative catalyst stock solution prep

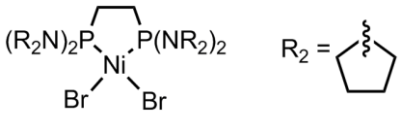

C1

To a 4 mL vial in the glovebox were added **C1** (10.0 mg) and THF (3.4 mL) and stirred until homogeneous (1 min) to yield a 5 mM solution.

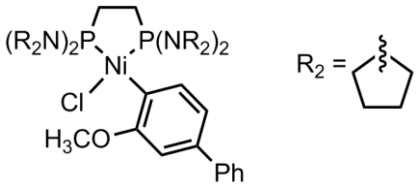

C2

To a 4 mL vial in the glovebox were added **C2** (2.5 mg) and THF (0.77 mL) and stirred until homogeneous (1 min) to yield a 5 mM solution.

Representative 1,4-dibromo-2,5-bishexyloxyphenylene Grignard Metathesis

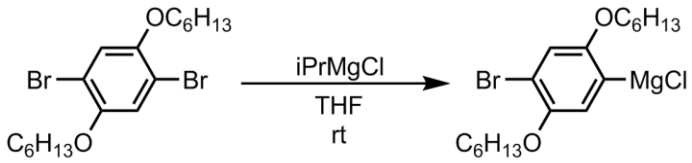

BHP

In the glovebox, 1,4-dibromo-2,5-bishexyloxyphenylene (763 mg, 1.75 mmol, 1.00 equiv) was added to a 20 mL vial equipped with a stir bar, followed by n-docosane (approx. 4.0 mg) and THF (2.10 mL). The mixture was stirred until homogeneous (5 min). To the stirring solution was added iPrMgCl (0.70 mL, 1.4 mmol, 2.0 M in THF, 0.80 equiv) and stirred for 16 h. **BHP** was titrated (see page 102) to be 0.40 M. An aliquot (0.3 mL) of **BHP** was quenched with aq. HCl (0.5 mL, 12 M) outside the box and the reaction mixture extracted with $CHCl_3$ (2.0 mL), dried over $MgSO_4$, filtered through glass wool and analyzed by GC.

i. BHP homopolymerizations using C1 and C2

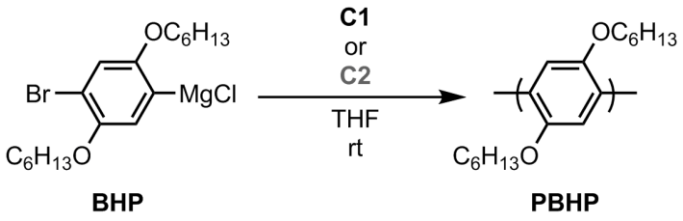

BHP **PBHP**

C1: In the glovebox to an 8 mL vial equipped with a stir bar were added **C1** (0.32 mL, 1.6 µmol, 1.0 equiv, 5 mM) and THF (0.58 mL). To the stirring solution was added **BHP** (0.3 mL, 0.12 mmol, 75 equiv, 0.40 M). The polymerization was stirred for 8 h before being poured into a 20 mL vial containing aq. HCl (5.0 mL, 12 M). The reaction was worked up according to the GC and GPC prep found on page 101.

C2: In the glovebox to an 8 mL vial equipped with a stir bar were added **C2** (0.32 mL, 1.6 µmol, 1.0 equiv, 5 mM) and THF (0.58 mL). To the stirring solution was added **BHP** (0.3 mL, 0.12 mmol, 75 equiv, 0.40 M). The polymerization was stirred for 8 h before being poured into a 20 mL vial containing aq. HCl (5.0 mL, 12 M). The reaction was worked up according to the GC and GPC prep found on page 101.

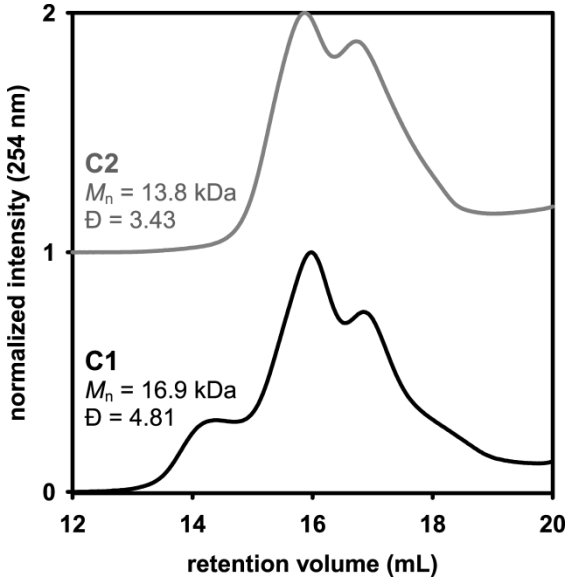

Figure S2.6. GPC trace for **BHP** polymerization using **C1** and **C2**.

ii. ^{31}P NMR BHP polymerization using C1

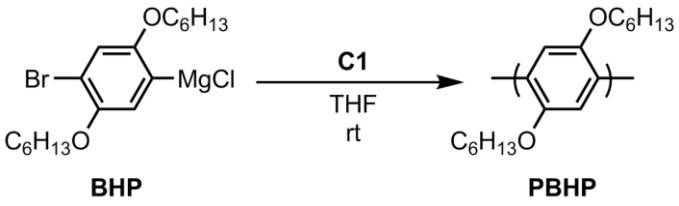

BHP **PBHP**

In the glovebox **C1** (6.3 mg, 0.011 mmol, 1.0 equiv) was dissolved in THF (0.7 mL) then added to a J. Young NMR tube which was sealed with a septum and placed in the spectrometer where an initial ^{31}P NMR spectrum was recorded. A solution of **BHP** (0.5 mL, 0.19 mmol, 15 equiv, 0.37 M) was added, and the tube was inverted twice to mix, placed back into the spectrometer, and the array immediately started. All ^{31}P NMR spectra were acquired with a time point taken at 5 min intervals over an 80 min period. (scan size = 16, d1 = 0.5 sec)

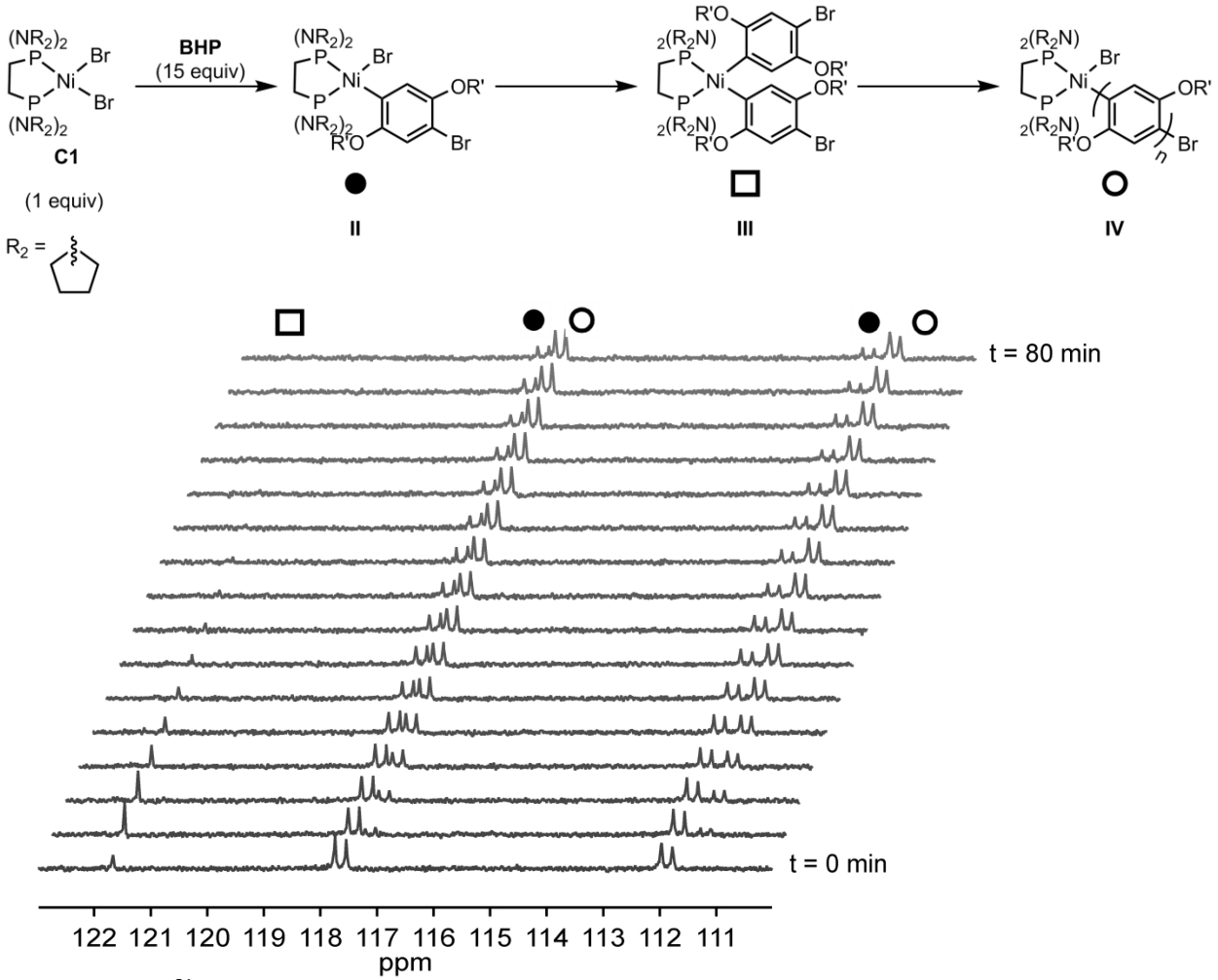

Figure S2.7 ^{31}P spectra for polymerizing **BHP** (15 equiv) with **C1** (1 equiv) and the various catalytic species throughout the polymerization

VI. 3HT polymerizations using C1 and C2

Representative catalyst stock solution prep

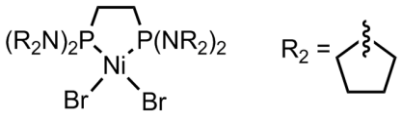

C1

To a 4 mL vial in the glovebox were added **cat 1** (10.0 mg) and THF (3.4 mL) and stirred until homogeneous (1 min).

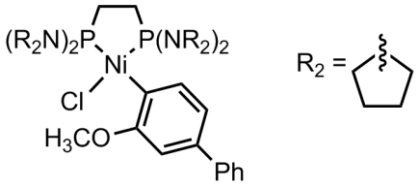

C2

To a 4 mL vial in the glovebox were added **cat 2** (5.5 mg) and THF (1.7 mL) and stirred until homogeneous (1 min).

Representative 2,5-dibromo-3-hexylthiophene Grignard Metathesis

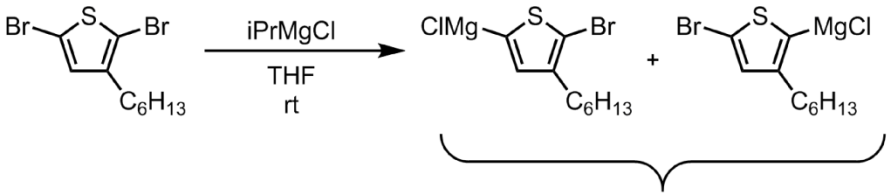

79:21

3HT

In the glovebox, 2,5-dibromo-3-hexylthiophene (107 mg, 0.328 mmol, 1.00 equiv) was added to a 20 mL vial equipped with a stir bar, followed by n-docosane (approx. 4.0 mg) and THF (2.18 mL). To the stirring solution was added iPrMgCl (115 µL, 0.230 mmol, 2.00 M in THF, 0.700 equiv) and stirred for 30 min. **3HT** was titrated (see page) to be 0.089 M. An aliquot (0.3 mL) of **3HT** was quenched with aq. HCl (0.5 mL, 12 M) outside the box and the reaction mixture extracted with $CHCl_3$ (2.0 mL), dried over $MgSO_4$, filtered through glass wool and analyzed by GC.

i. 3HT polymerization using C1

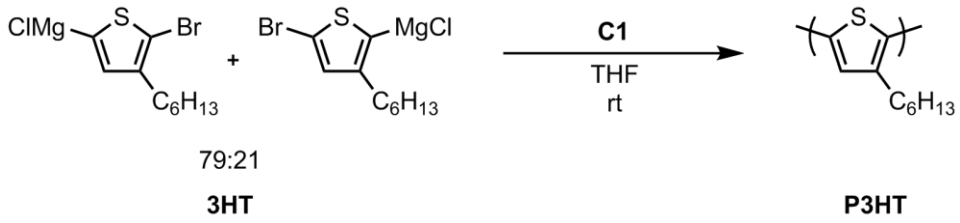

In the glovebox to an 8 mL vial equipped with a stir bar were added **cat 1** (0.10 mL, 0.50 µmol, 1.0 equiv, 5 mM) and THF (1.36 mL). To the stirring solution was added **3HT** (0.42 mL, 0.037 mmol, 75 equiv, 0.089 M). The polymerization was stirred for 90 min before being poured into a 20 mL vial containing aq. HCl (2.0 mL, 12 M). The reaction was worked up according to the GPC prep found on S2.

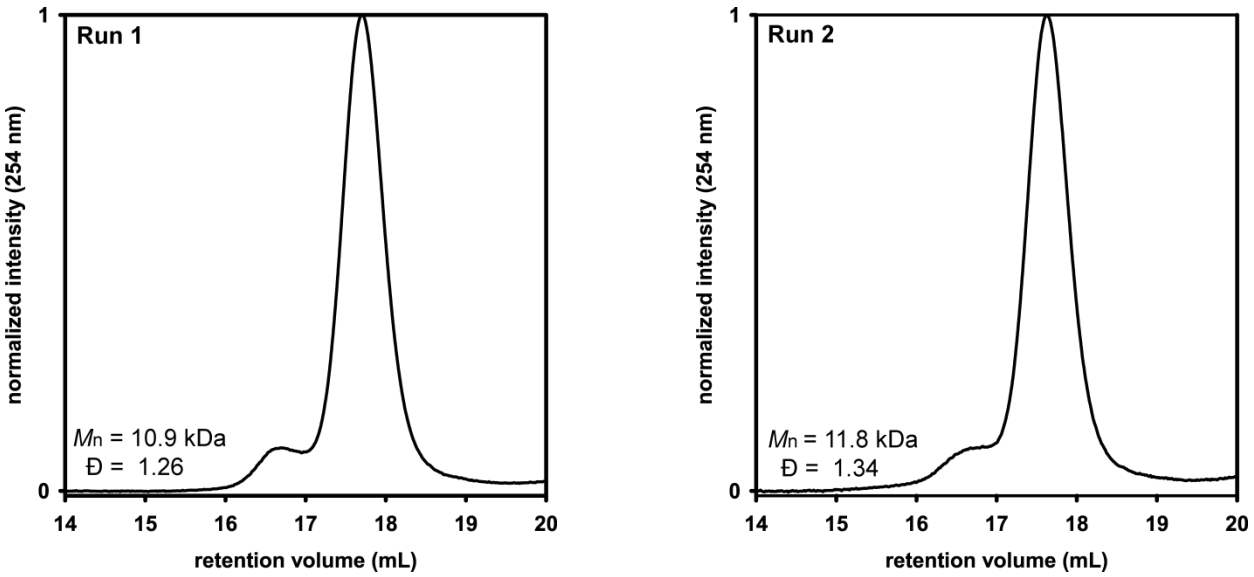

Figure S2.8. GPC trace for **3HT** polymerization using **C1**.

ii. 3HT polymerization using C2

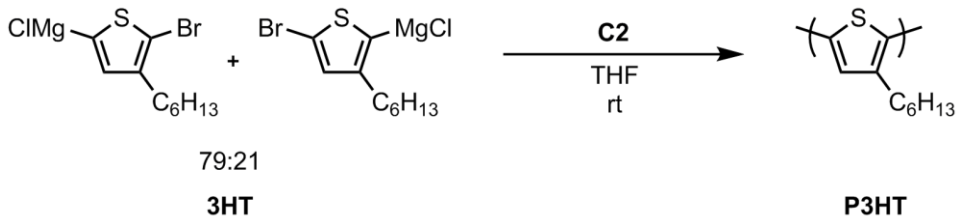

79:21

3HT **P3HT**

In the glovebox to an 8 mL vial equipped with a stir bar were added **C2** (0.10 mL, 0.50 µmol, 1.0 equiv, 5 mM) and THF (1.36 mL). To the stirring solution was added **3HT** (0.42 mL, 0.037 mmol, 75 equiv, 0.088 M). The polymerization was stirred for 90 min before being poured into a 20 mL vial containing aq. HCl (5.0 mL, 12 M). The reaction was worked up according to the GC and GPC prep found on S2. After GC and GPC analysis, both portions were recombined and the solvent removed *in vacuo* to yield a purple solid. The solid was dissolved in a minimum amount of $CHCl_3$ (0.5 mL), and precipitated with MeOH (15.0 mL). The mixture was then centrifuged, the solvent decanted, and the solid dried under vacuum to afford **P3HT** as a purple solid. (KDS-4-147)

Run 1: GC: major regioisomer consumed only (90%). 3.2 mg, 52% yield.
Run 2: GC: major regioisomer consumed only (99%). 3.0 mg, 48% yield.

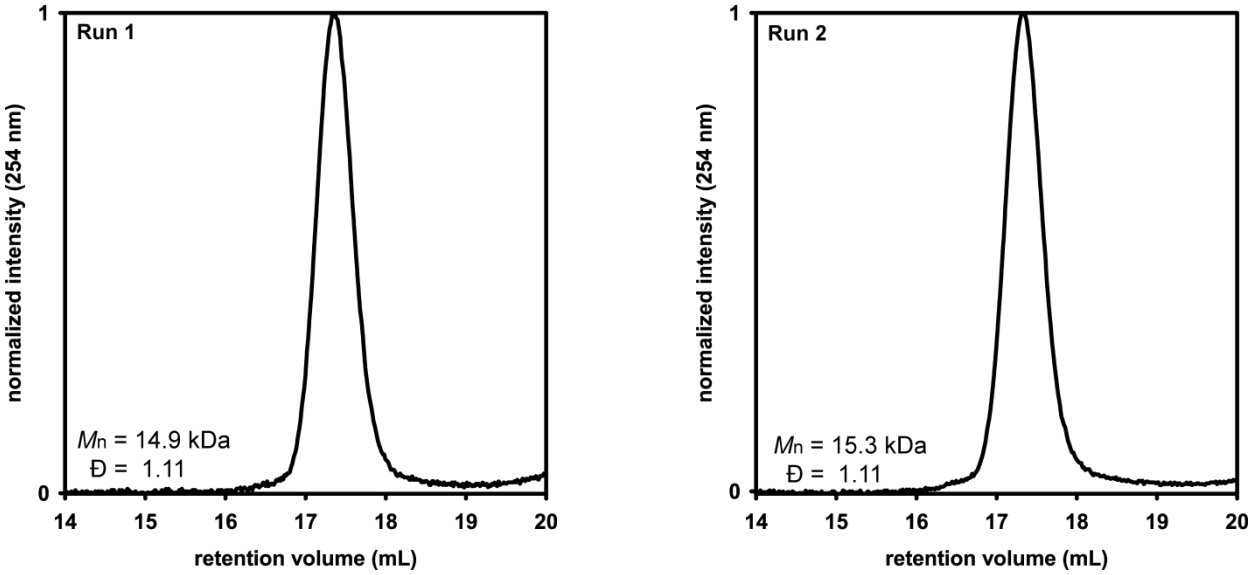

Figure S2.9. GPC trace for **3HT** polymerization using **C2**.

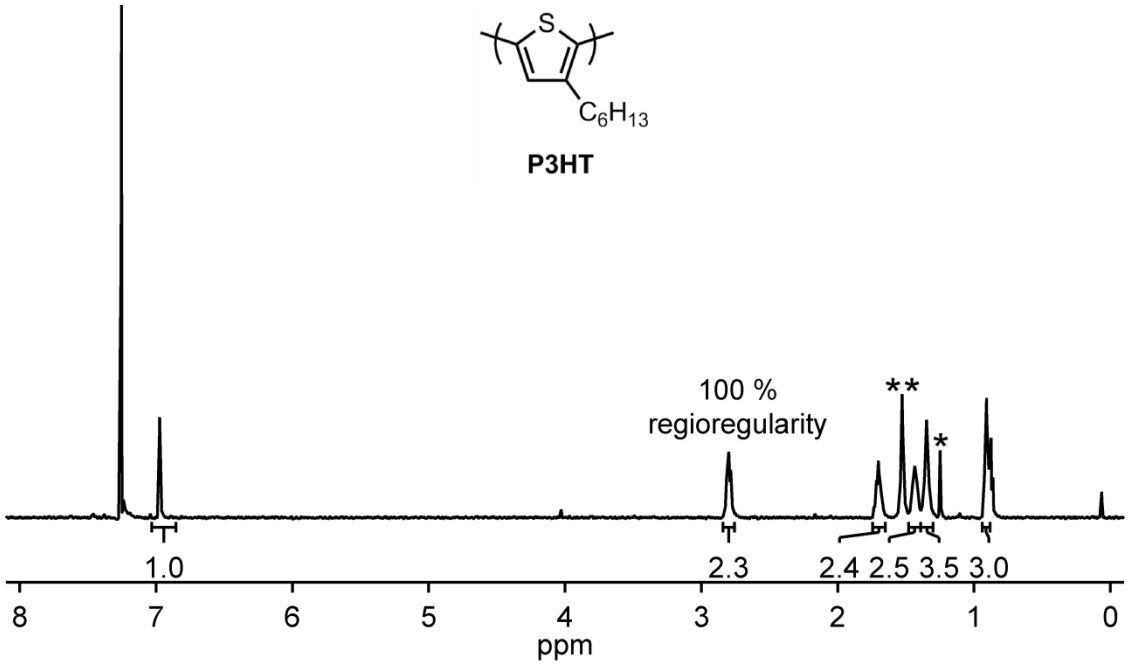

Figure S2.10. ^{1}H NMR spectrum for **3HT** polymerization using **C2**. *residual $C_{22}H_{46}$ standard, **H_2O

iii. Vary monomer:catalyst in 3HT homopolymerization with C2

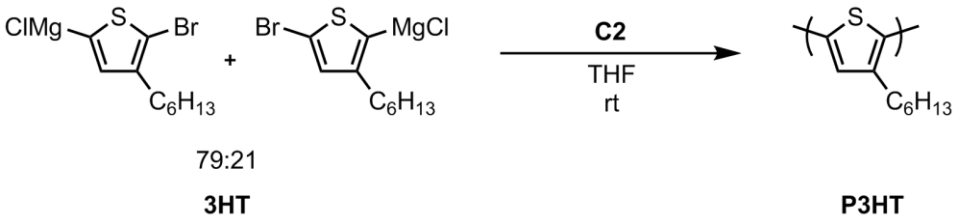

79:21

3HT **P3HT**

To three 8 mL vials equipped with stir bars were added the **C2** solution (100 µL, 0.5 µmol, 1.0 equiv, 5 mM) and the respective amounts of THF and **3HT** listed below.

Vial 1: THF (0.38 mL), **3HT** (0.10 mL, 0.013 mmol, 25 equiv)
Vial 2: THF (0.87 mL), **3HT** (0.20 mL, 0.025 mmol, 50 equiv)
Vial 3: THF (1.36 mL), **3HT** (0.40 mL, 0.037 mmol, 75 equiv)

The polymerizations were stirred for 90 min at rt, after which each vial was removed from the box and poured into a 20 mL vial containing aq. HCl (5.0 mL, 12 M) to quench. Each quenched reaction was worked up according to the GC (only major regioisomer consumed) and GPC prep found on 101.

Run 1

ratio 3HT:cat 2	% conversion major 3HT	M_n (kDa)	Đ	theor. M_n (kDa)
25:1	98.2	5.25	1.13	4.1
50:1	99	9.65	1.08	8.3
75:1	90.4	14.9	1.10	11.3

Run 2

ratio 3HT:cat 2	% conversion major 3HT	M_n (kDa)	Đ	theor. M_n (kDa)
25:1	99	5.08	1.13	4.1
50:1	99	11.2	1.11	8.3
75:1	99	15.3	1.11	12.4

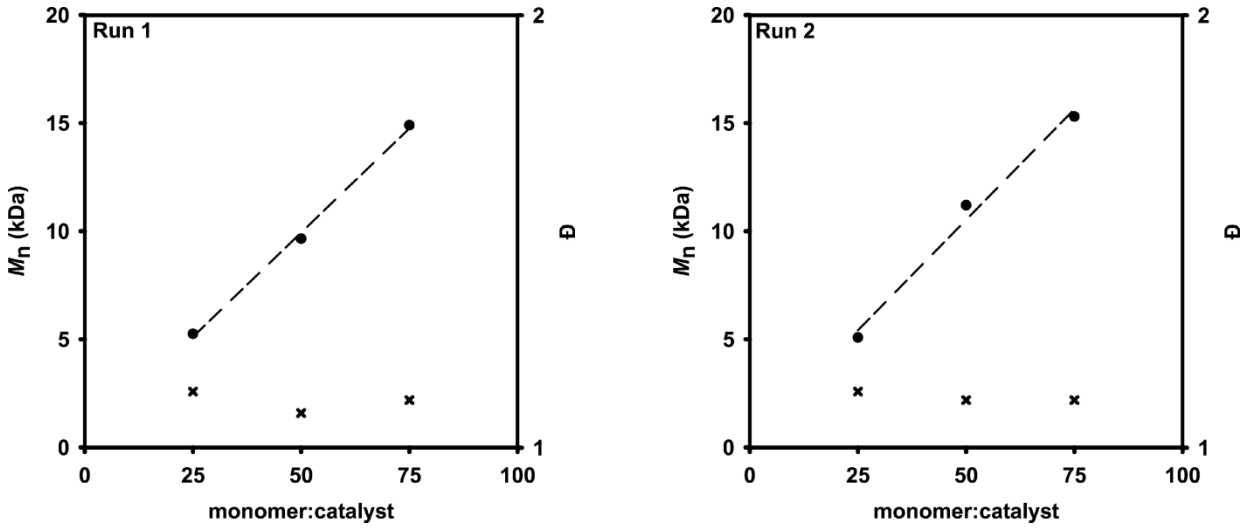

Figure S2.11. Plot of the number-average molecular weight versus monomer-to-catalyst ratio in polymerization of **3HT** with **C2**.

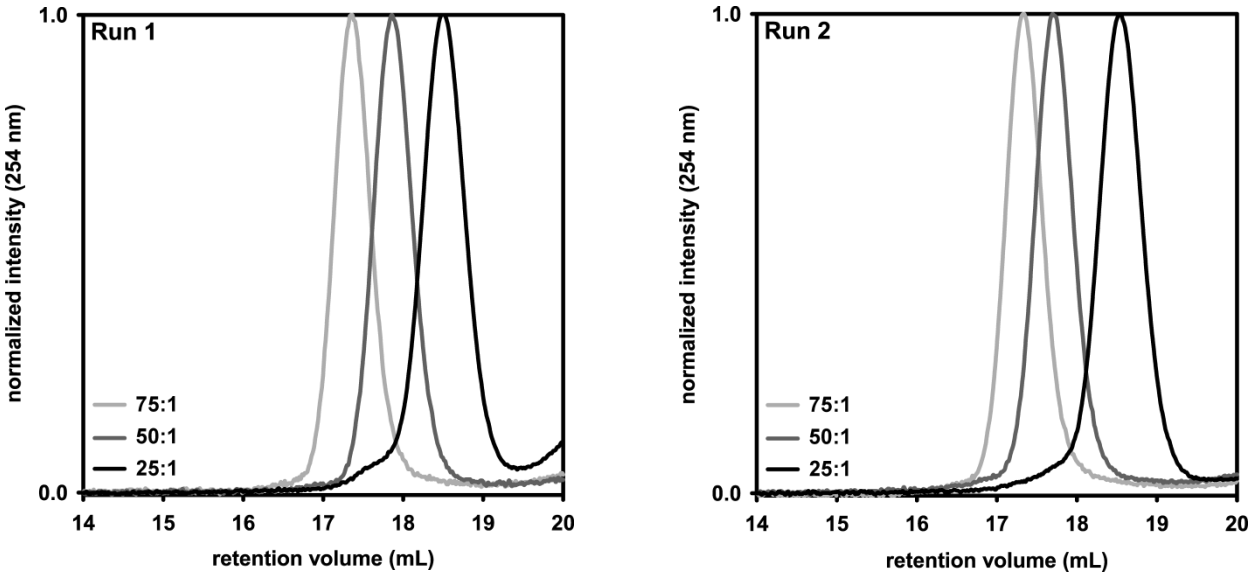

Figure S2.12. GPC traces for polymerization of **3HT** with **C2**.

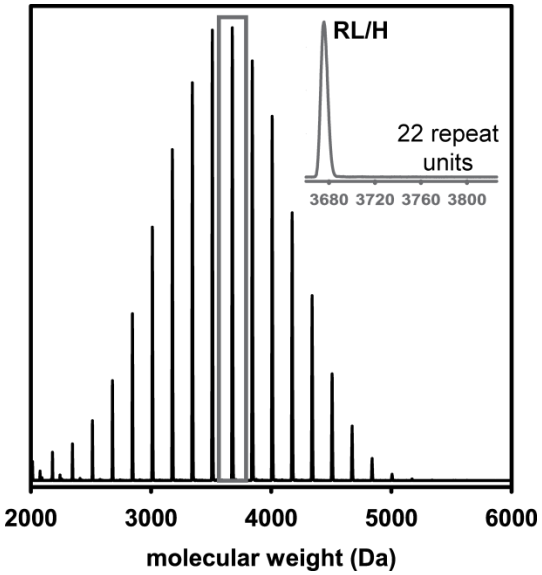

Figure S2.13 MALDI-TOF/MS spectrum for **3HT** polymerization using **C2** (25:1 mon:cat from above experiment).

iv. Number-average molecular weight versus percent conversion of monomer in 3HT homopolymerization using C2

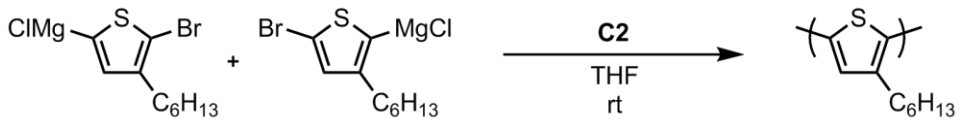

79:21

3HT **P3HT**

In the glovebox to a 20 mL vial equipped with a stir bar were added **C2** (0.20 mL, 1.0 µmol, 1.0 equiv, 5 mM) and THF (2.45 mL). To the stirring solution was added **3HT** (0.84 mL, 0.075 mmol, 75 equiv, 0.088 M). Aliquots (0.3 mL) were taken at 20, 30, 40, 50, and 60 min and quenched with aq. HCl (0.5 mL, 12 M) outside of the box. Each aliquot was worked up according to the GC (only major regioisomer consumed) and GPC prep found on page 101.

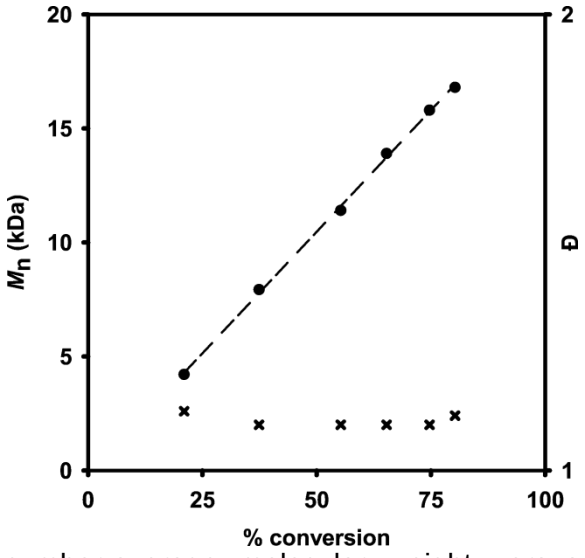

Figure S2.14. Plot of number-average molecular weight versus percent conversion for polymerization of **3HT** with **C2**.

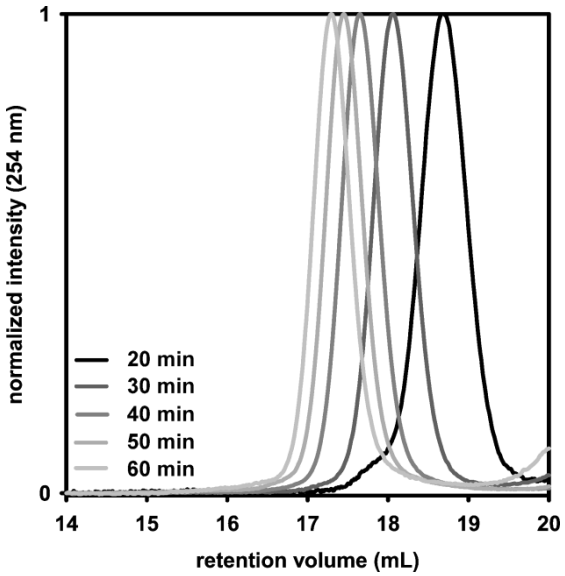

Figure S2.15. GPC traces of number-average molecular weight versus percent conversion for polymerization of **3HT** with **C2**.

v. Chain extending $P3HT_{initial}$ with 3HT using C2

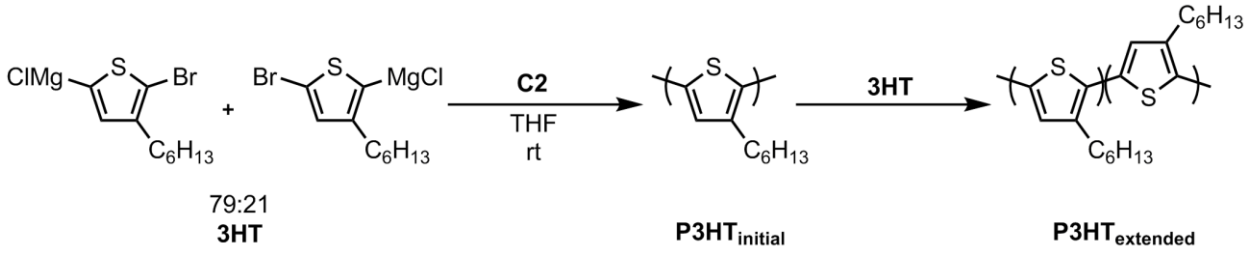

In the glovebox to an 8 mL vial equipped with a stir bar were added **cat 2** (0.10 mL, 0.50 µmol, 1.0 equiv, 5 mM) and THF (0.43 mL). To the stirring solution was added **3HT** (0.21 mL, 0.018 mmol, 37 equiv, 0.088 M). The polymerization was stirred for 30 min before an aliquot was taken and quenched outside the box with HCl (0.5 mL, 12M). The aliquot was worked up according to the GC and GPC prep found on S2. To the stirring **$P3HT_{initial}$** solution was added additional **3HT** (0.21 mL, 0.018 mmol, 37 equiv, 0.088 M) and the polymerization stirred for 30 min. The polymerization was then removed from the glovebox and poured into a 20 mL vial containing aq. HCl (5.0 mL, 12 M). The reaction was worked up according to GPC prep found on S2.

Run 1: $P3HT_{initial}$: GC: major regioisomer consumed only (98%). GC analysis not performed on **$P3HT_{extended}$**.
Run 2: $P3HT_{initial}$: GC: major regioisomer consumed only (99%). GC analysis not performed on **$P3HT_{extended}$**.

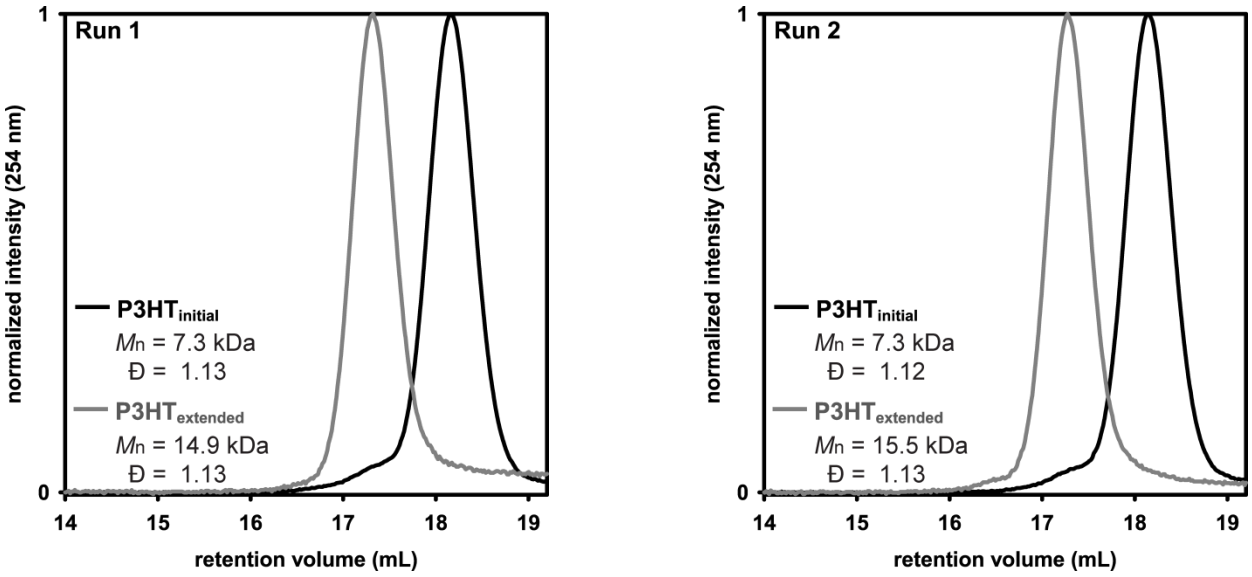

Figure S2.16. GPC traces for chain extending **$P3HT_{initial}$** with **3HT** using **C2**.

VI. 3HET Polymerization using C2

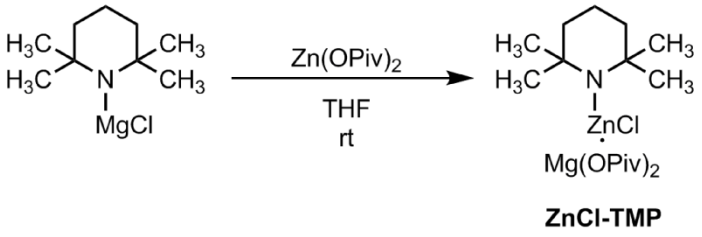

ZnCl-TMP

ZnCl-TMP: In the glovebox, $Zn(OPiv)_2$ (71 mg, 0.267 mmol, 1.10 equiv) was added to a 4 mL vial equipped with a stir bar. To the vial was added 2,2,6,6-tetramethylpiperidinylmagnesium chloride lithium chloride complex solution (310 µL, 0.242 mmol, 0.77 M in THF, 1.00 equiv) and the heterogeneous mixture stirred for 30 min. THF (0.17 mL) was added to the vial and the mixture stirred for an additional 5 min, turning a clear, light yellow solution.

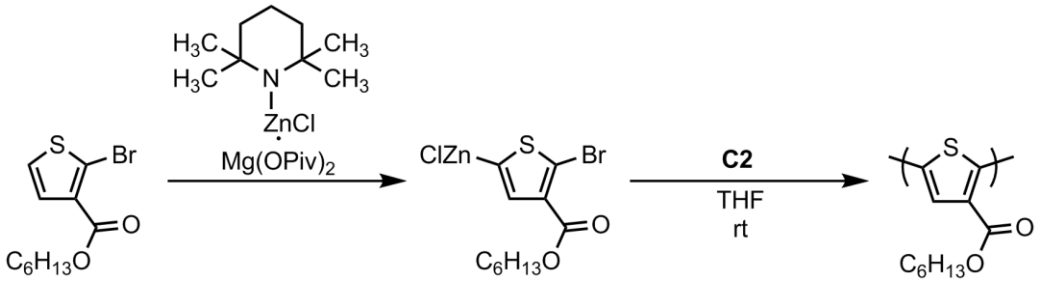

3HET **P3HET**

In the glovebox, hexyl 2-bromo-3-thiophenecarboxylate (25 mg, 0.086 mmol, 1.00 equiv) was added to a 4 mL vial equipped with a stir bar and THF (0.69 mL). To the stirring solution was added **ZnCl-TMP** (170 µL, 0.0860 mmol, 0.50 M in THF, 1.00 equiv) and stirred for 60 min. An aliquot (0.3 mL) of **3HET** was quenched with I_2 (4 mg) outside the box. Excess iodine was quenched with sat'd sodium thiosulfate, until the brown solution turned white (1.0 mL). The reaction mixture was extracted with $CHCl_3$ (2.0 mL), dried over $MgSO_4$, filtered through glass wool and analyzed by GC to show 58% active monomer. In the glovebox to a 4 mL vial equipped with a stir bar were added **C2** (0.10 mL, 0.50 µmol, 1.0 equiv) and THF (0.5 mL). To the stirring solution was added **3HET** (0.15 mL, 0.0087 mmol, 17 equiv, 0.058 M). The polymerization stirred for 3 h, before the polymerization was removed from the box and quenched with HCl (0.5 mL, 12 M). The reaction mixture was extracted with $CHCl_3$ (2.0 mL), dried over $MgSO_4$, and filtered through glass wool. The solvent was removed in vacuo, yielding an orange solid, and then redissolved in THF:PhMe (99:1) (1.5 mL) with mild heating, passed through a PTFE filter (0.2 µm), and analyzed by GPC and MALDI-TOF mass spectrometry.

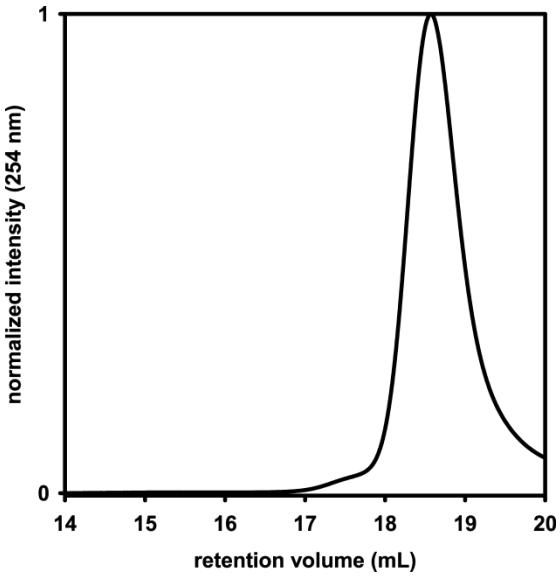

Figure S2.17. GPC trace for **3HET** polymerization using **C2** (M_n = 3.6 kDa, Đ = 1.31, theor. M_n = 3.2 kDa)

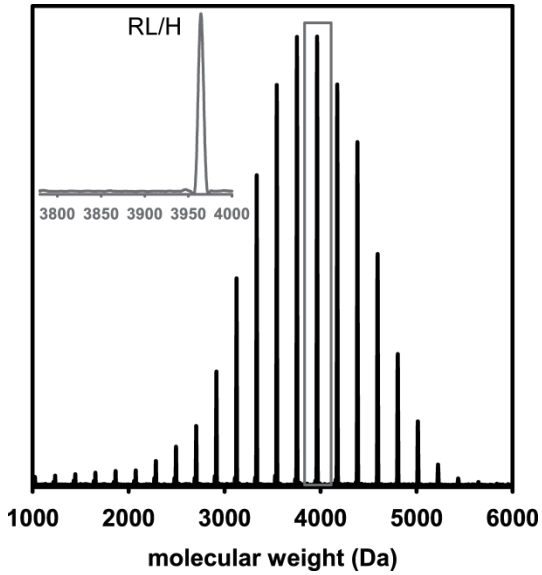

Figure S2.18. MALDI-TOF/MS spectrum for **3HET** polymerization using **C2**.

VIII. References

(1) Hall, A. O.; Lee, S. R.; Bootsma, A. N.; Bloom, J. W. G.; Wheeler, S. E.; McNeil, A. J. Reactive Ligand Influence on Initiation in Phenylene Catalyst-Transfer Polymerization. *J. Polym. Sci. Part A: Polym. Chem.* **2017**, *55*, 1530–1535.

(2) Beach, M. T.; Walker, J. M.; Wang, R.; Spivak, G. J. Ruthenium Piano-Stool Complexes Containing Mono- or Bidentate Pyrrolidinylalkylphosphines and Their Reactions with Small Molecules. *J. Organomet. Chem.* **2011**, *20*, 3198–3205.

(4) Souther, K. D.; Leone, A. K.; Vitek, A. K.; Palermo, E. F.; LaPointe, A. M.; Coates, G. W.; Zimmerman, P. M.; McNeil, A. J. Trials and Tribulations of Designing Multitasking Catalysts for Olefin/Thiophene Block Copolymerizations. *J. Polym. Sci. Part A: Polym. Chem.* **2018**, *56*, 132–137.

(4) Qiu, Y.; Worch, J. C.; Fortney, A.; Gayathri, C.; Gil, R. R.; Noonan, K. J. T. Nickel-Catalyzed Suzuki Polycondensation for Controlled Synthesis of Ester-Functionalized Conjugated Polymers. *Macromolecules* **2016**, *49*, 4757–4762.

Appendix 3

Supporting Information for Chapter 4

User-Friendly Synthesis for Conjugated Polymers

I. Materials

Flash chromatography was performed on SiliCycle silica gel (40–63 μm). Thin layer chromatography was performed on Merck TLC plates (pre-coated with silica gel 60 F254). iPrMgCl (2M in THF) was purchased in 25 mL quantities from Aldrich and titrated as described below before each reaction. All other reagent grade materials and solvents were purchased from Aldrich, Acros, ArkPharm, Oxchem or Fisher and used without further purification unless otherwise noted. 2,5-Dibromo-3-hexylthiophene from ArkPharm was purified via flash chromatography with hexanes as the eluent. THF was dried and deoxygenated using an Innovative Technology (IT) solvent purification system composed of activated alumina, a copper catalyst, and molecular sieves. The glovebox in which specified procedures were carried out was an MBraun LABmaster 130 with a N_2 atmosphere and H_2O levels below 0.1 ppm. Compounds **Zn(OPiv)$_2$**,[1] **IPentF**,[2] **IPentCF$_3$**[2] were prepared using modified literature procedures.

II. General Experimental

NMR Spectroscopy: Unless otherwise noted, ^{1}H and ^{19}F NMR spectra for all compounds were acquired at rt in $CDCl_3$ or CD_2Cl_2 on a Varian vnmr 500 operating at 500 and 470 MHz, respectively. For ^{1}H, ^{13}C, ^{19}F spectra in deuterated solvents, the chemical shift data are reported in units of δ (ppm) relative to tetramethylsilane (TMS) and referenced with residual solvent. Multiplicities are reported as follows: singlet (s), doublet (d), doublet of doublets (dd), triplet (t), doublet of quartets (dq), quartet (q), multiplet (m).

MALDI-TOF-MS: MALDI-TOF mass spectra were recorded using a Bruker AutoFlex Speed in linear or reflectron mode. The matrix trans-2-[3-(4-tert-butylphenyl)-2-methyl-2-propenylidene]malononitrile (DCTB), was prepared at a concentration of 0.1 M in THF. The instrument was calibrated with a sample of poly(3-decylthiophene) with H/Br endgroups. The polymer sample was dissolved in THF to obtain an approx.1 mg/mL solution. A 5.00 μL aliquot of polymer solution was mixed with 2.5 μL of the DCTB solution. This mixture (1 μL) was placed on the target plate and then air-dried. The data were analyzed using flexAnalysis.

Gas Chromatography: Gas chromatography was carried out using a Shimadzu GC 2010 containing a Shimadzu SHRX5 (crossbound 5% diphenyl – 95% dimethyl polysiloxane; 15 m, 0.25 mm ID, 0.25 μm df) column.

Gel-Permeation Chromatography: Polymer molecular weights were determined by comparison with polystyrene standards (Varian, EasiCal PS-2 MW 580–377,400) on a Malvern Viscotek GPCMax VE2001 equipped with two Viscotek LT-5000L 8 mm (ID) × 300 mm (L) columns and analyzed with Viscotek TDA 305 (with R.I., UV-PDA Detector Model 2600 (190–500 nm), RALS/LALS, and viscometer). Samples were dissolved in THF (with mild heating) and passed through a 0.2 μm PTFE filter prior to analysis. UV-PDA detection was used for all polymer MWs.

Titrations of the Grignard Reagents: An accurately weighed sample of salicylaldehyde phenylhydrazone[4] (typically between 90–100 mg) was dissolved in 5.00 mL of THF. An aliquot (0.25 mL) of this solution was stirred at rt while the Grignard of interest was added dropwise using a 500 μL syringe. The initial solution is yellow and turns bright orange at the end-point.

Measuring [ZnCl–Ar]: An aliquot (0.3 mL) of **ZnCl–Ar** was quenched with I_2 (4 mg) outside the box. Excess iodine was quenched with sat'd $Na_2S_2O_3$ until the brown solution turned white (1.0 mL). The reaction mixture was extracted with $CHCl_3$ (2.0 mL), dried over $MgSO_4$, filtered through glass wool and analyzed by GC. Active monomer was measured by comparing ratio of starting material to iodinated product.

III. Synthetic Procedures for $Zn(OPiv)_2$, IPentF, $IPentCF_3$, S1

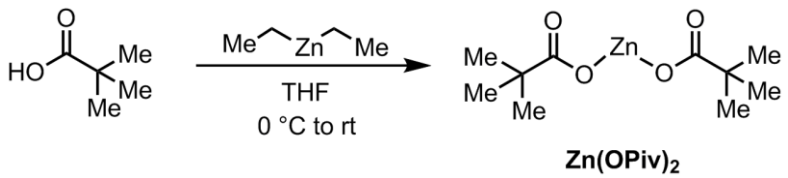

$Zn(OPiv)_2$

Zinc pivalate ($Zn(OPiv)_2$): A 50 mL oven-dried Schlenk flask equipped with a stir bar was cooled under N_2. Subsequently pivalic acid (1.21 g, 11.8 mmol, 2.00 equiv) and dry THF (6 mL) were added to the flask and the solution was cooled to 0 °C using an ice-water bath. After 20 min, diethyl zinc (5.66 mL, 5.66 mmol, 1.00 equiv, 1M in hexanes (not titrated)) was added to the flask and a white solid formed. The flask was removed from the ice-water bath and the mixture warmed to rt and then the solvent was removed under reduced pressure. The white fluffy solid was transferred to a 20 mL vial and dried under high vacuum at 90 °C to remove excess pivalic acid yielding 1.04 g of **$Zn(OPiv)_2$** (67.5% yield).

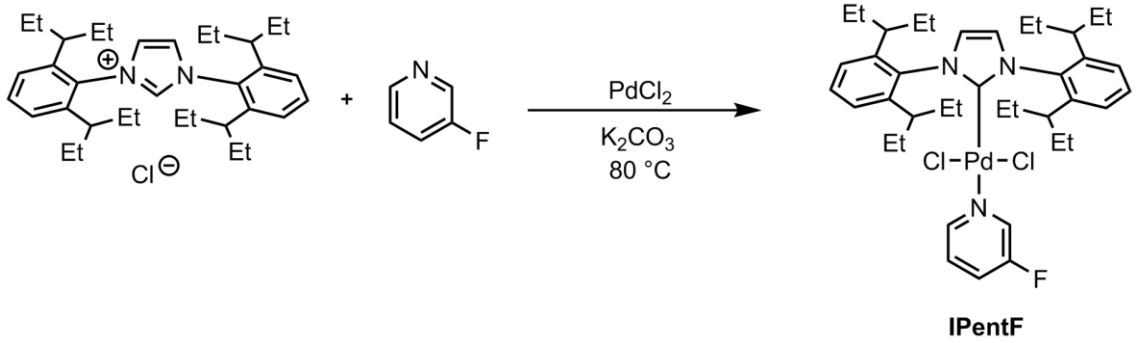

IPentF

(IPentF): To a 20 mL vial equipped with a stir bar were added sequentially, $PdCl_2$ (25.0 mg, 0.139 mmol, 1.00 equiv), K_2CO_3 (96.0 mg, 0.693 mmol, 5.00 equiv), 1,3-bis(2,6-di(pentan-3-yl)phenyl)-1H-imidazol-3-ium chloride (82.0 mg, 0.152 mmol, 1.10 equiv) and 3-fluoropyridine (0.50 mL, 5.8 mmol, 42 equiv). The vial was sealed with a teflon cap, and heated for at 80 °C for 24 h. The reaction mixture was cooled to rt, diluted with DCM (2.0 mL) and passed through a short plug of silica and celite. The filtrate was then concentrated in vacuo to yield a pyridine solution which was purified via flash chromatography (hexanes:EtOAc 1:1) to yield 57 mg of **IPentF** as a pale yellow solid (53 % yield).

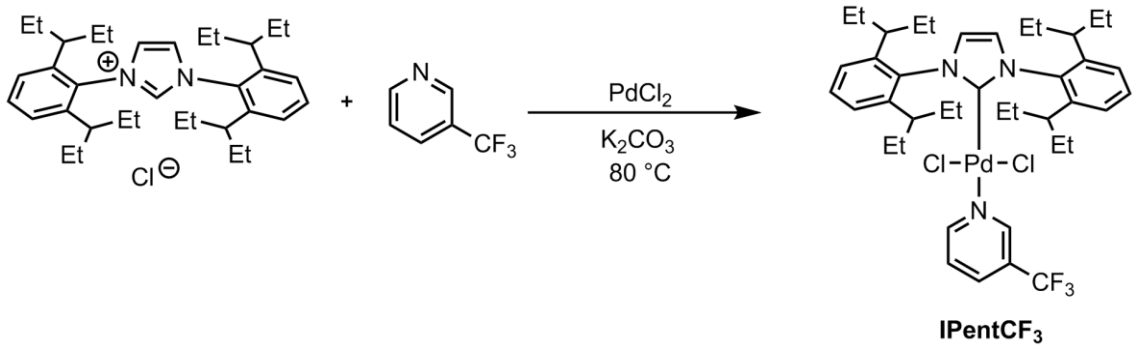

IPentCF$_3$

(IPentCF$_3$): To a 20 mL vial equipped with a stir bar were added sequentially, $PdCl_2$ (7.0 mg, 0.041 mmol, 1.00 equiv), K_2CO_3 (29.0 mg, 0.174 mmol, 5.00 equiv), 1,3-bis(2,6-di(pentan-3-yl)phenyl)-1H-imidazol-3-ium chloride (25.0 mg, 0.0456 mmol, 1.10 equiv) and 3-fluoropyridine (0.20 mL, 1.7 mmol, 42 equiv). The vial was sealed with a teflon cap, and heated for at 80 °C for 24 h. The reaction mixture was cooled to rt, diluted with DCM (2.0 mL) and passed through a short plug of silica and celite. The filtrate was then concentrated in vacuo to yield a pyridine solution which was purified via flash chromatography (hexanes:EtOAc 1:1) to yield 57 mg of **IPentCF$_3$** as a pale yellow solid (67 % yield).

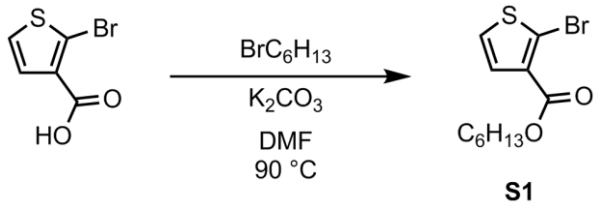

S1

Hexyl 2-bromothiophene-3-carboxylate (S1): To an oven-dried 25 mL round-bottom flask equipped with a stir bar were added 2-bromothiophene-3-carboxylic acid (1.015 g, 4.902 mmol, 1.00 equiv), K_2CO_3 (2.03 g, 14.7 mmol, 3.00 equiv) and DMF (6.5 mL). Then 1-bromohexane (1.37 mL, 9.80 mmol, 2.00 equiv) was added. The flask was sealed with a rubber septum, placed under N_2, and stirred at 90 °C for 12 h. The reaction mixture was then cooled to rt after which H_2O (20 mL) was added. The mixture was added to a separatory funnel and the aqueous layer extracted with Et_2O (3 x 10 mL) and the combined organic extracts washed with brine (2 x 10 mL), dried over $MgSO_4$, and filtered. The filtrate was concentrated in vacuo to give a yellow oil. The yellow oil was subjected to flash chromatography with a gradient of hexanes/EtOAc (99:1 to 94:6) as the eluent to afford 956 mg of S1 as a clear oil (67% yield)

IV. NMR spectra of IPentF and IPentCF$_3$

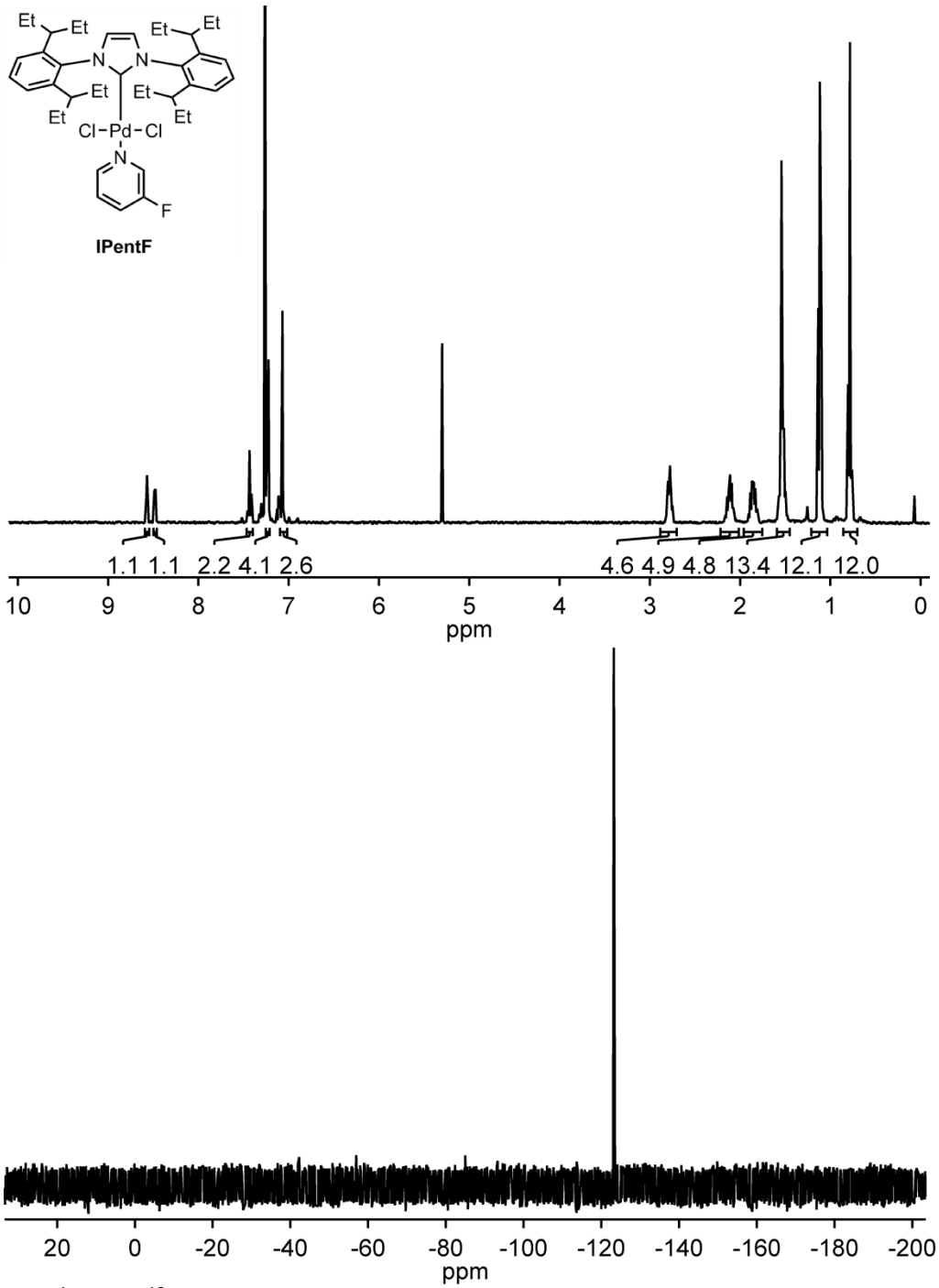

Figure S3.1. ^{1}H and ^{19}F NMR spectra of **IPentF**

^{1}H NMR (500 MHz, $CDCl_3$) δ 8.57 (d, *J* = 2.9 Hz, 1H), 8.48 (d, *J* = 5.4 Hz, 1H), 7.43 (t, *J* = 7.8 Hz, 2H), 7.27–7.18 (m, 4H), 7.07 (s, 2H), 2.78 (dq, *J* = 10.3, 5.5Hz, 4H), 2.11 (ddd, *J* = 12.7, 7.4, 4.8 Hz, 4H), 1.94–1.76 (m, 4H), 1.59–1.44 (m, 12H), 1.12 (t, *J* = 7.3 Hz, 12 H), 0.78 (t, *J* = 7.5 Hz, 12 H) ppm. (4H additional protons in spectrum from unknown source).

^{19}F NMR (470 MHz, $CDCl_3$) δ -121.39 ppm.

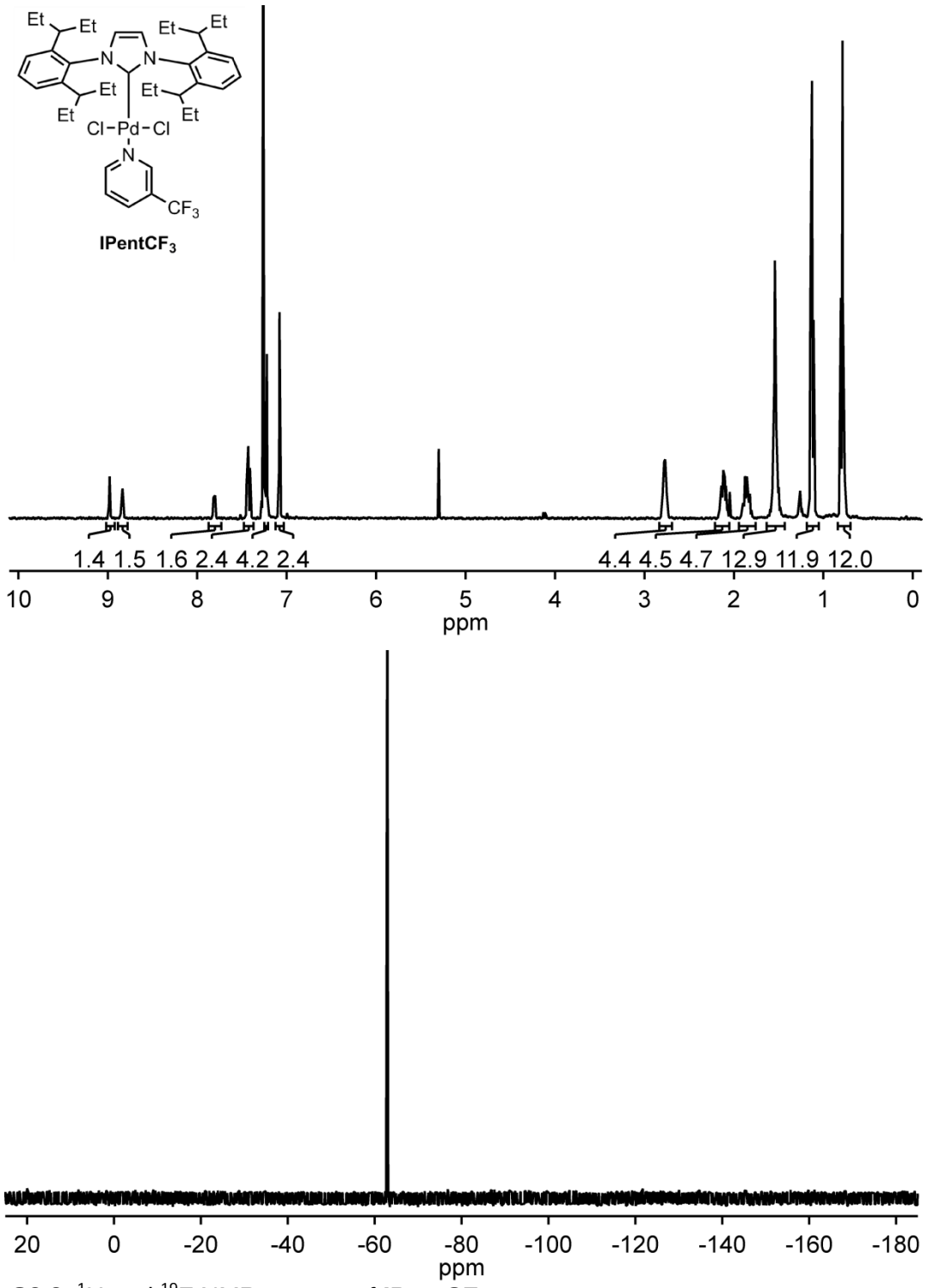

Figure S3.2. ^{1}H and ^{19}F NMR spectra of **$IPentCF_3$**

^{1}H NMR (500 MHz, $CDCl_3$) δ 8.98 (d, *J* = 2.1 Hz, 1H), 8.84 (d, *J* = 5.6 Hz, 1H), 7.81 (d, *J* = 8.0 Hz, 2H), 7.43 (t, *J* = 7.8 Hz, 2H), 7.28–7.19 (m, 4H), 7.08 (s, 2H), 2.77 (dd, *J* = 9.7, 4.9 Hz, 4H), 2.11 (dd, *J* = 6.6, 2.0 Hz, 4H), 1.87 (dd, *J* = 6.7, 2.5 Hz, 4H), 1.64–1.44 (m, 12H), 1.13 (t, *J* = 7.3 Hz, 12 H), 0.79 (t, *J* = 7.5 Hz, 12 H) ppm. (4H additional protons in spectrum from unknown source).

^{19}F NMR (470 MHz, $CDCl_3$) δ -62.89 ppm.

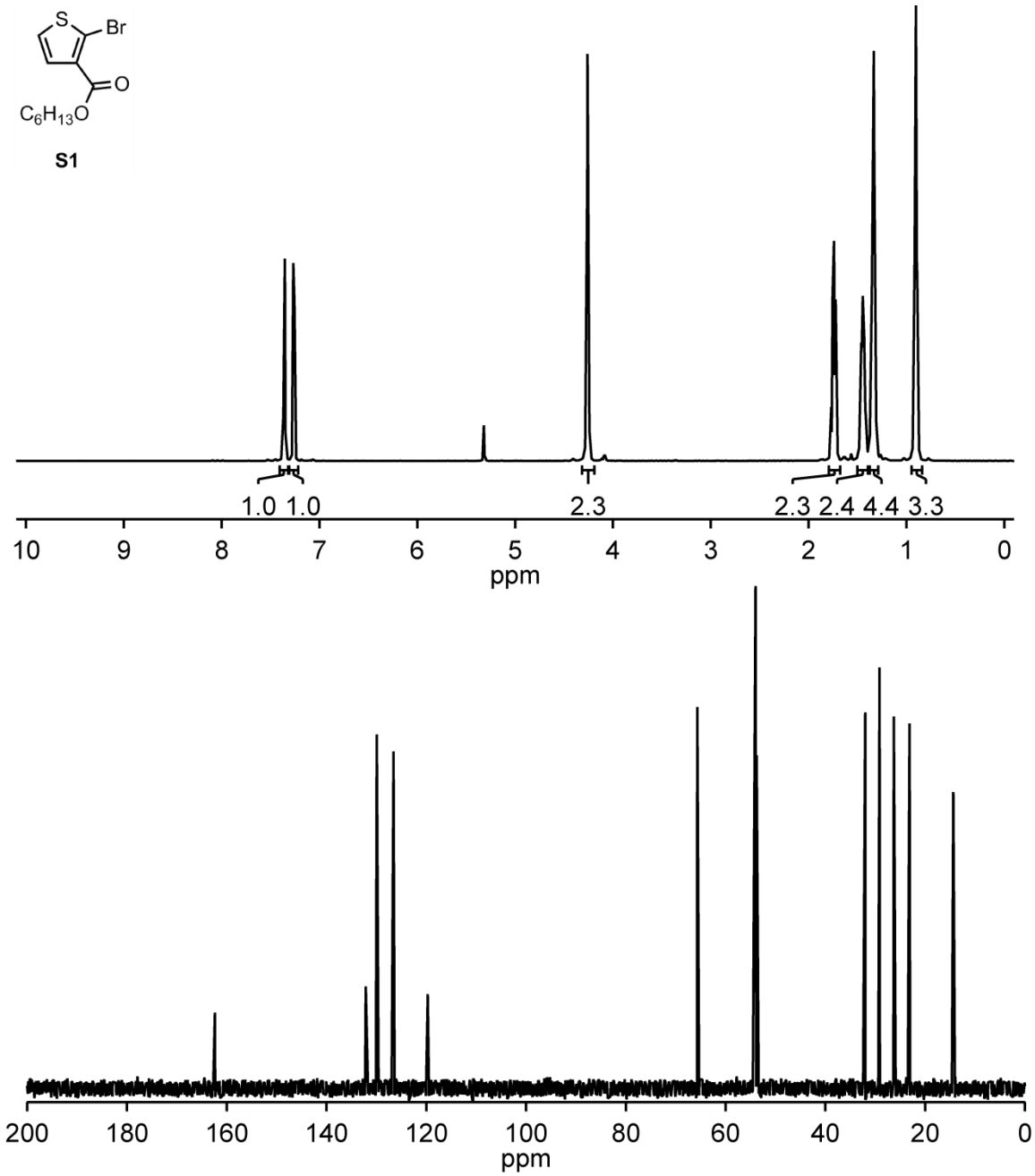

Figure S3.3. ^{1}H and ^{13}C NMR spectra of **S1**
^{1}H NMR (500 MHz, CD_2Cl_2) δ 7.36 (d, *J* = 5.8 Hz, 1H), 7.26 (d, *J* = 5.7 Hz, 1H), 4.26 (t, *J* = 6.6 Hz, 2H), 1.81–1.67 (m, 2H), 1.51–1.39 (m, 2H), 1.39–1.27 (m, 4H), 0.99–0.81 (m, 3H) ppm.
^{13}C NMR (126 MHz, CD_2Cl_2) δ 162.37, 132.13, 129.92, 126.56, 119.70, 65.68, 32.02, 29.15, 26.29, 23.13, 14.36 ppm.

V. Zn-3HT polymerization catalyst screen

Chart S3.1 Commercially available precatalysts

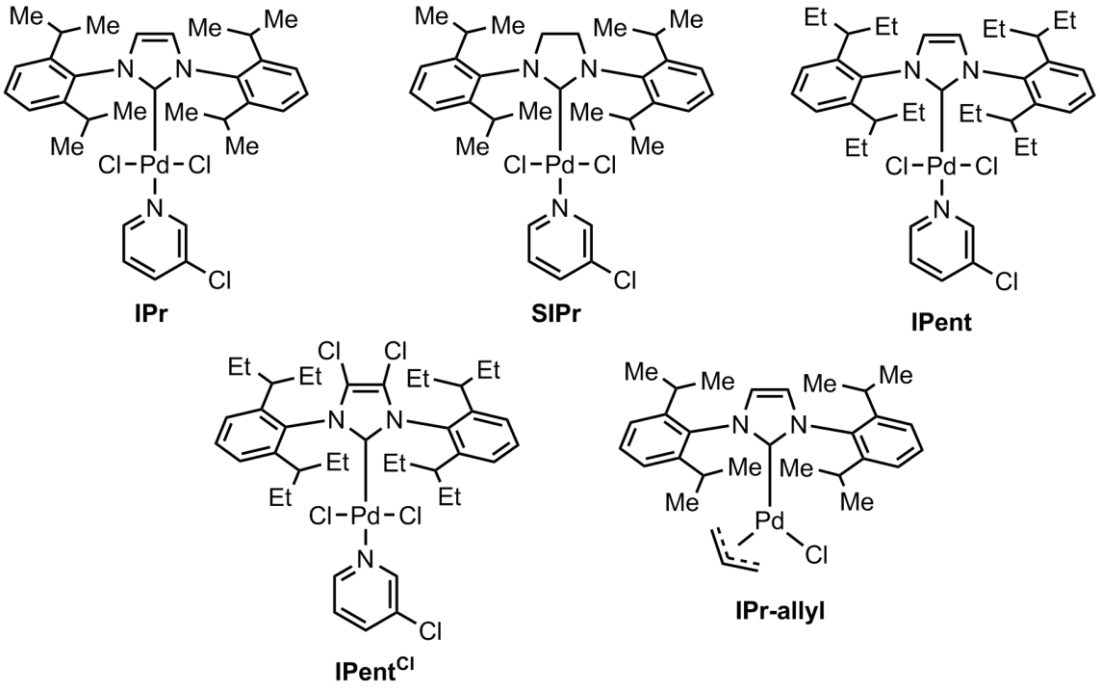

Precatalyst stock solution prep

To a 4 mL vial in the glovebox were added the respective **precatalyst** and THF in the quantities listed below sequentially and stirred until homogeneous to yield a 5 mM solution (approx. 1 min).

precatalyst	mg	THF
IPr	6.0	1.77
SIPr	6.7	1.97
IPent	3.0	0.96
IPent^{Cl}	6.2	1.44
IPr-allyl	8.3	2.89

Grignard Metathesis

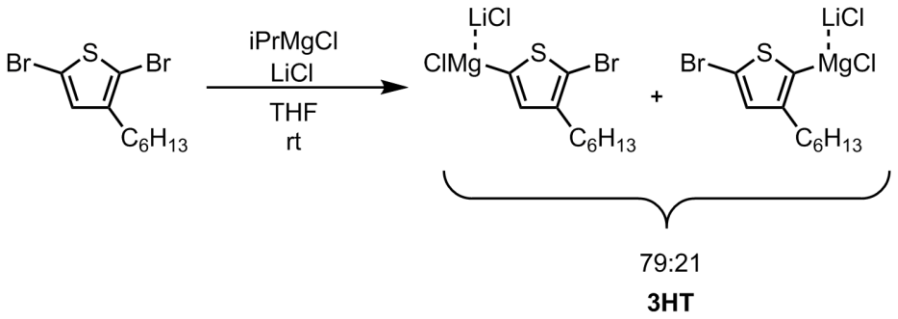

In the glovebox, 2,5-dibromo-3-hexylthiophene (111 mg, 0.341 mmol, 1.00 equiv) was added to a 20 mL vial equipped with a stir bar, followed by n-docosane (approx. 2.0 mg), LiCl (2.38 mL, 0.238 mmol, 0.7 equiv, 0.1 M in THF) and THF (1.03 mL). To the stirring solution was added iPrMgCl (130 µL, 0.238 mmol, 0.700 equiv, 1.85 M in THF) and stirred for 30 min. An aliquot (0.3 mL) of **3HT** was quenched with aq. HCl (0.5 mL, 12 M) outside the box and the reaction mixture extracted with $CHCl_3$ (2.0 mL), dried over $MgSO_4$, filtered through glass wool and analyzed by GC to show a mixture of regioisomers. An additional aliquot (0.1 mL) was quenched with I_2 (approx. 5 mg) outside of the box, yielding a dark brown solution. To quench excess I_2, saturated aq. $Na_2S_2O_3$ (1 mL) was added to the vial, capped and shaken until the solution turned cloudy white. The resulting solution was extracted with $CHCl_3$ (2.0 mL), dried over $MgSO_4$, and analyzed by GC to show [**3HT**] = 0.070 M.

$Zn(OPiv)_2$ Transmetalation with 3HT

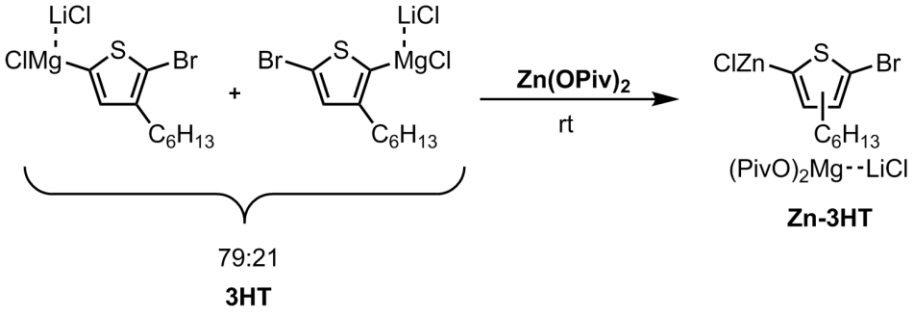

To a 20 mL vial equipped with a stirbar was added sequentially $Zn(OPiv)_2$ (56.0 mg, 0.210 mmol, 1.00 equiv) and **3HT** (3.0 mL, 0.21 mmol, 0.07 M, 1.0 equiv). The reaction stirred for 15 min, becoming yellow over time. An aliquot of **Zn-3HT** (0.1 mL) was quenched with I_2 (approx. 5 mg) outside of the box, yielding a dark brown solution. To quench excess I_2, saturated aq. $Na_2S_2O_3$ (1 mL) was added. The vial was capped and shaken until the solution turned opaque. The resulting solution was extracted with $CHCl_3$ (2.0 mL), dried over $MgSO_4$, and analyzed by GC to show [**Zn-3HT**] = 0.066 M.

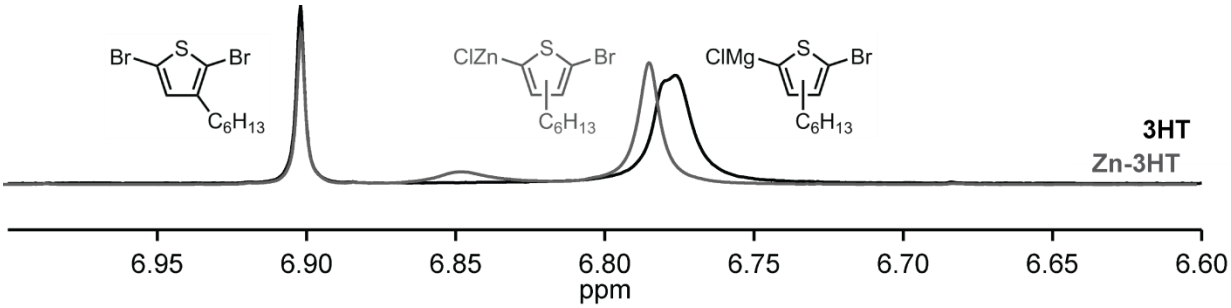

Figure S3.4 ^{1}H NMR spectrum of 3HT before and after reacting with $Zn(OPiv)_2$.

General Zn-3HT polymerization for catalyst screen

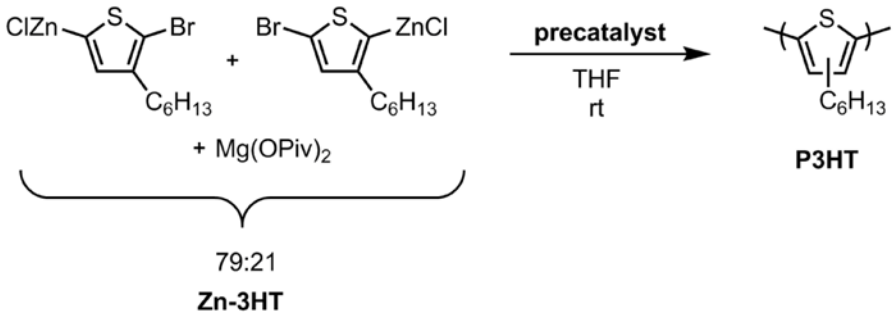

In the glovebox to a 4 mL vial equipped with a stir bar was added **Zn-3HT** (0.5 mL, 0.028 mmol, 100 equiv) and THF (0.84 mL) to give an overall [**Zn-3HT**] of 0.02 M. To the stirring solution was added **precatalyst** solution (60 µL, 0.28 µmol, 1.0 equiv). The polymerization was stirred for 30 min before being quenched outside of the box with aq. HCl (2.0 mL, 12 M). The reaction mixture was extracted with $CHCl_3$ (2.0 mL), the organic layer dried over $MgSO_4$, and filtered through glass wool. The solvent was removed in vacuo and the remaining residue redissolved in THF:PhMe (99:1) (1.5 mL) with mild heating, passed through a PTFE filter (0.2 µm), and analyzed by GPC.

precatalyst	M_n (kDa)	Đ	% conversion (major & minor)
IPr	17.7	2.25	99
SIPr	12.3	2.10	98
IPent	9.9	1.55	99
IPent^{Cl}	12.0	1.33	99
IPr-allyl	87.0	2.57	< 1%

theor. M_n = 16.7 kDa

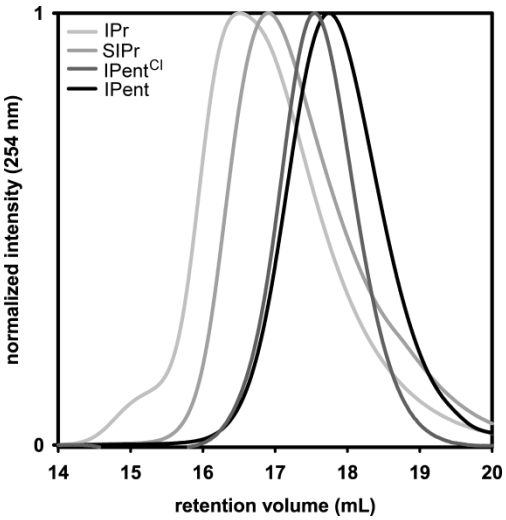

Figure S3.5 GPC overlay of **P3HT** generated with various precatalysts

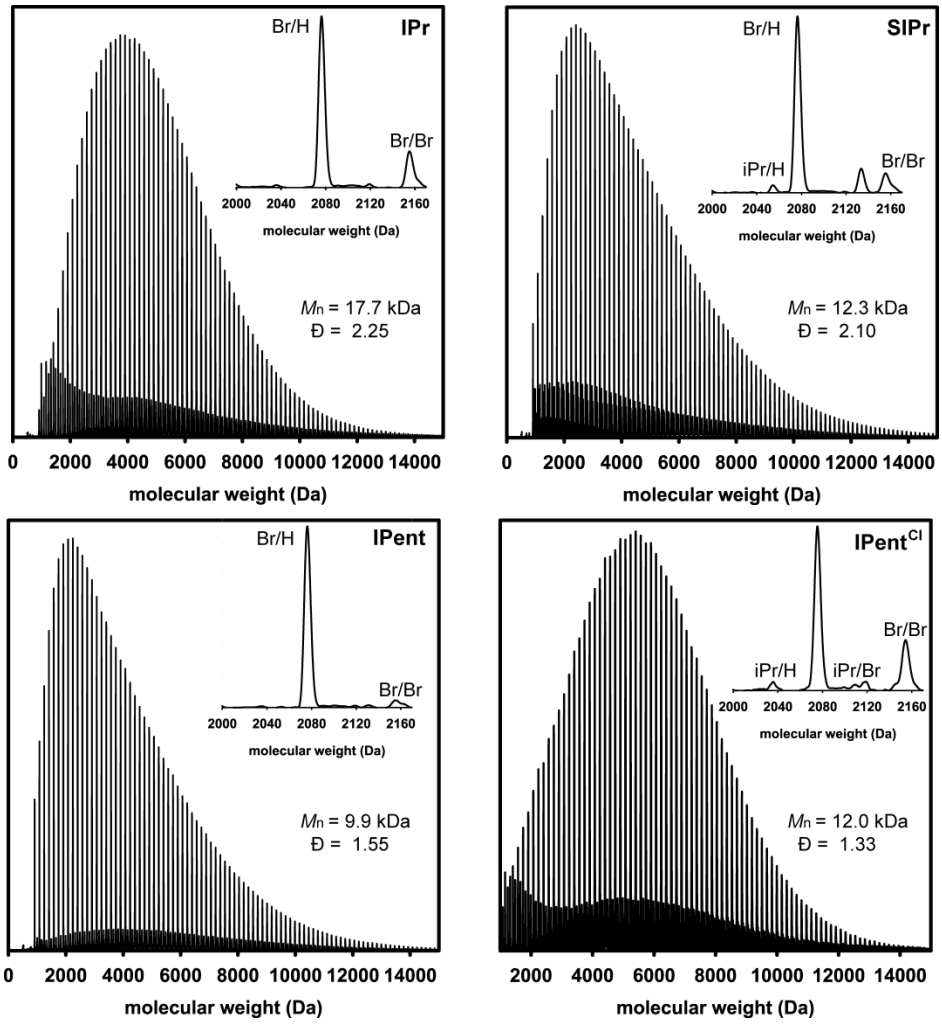

Figure S3.6 MALDI-TOF/MS spectra of **P3HT** generated with various precatalysts

VI. Zn-3HT polymerization using IPent with 3-Xpyridine

Precatalyst stock solution prep

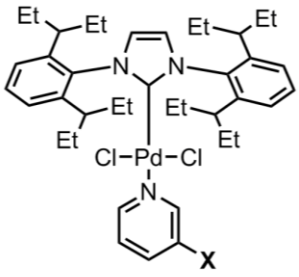

IPentX

X = Cl, CF_3, or F

To a 4 mL vial in the glovebox were added the respective **precatalyst** and THF in the quantities listed below sequentially and stirred until homogeneous to yield a 5 mM solution (approx. 1 min).

precatalyst	mg	THF
IPentCl	9.0	2.27
IPentCF$_3$	4.0	0.97
IPentF	6.0	1.55

3HT synthesis

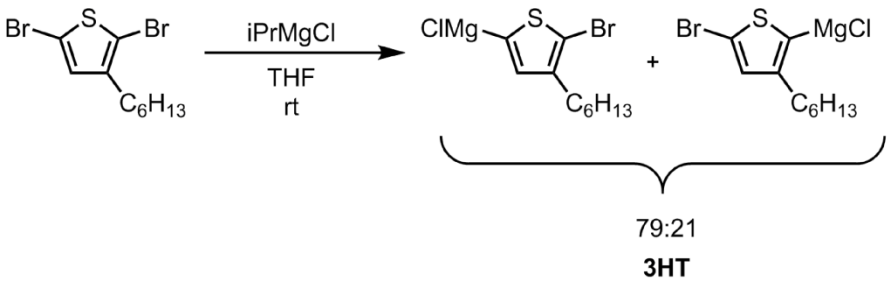

In the glovebox, 2,5-dibromo-3-hexylthiophene (69.0 mg, 0.212 mmol, 1.00 equiv) was added to a 20 mL vial equipped with a stir bar and THF (2.04 mL). To the solution was added iPrMgCl (74 µL, 0.15 mmol, 0.70 equiv, 2.0 M in THF) and stirred for 30 min. An aliquot (0.3 mL) of **3HT** was quenched with HCl (0.5 mL, 12 M) outside the box and the reaction mixture extracted with $CHCl_3$ (2.0 mL), the organic layer dried over $MgSO_4$, filtered through glass wool and analyzed by GC to show a mixture of regioisomers.

Zn(OPiv)$_2$ transmetalation with 3HT

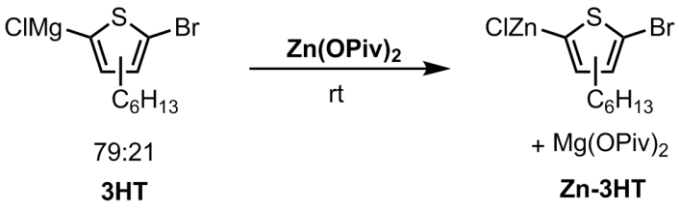

79:21
3HT

Zn-3HT

To a 20 mL vial equipped with a stir bar was added sequentially $Zn(OPiv)_2$ (37.0 mg, 0.139 mmol, 1.00 equiv) and **3HT** (2.0 mL, 0.14 mmol, 0.070 M, 1.0 equiv). The reaction was stirred for 15 min, becoming yellow over time.

Polymerization

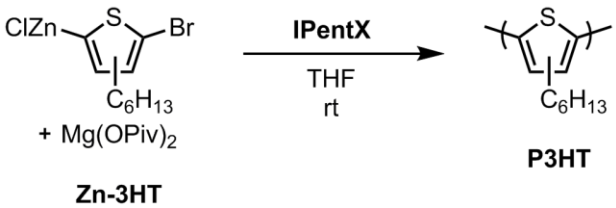

Zn-3HT

P3HT

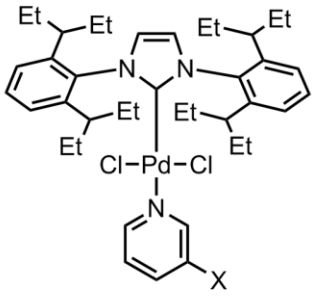

IPentX

X = Cl, CF_3, F

In the glovebox to a 4 mL vial equipped with a stir bar was added **Zn-3HT** (0.50 mL, 0.028 mmol, 100 equiv) and THF (0.84 mL) to give an overall [**Zn-3HT**] of 0.02 M. To the stirring solution was added **precatalyst** solution (60 µL, 0.28 µmol, 1.0 equiv). The polymerization was stirred for 30 min before being quenched outside of the box with aq. HCl (2.0 mL, 12 M). The reaction mixture was extracted with $CHCl_3$ (2.0 mL), the organic layer dried over $MgSO_4$, and filtered through glass wool. The solvent was removed in vacuo and the remaining residue redissolved in THF:PhMe (99:1) (1.5 mL) with mild heating, passed through a PTFE filter (0.2 µm), and analyzed by GPC.

precatalyst	M_n (kDa)	Đ
IPentCl	12.4	1.49
IPentCF_3	15.5	1.41
IPentF	15.6	1.39

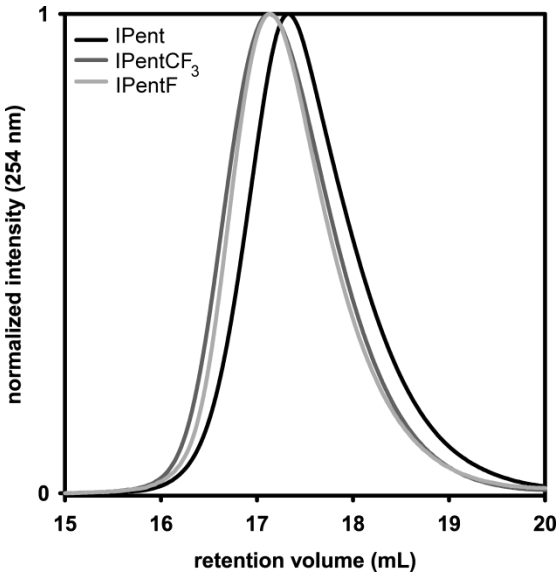

Figure S3.7 GPC traces for the polymerization of **3HT** with **IPentX**.

VII. Zn-3HT polymerizations in air using IPentF

Representative 3HT synthesis

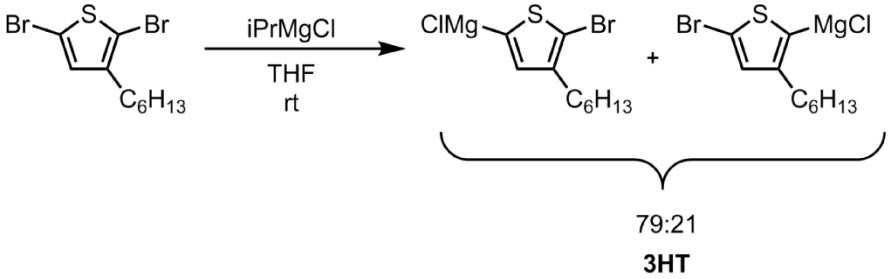

In the glovebox, 2,5-dibromo-3-hexylthiophene (110 mg, 0.285 mmol, 1.00 equiv) was added to a 20 mL vial equipped with a stir bar, followed by n-docosane (approx. 2.0 mg) and THF (2.75 mL). To the stirring solution was added iPrMgCl (100 µL, 0.200 mmol, 0.700 equiv, 1.85 M in THF) and stirred for 30 min. An aliquot (0.3 mL) of **3HT** was quenched with aq. HCl (0.5 mL, 12 M) outside the box and the reaction mixture extracted with $CHCl_3$ (2.0 mL), the organic layer dried over $MgSO_4$, filtered through glass wool and analyzed by GC to show a mixture of regioisomers.

Representative $Zn(OPiv)_2$ Transmetalation with 3HT

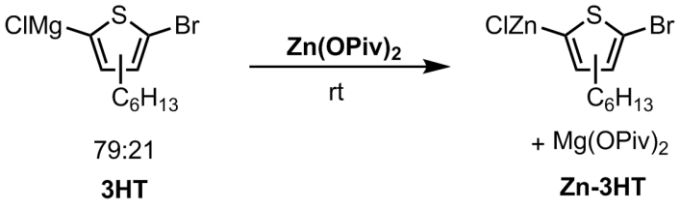

To a 20 mL vial equipped with a stir bar was added sequentially $Zn(OPiv)_2$ (47.0 mg, 0.176 mmol, 1.00 equiv) and 3HT (2.5 mL, 0.14 mmol, 0.070 M, 1.0 equiv). The reaction was stirred for 15 min, becoming yellow over time.

Zn-3HT polymerization with 1.2 mol% IPentF

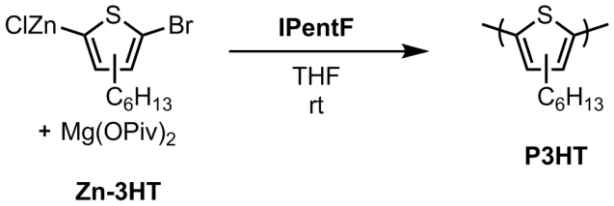

In the glovebox to a 4 mL vial equipped with a stir bar were added **IPentF** (0.10 mL, 0.50 µmol, 1.0 equiv) and THF (1.40 mL). To another 4 mL vial was added **Zn-3HT** (0.60 mL, 0.042 mmol, 84 equiv). Both vials were capped and removed from the glovebox. Outside the box, **Zn-3HT** solution was added to the **IPentF solution** and the vial capped. The polymerization was stirred for 10 min before being quenched with aq. HCl (1.0 mL, 12 M). The reaction mixture was

extracted with $CHCl_3$ (2.0 mL), the organic layer dried over $MgSO_4$, and filtered through glass wool. An aliquot of the organic layer (1.0 mL) was split into two equal portions. The first portion was diluted with additional $CHCl_3$ (2.0 mL) and analyzed by GC. The other portion was concentrated in vacuo and then redissolved in THF:PhMe (99:1) (1.5 mL) with mild heating, passed through a PTFE filter (0.2 μm), and analyzed by GPC. Both the GC and GPC aliquots were recombined with the original organic layer and the solvent removed under reduced pressure to yield a maroon solid. The solid was dissolved in a minimum amount of $CHCl_3$ (0.1 mL), and precipitated with MeOH (10.0 mL). The mixture was then centrifuged, the solvent decanted, and the solid dried under vacuum to afford **P3HT** as a maroon solid.

Run 1: M_n **=** 19.7 kDa, **Đ =** 1.40, 97.7% conversion of **Zn-3HT** (4.8 mg, 69% yield)
Run 2: M_n **=** 23.5 kDa, **Đ =** 1.38, 96.7% conversion of **Zn-3HT** (4.4 mg, 63% yield)

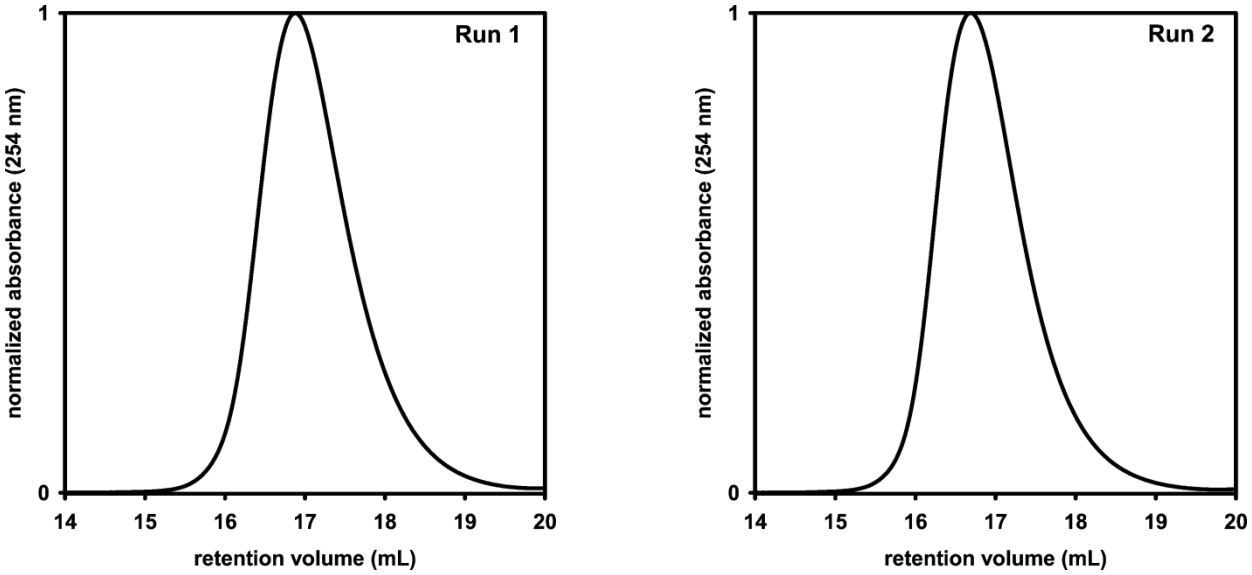

Figure S3.8. GPC trace of **P3HT** from **Zn-3HT** polymerization using **IPentF**.

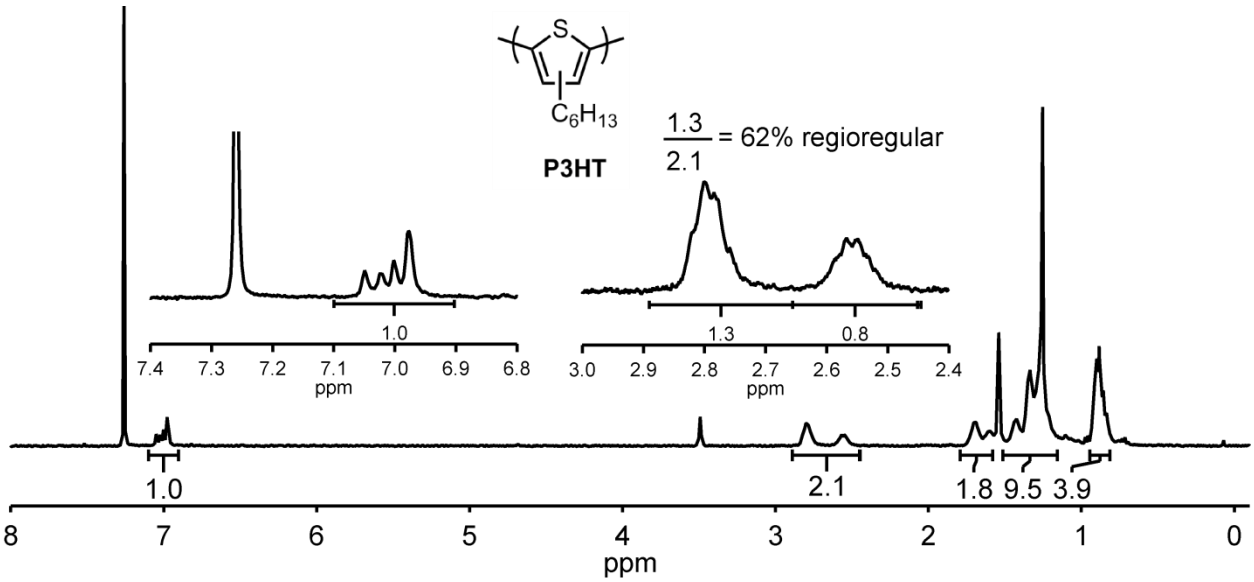

Figure S3.9. ^{1}H NMR spectrum of **P3HT** from **Zn-3HT** polymerization using **IPentF** (Run 1).

Zn-3HT polymerization with 3.6 mol% IPentF

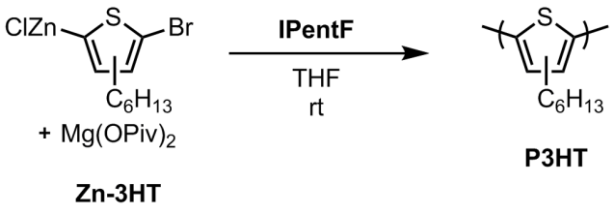

In the glovebox to a 4 mL vial equipped with a stir bar were added **IPentF** (0.10 mL, 0.50 µmol, 1.0 equiv) and THF (0.5 mL). To another 4 mL vial was added **Zn-3HT** (0.20 mL, 0.014 mmol, 27 equiv). Both vials were capped and removed from the glovebox. Outside the box, **Zn-3HT** solution was added to the **IPentF solution** via syringe and the vial capped. The polymerization was stirred for 10 min before being quenched with aq. HCl (1.0 mL, 12 M). The reaction mixture was extracted with $CHCl_3$ (2.0 mL), the organic layer dried over $MgSO_4$, and filtered through glass wool. An aliquot of the organic layer (1.0 mL) was split into two equal portions. The first portion was diluted with additional $CHCl_3$ (2.0 mL) and analyzed by GC. The other portion was concentrated in vacuo and then redissolved in THF:PhMe (99:1) (1.5 mL) with mild heating, passed through a PTFE filter (0.2 µm), and analyzed by GPC.

Run 1: M_n **=** 4.11 kDa, **Đ =** 1.70, 84.1% conversion of **Zn-3HT**
Run 2: M_n **=** 4.23 kDa, **Đ =** 1.71, 75.9% conversion of **Zn-3HT**

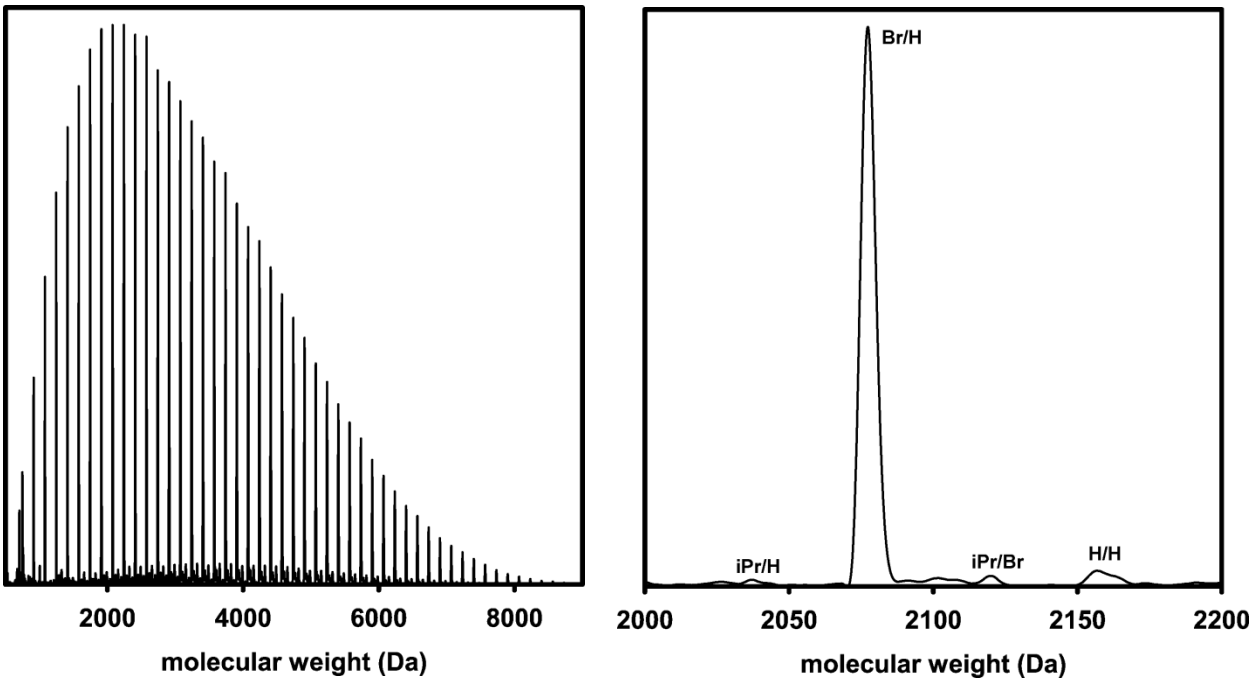

Figure S3.10. MALDI-TOF/MS spectrum of **P3HT** from **Zn-3HT** polymerization using **IPentF (Run 1)**.

Chain Extending P3HT$_{initial}$ with Zn-3HT using IPentF

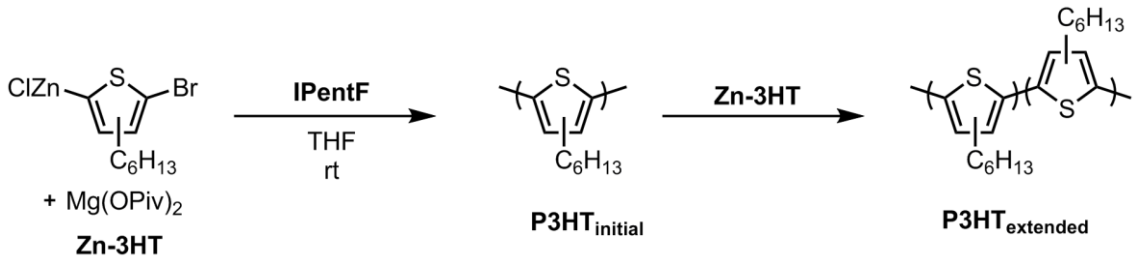

In the glovebox to a 4 mL vial equipped with a stir bar were added **IPentF** (0.10 mL, 0.50 µmol, 1.0 equiv) and THF (1.40 mL). To two additional 4 mL vials was added **Zn-3HT** (0.30 mL, 0.021 mmol, 42 equiv). All vials were capped and removed from the glovebox. Outside the box, **Zn-3HT** solution (0.3 mL) was added to the **iPentF** solution via syringe and the vial capped. The polymerization was stirred for 10 min before an aliquot (0.1 mL) was taken and quenched with aq. HCl (0.5 mL, 12 M). To the stirring **P3HT$_{initial}$** solution was added additional **Zn-3HT** (0.3 mL), the vial was capped and the reaction stirred 10 min before being quenched with aq. HCl (1.0 mL, 12 M). Both the **P3HT$_{initial}$** and **P3HT$_{extended}$** reaction mixtures were extracted with $CHCl_3$ (1.0 mL), dried over $MgSO_4$, and filtered through glass wool. The **P3HT$_{initial}$** organic layer was split into two equal portions. The first portion was diluted with additional $CHCl_3$ (2.0 mL) and analyzed by GC to show 93% conversion. The other **P3HT$_{initial}$** portion and the **P3HT$_{extended}$** organic layer were concentrated in vacuo and then redissolved in THF:PhMe (99:1) (1.5 mL) with mild heating, passed through a PTFE filter (0.2 µm), and analyzed by GPC.

Run 1: P3HT$_{initial}$: M_n = 8.96 kDa, **Đ** = 1.51, 93% conversion of **Zn-3HT**. **P3HT$_{extended}$: M_n** = 18.3 kDa, **Đ** = 1.38. GC analysis not performed on **P3HT$_{extended}$**
Run 2: P3HT$_{initial}$: M_n = 9.67 kDa, **Đ** = 1.44, 94% conversion of **Zn-3HT**. **P3HT$_{extended}$: M_n** = 18.8 kDa, **Đ** = 1.37. GC analysis not performed on **P3HT$_{extended}$**

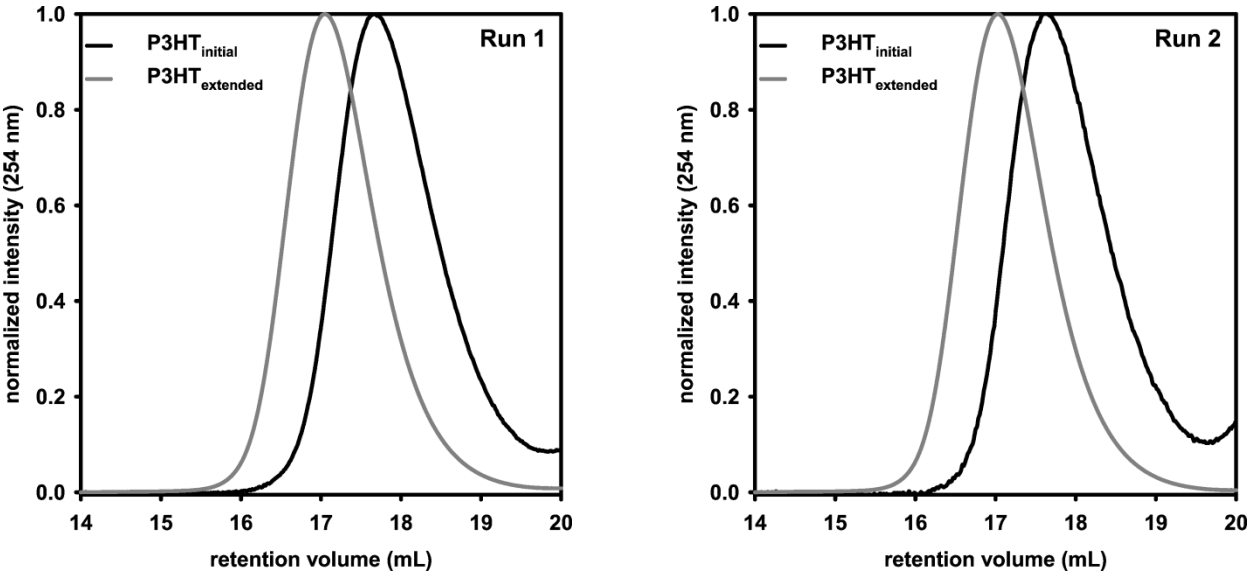

Figure S3.11. GPC traces of extending **P3HT$_{initial}$** with **Zn-3HT.**

VIII. Zn-3HET Polymerization using IPentF

2,2,6,6-tetramethylpiperidinylzinc chloride synthesis

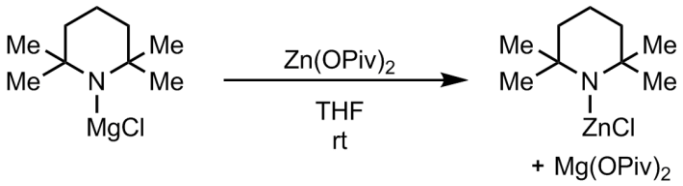

Zn-TMP

In the glovebox $Zn(OPiv)_2$ (74.0 mg, 0.277 mmol, 1.10 equiv) was added to a 4 mL vial equipped with a stir bar. To the vial was added 2,2,6,6-tetramethylpiperidinylmagnesium chloride lithium chloride complex solution (330 µL, 0.252 mmol, 0.76 M in THF (titrated), 1.00 equiv) and the heterogeneous mixture stirred for 30 min. THF (0.17 mL) was added to the vial and the mixture stirred for 5 min, turning a clear, light yellow solution.

Zn-3HET synthesis using Zn-TMP

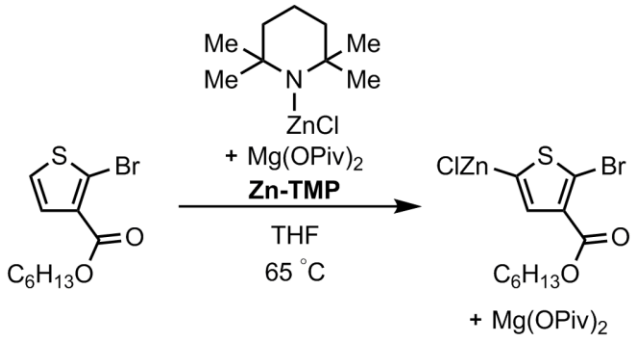

Zn-3HET

In the glovebox, **S1** (56.0 mg, 0.193 mmol, 1.00 equiv) was added to a 4 mL vial equipped with a stir bar and THF (1.65 mL). To the stirring solution was added **ZnCl-TMP** (170 µL, 0.0860 mmol, 0.50 M in THF, 1.00 equiv). The vial was sealed and heated to 65 °C and stirred at this temperature for 4 h. An aliquot (0.3 mL) of **Zn-3HET** was quenched with I_2 (4 mg) outside the box. Excess iodine was quenched with sat'd aq. $Na_2S_2O_3$ until the brown solution turned white (approx. 1.0 mL). The reaction mixture was extracted with $CHCl_3$ (2.0 mL), dried over $MgSO_4$, filtered through glass wool and analyzed by GC to show 51% active monomer.

Zn-3HET polymerization with IPent in glovebox

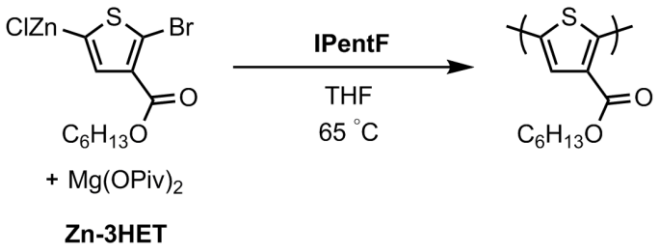

Zn-3HET

In the glovebox to a 4 mL vial equipped with a stir bar were added **IPentF** (70 µL, 0.35 µmol, 1.0 equiv) and THF (0.93 mL). The vial was sealed and heated to 65 °C (the desired polymerization temperature) for 15 min. The cap was then removed and to the stirring solution was added **Zn-3HET** (0.40 mL, 0.028 mmol, 58 equiv, 0.051 M). The vial was sealed and the polymerization stirred for 10 min before being quenched with aq. HCl (1.0 mL, 12 M) outside the box. The reaction mixture was extracted with $CHCl_3$ (2.0 mL), the organic layer dried over $MgSO_4$, and filtered through glass wool. The solution was concentrated in vacuo and then the residue redissolved in THF:PhMe (99:1) (1.5 mL) with mild heating, passed through a PTFE filter (0.2 µm), and analyzed by GPC.

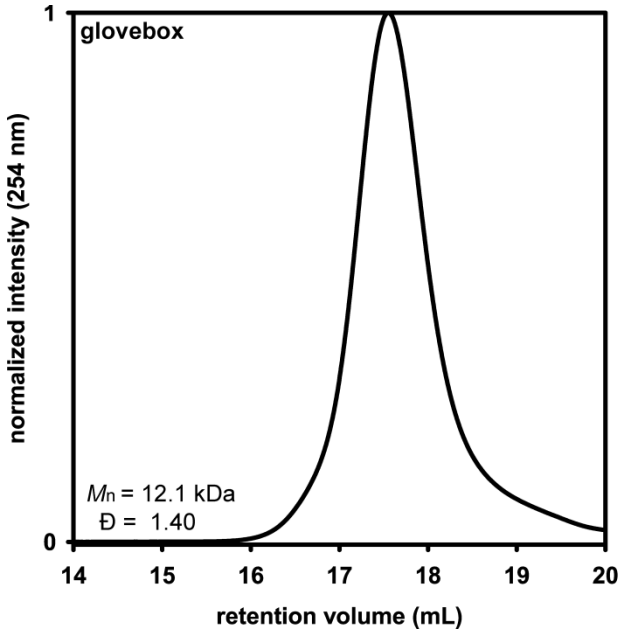

Figure S3.12. GPC trace of **Zn-3HET** polymerized with **IPentF** in the glovebox (theor. M_n = 12.2 kDa based on initial monomer:catalyst ratio).

Zn-3HET polymerization with IPent open-to-air

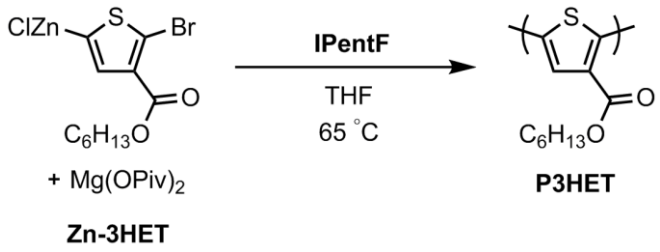

In the glovebox to a 4 mL vial equipped with a stir bar were added **IPentF** (70 µL, 0.35 µmol, 1.0 equiv) and THF (0.93 mL). To another 4 mL vial were added **Zn-3HET** (0.40 mL, 0.028 mmol, 58 equiv, 0.051 M). All vials were capped and removed from the glovebox. Outside the box, the vial containing **IPentF** was heated to 65 °C (desired polymerization temperature) for 10 min after which the cap was removed and **Zn-3HET** solution (0.4 mL) was added to the catalyst vial. The polymerization vial left open to air. After 15 min of stirring, the polymerization was quenched with aq. HCl (1.0 mL, 12 M). The reaction mixture was extracted with $CHCl_3$ (2.0 mL), dried over $MgSO_4$, and filtered through glass wool. The solution was concentrated in vacuo and then the residue redissolved in THF:PhMe (99:1) (1.5 mL) with mild heating, passed through a PTFE filter (0.2 µm), and analyzed by GPC.

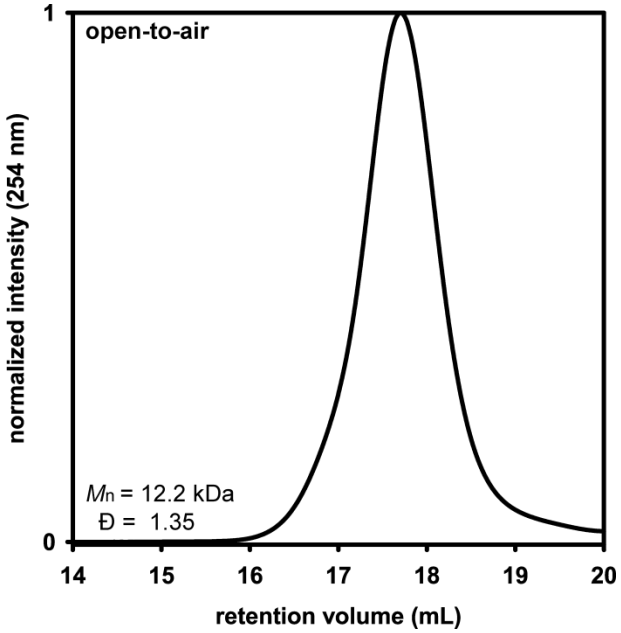

Figure S3.13. GPC trace of **Zn-3HET** polymerized with **IPentF** open-to-air (theor. M_n = 12.2 kDa based on initial monomer:catalyst ratio).

Zn-3HET polymerization with IPent open-to-air for MALDI-TOF/MS analysis

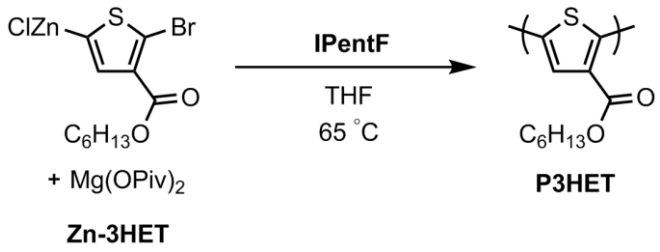

In the glovebox to a 4 mL vial equipped with a stir bar were added **IPentF** (70 µL, 0.35 µmol, 1.0 equiv) and THF (0.93 mL). To another 4 mL vial were added **Zn-3HET** (0.10 mL, 0.0051 mmol, 14 equiv, 0.051 M). The vials were capped and removed from the glovebox. Outside the box, the vial containing **IPentF** was heated to 65 °C (desired polymerization temperature) for 10 min after which the cap was removed and **Zn-3HET** solution (0.4 mL) was added to the catalyst vial. The polymerization vial left open to air. After 15 min of stirring, the polymerization was quenched with aq. HCl (1.0 mL, 12 M). The reaction mixture was extracted with $CHCl_3$ (2.0 mL), dried over $MgSO_4$, and filtered through glass wool. The solution was concentrated in vacuo and then the residue redissolved in THF:PhMe (99:1) (1.5 mL) with mild heating, passed through a PTFE filter (0.2 µm), and analyzed by GPC.

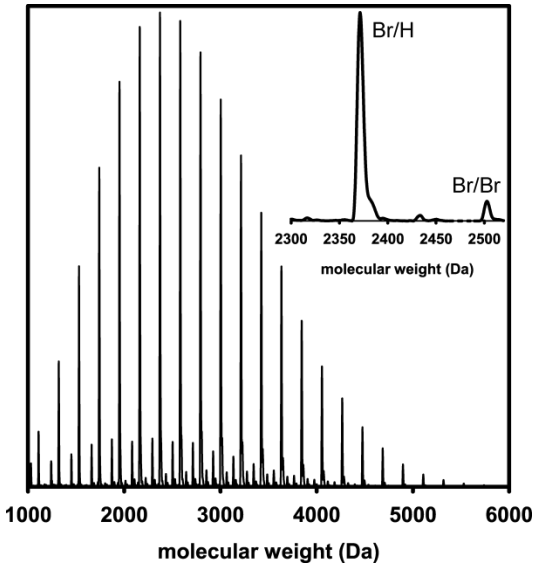

Figure S3.14. MALDI-TOF/MS spectrum of **Zn-3HET** polymerized with **IPentF** open-to-air (M_n = 2.56 kDa, Đ = 1.40).

IX. References

(1) Stathakis, C. I.; Bernhardt, S.; Quint, V.; Knochel, P. Improved Air-Stable Solid Aromatic and Heterocyclic Zinc Reagents by Highly Selective Metalations for Negishi Cross–Couplings. *Angew. Chem. Int. Ed.* **2012**, 51, 9428–9432.

(2) Organ, M. G.; Avola, S.; Dubovyk, I.; Hadei, N.; Kantchev, E. A. B.; O'Brein, C. J.; Valente, C. A User-Friendly, All-Purpose Pd–NHC (NHC = N-Heterocyclic Carbene) Precatalyst for the Negishi Reaction: A Step Towards a Universal Cross–Coupling Catalyst. *Chem. Eur. J.* **2006**, *12*, 4749–4755.